



HAL
open science

New approach to hematite recovery from ultrafine iron ore processing tailings : From fundamental studies to on-site pilot testing

Klaydison Silva

► **To cite this version:**

Klaydison Silva. New approach to hematite recovery from ultrafine iron ore processing tailings : From fundamental studies to on-site pilot testing. Geochemistry. Université de Lorraine, 2022. English. NNT : 2022LORR0287 . tel-04227510

HAL Id: tel-04227510

<https://theses.hal.science/tel-04227510>

Submitted on 3 Oct 2023

HAL is a multi-disciplinary open access archive for the deposit and dissemination of scientific research documents, whether they are published or not. The documents may come from teaching and research institutions in France or abroad, or from public or private research centers.

L'archive ouverte pluridisciplinaire **HAL**, est destinée au dépôt et à la diffusion de documents scientifiques de niveau recherche, publiés ou non, émanant des établissements d'enseignement et de recherche français ou étrangers, des laboratoires publics ou privés.



**UNIVERSITÉ
DE LORRAINE**

**BIBLIOTHÈQUES
UNIVERSITAIRES**

AVERTISSEMENT

Ce document est le fruit d'un long travail approuvé par le jury de soutenance et mis à disposition de l'ensemble de la communauté universitaire élargie.

Il est soumis à la propriété intellectuelle de l'auteur. Ceci implique une obligation de citation et de référencement lors de l'utilisation de ce document.

D'autre part, toute contrefaçon, plagiat, reproduction illicite encourt une poursuite pénale.

Contact bibliothèque : ddoc-theses-contact@univ-lorraine.fr
(Cette adresse ne permet pas de contacter les auteurs)

LIENS

Code de la Propriété Intellectuelle. articles L 122. 4

Code de la Propriété Intellectuelle. articles L 335.2- L 335.10

http://www.cfcopies.com/V2/leg/leg_droi.php

<http://www.culture.gouv.fr/culture/infos-pratiques/droits/protection.htm>



**Ecole Doctorale SIRENa
Laboratoire Georessources**



Thèse

Présentée et soutenue publiquement pour l'obtention du titre de

DOCTEUR DE L'UNIVERSITE DE LORRAINE

Mention : GÉOSCIENCES

par **Klaydison SILVA**

Sous la direction de Lev FILIPPOV

**New approach to hematite recovery from ultrafine iron
ore processing tailings.**

From fundamental studies to on-site pilot testing.

24 novembre 2022

Membres du jury :

Directeur de thèse :	Lev FILIPPOV	Professeur, Université de Lorraine, Nancy
Président de jury :	Saija LUUKKANEN	Professeur, Université de Oulu, Oulu, Finlande
Rapporteurs :	Saija LUUKKANEN	Professeur, Université de Oulu, Oulu, Finlande
	George VALADÃO	Professeur, Univ. Fédérale de Minas Gerais, Belo Horizonte, Brésil
Examineurs :	Belinda MCFADZEAN	Professeur Adj., Univ. de Cape Town, Cape Town, Afrique du Sud
	Henrique TURRER	Chef du Service de Minéral Processing, ArceloMittal, Metz
	Inna FILIPPOVA	Enseignant-Chercheur, Université de Lorraine, Nancy
Membres invités :	Otávia RODRIGUES	Professeur, Université Fédérale de Ouro Preto, Ouro Preto, Brésil

Acknowledgments

More challenging than completing this work is to express, in a few words, all the feeling of gratitude to those who accompanied me on this journey.

This thesis was only possible due to the support I received from several people.

First, I thank God for putting so many generous people in my life.

I thank my parents Osvaldo and Theresinha (in memoriam) who worked so hard in life so that I had the opportunities they didn't have. My parents were my main encouragers, through the example of life. My mother, as a teacher, always showed me the importance of the search for knowledge. May God allow me to be an example to my children as my parents were an example to me.

I thank all my family and, above all, my wife Cléia Fernandes and my children João Pedro and Thomás Augusto for giving up part of their lives to accompany me and for making me believe that everything would be worth it. Thank you for dreaming with me!

I also thank Vale Company S.A., especially Marco Tulio, who believed me more than once, and all my friends from the Iron Ore Treatment Process Development Department, especially Neymayer, Mauricio Segato, Ivan, Samuel and Edison.

I thank Prof. Lev Filippov and to Dr. Inna Filippova for understanding my challenges and guiding me so brilliantly in this work.

I thank Alexandre Piçarra who, in addition to being my support in the laboratory, became a friend.

I thank the members of the "*Comité de Suivi de Thèse*" Daniel Fornasiero, José Paulo Pinheiro and Saeed for their patience. Thanks to Toninho Peres for all the valuable advice and for the very important help; to the CETEM team (mainly Elves Matiolo, Julio Guedes and Lucas Andrade), Clariant, ITV (Vale), Ms. Catherine and Filipe Guimarães for their support.

I also thank the members of the jury: Saija Luukkanen, George E. S. Valadão, Belinda McFadzean, Henrique D. G. Turrer, Otávia M. S. Rodrigues for their cordiality and valuable comments on this work.

My list of people to thank is very long. There are still several people who encouraged me in some way, but who were not mentioned. Rest assured that I am grateful to all of you and I wish the world to be as generous to you as you have been to me.

Thank you very much !

Agradecimentos

Mais desafiador do que concluir este trabalho é expressar, em poucas palavras, todo o sentimento de gratidão a quem me acompanhou nesta jornada. Esta tese só foi possível devido ao apoio que recebi de várias pessoas.

Primeiramente, agradeço a Deus por colocar tantas pessoas generosas em minha vida.

Agradeço aos meus pais Theresinha (in memoriam) e Osvaldo, que trabalharam tanto na vida para que eu tivesse as oportunidades que eles não tiveram. Meus pais foram meus principais incentivadores, através do exemplo de vida. Minha mãe, como professora, sempre me mostrou a importância da busca pelo conhecimento. Que Deus me permita ser exemplo para meus filhos assim como meus pais foram exemplo para mim.

Agradeço a toda a minha família e, principalmente, à minha esposa Cléia Fernandes e aos meus filhos João Pedro e Thomás Augusto por cederem parte de suas vidas para me acompanhar e por me fazer acreditar que tudo valeria a pena. Obrigado por sonharem comigo!

Agradeço também à Companhia Vale S.A., em especial ao Marco Tulio, que acreditou em mim mais de uma vez, e a todos os meus amigos do Departamento de Desenvolvimento de Processos de Tratamento de Minério de Ferro, especialmente ao Neymayer, Mauricio Segato, Ivan Pena, Samuel e Edison.

Agradeço ao Professor Lev Filippov e a Dr. Inna Filippova por compreenderem meus desafios e me guiarem de forma tão brilhante neste trabalho.

Agradeço ao Alexandre Piçarra que, além de ser meu apoio constante no laboratório, se tornou um amigo.

Agradeço aos membros do "*Comité de Suivi de Thèse*" Daniel Fornasiero, José Paulo Pinheiro e Saeed pela paciência. Obrigado ao Toninho Peres por todos os valiosos conselhos e pela importantíssima ajuda, à equipe do CETEM (especialmente ao Elves Matiolo, Julio Guedes e Lucas Andrade), a Clariant, ITV (Vale), Sra. Catherine e Filipe Guimarães pelo apoio.

Agradeço também aos membros do jury: Saija Luukkanen, George E. S. Valadão, Belinda McFadzean, Henrique D. G. Turrer, Otávia M. S. Rodrigues pela cordialidade e valiosos comentários sobre este trabalho.

Minha lista de agradecimento é muito extensa. Ainda há várias pessoas que me incentivaram de alguma forma, mas que não foram citadas. Tenham certeza de que sou grato a todas e desejo que o mundo seja tão generoso com vocês quanto vocês foram comigo.

Muito obrigado !

Forewords

About the structure of this thesis

This thesis presents studies concerning the adoption of a new reagent as collector for iron ore slimes concentration process by flotation, without depressant.

Except for the first chapter (which presents the context of the thesis) and the last chapter (which presents the final comments), this thesis is composed of scientific articles written during the development of studies in Brazil (at Vale Mining Company and CETEM - Mineral Technology Center) and France (University of Lorraine).

The **First Chapter** aims to emphasize the importance of this study, presenting information on the reduction of iron content in ores from the Iron Quadrangle region, in Brazil, over the years, with the consequent increase in the number of tailings dams. A brief literature review is presented to justify the scientific hypothesis to be studied.

The investigation of the scientific hypothesis presented in chapter 1 is carried out throughout the scientific articles presented in chapters 2 to 6. Chapters 2, 3, 5 and 6 have already been published, while chapter 4 refers to an article submitted and awaiting publication. A brief description of each article/chapter is presented below:

- **Chapter 2 - The Characteristics of Iron Ore Slimes and Their Influence on The Flotation Process**

Minerals 2020, 10 (8), 675; <https://doi.org/10.3390/min10080675>

This paper shows the study of characterization of a typical iron ore slime, aiming to create a better understanding of its role on the iron ore concentration by flotation.

- **Chapter 3 - New perspectives in iron ore flotation: use of collector reagents without depressants in reverse cationic flotation of quartz**

Minerals Engineering 170 (2021) 107004; <https://doi.org/10.1016/j.mineng.2021.107004>

This paper aims to propose a new amidoamine collector for iron ore reverse flotation with a potential of removing the iron oxides depressant.

- **Chapter 4 - Comparison Between Etheramine and Amidoamine (N-[3-(dimethylamino)propyl]dodecanamide) Collectors: Adsorption Mechanisms on Quartz and Hematite Unveiled by Molecular Simulations**

Minerals Engineering 180 (2022) 107470; <https://doi.org/10.1016/j.mineng.2022.107470>

This work describes, at the molecular level, the differences in adsorption between etheramine and amidoamine N-[3-(dimethylamino)propyl]dodecanamide, explaining the behavior of this amidoamine, which allows its use, without a depressant, for the flotation process of some ore iron slimes.

- **Chapter 5 - Improving recovery of iron using column flotation of iron ore slimes**

Minerals Engineering 158 (2020) 106608; <https://doi.org/10.1016/j.mineng.2020.106608>

This work aims at evaluating the technical feasibility of concentration of two slimes samples from two different plants in operation at the Iron Quadrangle, using the column flotation.

- **Chapter 6 - Iron Ore Slimes Flotation Tests Using Column and Amidoamine Collector Without Depressant**

Minerals 2021, 11(7), 699; <https://doi.org/10.3390/min11070699>

This work describes the pilot scale iron ore slimes flotation tests, with a 500mm diameter column, operating in series with the industrial plant, adopting amidoamine N-[3-(dimethylamino)propyl]dodecanamide as collector, without depressant. The objective is to present the variability in slimes characteristics and discuss its effect on process efficiency and main control parameters.

The **Chapter 7** presents, in summary, the comparison between two different processes: slimes flotation, presented in this thesis, and magnetic concentration. This topic shows that, for the specific case of Vargem Grande 2 plant, a suitable process route could be the adoption of flotation (with amidoamine N-[3-(dimethylamino)propyl]dodecanamide) as the rougher stage and the magnetic concentration as a cleaner stage.

The **Final Comments** present the relationship between each chapter and also some suggestions for the development of new research related to this subject.

As this thesis is mainly composed of articles published during the research, each chapter presents its own Literature Review and of References.

Avant-Propos

À propos de la structure de cette thèse

Cette thèse présente des études concernant l'adoption d'un nouveau réactif comme collecteur pour le procédé de concentration de boues de minerai de fer par flottation, sans dépresseur.

A l'exception du premier chapitre (qui présente le contexte de la thèse) et du dernier chapitre (qui présente les commentaires finaux), cette thèse est composée d'articles scientifiques rédigés lors du développement d'études au Brésil (chez Vale Mining Company et CETEM - Centre de Technologie Minérale) et en France (Université de Lorraine).

Le **Premier Chapitre** vise à souligner l'importance de cette étude, en présentant des informations sur la réduction de la teneur en fer dans les minerais de la région du quadrilatère de fer, au Brésil, au fil des ans, avec l'augmentation conséquente du nombre de barrages de résidus. Une brève revue de la littérature est présentée afin de justifier l'hypothèse scientifique à étudier.

L'investigation de l'hypothèse scientifique présentée dans le chapitre 1 est réalisée à travers les articles scientifiques présentés dans les chapitres 2 à 6. Les chapitres 2, 3, 4, 5 et 6 ont déjà été publiés, tandis que le chapitre 4 fait référence à un article soumis le 28 septembre. Une brève description de chaque article/chapitre est présentée ci-dessous :

- **Chapitre 2 - Les caractéristiques des boues de minerai de fer et leur influence sur le processus de flottation**

Minerals 2020, 10 (8), 675; <https://doi.org/10.3390/min10080675>

Cet article montre l'étude de la caractérisation d'une boue de minerai de fer typique, visant à créer une meilleure compréhension de son rôle sur la concentration de minerai de fer par flottation.

- **Chapitre 3 - Nouvelles perspectives dans la flottation du minerai de fer : utilisation de réactifs de collecte sans dépresseur dans la flottation cationique inversée du quartz**

Minerals Engineering 170 (2021) 107004 ; <https://doi.org/10.1016/j.mineng.2021.107004>

Cet article vise à présenter un nouveau collecteur de type amidoamine pour la flottation inverse du minerai de fer avec le potentiel d'éliminer le besoin d'un réactif dépresseur d'oxyde de fer.

- **Chapitre 4 - Comparaison entre collecteurs étheramine et l'amidoamine (N-[3-(diméthylamino)propyl]dodécaneamide: mécanismes d'adsorption sur quartz et hématite révélés par simulations moléculaires**

Minerals Engineering 180 (2022) 107470; <https://doi.org/10.1016/j.mineng.2022.107470>

Ce travail décrit, au niveau moléculaire, les différences d'adsorption entre l'étheramine et l'amidoamine N-[3-(diméthylamino)propyl]dodécaneamide, expliquant le comportement de cette amidoamine, qui permet son utilisation, sans dépresseur, pour le procédé de flottation de certaines boues de minerai de fer.

- **Chapitre 5 – Optimisation de la récupération du fer par flottation sur colonne de boues de minerai de fer**

Minerals Engineering 158 (2020) 106608; <https://doi.org/10.1016/j.mineng.2020.106608>

Ce travail vise à évaluer la faisabilité technique de la concentration de deux échantillons de boues provenant de deux usines différentes opérant au Iron Quadrangle, par flottation sur colonne.

- **Chapitre 6 - Tests de flottation des boues de minerai de fer utilisant une colonne et amidoamine comme collecteur, sans dépresseur**

Minerals 2021, 11(7), 699; <https://doi.org/10.3390/min11070699>

Ce travail décrit les essais pilotes de flottation de boues de minerai de fer, avec une colonne de 500 mm de diamètre, fonctionnant en série avec l'installation industrielle, en adoptant l'amidoamine N-[3-(diméthylamino)propyl]dodécaneamide comme réactif collecteur, sans dépresseur. L'objectif est de présenter la variabilité des caractéristiques des boues et de discuter l'effet sur l'efficacité du procédé des principaux paramètres de contrôle.

Le **Chapitre 7** présente, en résumé, la comparaison entre deux procédés différents : la flottation des boues, présentée dans cette thèse, et la concentration magnétique. Ce sujet montre que, pour le cas spécifique de l'usine Vargem Grande 2, une voie de traitement appropriée pourrait être l'adoption de la flottation (avec amidoamine N-[3-(diméthylamino)propyl]dodécaneamide comme étape rougher et de la concentration magnétique comme étape cleaner.

Les **Commentaires Finaux** présentent la relation entre chaque chapitre ainsi que quelques suggestions pour le développement de nouvelles recherches liées à ce sujet.

Comme cette thèse est principalement composée d'articles publiés au cours de la recherche, chaque chapitre présente sa propre revue de la littérature et références bibliographiques.

SUMMARY

Présentation de la thèse avec commentaires sur les principaux sujets	1
Chapter 1 - Contextualization.....	7
1. Introduction	7
1.1. Decreased iron content in the Iron Quadrangle deposits - The “Third Wave” of iron ore processing plants in Brazil.....	7
1.2. Tailings Dam - One of the biggest problems related to the Third Wave.	8
1.3. Chemical and granulometric characteristics of Brazilian iron ore slimes.....	11
2. Literature Review	14
2.1. The Role of Starch in the Iron Ore Flotation Plants from the Iron Quadrangle Region.....	14
2.2. Starch Adsorption Mechanism	15
2.3. Issues that hinder the selective action of starches in the iron ore cationic reverse flotation process.....	16
2.4. Amidoamines	19
Amidoamine (N-[3(dimethylamino)propyl]dodecanamide)	20
2.5. Development of Selective Collectors.....	22
3. Scientific Hypothesis	25
4. Purpose of this PhD Thesis	26
References.....	27
Chapter 2 - The characteristics of iron ore slimes and their influence on the flotation process	36
1. Introduction	37
2. Materials and Methods	40
2.1. Samples.....	40
2.2. Characterizations	41
3. Results and Discussion	42
4. Conclusions	48
References.....	49
Chapter 3 - New perspectives in iron ore flotation: use of collector reagents without depressants in reverse cationic flotation of quartz.....	51
5. Introduction	52

6. Materials and methods.....	54
6.1. Minerals and reagents	54
6.2. X-Ray fluorescence (XRF) analysis.....	54
6.3. Modified water	55
6.4. Contact angle measurements	57
6.5. Zeta potential.....	58
6.6. Flotation.....	58
6.7. Infrared measurements	59
7. Results and discussions	60
7.1. Contact angle measurements	60
7.2. Zeta potential measurements	65
7.3. Flotation of pure minerals	71
Hematite	72
Kaolinite	73
Quartz	75
7.4. Flotation of mineral mixtures	76
Mixture: 85% hematite and 15% quartz	76
Mixture: 85% hematite and 15% kaolinite.....	78
7.5. Infrared measurements	81
8. Conclusions	86
References.....	87

Chapter 4 - Comparison Between Etheramine and Amidoamine (N-[3-(dimethylamino)propyl]dodecanamide) Collectors: Adsorption Mechanisms on Quartz and Hematite Unveiled by Molecular Simulations	91
1. Introduction	92
1.1. Nomenclatures and abbreviations.....	92
1.2. Development of new more selective collectors in the iron ore flotation	92
1.3. The quartz and hematite mineral surfaces.....	93
1.4. Amidoamine Flotisor 5530	94
1.5. Molecular modeling.....	96
2. Methodology	96
2.1. Measurement of the pKa	96
2.2. Systems Modeling.....	97
2.3. Molecular Dynamics Simulations.....	100
2.4. Analysis	102
3. Results.....	103
3.1. Study 1 - Single collector adsorption	103

3.2. Study 2 - Adsorption Layer Stability.....	106
Interaction Energies.....	106
1D Atomic Concentration Profiles	107
Surface Normal Angle Profiles	108
Hydrogen Bonds.....	110
4. Conclusion	113
References.....	114

Chapter 5 - Improving recovery of iron using column flotation of iron ore slimes .120

1. Introduction	121
2. Experimental.....	130
2.1. Slimes samples.....	130
2.2. Samples characterization.....	130
2.3. Flotation studies	132
Reagents	132
Sample 1 - Column flotation 2"	132
Sample 1 - Column flotation 6"	134
Sample 2 - Column flotation 3"	135
Sample 2 - Column flotations 6" and 4"	136
3. Results and Discussion	137
3.1. Flotation Studies – Sample 1	137
3.2. Flotation Studies – Sample 2	146
4. Conclusions	150
References.....	150

Chapter 6 - Iron ore slimes flotation tests using column and amidoamine collector without depressant156

1. Introduction	157
1.1. Iron ore ultrafine concentration	157
1.2. Equipment Improvements for Ultrafine Flotation — Microbubbles.....	158
1.3. Developments of Collectors Regarding the Brazilian Iron Ores Slimes Characteristics	158
1.4. Objectives of this Paper	160
2. Materials and Methods	161
2.1. Industrial Plant.....	161
2.2. Pilot Plant.....	162
2.3. Reagents	162
2.4. Characterization.....	162
2.5. Operational Parameters of Flotation Column	163

3. Results.....	163
3.1. Sample Characterization.....	163
3.2. Pilot Flotation General Conditions.....	167
3.3. Variability of the Slimes in the Industrial Plant	167
3.4. Initial Pilot Flotation Tests — Summary Results for a 6 Day Test Period	170
3.5. Analysis of the Influence of Feed Variability and Operational Parameters on Flotation Results during the 67 Pilot Test Campaign	174
Results.....	174
Influence of Collector Dosage.....	176
Influence of Water Recovery	177
Influence of Washing Water	178
Carrying Rates	180
3.6. General Discussions	181
Control System.....	181
Product Quality and the Challenge of Slimes Concentration in Brazil	181
4. Conclusion	183
References.....	184
Chapter 7 - Why flotation for iron ore slimes?	188
References.....	195
Chapter 8 - Final comments	196

Présentation de la thèse avec commentaires sur les principaux sujets

Ce chapitre a une particularité, car il peut être présenté sous forme de Conclusions ou de Résumé, au début ou à la fin de cette thèse. J'ai choisi de le présenter au début, en français.

L'objectif est de discuter, de manière simplifiée, une relation entre les thèmes abordés et de présenter les principales conclusions de cette thèse. Ce chapitre vise aussi, en quelque sorte, à souligner l'importance de développer de nouveaux réactifs pour la flottation du minerai de fer, afin, peut-être, d'initier de nouvelles recherches sur le sujet.

Dans le chapitre 1 de la thèse, il est indiqué que l'industrie minière du fer dans le Quadrilatère Ferrífero, au Brésil, est actuellement dans la phase, appelée par certains auteurs, la troisième vague et, en raison des caractéristiques du minerai de fer de la région, le processus de concentration est la flottation cationique inverse du quartz présent dans l'itabirite. La troisième vague de l'industrie minière du minerai de fer génère des conséquences indésirables, telles que des impacts environnementaux accrus associés aux barrages de résidus. Par conséquent, l'étude du processus de concentration contribuant à la réduction de la quantité de résidus miniers est très importante pour le progrès de l'industrie minière dans la région.

Les problèmes liés à l'utilisation de l'amidon dans certaines conditions spécifiques pouvant entraver le processus de flottation ont été discutés. Certains auteurs ont montré que l'amidon peut être adsorbé sur des surfaces de silicate contenant Fe-Mg-Al, ce qui nuit à la flottation. A des doses élevées d'amine et/ou d'amidon il est possible que des interactions entre ces réactifs se produisent, réduisant l'efficacité du procédé. D'autre part, certains travaux visant à développer de nouveaux collecteurs de flottation plus sélectifs, qui éliminent le besoin de dépresseurs, ont montré que certains réactifs, à tête polaire volumineuse, peuvent présenter un comportement sélectif dans la flottation de certains minéraux, en raison du phénomène d'empêchement stérique dû à la particularité de conformation moléculaire sur la surface des minéraux.

Ainsi, il a été proposé dans cette thèse de développer des études sur l'hypothèse scientifique que certains collecteurs, avec une structure moléculaire contenant une tête polaire volumineuse, peuvent améliorer la sélectivité de flottation de certains minerais de fer complexes. Compte tenu de la teneur en fer des boues de la région du Quadrilatère du Fer, de leur composition minérale (contenant d'autres minéraux en plus de l'hématite et du quartz, avec une présence importante de kaolinite) et la distribution granulométrique (générant une surface spécifique élevée, augmentant la consommation de réactifs et perte de fer dans les résidus par l'entraînement mécanique), on peut considérer ces boues comme un « minerai de fer complexe

». Afin de tester l'hypothèse scientifique, nous avons étudié l'amidoamine N-[3-(diméthylamino)propyl]dodécaneamide comme collecteur. Le développement d'un procédé de flottation des boues de minerai de fer réduira la quantité de résidus ultrafins, augmentera la récupération métallurgique de l'usine et contribuera au remplacement des digues à stériles par des piles, puisque certaines études ont montré qu'il existe un ratio maximal entre les résidus ultrafins et les résidus de flottation, rendant viable le filtrage et l'empilement des résidus totaux.

Le chapitre 2 a été consacré à la discussion des effets néfastes des boues de fer sur la flottation inversée du quartz (les principaux effets se réfèrent à une consommation accrue de réactifs, une diminution de la sélectivité et de la stabilité de la mousse). Il a également été discuté du comportement de flottation anormal de la kaolinite, qui peut être expliqué selon la structure cristalline.

Un échantillon de boue de minerai de fer du quadrilatère de fer a été analysé, dont près de 91 % de l'alumine (principalement de la kaolinite) était distribuée dans la fraction granulométrique inférieure à 20 μm . Des tests de flottation ont montré que l'ajout d'amidon de maïs lors des tests de sédimentation du minerai augmentait la dépression de la kaolinite. Étant donné que la kaolinite est le principal minéral d'alumine dans les boues de minerai de fer de la région du quadrilatère de fer, sa présence peut affecter la flottation du quartz en raison de la dépression de la kaolinite par l'amidon de maïs. L'adsorption d'amidon à la surface de la kaolinite peut réduire la quantité d'amidon à adsorber sur l'hématite, augmentant la teneur en fer dans le rejet de flottation. La dépression de la kaolinite due à l'adsorption de l'amidon altère également la qualité du produit en raison de l'augmentation de la teneur en silice et en alumine dans le concentré de flottation. Ainsi, compte tenu d'un minerai de fer à forte teneur en kaolinite, augmenter le dosage d'amidon pour augmenter la dépression de l'hématite peut entraîner, par conséquent, la diminution de la sélectivité du procédé de flottation.

Autre problème important présenté dans ce chapitre concerne la distribution granulométrique des minéraux présents dans les boues de minerai de fer. Il a été possible de vérifier que l'hématite présente dans l'échantillon de boue étudié se concentre dans les fractions plus fines que les silicates (d₅₀ de l'hématite était de 9 μm , tandis que le d₅₀ des silicates est de 20 μm). La surface spécifique élevée de l'hématite dans les boues peut nécessiter des dosages d'amidon plus élevés dans le processus de flottation. De fortes doses d'amidon peuvent générer une dépression de la kaolinite et également une dépression du quartz due à la co-adsorption de l'amidon avec l'amine à la surface du quartz (de fortes doses de ces réactifs peuvent altérer le processus de flottation en raison de la formation de clathrates).

Par conséquent, les études réalisées au chapitre 2 ont démontré que l'hypothèse scientifique présentée au chapitre 1 (*le développement d'un collecteur qui élimine la nécessité d'utiliser un réactif dépresseur dans la flottation cationique inverse du minerai de fer peut contribuer au développement d'un système de flottation des boues efficace*) est une hypothèse appropriée.

Il est important de noter, cependant, que les résultats de concentration magnétique présentés au chapitre 2 ont montré que, même après trois étapes de d'épuisage, les résidus contenaient 17,06 % de Fe, indiquant une certaine association entre les minéraux de gangue et les minéraux de Fe. Par conséquent, la distribution granulométrique des minéraux de fer dans les boues et leurs associations avec les minéraux de gangue indiquent des défis et des difficultés à concentrer les boues de minerai de fer, même avec un collecteur sélectif.

Du chapitre 3 au chapitre 6, les études ont été basées sur l'analyse de l'amidoamine N-[3-(diméthylamino)propyl]dodécaneamide comme réactif collecteur, sans dépresseur.

Le chapitre 3 s'est concentré sur les études fondamentales classiques liées à l'interaction entre les minéraux d'hématite, de quartz et de kaolinite avec l'amidoamine, l'amine et l'amidon. Il a été discuté des résultats du potentiel zêta, des mesures d'angle de contact, des tests de flottation des minéraux purs et mixtes et de l'analyse FTIR. Bien que plus petits que les angles de contact de l'étheramine, les angles obtenus avec l'amidoamine à pH 8 et 10 ont montré que ce collecteur pouvait rendre la surface du quartz hydrophobe. Le potentiel zêta a augmenté de manière significative à pH 8 pour l'amidoamine, tandis que la variation du potentiel zêta pour l'étheramine était légèrement prononcé à pH 10. Ainsi, la plus grande différence dans le comportement d'adsorption entre les deux collecteurs se produit à pH 8 et 10 (cette différence s'explique par le pKa de chaque réactif, alors que le pKa d'étheramine est proche de 10, le pKa d'amidoamine est proche de 8).

Des essais ont montré qu'il est possible d'obtenir une flottation sélective du quartz dans le minerai de fer, sans dépresseur. Cependant, pour atteindre le même niveau de récupération obtenu avec le collecteur d'amines, il est nécessaire d'adopter un dosage plus élevé d'amidoamine que d'étheramine.

Les résultats de la spectroscopie infrarouge ont montré qu'une augmentation de la concentration en amidoamine n'a pas entraîné de changement significatif de l'intensité du pic (extension des bandes CH₃ et CH₂) pour le spectre de l'hématite, tandis que l'intensité du pic dans le quartz et la kaolinite a été significativement augmentée, ce qui signifie qu'il y a un effet inhibiteur de l'adsorption du réactif à la surface de l'hématite. Ainsi, l'amidoamine N-[3-(diméthylamino)propyl]dodécaneamide est capable de favoriser la flottation sélective du quartz

sans agent dépressur, tel que l'amidon. Bien que le comportement de flottation de la kaolinite, adoptant l'amidoamine, soit similaire à celui de l'hématite, l'analyse du spectre FTIR était similaire à celle du quartz. La surface spécifique élevée couplée à la structure en double feuille peut être une explication de ce comportement. Par conséquent, ce réactif peut être une alternative avantageuse aux amines conventionnelles dans la flottation cationique inverse de boues de minerai de fer, en fonction de la quantité de kaolinite présente, car la teneur élevée en kaolinite peut également nuire à la sélectivité du minerai.

Une connaissance approfondie du mécanisme d'adsorption lié à cette amidoamine spécifique peut contribuer au développement d'une nouvelle classe de réactifs, plus efficace pour la flottation inverse du minerai de fer, réduisant ou éliminant le besoin d'un réactif dépressur, contribuant également à la réduction de la perte de fer dans les résidus. Par conséquent, dans le chapitre 4, des études sur la modélisation moléculaire, comparant l'adsorption d'étheramine et d'amidoamine à la surface de l'hématite et du quartz, ont été menées pour expliquer le mécanisme présenté par l'analyse FTIR (chapitre 3).

Des études de modélisation moléculaire ont montré que, par rapport à la surface D2 de l'hématite, le comportement de sélectivité pour la flottation du système quartz-hématite avec l'amidoamine peut s'expliquer par la combinaison du « bouclier » formé par la coordination des molécules d'eau sur cette surface avec le grand volume moléculaire de tête de cette amidoamine, dû au méthyle lié à l'azote dans l'amine tertiaire, générant un empêchement stérique et entravant l'adsorption du réactif à la surface de l'hématite, même en considérant l'amidoamine protonée (pH 8,5). En ce qui concerne l'étheramine, l'adsorption du collecteur neutre est réduite par la coordination de l'eau à la surface de l'hématite-(D2), mais la molécule protonée (Etherammonium) peut pénétrer et se lier sur cette surface en raison de la force motrice électrostatique. Ainsi, l'analyse présentée au chapitre 4 a permis d'expliquer l'apparition d'empêchement stérique à la surface de l'hématite et l'absence de ce comportement à la surface du quartz. D'autres surfaces d'hématite n'ont pas été étudiées, par conséquent, selon les caractéristiques du minerai de fer, le comportement de sélectivité de cette amidoamine peut être différent.

Afin d'évaluer l'application industrielle de l'amidoamine sur la flottation des boues de minerai de fer, le chapitre 5 est dédié à l'étude de deux échantillons de des schlammes différents dans une colonne pilote de flottation. L'échantillon de boue contenant une plus grande quantité de kaolinite présentait les performances de flottation médiocres. Ces résultats sont conformes à l'analyse liée aux études fondamentales menées dans cette thèse. L'amidoamine a montré le

potentiel d'un collecteur efficace, sans dépresseur, dans un procédé de flottation de boues pour l'échantillon avec le plus faible pourcentage de kaolinite.

Ces différents tests ont été effectués dans une installation pilote, ils n'ont donc pas pris en compte les variations dues au fonctionnement ou même la variabilité des caractéristiques des boues qui se produit dans une usine industrielle. Par conséquent, pour conclure sur l'application industrielle de l'amidoamine dans la flottation des boues de minerai de fer, sans dépresseur, il était nécessaire d'évaluer ses performances en fonctionnement en continu.

Ainsi, les études présentées dans le chapitre 6 ont démontré que, concernant une application industrielle de la flottation des boues de minerai de fer avec l'amidoamine N-[3-(diméthylamino)propyl]dodecanamide, sans dépresseur, la variabilité du processus altère significativement les résultats. L'influence des paramètres opérationnels ont été analysés et il a été possible de conclure que, à la différence des résultats obtenus dans un environnement contrôlé présentés dans le chapitre 5, il n'était pas possible de maintenir une efficacité de flottation acceptable pendant le fonctionnement en continu, en adoptant une seule étape de concentration. Ce travail permet déduire l'importance de la mise en œuvre d'un système de contrôle automatisé de silice et de fer, ainsi que des contrôles automatiques des paramètres, tels que le débit de l'eau de lavage et le dosage des réactifs dans une éventuelle application industrielle.

Le chapitre 7 suggère la séparation magnétique comme une étape de relavage du concentré de flottation avec l'amidoamine N-[3-(diméthylamino) propyl]dodecanamide en permettant de générer un concentré de fer avec une teneur > 67 % Fe à partir des schlammes de l'usine de Vargem Grande 2. Ce chapitre présente des études exploratoires, qui pourraient être considéré comme une perspective de cette thèse et devraient être approfondies.

Cette thèse s'est concentrée sur le comportement de sélectivité lié à l'amidoamine N-[3-(diméthylamino)propyl]dodecanamide dans la flottation de schlammes de minerai de fer composées essentiellement d'hématite et de quartz et représente une contribution modeste au développement de nouveaux collecteurs de flottation de minerai de fer .

Avec l'avancée de la technologie, l'utilisation d'outils informatiques prend une place de plus en plus importante dans les domaines de connaissances les plus variés, comme en témoigne l'utilisation de la modélisation moléculaire dans cette thèse, par exemple.

Le développement scientifique d'un sujet donné se fait par plusieurs mains. C'est une construction dans laquelle chaque chercheur place une brique pour construire des connaissances nouvelles et plus solides. Ainsi, il reste encore plusieurs questions liées aux recherches présentées dans cette thèse qui peuvent être approfondies, telles que : le comportement

d'adsorption par rapport aux différentes tailles de particules minérales, l'influence du pourcentage de solides et des caractéristiques de mousse sur l'hydrodynamique et efficacité du processus. De plus, l'étude de l'optimisation des réactifs par des changements dans sa structure ou son mélange avec d'autres réactifs est un axe de recherche important à évaluer.

Chapter 1 - Contextualization

1. Introduction

1.1. Decreased iron content in the Iron Quadrangle deposits - The “Third Wave” of iron ore processing plants in Brazil

In 2007, concerning the primary minerals products, iron represented about 87% of the Brazilian exportations (approximately US\$ 19 billions). Approximately 49% of these products were destined for China. Most of the Brazilian iron ore production in this period originated from the region known as Iron Quadrangle, in the state of Minas Gerais (ANM, 2020).

The Iron Quadrangle comprises an area of approximately 7,000 km², in the central portion of Minas Gerais. The abundant occurrences of Banded Iron Formations (BIF) have made this area the largest iron deposit in Brazil during the sixties and seventies (Mapa, 2006). The iron ore in this region is composed of hematite and itabirite. Itabirite is a laminated, metamorphosed iron formation of iron oxides (hematite, magnetite, martite), abundant in quartz, but very rarely containing mica and other accessory minerals (Dorr & Barbosa, 1963).

It can be said that the history of iron mining in Brazil began in the Iron Quadrangle region. At the end of the 19th century, Pico do Cauê, located in Itabira, was mapped as the largest iron ore deposit in the world. The first stone block was extracted directly from the 1370-meter peak by CVRD (in 2007, the company was renamed Vale) in October 1944. At the same time, the first mine equipment arrived in the city and, from that time to the present day, the extraction of iron ore in the Iron Quadrangle region can be divided into 3 waves (Alexandrino, et al., 2017):

- First wave (from 1942 to 1972): exploration of hematite, with iron content greater than 60%, which did not require complex industrial processes.
- Second wave (from 1972 to 2013): processing of friable itabirite (iron contents ranging from 50% to 60%) producing sinter feed and pellet feed. Concentration methods by magnetic separation, gravity concentration and flotation were introduced.
- Third wave (from 2013): processing of low-grade itabirite (iron content below about 42%). The main concentration process is flotation.

According Fiscor (2015), during the “third wave”, mining companies seek to concentrate the unexploited or discarded itabirites in previous operations (second wave)

through new iron ore beneficiation plants or modification on the existing plants through addition of grinding circuits.

The decline of the iron content in the world deposits is, mainly, due the substantial increase of the Chinese iron ore production, with iron content between 30% and 34% (Mudd, 2010). It is noteworthy, however, that, with regard to Brazilian iron ore mines, the decrease in the iron content occurs mainly in the Iron Quadrangle. In this region, due to factors such as the increase in world demand for iron ore, infrastructure and existing workforce, new projects for beneficiation plants have emerged, including, more recently, projects for compact itabirite concentration. This means that the third wave of iron ore processing in Brazil takes place in Minas Gerais, while the iron ore processing plants located in the northern region of the country (Carajás Mineral Province) are still in the first wave, with iron ore content in the run of mine above 60%.

The Itabiritos Project, implemented by VALE, is the main example that resulted from the reduction of Iron Quadrangle deposits iron content. This project aimed to process itabirite with about 40% iron, through the construction of new plants or modification of existing beneficiation plants, in order to concentrate the material that was previously considered waste (Alexandrino, et al., 2017), and had CAPEX estimated at US\$ 5.5 billion with 65Mty of nominal production, of which 26 million representing a real increase in capacity.

Recently, it can be said that the fourth wave is starting in the Iron Quadrangle due to the new projects of dry iron ore concentration plants. These new plants will include dryers to reach ROM moisture below 1% and the concentration process will be carried out by dry magnetic concentrators. In this case, the introduction of a fourth generation of iron ore treatment plants is not correlated with the decrease in the iron content in the ore, but with issues related to the need to eliminate the use of tailings dams. In this way, the production of dry tailings would make it possible to replace these dams with piles.

Torquato have demonstrated the technical feasibility of filtering and disposing of the tailings from the Iron Quadrangle iron ore beneficiation plants in piles, if the ratio between ultrafine tailings and flotation tailings is not greater than 20/80 (Torquato, et al., 2019). Then, in some plants, it is necessary reducing the amount of ultrafine tailings (slimes) to obtain this proportion.

1.2. Tailings Dam - One of the biggest problems related to the Third Wave.

A negative aspect, considering the impacts caused by the mineral activity, is the “NIMBY syndrome” (acronym for the expression Not In My Back Yard), which, in the case of

mining, means: “You can mine anywhere, but not in my yard” (Gomes, 2017). The presence of tailings dams is an important factor that can potentiate this “NIMBY syndrome”.

The low-grade iron ore concentration process increased the amount of material disposed in the Iron Quadrangle tailings dams, resulting in the need to build new structures. A survey prepared by Gomes (2017) showed that, in 2014, there were 15 mines in the Iron Quadrangle and about 111 million tons of tailings were produced during that year.

Tailings dams are structures for receiving tailings and discharges from the ore beneficiation process. Their construction (and factors ranging from the choice of location to the decommissioning process) is governed by specific environmental standards, in addition to economic, geotechnical, structural, social and safety criteria. The state of Minas Gerais has more than 200 tailings dams produced as a result of mining operations; almost 40% are related to the extraction of iron ore (Gomes, 2017).

In 2020, Vale Mining Company had 124 iron ore tailings dams, 82% of them located in the state of Minas Gerais (Vale, 2020). The material disposed in these dams are majorly constituted by slimes produced from the desliming process and by the tailings from some concentration process such as flotation or magnetic separation (Aguiar, 2013).

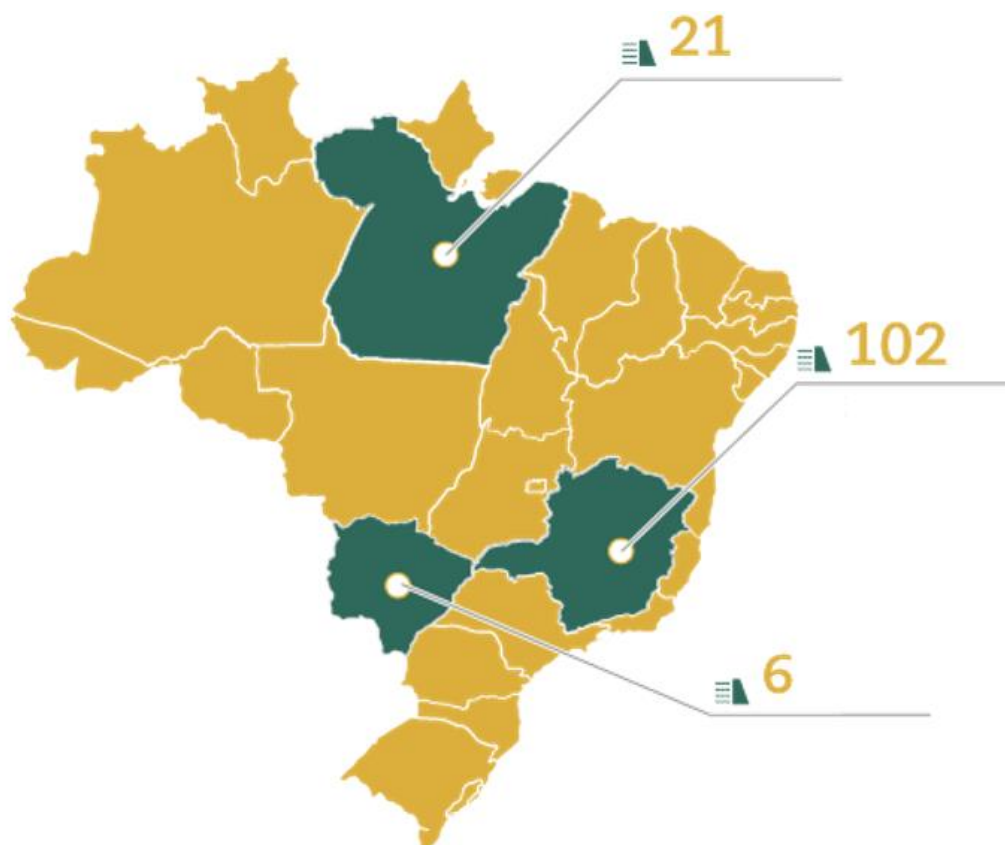


Figure 1 – Tailings dams owned by Vale in Brazil, by region. (Vale, 2020)

A survey carried out in the 20 largest iron ore mines from Minas Gerais showed that, in 2015, to obtain around 264 million tons of products (Granulado, Hematitinha, Sinter Feed and Pellet Feed), approximately 300 million tons of waste were generated, 183 Mt of materials such as topsoil overburden (which are removed to gain access to mineral resources), and waste rock and 112 Mt (70 Mm³) of tailings (considering an average density of 1.6 t/m³) (Heider, 2020). This high volume of tailings from iron mining has generated pressure on mining companies, in the sense of seeking solutions that minimize the resulting impacts reducing the risks of future accidents and disasters related with tailings dams (Heider, 2020).

In 2020, the National Mining Agency of Brazil (ANM) classified 22 ore tailings dams located in Minas Gerais as having a high risk of failure and high potential for damage in the event of failure (Table 1) and the total volume of material estimated in these dams was in around 650 million cubic meters (ANM, 2020).

Table 1 - Iron ore tailings dams with high potential for damage in the event of collapse (ANM, 2020)

Tailings Dam	City	Current Height (m)	Current Volume (m ³)
1 5 (MAC)	NOVA LIMA	78	15,553,688
2 Borrachudo II	ITABIRA	20	525,009
3 Campo Grande	MARIANA	99	22,978,889
4 Dicão Leste	MARIANA	23	150,000
5 Doutor	OURO PRETO	77	37,683,207
6 ED Xingu	MARIANA	70	6,117,000
7 Forquilha I	OURO PRETO	98	12,763,177
8 Forquilha II	OURO PRETO	96	22,778,398
9 Forquilha III	OURO PRETO	77	19,476,113
10 Forquilha IV	OURO PRETO	105	4,306,560
11 Grupo	OURO PRETO	43	1,249,249
12 Itabiruçu	ITABIRA	71	159,240,000
13 Maravilhas II	ITABIRITO	98	90,122,658
14 Marés I	BELO VALE	13	154,508
15 Marés II	BELO VALE	16	340,000
16 Menezes II	BRUMADINHO	21	325,556
17 Norte/Laranjeiras	BARÃO DE COCAIS	59	32,310,000
18 Pontal	ITABIRA	69	209,714,145
19 Santana	ITABIRA	52	11,456,940
20 Sul Inferior	BARÃO DE COCAIS	35	595,348
21 Sul Superior	BARÃO DE COCAIS	85	6,016,849
22 VI	BRUMADINHO	40	502,671
Total			654,359,965

Brazilian mining companies have not yet achieved a successful method of reducing the environmental damage caused by mining activities while the volume of waste in the country

grows exponentially as new ore treatment technologies are developed, also enabling the processing of ultrafine and low iron content ores (Sant'Ana Filho, 2013).

According to Aguiar (2013), maximizing the recovery of mineral resources is revealed as the greatest and most noble engineering challenge for the present and the future of iron ore treatment.

According to Carvalho (2012), iron ores have, historically, shown little evolution in relation to other commodities in their beneficiation process. The decrease in iron content related to the greater dissemination of itabirites has resulted in an increased demand for beneficiation processes adapted to ores with low iron content (Carvalho, 2012). Studies for the development of new low-grade iron ore processing routes should be concerned with environmental issues caused, for example, by the slimes generated by desliming stages before the flotation process.

Although the mining industry plays a very important role in generating wealth in Brazil, this activity can also represent a strong impact on the environment and these impacts have caused concern to the population and government agencies. Mining companies are looking for a way to increase the sustainability of their operations by improving mineral recovery by implementing new tailings concentration routes and replacing dams with tailings piles (adopting tailings filtration or, recently, developing the dry concentration process).

Among the tailings, the material that presents the greatest processing challenges is the ultrafine tailings (slimes). Therefore, the need for implementation of efficient recovery processes of the iron from ultrafine tailings goes beyond economic importance and covers, above all, issues related to sustainability (Nykänen, et al., 2018). According to Mudd (2009), the true sustainability of mineral resources is much more complex and involves exploration, technology, economics, social and environmental problems and the advancement of scientific knowledge.

1.3. Chemical and granulometric characteristics of Brazilian iron ore slimes

The deleterious effect of the slimes in the iron ore concentration process is quite widespread, but the understanding of the interaction mechanism of slime with ore is not unanimous in the literature and has been the subject of extensive debate (Marques, 2013).

According to Marques, as the iron content in the deposits is decreasing every day, grinding is increasingly necessary to obtain the liberation between gangue minerals and iron oxide minerals (Marques, 2013). Grinding increases the amount of ultrafine particles generated in the plants, which means that more slimes will be sent to the tailings dams, therefore, concomitantly with the increase in low-grade iron ore, slimes generation tends to increase. The

optimization of iron ore concentration processes, either through the implementation of new routes aimed at reducing iron in coarse tailings or through the development of new processes that allow the recovery of iron in the slimes, has become an increasingly important item for the feasibility of the mining industry in the Iron Quadrangle region.

The granulometric range of conventional iron ore flotation plants in the Iron Quadrangle is generally constituted of particles smaller than 150 micrometers (the range is around d85 to d95 depending on the plant), having previously been removed the particles smaller than 10 micrometers in the desliming process by hydrocyclones (to obtain the maximum around 5% of ultrafine particles in the flotation feed, there are about 30% to 60% of particles above 10 micrometers may be present in the slimes).

Due to the characteristics of the slimes and the use of hydrocyclones in the desliming process, there is a large amount of ultrafine iron particles in the slimes (Aguiar, 2013). According to Wolff et al. (2011), the amount of slimes varies from mine to mine and depends on the ore characteristics.

Marques (2013) analyzed 4 different iron ore slimes samples from Brazil during a study on the behavior of flotation of iron ore with slimes. The iron content in the slimes in these analyzes ranged from about 28% to approximately 53%.

Table 2 - Chemical analysis of slimes samples from Iron Quadrangle beneficiation plants. Copied from (Marques, 2013)

ID	Fe	SiO ₂	P (%)	Al ₂ O ₃	Mn (%)	TiO ₂ (%)	CaO (%)	MgO (%)	PPC
Sample 1	27.8	36.4	0.200	13.34	1.000	0.290	0.120	0.000	8.1
Sample 2	45.2	18.7	0.200	6.34	0.000	0.050	0.050	0.200	8.4
Sample 3	43.6	20.2	0.200	9.05	0.000	0.030	0.020	0.050	7.3
Sample 4	53.4	12.4	0.100	1.93	0.000	0.040	0.010	0.080	8.9

Wolff et al. (2011) collected 9 iron ore slimes samples from 7 mines located in the Quadrilátero Ferrífero and Carajás Mineral Province regions. The analyzes showed a variation in the iron content in the Iron Quadrangle slimes samples from 44.3% to 56.3% (the slimes from Carajás Mineral Province presented 64% iron).

Table 3 - Chemical analysis and D80 of some Slimes from Brazilian iron ore plants. Copied from (Wolff, et al., 2011)

Sample/Mine	Fe (%)	Al (%)	Mn (%)	P (%)	D80 (μm)
Brucutu	44.8	3.1	0.2	0.16	15
Córrego do Feijão I	56.3	1.3	4.6	0.27	10
Córrego do Feijão II	46.5	2.0	1.1	0.11	22
Conceição	44.3	1.0	1.9	0.11	27
Cauê	45.6	1.1	2.1	0.12	25
Fábrica Nova	53.4	1.1	0.3	0.17	14
Alegria I	51.8	2.4	0.2	0.21	13
Alegria II	48.6	1.2	0.4	0.17	16
Carajás	64.0	0.8	0.9	0.08	10

Queiroz (2003) analyzed, in the laboratory, the effect, in the reverse flotation, of the attrition and dispersion process in iron ore samples from the Alegria and Fábrica Nova mines (located in the Iron Quadrangle). He performed bench scale desliming tests adopting different pH and attrition time before desliming. Flotation tests were performed with underflow from these previously performed desliming tests. Depending on the conditions adopted in the attrition process, the iron content in the slimes varied from 28.71% to 50.85% and the percentage of mass in relation to the total mass varied from 3.85% to 14.46%.

Table 4 - Iron content in the slimes from the plants Fábrica Nova and Alegria, obtained on a laboratory scale, considering different conditions of attrition. Adapted from (Queiroz, 2003)

Samples	"Natural" pH			pH 9,80		
	0min	5min	20min	0min	5min	20min
Sample 1 - Fábrica Nova	48.36	47.63	47.08	44.66	44.76	44.48
Sample 2 - Fábrica Nova	50.85	47.72	46.24	43.78	43.40	43.40
Sample 3 - Fábrica Nova	46.64	45.68	46.61	42.91	42.09	41.89
Sample 1 - Alegria	--	--	--	30.42	28.71	28.78
Sample 2 - Alegria	--	--	--	50.52	51.49	52.23
Sample 3 - Alegria	--	--	--	48.63	48.85	49.38

Table 5 - Slimes amount (%) concerning Fábrica Nova and Alegria mines, obtained on a laboratory scale, considering different attrition conditions. Adapted from (Queiroz, 2003)

Samples	pH Natural			pH 9,80		
	0min	5min	20min	0min	5min	20min
Sample 1 - Fábrica Nova	3.85	4.26	5.43	6.03	6.39	6.60
Sample 2 - Fábrica Nova	3.92	5.56	5.80	11.21	11.74	11.93
Sample 3 - Fábrica Nova	8.23	0.84	0.55	8.26	8.61	8.97
Sample 1 - Alegria	0.00	0.00	0.00	6.01	6.15	6.30
Sample 2 - Alegria	--	--	--	9.19	11.51	12.20
Sample 3 - Alegria	0.00	0.00	0.00	11.84	13.43	14.46

Several other studies about the Iron Quadrangle iron ore slimes have been carried out in recent years. For example, Oliveira (2006) studied the development of process routes to recover

the iron contained in Conceição plant slimes (the average iron content in these slimes was about 41%).

As mentioned early, the slimes amount generated in the Iron Quadrangle region can vary considerably from one plant to another, depending on the mineralogical composition of the run of mine (ROM). According Guimarães (2011) the amount of slimes from the Vargem Grande 2 plant constituted about 19% of the ROM in 2011, representing a mass of 546 t/h of material containing about 42% Fe. The pilot tests results presented by Pinto (2016), referring to the compact itabirites of Jangada Mine plant, presented slimes mass partition values varying from 13.6% to 14.7%, depending on the comminution route adopted.

2. Literature Review

2.1. The Role of Starch in the Iron Ore Flotation Plants from the Iron Quadrangle Region

The iron ore beneficiation plants flotation feed from the Iron Ore Quadrangle region is basically constituted by particle size with d_{85} to d_{95} of around 0.15 mm. The main gangue mineral in Brazilian iron ores is quartz and the main concentration process adopted is reverse cationic flotation, requiring a previous desliming step to remove particles smaller than 10 microns (slimes), as the presence of these ultrafine particles impairs the flotation process (Filippov, et al., 2014).

The reverse cationic flotation is also adopted to reduce the silica content in the iron concentrate obtained through magnetic separation in other countries and, according Filippov et al., (2014), this is the most efficient upgrading process for simple systems composed of hematite/magnetite and quartz.

The amine adsorption mechanism on mineral surfaces is basically electrostatic and both, hematite and quartz, can be floated by this type of reagent, therefore, it is necessary to adopt iron oxide depressant reagents to obtain the necessary selectivity in the flotation process. These depressant reagents play a crucial role in selectively making the iron oxides hydrophilic and prohibiting them from reporting to the gangue-rich froth phase (Swagat & Hrushikesh, 2020).

In fact, it can be stated that, in the Iron Quadrangle mines, the reverse cationic flotation of iron ore is possible due to the action of the collector/depressant system. This means that it is not possible to obtain high quality concentrates with high metallurgical recovery without the use of a depressant. Therefore, currently, starch is as essential as the amine in this type of process.

Starches are the universal iron oxides depressants (Araujo, et al., 2005). Corn starch is the most used depressant in the reverse flotation of iron ore due to its availability, cost and low environmental impact (Shrimali & Miller, 2016). Thus, in Brazil, this type of starch plays an important role in the iron ore beneficiation plants (Kar, et al., 2013).

2.2. Starch Adsorption Mechanism

A depressant is considered effective if it can, selectively, inhibit collector adsorption onto undesired minerals without disturbing the floatability of the target minerals (Urbina, 2003). However, depression is a complex phenomenon, in which adsorption is only one step, although being the most important one (Pavlovic & Brandão, 2003).

According to Peres et al. (1992) and Xia et al. (2009), the adsorption of starch on the hematite surface is due to hydrogen bonds, salt formation and electrostatic interactions. Liu-yin et al. (2009) have suggested that hydrogen bonding is the underlying adsorption mechanism for starches with the oxide minerals due to the presence of the hydroxyl group both in starch and mineral oxides. According to Balajee and Iwasaki (1969), the adsorption of starch in hematite is mainly due to the presence of a large number of hydroxyl groups on starch and hematite molecules surface, which facilitates non-selective hydrogen bonding and electrostatic attraction force. Based on Fourier transform infrared (FTIR) spectroscopy data, Severov et al. (2013) showed that starch can also adsorb on the quartz surface owing to the formation of hydrogen bonds between the hydroxyl groups of the polysaccharides and silanol groups presents on the quartz surface at pH 10.

Subramanian and Natarajan (1988) confirmed the partially irreversible adsorption of starch on hematite by application hot water in an autoclave for several minutes. The partial irreversibility suggested the involvement of non-electrostatic forces in the adsorption process. These authors studied the effect of the temperature in the adsorption of the starch on the hematite surface. At a constant pH, the starch adsorption increased with an increase in the temperature. In general, the physisorption process is characterized by an exothermic heat of adsorption, and as a result, adsorption is expected to decrease with increasing temperature. In contrast, higher temperature favors the chemisorption due to faster reaction kinetics. Therefore, the temperature effect in the studies of Subramanian and Natarajan confirmed the chemical adsorption of starch on hematite (Rath & Sahoo, 2020).

Weissenborn, et al (1995) investigated the adsorption mechanisms of wheat starch on hematite. Spectroscopy results indicated that a complex was formed on the mineral's surface,

but the existence of hydrogen bonds between the starch and the mineral surface has not been ruled out. Thus, the authors suggested the adsorption scheme illustrated in Figure 2.

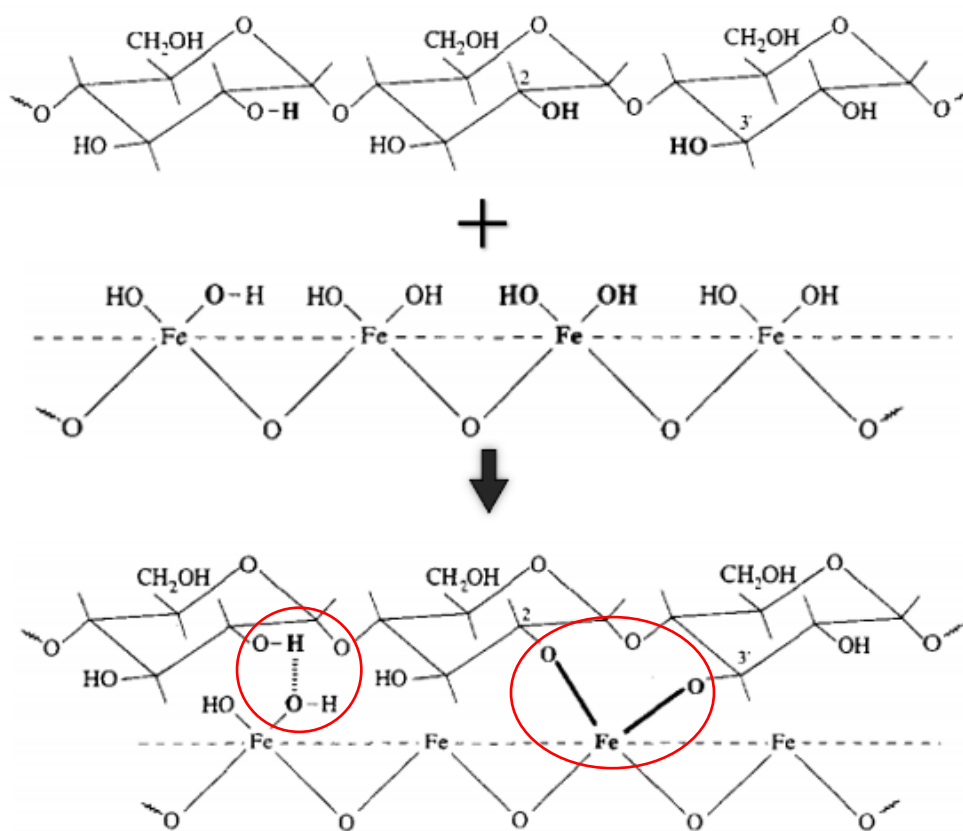


Figure 2 – Reaction scheme for surface complex formation and hydrogen-bonding mechanisms. Copied from Weissenborn, et al (1995).

2.3. Issues that hinder the selective action of starches in the iron ore cationic reverse flotation process.

The starch adsorption on quartz and hematite surfaces are different not merely in terms of the magnitude, but also in terms of the bonding strength. This is because the polysaccharides adsorption on the iron oxides and Fe-bearing silicates is mainly controlled by their chemical bonding with the iron in the mineral structure (Weissenborn, et al., 1995) (Filippov, et al., 2013); however, hydrogen bond is the main adsorption mechanism on the quartz surface. Thus, amine collectors can replace the starch molecules on the quartz surface because of their stronger electrostatic interactions with the negatively charged quartz surface.

Starch adsorbs extensively on hematite and to a lesser extent on quartz, but in some cases, the adoption of starch is not sufficient to obtain satisfactory selectivity in the flotation process. For example, the influence of clay minerals on the starch-hematite interaction cannot be ruled out and, similarly, the effect of starch on the collector action is also worth exploring

(Rath & Sahoo, 2020). Another important issue that influences the effectiveness of starch as a selective depressant is the presence of Fe-Mg-Al bearing silicates in the ore. According Veloso et al., (2018), the concentration of iron ore by flotation, when gangue minerals are composed of Fe-Mg-Al, is a challenge due to the depression of these minerals due to the presence of metal ions on the mineral surface, which can form a strong chemical complex with starch molecules used as iron oxide depressants.

According to Turrer (2007) it is expected that an excessive increase in starch dosage during the cationic reverse flotation of iron ore will increase the silica content in the concentrate due to the excess of this reagent, which would also act in the quartz depression.

The starch/amine ratio is also an important parameter that influences the flotation efficiency. Amine consumption tends to increase if the particle size of the flotation feed is reduced (more specifically, for the same ore, increasing specific surface results in increasing collector dosage) and, under some conditions, (starch composition, pH and reagent dosages) starch and the collector interact with each other, forming clathrates, increasing, as consequence, the SiO₂ content in the flotation concentrate (Aguiar, et al., 2017).

Partridge & Smith (1972) e Hendrix & Smith (1972) attributed the clathrates formation to the follow mechanisms: electrostatic attraction between RNH₃⁺ and the starch molecule with negative charge, Van der Waals forces and hydrogen bonds.

Aguiar (2014) studied clathrate formations in the reverse cationic iron ore flotation and concluded that:

- The co-adsorption of starch and amine at the quartz-solution interface can be explained in terms of the clathrate formed between the starch in its helical form and the amine adsorbed inside the helices.
- The increase of amine and starch dosages favors the clathrate formation. The quartz floatability decreased from 95% to 35% due the increase of the amine dosage.
- At high pH levels, a progressive decrease in quartz floatability is observed.
- There was an increase in the quartz zeta potential with starch and amine adsorption under conditions that favored clathrate formation, when compared to the same conditions, without starch adsorption. Thus, it is believed that the drop in quartz floatability occurs due to the co-adsorption of starch and amine at the quartz-solution interface.

Figure 3 shows the variation in the floatability of quartz, at pH 10.0, with different concentrations of amine and corn starch according to the author.

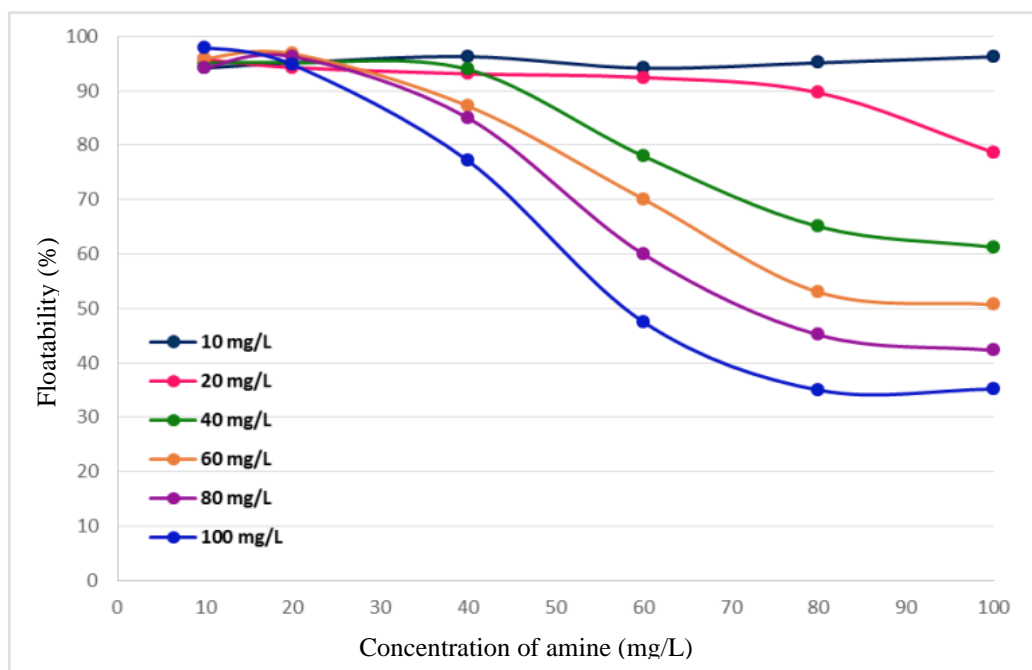


Figure 3 – Quartz floatability due to different dosages of amine and corn starch at pH 10. Copied from AGUIAR, et al., (2017)

According to Filippov, et al. (2010), Fe–Mg–Al-bearing silicates are widely present in magnetite ores and account for the difficulties of their separation by flotation when amine collectors and starch are used. The authors demonstrated that the starch cannot be considered as a selective depressant for magnetite at pH of approximately 10 in the process of the reverse cationic flotation of iron ores when the Fe–Mg–Al-bearing silicates as amphiboles are present in the flotation system (Filippov et al., 2013). The flotation process separation efficiency decreases when, as a part of the gangue minerals, there are Fe/Mg silicates because the surface properties of these silicates are similar to those of iron oxides, resulting in the non-selective action of depressants such as starch (Turrer & Peres, 2010) (Filippov, et al., 2010; Filippov, et al., 2013).

Detailed studies on reverse cationic flotation with iron ore samples from different deposits over the world (Brazil, Russia, Mexico) performed by Filippov and co-workers confirmed the inefficiency of starch when the silica content in the concentrate is controlled by Fe-Mg-bearing minerals such as amphiboles, epidote, chamosite, and diopside (Filippov, et al., 2010; Severov, et al., 2013; Veloso et al., 2018). The studies suggest that starch attaches to the amphibole surface not only by hydrogen bonding with the surface hydroxyls, but also through

the formation of a surface chemical complex with metal atoms. Thus, the chemical complexation adsorption mechanism can explain the strong depression effect of the starch during the magnetite and Fe–Mg–Al-bearing amphibole flotation.

Nykänen et al (2018) demonstrated that, in industrial circuits, starch may not be effective in preventing iron loss in flotation tailings. The authors performed two-liquid flotation (water and isooctane) experiments with the flotation tailings from the Conceição Mine and Pico Mine, localized in the Iron Quadrangle, to quantify the amount of iron loss in the -44 μ m fraction of these plants due the drag flotation (entrainment and entrapment) and real flotation (iron oxides hydrophobization by the collector).

Table 6 shows that, while in Conceição Mine most of the iron (97.7%) was lost due to dragging flotation, in Pico Mine the main problem concerning the loss of iron in the tailings was the hydrophobization of iron oxides, being 65.4% of the iron in the flotation tailings reported for the hydrophobic phase (isooctane).

Table 6 - Two liquid flotation tests results. A – <44 μ m Pico mine tailings flotation sample, B – <44 μ m Conceição mine tailings flotation sample. Copied from (Nykänen, et al., 2018)

Analyte Sample A	Final tail (-44 μ m)		Hydrophilic phase		Hydrophobic phase	
	Contents (wt%)	Dist (%)	Contents (wt%)	Dist (%)	Contents (wt%)	Dist (%)
Fe	47.9 \pm 0.9	100.0	43.0 \pm 1.4	34.6 \pm 2.4	51.0 \pm 0.8	65.4 \pm 2.4
SiO ₂	28.2 \pm 1.0	100.0	34.9 \pm 1.6	47.6 \pm 2.2	24.1 \pm 0.8	52.1 \pm 2.2

Analyte Sample B	Final tail (-44 μ m)		Hydrophilic phase		Hydrophobic phase	
	Contents (wt%)	Dist (%)	Contents (wt%)	Dist (%)	Contents (wt%)	Dist (%)
Fe	57.6 \pm 0.3	100.0	57.6 \pm 0.3	97.7 \pm 1.2	56.3 \pm 1.0	2.3 \pm 1.5
SiO ₂	12.6 \pm 0.2	100.0	12.7 \pm 1.2	98.7 \pm 1.0	6.5 \pm 2.1	1.3 \pm 1.0

Thus, even using starch as depressant, significantly loss of iron in the tailings can be occur in some industrial flotation plants. According to the author, the cause of the loss of iron in flotation tailings by true flotation could be an insufficient addition or inefficiency of the depression agent.

2.4. Amidoamines

Amidoamines were suggested and tested as effective agents for the flotation process, with diethylenetriamine monoamide being the most used compound (Friedli, 1990). These reagents are obtained by the reaction between polyamines and organic acids (Balduino, 2017) and may provide several advantages for the flotation process, i.e., selectivity and cost reduction (Friedli, 1990).

In phosphate ore concentration processes, amidoamines are more tolerant toward sulphate ions. They are also inexpensive and have fewer complications due to possible overdosage (Friedli, 1990). The reverse cationic flotation of phosphate ores from Bayovar deposits with amidoamines showed better results when compared to those obtained using amines (Baldoino, 2017). Amidoamines are the most suitable compounds in unfavorable conditions, such as temperature fluctuations (25-40 °C), high concentration of electrolytes in the process water (ionic strength 0.71 mol/L), and variation in electrolyte concentration in the pulp caused by evaporation (2237 g/L of chloride) when sea water is used during the beneficiation process.

As reported in some studies, iron ore slimes are generally composed by other minerals in addition to iron oxides and quartz. Some slimes from the Iron Quadrangle in Brazil, for example, have considerable amounts of kaolinite in their composition. Kaolinite flotation is difficult to perform (i.e., with amines) owing to the structural properties of this mineral (Xu, et al., 2015). Kaolinite flotation studies carried out by Souza (2014) using manganese ore from the Azul mine, in Brazil, showed that amidoamine collector was more effective compared to etheramine collector. The best flotation result was obtained at 20% solids, pH>10, using a depressant dosage of 900 g/t (cornmeal or Fox Head G2241), and amidoamine dosage of 1360 mg/L (5333 g/t).

There are very few studies reporting the use of amidoamine molecules in iron ore flotation. However, they can be efficient quartz collectors in conventional iron ore reverse flotation, using starch as the depressant of iron oxides (Budenberg, 2016).

Amidoamine (N-[3(dimethylamino)propyl]dodecanamide)

The structure of the N-[3(dimethylamino)propyl]dodecanamide molecule (molecular formula: $C_{17}H_{36}N_2O$) is presented in the Figure 4:

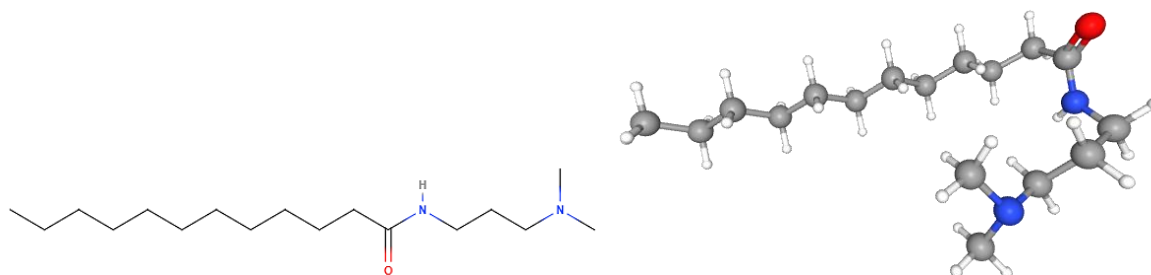


Figure 4 – N-[3(dimethylamino)propyl]dodecanamide molecule. Copied from (s.d., p. <https://pubchem.ncbi.nlm.nih.gov/compound/lauramidopropyldimethylamine>)

The chemical reaction, described by Budenberg (2016), for the synthesis of this amidoamine is shown in the Figure 5.

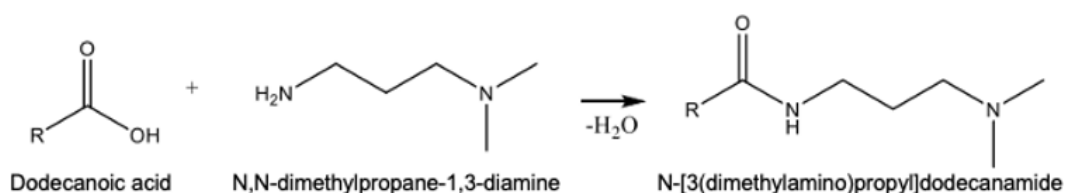


Figure 5 – Synthesis of the N-[3(dimethylamino)propyl]dodecanamide molecule. Copied from (Budenberg, 2016)

The N-[3(dimethylamino)propyl]dodecanamide pKa value obtained according to the methodology described by Mhonde (2016) is about 8.2 (Figure 6).

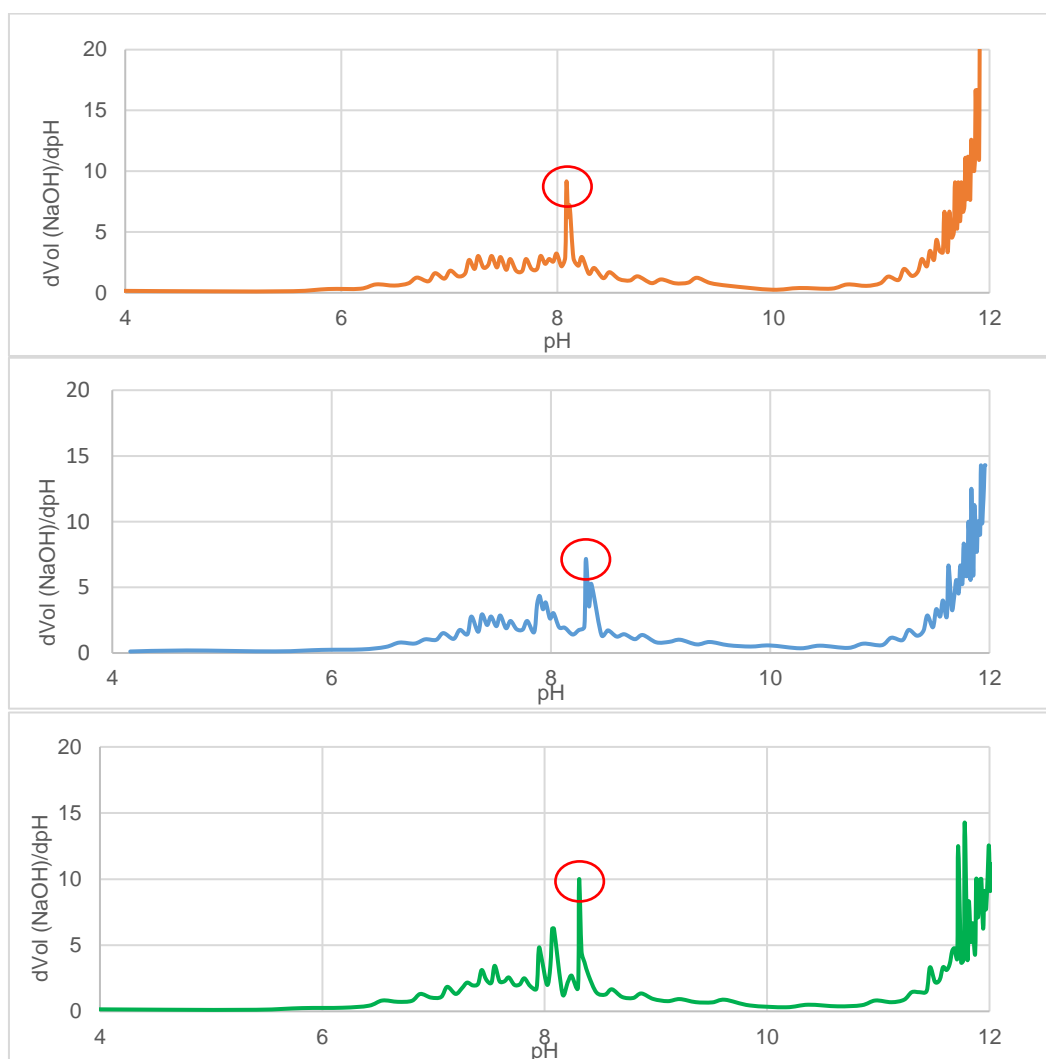


Figure 6 – Establishing the pKa value of N-[3(dimethylamino)propyl]dodecanamide using the first derivative method. From the data obtained in acid-base potentiometric titrations of a collector solution with a NaOH titrant solution, the curve of the first derivative (Δ Volume of NaOH/ Δ pH) was plotted by pH. The point on the pH axis with the highest peak on this curve represents the approximate pKa value of each collector. (These data refer to studies carried out by the author)

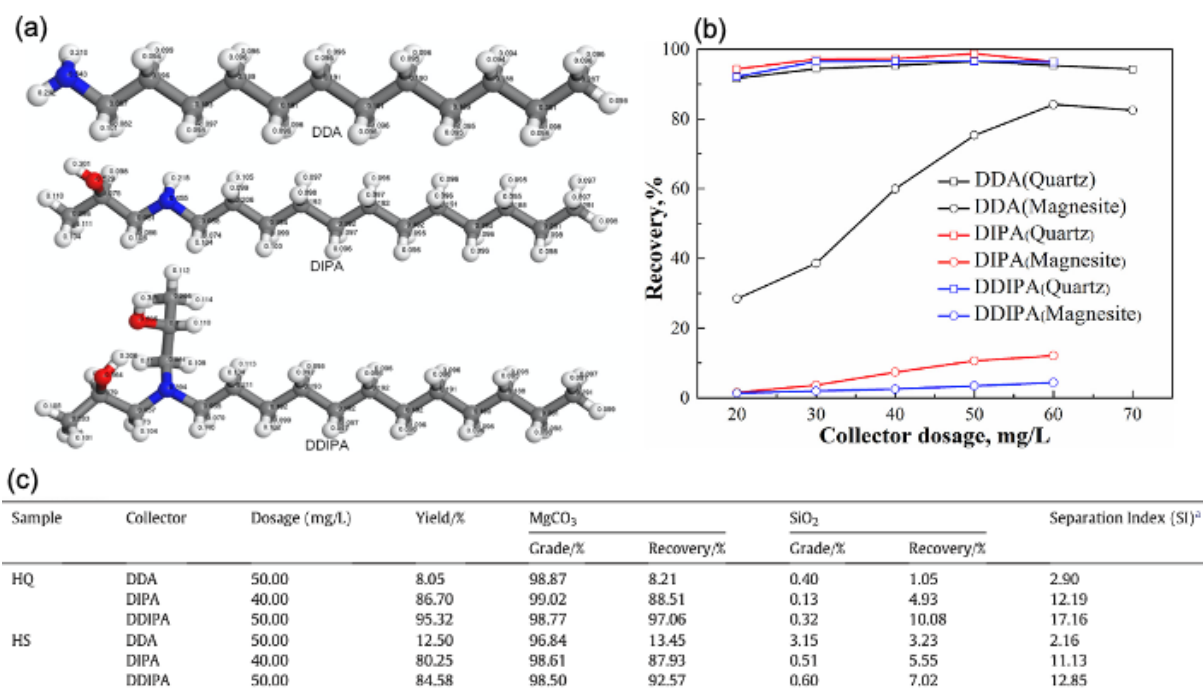
2.5. Development of Selective Collectors

As mentioned by Chen et al (2017), surfactants initially adsorb on mineral surfaces through electrostatic forces as individual ions; further, with the increase in the coverage of the surfactant on the mineral surface, steric hindrance gradually occurs.

Budenberg (2016) analyzed and compared some different structures of amidoamines with commercial amines used in the iron ore flotation. The studies were carried out using the iron ore from the Alegria mine in the Iron Quadrangle region. One of the amidoamines tested was the N-[3(dimethylamino)propyl]dodecanamide and, according to the author, this amidoamine presents steric hindrance, resulting from the bonding between the methyl and amine groups (Figure 4).

The bench scale flotation tests results, when using the amidoamine N-[3(dimethylamino)propyl]dodecanamide, were very similar to those obtained using a commercial amine, however, the amidoamine dosage was higher than that of the conventional amine to obtain these similar results. The SiO₂ content in the concentrate, obtained using the commercial amine, was 1.8%, with a loss of 11.03% Fe in the tailings at pH 9.5 and a collector dosage of 180g/t, compared to 1.85% of SiO₂ in the concentrate, with a loss of 11.05% Fe in the tailings at pH 9.5 and an amidoamine dosage of 400g/t. For both tests carried by Budenberg, starch was used as depressant (600g/t) therefore, it was not possible to verify whether, by adopting this amidoamine in the absence of starch, it would be possible to obtain good results, with low iron content in the tailings, without significantly reducing the quartz floatability.

The high selectivity to float quartz in a mixture with magnesite, without depressant, due the steric hindrance was demonstrated by Liu et al. (2019). The authors used surface tension measurements, molecular dynamics simulations and density functional theory to investigate the effects of introducing an isopropanol substituent in amine collectors in the flotation process for a mineral system composed by quartz and magnesite. The results showed that introducing this isopropanol substituent in dodecyl amine (Figure 7) weakened the electrical properties of the polar groups and increased the cross-sectional size of these groups; this can decrease the electrostatic effect and increase steric hindrance, thereby improving the selectivity of the reagent, providing a high floatability of the quartz and low floatability of the magnesite.



^a Separation index (SI), $SI = (\epsilon_1 \times (100 - \epsilon_2)) / (\epsilon_2 \times (100 - \epsilon_1))^{0.5}$, ϵ_1 - MgCO₃ recovery in concentrate, ϵ_2 - SiO₂ recovery in concentrate.

Figure 7 – (a) Collector structures, (b) the flotation behavior of pure minerals (quartz and magnesite) as a function of collector concentration, (c) results of the flotation tests. Copied from Liu et al. (2019).

Analysis of the BHDA and DDA reagents on quartz, magnesite and dolomite flotation (Figure 8) showed that BHDA is more selective than DDA and these results were attributed to BHDA's relatively weaker electronegativity and stronger steric hindrance (Liu, et al., 2019).

Regarding the adsorption mechanism, the authors demonstrated that the density of oxygen atoms on the quartz surface ($26.79 \mu\text{mol}/\text{m}^2$) was twice that was presented on the dolomite surface ($12.43 \mu\text{mol}/\text{m}^2$) and four times that of the magnesite surface ($6.74 \mu\text{mol}/\text{m}^2$). Thus, the oxygen atoms exposed on the surface not only affected the electronegativity of the mineral's surface, but also provided adsorption sites for hydrogen bonds.

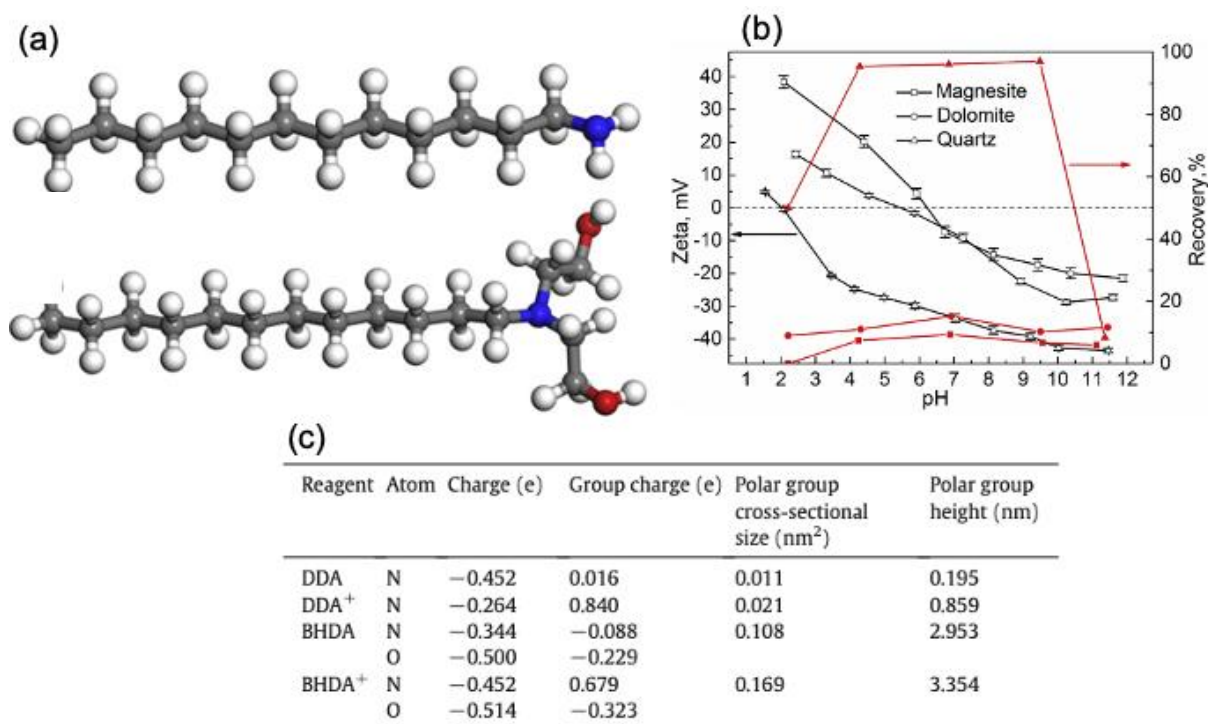


Figure 8 – (a) Collectors structures (DDA and BHDA), (b) zeta potentials and flotation recoveries (magnesite, dolomite and quartz), (c) collectors properties analysis. Copied from Liu, et al. (2019).

Liu, et al. (2019) analyzed the collectors: DPDA, NDEA and DDA for the separation of quartz and hematite by flotation. According to the authors, the DPDA²⁺ adsorbed on the negative surfaces of hematite and quartz and formed the hydrogen bonds with the exposed oxygen atoms on quartz and hematite surfaces. Thus, the adsorption behaviors could be attributed to electrostatic attraction and hydrogen bond. The properties analysis using DFT calculation and MS simulation indicate that DPDA had the great collecting ability, which was similar to NDEA, but it had better selectivity than NDEA and DDA (Figures 9 and 10).

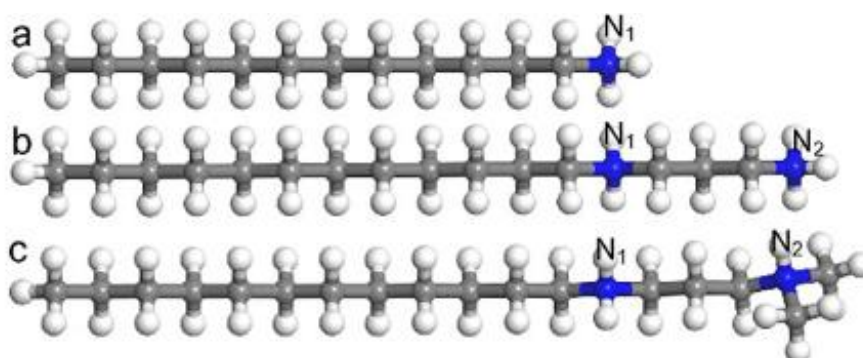


Figure 9 – Optimized geometry of DDA⁺ (a), NDEA²⁺(b) and DPDA²⁺(c). Copied from Liu, et al. (2019).

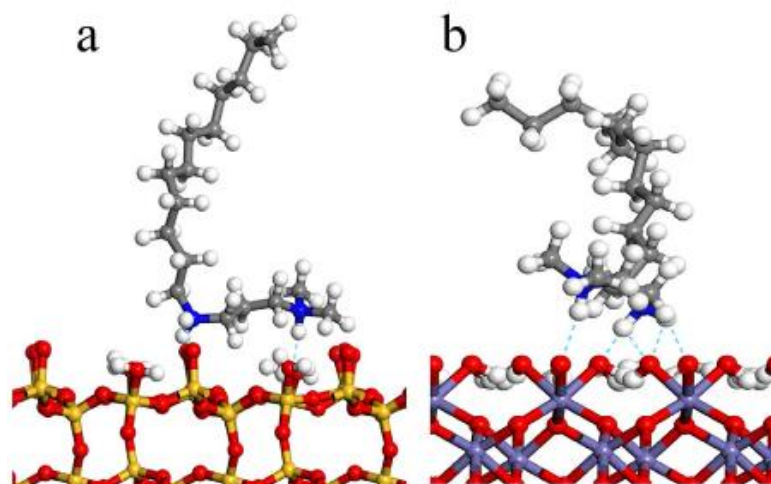


Figure 10 – Snapshots of adsorption configuration after equilibrium state of quartz (a) and hematite (b) with DPDA^{2+} . The hydrogen bond is by the sky-blue dotted line. Copied from Liu, et al. (2019).

3. Scientific Hypothesis

Some authors have shown that the use of depressant can be harmful to the flotation process when gangue minerals have more complex mineralogy. The loss of iron in tailings by real flotation with conventional collectors (amines) was also demonstrated.

The main approaches for solving these issues focus on using new collector formulations or new alternative depressants such as guar gum (Turrer & Peres, 2010) humic acid (Dos Santos & Oliveira, 2007; Veloso, et al., 2018), lignosulfonate, and carboxymethyl cellulose (Turrer & Peres, 2010; Veloso, et al., 2020), leading to better flotation selectivity between hematite and silicates. However, the alternative depressants tested inhibited flotation of quartz owing to physical adsorption on their surfaces (Turrer & Peres, 2010).

The investigations on new flotation collectors, more selective, may contribute toward unlocking new iron ore resources related to primary deposits with complex gangue mineralogy (i.e., Fe-bearing silicates, kaolinite) or processing of old tailings with high degrees of alterations.

Regarding some iron ore slimes, it is possible to infer that:

- Due to the high specific surface of slimes, high dosages of reagents may be necessary for satisfactory adsorption on mineral surfaces. However, high dosages of starch and amine may also result in reduced efficiency in the flotation process.
- Some iron ore slimes have more complex mineralogy than conventional flotation feed, mainly due to clay minerals in their composition, such as kaolinite.

Considering that high dosages of starch or high starch/amine ratio may result in a reduction in the efficiency of the flotation process, the search for more selective collectors, which do not require the adoption of a depressant, can also contribute to the development of a viable flotation process for iron ore slimes.

Some authors have shown that the N-[3(dimethylamino)propyl]dodecanamide has potential to be a quartz collector (Budenberg, 2016) and kaolinite collector (Souza, 2014), using depressant in the flotation process. However, considering that this reagent also has a molecular structure with a bulky polar head that can generate steric hindrance, the scientific hypothesis to be presented in this doctoral thesis is that the amidoamine N-[3(dimethylamino)propyl]dodecanamide can be adopted in some flotation process (mainly, iron ore slime flotation) without the need for a depressant.

4. Purpose of this PhD Thesis

Considering what has been exposed so far, this thesis aims to contribute to increasing the environmental sustainability of iron ore processing plants, generating knowledge that can assist in the development of more selective collector reagents for iron ore flotation, with the possibility to eliminate the need for depressants.

The development of a collector for cationic reverse flotation of iron ore that does not require the use of depressants can contribute to obtaining concentrates, via flotation, from ores with complex gangue or even from slimes that are currently disposed in tailings dams. The loss of iron by hydrophobization in the existing Iron Quadrangle flotation plants may also be reduced.

As mentioned earlier, amidoamine N-[3(dimethylamino)propyl]dodecanamide was chosen to be studied as a flotation collector, without depressant due to the voluminous polar head group in its molecular structure.

Regarding the type of sample to be studied together with this collector, it was to evaluate the use of this reagent in iron some ore slimes samples from the Iron Quadrangle. As presented

throughout this chapter, the main justifications for studying the slime concentration with this amidoamine are:

- Issues related to tailings dams in the Iron Quadrangle due to the increase in the volume of tailings generated in the “third wave” of iron ore processing plants.
- The high iron content in these slimes.
- The need to reduce, for some plants, the ratio between sludge and flotation tailings to less than 20/80 in order to allow the replacement of dams by piles, filtering the total tailings.

It is important to highlight that the choice of a suitable reagent is not the only factor that needs to be considered for developing a flotation process. Mainly considering the particle size distribution of the mineral samples to be studied in this thesis, studies on hydrodynamic issues also need to be carried out (Fornasiero & Filippov, 2017). However, to determine the ideal hydrodynamic conditions, it is first necessary to develop reagents that make the process viable.

References

Aguiar, M. A. M., 2014. Dissertação de mestrado: CLATRATOS NA FLOTAÇÃO CATIONICA REVERSA DE MINÉRIOS DE FERRO, Belo Horizonte: Escola de Engenharia da UFMG.

Aguiar, F. L. d., 2013. Monografia. Belo Horizonte(Minas Gerais): Universidade Federal de Minas Gerais.

Aguiar, M., Furtado, R. & Peres, A., 2017. Seletividade na flotação catiônica reversa de minério de ferro. *Holos*, 24 11, pp. 126-135.

Alexandrino, J. S., Barros, A. J. d., Silva, C. C. M. & Dornelas, C. A. d. S., 2017. Estudo de caso: tecnologias e processos utilizados no tratamento de minérios de ferro de baixo teor. *Contribuciones a las Ciencias Sociales*, pp. <http://www.eumed.net/rev/cccss/2017/04/tratamiento-minerios-ferro.html>.

Amorim, L. Q. & Alkimim, F. F., 2011. New ore types from the cauê banded iron formation, Quadrilátero Ferrífero, Minas Gerais, Brazil - responses to the growing demand.. Perth, s.n., pp. p. 59-71.

ANM, 2020. Agência Nacional de Mineração. [Online] Available at: <https://app.anm.gov.br/SIGBM/Publico/ClassificacaoNacionalDaBarragem>

Araujo, A. C., Amarante, S. C., Souza, C. C. & Silva, R. R. R., 2003. Ore mineralogy and its relevance for iron ores methods in processing of Brazilian iron ores. s.l.:s.n.

Araujo, A., Viana, P. & Peres, A., 2005. Reagents in iron ores flotation. *Miner. Eng.* 18(2), pp. 219-224, DOI: 10.1016/j.mineng.2004.08.023.

Baldoino, R. d. O., 2017. Tese de Doutorado. São Paulo(São Paulo): Universidade de São Paulo. Escola Politécnica. Departamento de Engenharia de Minas e Petroleo.

Barcelos, H. O., 2010. Dissertação de Mestrado. Ouro Preto(Minas Gerais): Universidade Federal de Ouro Preto.

Brandão, P., 2005. A SELETIVIDADE NA FLOTAÇÃO REVERSA DE MINÉRIO DE FERRO: ADSORÇÃO DOS REAGENTES. Natal - RN, s.n., p. 23.

Brasil. Agência Nacional de Mineração, 2019. ANUÁRIO MINERAL BRASILEIRO. Brasília: ANM - Equipe Técnica por Marina Dalla Costa.

Brown, E. H. & Tartaron, F. X., 1943. United States, Patente N° US496582A - Concentration of oxidized iron ores.

Bruckard, L. W., Smith, K. & Heyes, G., 2015. Developments in the physiochemical separation of iron ore. s.l.:s.n.

Budemberg, G., 2016. Dissertação de Mestrado. Lorena(São Paulo): Universidade de São Paulo. Escola de Engenharia de Lorena.

Carvalho, B. C. L. d., 2012. Dissertação de Mestrado. Ouro Preto(Minas Gerais): Universidade Federal de Ouro Preto.

Carvalho, P. S. L. d., Silva, M. M. d., Rocio, M. A. R. & Moszkowicz, J., 2014. Insumos Básicos - BNDES Setorial 39, p. 197-234. s.l.:<http://www.bndes.gov.br/bibliotecadigital>.

Chen, P. et al., 2017. Discovery of a Novel Cationic Surfactant: Tributyltetradecyl-Phosphonium Chloride for Iron Ore Flotation: From Prediction to Experimental Verification. *Minerals*, 2 December.

Cloud, J. & Manuel, J., 2015. Iron Ore-Mineralogy, Processing and Environmental Sustainability, 1. s.l.:s.n.

Dorr J. V. N. & Barbosa A. L. M. Geology and ore deposits of the Itabira District, Minas Gerais, Brazil. .U. S. Geological Survey Prof. Paper 341-C. Washington, DC, 1963. 110p.

Dos Santos, I. & Oliveira, J., 2007. Utilization of humic acid as a depressant for hematite in the reverse flotation of iron ore. *Miner. Eng.* 20, p. 1003–1007.

Farrokhpay, S., 2012. The importance of rheology in mineral flotation: A review. *Minerals Engineering*, 14 June.

Figueirôa, S. F., 2006. "Metais aos pés do Trono": exploração mineral e o início da investigação da terra no Brasil. *Revista USP*, São Paulo n. 71, pp. 10 - 19.

Filippov, L., Filippova, I. V. & Severov, V. V., 2010. The use of collectors mixture in the reverse cationic flotation of magnetic ore: The role of Fe-bearing silicates. s.l.:s.n.

Filippov, L., Severova, V. & Filippova, I., 2014. An overview of the beneficiation of iron ores via reverse cationic flotation. *International Journal of Mineral Processing*, pp. 127, 62-69.

Filippov, L., Severov, V. & Filippova, I., 2013. Mechanism of starch adsorption on Fe-Mg-Al-bearing amphiboles. s.l.:s.n.

Fiscor, S., 2015. Vale Launches Third Wave. *Engineering and Mining Journal*; Jacksonville Vol. 216, Ed. 11, Nov., pp. 28 - 32.

Fornasiero, D. & Filippov, L., 2017. Innovations in the flotation of fine and coarse particles. *J. Phys. Conf. Ser.*, pp. 879, 012002, doi:10.1088/1742-6596/879/1/012002.

Friedli, F. E., 1990. Amidoamine Surfactants. Em: *Cationic Surfactants - Organic Chemistry (Surfactant science series; v34)*. New York: Marcel Dekker, Inc., pp. 52-83.

Frommer, D. W. & Colombo, A. F., 1964. United States, Patente N° US3292780A.

Fuerstenau, M. C., Jameson, G. & Yoon, R.-H., 2007. *Froth Flotation - A Century of Innovation*. Littleton, Colorado: Society for Mining, Metallurgy, and Exploration, Inc. (SME).

Gomes, A. C. F., 2017. *Dissertação de Mestrado*. Belo Horizonte(Minas Gerais): Universidade Federal de Minas Gerais.

Guimarães, N. C., 2011. *Dissertação de Mestrado*. Belo Horizonte(Minas Gerais): Universidade Federal de Minas Gerais.

Gupta, V. & Miller, J., 2010. Surface force measurements at the basal planes of ordered kaolinite particles. *J Colloid Interface Sci.*, pp. 344 (2):362-71.

Habashi, F., 2006. *A short history of mineral processing*. Istanbul, s.n., pp. 3 - 8.

Haselhuhn III, H. J., 2015. The dispersion and selective flocculation of hematite ore. s.l.:Michigan Technological University, <http://digitalcommons.mtu.edu/etds/945>.

Heider, M., 2020. REAPROVEITAMENTO DE RESÍDUOS DE MINÉRIO DE FERRO. [Online]

Available at: <https://www.inthemine.com.br/site/reaproveitamento-de-residuos-de-minerio-de-ferro/>

Houot, R., 1982. Beneficiation of iron ore by flotation - Review of industrial and potential applications. *International Journal of Mineral Processing*, vol10, pp. 183-204.

<http://bibocaambiental.blogspot.com/2011/05/mina-do-caue-e-itabira.html>, 2017. [Online] Available at: <http://bibocaambiental.blogspot.com/2011/05/mina-do-caue-e-itabira.html>

Kar, B., Sahoo, H., Rath, S. & Das, B., 2013. Investigations on different starches as depressant for iron ore flotation. *Miner. Eng.* 49, pp. 1-6, <http://dx.doi.org/10.1016/j.mineng.2013.05.004>..

Khosla, N. & Biswas, A., 1984. Mineral-collector-starch constituent interactions. *Colloids Surf.* 9 (3), pp. 219-235.

Lima, N. P., Pinto, T. C. d. S., Tavares, A. C. & Sweet, J., 2016. The entrainment effect on the performance of iron ore reverse flotation. *Minerals Engineering*, 22 May.

Lima, N., Silva, K., Souza, T. & Filippov, L., 2020. The Characteristics of Iron Ore Slimes and Their Influence on the Flotation Process. *Minerals*, p. 10. 675. [10.3390/min10080675](https://doi.org/10.3390/min10080675).

Lima, N. P., Valadão, G. E. & Peres, A. E., 2013. Effect of amine and starch dosages on the reverse cationic flotation of an iron ore. *Minerals Engineering*, Volume 45, pp. 180-184, <https://doi.org/10.1016/j.mineng.2013.03.001>.

Liu, J., 2015. Dissertation PhD. s.l.:The University of Utah.

Liu, W. et al., 2019. Molecular-level insights into the adsorption of a hydroxy-containing tertiary amine collector on the surface of magnesite ore. *Powder Technology* 355, 30 July, pp. 700 - 707.

Liu, W. et al., 2019. Effect mechanism of the iso-propanol substituent on amine collectors in the flotation of quartz and magnesite. *Powder Technology*, 12 October.

Liu, W. et al., 2019. Investigating the performance of a novel polyamine derivative for separation of quartz and hematite based on theoretical prediction and experiment. *Separation and Purification Technology*, 30 November.

Longhua, X. et al., 2014. Effects of particle size and chain length on flotation of quaternary ammonium salts onto kaolinite. *Miner Petrol*, 29 May, pp. 309 - 316.

Lopes, G. M., 2009. Dissertação de Mestrado. Ouro Preto(Minas Gerais): Universidade Federal de Ouro Preto - Escola de Minas.

Mapa, P. S., 2006. Dissertação Mestrado. Belo Horizonte(Minas Gerais): Escola de Engenharia da UFMG.

Marques, M., 2013. Dissertação de Mestrado. Belo Horizonte(Minas Gerais): Universidade Federal de Minas Gerais.

Martins, M., Lima, N. P. & Leal Filho, L. S., 2012. Depressão de Minerais de Ferro: influência da mineralogia, morfologia e pH no condicionamento. *Revista Escola de Minas* v65, pp. n.3, p. 393-399.

Mathur, S., 2002. Kaolin Flotation. *Journal of Colloid and Interface Science* 256, 13 August, pp. 153-158.

Matiolo, E. et al., 2020. Improving recovery of iron using column flotation of iron ore slimes. *Minerals Engineering* 158 - <https://doi.org/10.1016/j.mineng.2020.106608>, 1 november.

Ma, X. & Bruckard, W., 2010. The effect of pH and ionic strength on starch-kaolinite interactions. *Int. J. Miner.*, pp. 94, 111–114, doi:10.1016/j.minpro.2010.01.004.

MHONDE, N., 2016. Investigating collector and depressant performance in the flotation of selected iron ores, Cape Town: University of Cape Town, 145p. (Dissertation, Master of Science in Engineering)..

Motta, E. et al., 2016. INCORPORATING MINERALOGICAL AND DENSITY PARAMETERS IN FERROUS RESOURCE EVALUATION USING MINERALOGICAL NORM CALCULATION – MNC. Rio de Janeiro, s.n., pp. 210 - 221.

Mudd, G. M., 2009. The Environmental sustainability of mining in Australia: key mega-trends and looming constraints. *ResourcesPolicy* 35, pp. 98 - 115.

Mudd, G. M., 2010. The “Limits to Growth” and ‘Finite’ Mineral Resources: Re-visiting the Assumptions and Drinking From That Half-Capacity Glass. Auckland: s.n.

Nascimento, A. E. D., 2018. Monografia. Mariana(Minas Gerais): Universidade Federal de Ouro Preto.

Nascimento, H. N., 2014. Dissertação Mestrado. Belo Horizonte(Minas Gerais): Universidade Federal de Minas Gerais - Escola de Engenharia.

National Institutes of Health (NIH), s.d. PubChem DOCS. [Online] Available at: <https://pubchem.ncbi.nlm.nih.gov/compound/lauramidopropyltrimethylamine> [Acesso em January 15 2020].

Navarro, R., 2006. A Evolução dos Materiais. Parte 1: da Pré-história ao Início da Era Moderna. s.l.:www.dema.ufcg.edu.br/revista.

Nonnenberg, M. J. B., 2010. China: Estabilidade e crescimento econômico. s.l.:s.n.

Nykänen, V. P. S. et al., 2018. True flotation versus entrainment in reverse cationic flotation for the concentration of iron ore at industrial scale. *Mineral Processing and Extractive Metallurgy Review*, 10 October, pp. 1-11.

Oliveira, P. S., 2006. Dissertação de Mestrado. Belo Horizonte(Minas Gerais): Universidade Federal de Minas Gerais.

Pavlovic, S. & Brandao, P., 2003. Adsorption of starch, amylose, amylopectin and glucose monomer and their effect on the flotation of hematite and quartz. *Minerals Engineering*, Volume 16, pp. 1117–1122, doi:10.1016/j.mineng.2003.06.011.

Pinto, P. H. F., 2019. Tese de Doutorado. São Paulo(São Paulo): Universidade de São Paulo. Escola Politécnica. Departamento de Engenharia de Minas e de Petróleo.

Pinto, P. P., 2016. Dissertação de Mestrado. São Paulo: Biblioteca digital USP.

Piorek, S., 1997. Field-portable X-Ray Fluorescence Spectrometry: Past, Present and Future. *Analytical Chemistry and Technology* 1(6), pp. 317-329.

Queiroz, L. d. A., 2003. Dissertação de Mestrado. Belo Horizonte(Minas Gerais): Universidade Federal de Minas Gerais.

Rao, S. R., 2004. 744 p.. New York: Kluwer Academic / Plenum Publishers.

Rath, S. S. & Sahoo, H., 2020. A Review on the Application of Starch as Depressant in Iron Ore Flotation. *Mineral Processing and Extractive Metallurgy Review*, p. DOI: 10.1080/08827508.2020.1843028.

Reis, J. M. d., 2015. Dissertação de Mestrado. Belo Horizonte(Minas Gerais): Universidade Federal de Minas Gerais.

Robinson, M. R., Abdelmoula, M., Mallet, M. & Coustel, R., 2019. Starch functionalized magnetite nanoparticles: New insight into the structural and magnetic properties. *Journal of Solid State Chemistry* 277 (2019), p. 587–593.

Rocha, L., 2008. Dissertação de Mestrado. Belo Horizonte(Minas Gerais): Universidade Federal de Minas Gerais.

Rodrigues, O. M. S., Martins, L. V. F., Viana, P. R. M. & Araujo, A. C., 2009. Investigação da Cinética de Flotação de caulinita e do Quartzo e sua Implicação na Flotação Reversa de Minérios de Ferro. Belo Horizonte, s.n.

Roe, L. A., 1957. Book: Iron Ore Beneficiation, Edited by Edwards Brothers INC. Ann Arbor,(Michigan): Edwards Brothers, INC, in <https://babel.hathitrust.org/cgi/pt?id=mdp.39015024221353&view=1up&seq=8>.

Rosière, C. & Chemale, F., 1993. Um modelo para a Evolução microestrutural dos minérios de ferro do Quadrilátero Ferrífero. Parte I-Estruturas e Recristalização. *Revista Geonomos* V.1, pp. 65 - 84.

Sales, C. G., 2012. Dissertação de Mestrado. Belo Horizonte(Minas Gerais): Universidade Federal de Minas Gerais.

Sales, C. G. d., 2012. Dissertação de Mestrado. Belo Horizonte(Minas Gerais): Universidade Federal de Minas Gerais - Escola de Engenharia.

Sant'Ana Filho, J. N. d., 2013. Dissertação de Mestrado. Belo Horizonte(Minas Gerais): Centro Federal de Educação Tecnológica - CEFET.

Santos, I. J. d., 2003. Dissertação de Mestrado. Ouro Preto(Minas Gerais): Universidade Federal de Ouro Preto.

Severov, V., Filippova, I. & Filippov, L., 2013. Floatability of Fe-bearing silicates in the presence of starch: adsorption and spectroscopic studies. J. Phys. Conf. Ser. <http://dx.doi.org/10.1088/1742-6596/416/1/012017..>

Shrimali, K. & Miller, J., 2016. Polysaccharide Depressants for the Reverse Flotation of Iron Ore. Trans Indian Inst Met, Volume 69, pp. 83-95, <https://doi.org/10.1007/s12666-015-0708-4>.

Silva, R. V. G., 1999. Dissertação de Mestrado em Engenharia Metalúrgica e de Minas. Belo Horizonte(Minas Gerais): Universidade Federal de Minas Gerais - Escola de Engenharia.

Singh, S. et al., 2014. Recovery of iron minerals from Indian iron ore slimes using colloidal magnetic coating. Powder Technology 269 (2015), 6 september, p. 38–45.

Souza, H. S., 2014. Dissertação de Mestrado. São Paulo(São Paulo): Universidade de São Paulo. Escola Politécnica. Departamento de Engenharia de Minas e Petróleo.

Svoboda, J. & Fujita, T., 2003. Recent developments in magnetic methods of material. Minerals Engineering, Cornwall, n.16, pp. 785-792.

Swagat, S. R. & Hrushikesh, S., 2020. A Review on the Application of Starch as Depressant in Iron Ore Flotation. Mineral Processing and Extractive Metallurgy Review, p. DOI: 10.1080/08827508.2020.1843028.

Taner, H. A. & Onen, V., 2016. Control of clay minerals effect in flotation. A review. s.l., s.n.

Torquato, N. C., Silva, W. P. & Ferreira, M. T. S., 2019. MÉTODOS ALTERNATIVOS PARA DISPOSIÇÃO DE REJEITOS. São Paulo, Associação Brasileira de Metalurgia, Materiais e Mineração.

Turrer, H. D. G., 2007. Tese de doutorado: Polímeros depressantes na flotação de minério de ferro, Belo Horizonte: UNIVERSIDADE FEDERAL DE MINAS GERAIS - Curso de Pós-Graduação em Engenharia Metalúrgica e de Minas.

Turrer, H. & Peres, A., 2010. Investigation on alternative depressants for iron ore flotation. *Miner. Eng.* 23, pp. 1066-1069, <https://doi.org/10.1016/j.mineng.2010.05.009>.

Universidade de São Paulo & Instituto Tecnológico Vale, 2018. Relatório interno da Vale S.A - Relatório Parcial do Projeto. Ouro Preto(Minas Gerais): s.n.

Universidade de São Paulo; Vale Technological Institute. Vale S.A; , 2018. Relatório interno da Vale S.A - Relatório Parcial do Projeto. Ouro Preto(Minas Gerais): s.n.

Urbina, R. Herrera (2003) Recent developments and advances in formulations and applications of chemical reagents used in froth flotation, *Mineral Processing and Extractive Metallurgy Review*, 24:2, 139-182, DOI: 10.1080/08827500306898

Vale S.A., 2012. Em: Nossa História 2012. s.l.:Verso Brasil Editora.

Vale S.A., 2014. Geologia dos Itabiritos Compactos no Quadrilátero Ferrífero, Belo Horizonte: s.n.

Vale S.A., 2020. Conheça mais sobre a história de Carajás, a maior mina de minério de ferro do mundo. [Online] Available at: <http://www.vale.com/hotsite/PT/Paginas/conheca-mais-sobre-historia-carajas-maior-mina-minerio-ferro-mundo.aspx>

Vale S.A., Fevereiro, 2017. Relatório Interno - Concentração de Lama de Minério de Ferro, Belo Horizonte: s.n.

VALE, 2007. Itabirito compacto conceição variabilidade de processos e produtos: relatório interno. Belo Horizonte, s.n.

Vale, 2020. Entenda as Barragens da Vale. Available at: http://www.vale.com/brasil/PT/aboutvale/servicos-para-comunidade/minasgerais/atualizacoes_brumadinho/Documents/PT/entenda-as-barragens-da-vale-pt.html

Veloso, C., Filippov, L., Filippova, I. & Araujo, A., 2018. Investigation of the interaction mechanism of depressants in the reverse cationic flotation of complex iron ores. *Minerals Engineering* 125, pp. 133-139.

Veloso, C. et al., 2020. Adsorption of polymers onto iron oxides. *J Mater Res Technology* 9(1), pp. 779-788.

Vieira, A. M., 1994. Dissertação de Mestrado. Belo Horizonte(Minas Gerais): Universidade Federal de Minas Gerais.

Wang, L., 2016. PhD Thesis. s.l.:The University of Queensland .

Weissenborn, P., Warren, L. & Dunn, J., 1995. Selective flocculation of ultrafine iron ore. 1. Mechanism of adsorption of starch onto hematite. *Colloids and Surfaces - A: Physicochemical and Engineering Aspect*, Volume 99, pp. 11 - 27.

Whitbeck, R. H., 1919. *Our Iron-Clad Civilization*. s.l.:American Association for the Advancement of Science, <https://www.jstor.org/stable/6734>.

Wolff, A. P., Costa, G. M. d. & Dutra, F. C., 2011. A COMPARATIVE STUDY OF ULTRA-FINE IRON ORE TAILINGS FROM BRAZIL. *Mineral Processing & Extractive Metall. Rev.*, 32, p. 47–59.

Xiaodong, Z., 2012. *Understanding China's Growth: Past, Present, and Future*. s.l.:s.n.

Xu, L. et al., 2015. Effects of particle size and chain length on flotation of quaternary ammonium salts onto kaolinite. *Mineral Petrol.* , pp. 109, 309-316.

Yianatos, J., Contreras, F., Díaz, F. & Villanueva, A., 2008. Direct measurement of entrainment in large flotation cells. *Powder Technology*, 8 June.

Yuehua, H., Wei, S., Haipu, L. & Xu, Z., 2004. Role of macromolecules in kaolinite flotation. *Minerals Engineering* 17, 27 April, pp. 1017-1022.

Chapter 2 - The characteristics of iron ore slimes and their influence on the flotation process

Neymayer P. Lima ¹, Klaydison Silva ¹, Thiago Souza ², and Lev O. Filippov ^{3,*}

¹ Av. Dr. Marco Paulo Simon Jardim, 3580, Bairro Piemonte, Nova Lima, CEP 34.006-200, MG, Brazil; neymayer.lima@vale.com (N.P.L.); klaydison.silva@vale.com (K.S.)

² Mineral Development Center – CDM/Vale, BR381 KM450, Postal Code 33040-900, Santa Luzia - MG - Brasil, thiago.souza@vale.com.

³ Université de Lorraine, CNRS, GeoRessources, F54000 Nancy, France, lev.filippov@univ-lorraine.fr.

Minerals 2020, 10(8), 675 <https://doi.org/10.3390/min10080675>

Received: 21 May 2020; Accepted: 22 July 2020; Published: 30 July 2020

Abstract: The flotation has been successfully applied to process the iron ore for the particle size (Ps) from 10 µm up to 150 µm. The presence of the slimes (Ps < 10 µm) is harmful on the reverse flotation of quartz, so they are usually prior removed by hydrocyclones. The main effects of the presence of slimes on the flotation are related to the increase on reagents consumption, the froth stability, and decrease on the selectivity. The lower floatability of coarse quartz particles (+74 µm) combined with the presence of slimes, even in small quantities, drastically affect the flotation response. This paper shows a study of characterization of a typical iron ore slime, aiming to create a better understanding of its role on the concentration by flotation. The main characteristics of typical slimes from the Iron Ore Quadrangle in Brazil are the presence of almost 70% of hematite, 25% of quartz, and 5% of kaolinite, as the main silicates gangue minerals. Furthermore, the particle size distribution revealed that 80% of the hematite and the kaolinite are below 20 µm. The affinity between the ultrafine kaolinite of the slimes with the corn starch is harmful to the reverse flotation of quartz, as the starch has an important depressing action over the hematite. The presence of 20% of hematite –20 µm decreased the recovery to the froth of quartz + 74 µm from 97% to 62%, where the slimes coating seems to be the main responsible.

Keywords: iron ore; slimes; kaolinite; flotation

1. Introduction

The flotation of iron ores is performed in circuits that consist of mechanical cells, columns, or a combination of both types of machines. The feed consists of particles in the size range between 10 μm and 150 μm [1]. The slimes (fraction < 10 μm) are removed in hydrocyclones and the top size is limited to 5% to 10% > 150 μm . This wide range of particles size impairs process selectivity due to the possible differences in behavior concerning properties, such as hydrophobicity, specific surface area, weight, etc. [2]. Understanding the characteristics and behavior of the slimes is of fundamental importance on the iron ore flotation industry, as the operational conditions can be better adjusted to maximize Fe recovery and product quality [3]. The harmful effects of iron slimes on the reverse flotation of quartz have been known since the beginning of its operation [1]. The main effects refer to the increase of reagents consumption, the lower selectivity and the froth stability [4]. The removal of iron ore slimes using hydrocyclones was introduced with the USBM process [5]. Investigations that were carried out by Lima and coworkers for different iron ores from the Iron Quadrangle in the Southeast of Brazil indicated that the by-pass levels on the desliming hydrocyclones lower than 4% did not affect the flotation recoveries or the quality of the concentrates [6]. The results of this study indicated that the specific surface area with different bypass levels can explain the flotation response on the presence of slimes. Filippov and coworkers reported the effect of desliming in wet magnetic separation, applied to tailings from magnetite ores processing, at the Mikhailovsky plant in Russia [7]. The authors demonstrated that desliming at 10 μm reveals higher mass pull and lower iron grades when desliming at 20 μm . Despite 10% higher mass pull at 10 μm , cutting at 20 μm have shown a dramatic increase on the flotation selectivity. Table 1 shows the effect of the desliming size on the flotation response.

Table 1. Influence of desliming on the reverse cationic flotation of hematite containing tailings of magnetic separation from magnetite ore at the Mikhailovsky plant, Russia [6].

Desliming	Products	wt%	Grade%		Fe Recovery%
			Fe	SiO ₂	
<10 μm	Concentrate	58.5	39.2	35.8	72.8
	Tailings	41.5	20.6	62.3	27.2
	Magnetic product	100	31.5	46.8	100
<20 μm	Concentrate	49.8	54.9	10.8	73.5
	Tailings	50.2	19.6	66.5	26.5
	Magnetic product	100	37.2	38.8	100

Studies that were conducted by Thella and coworkers with the iron slimes stored in slimes pond showed the possibility to obtain concentrates with 64.46% Fe, 2.66% Al₂O₃, and 2.05% SiO₂ with the combination of two stages of hydrocyclones of 50 mm of diameter with vortex finders of 14.3 mm and 11 mm of diameters to remove the particles with high content of Al₂O₃ and enhance the flotation selectivity while using amines and starch [8]. Ma and coworkers observed that starch adsorption in kaolinite is pH dependent, with starch adsorption decreasing with increasing pH from 7 to 10.5 [9] at pH 10.5, increasing ionic strength significantly enhances the adsorption density of starch on kaolinite. Weissenborn and coworkers studied the optimization of selective flocculation of ultrafine iron ore aiming the increase of Fe content in tailings samples where kaolinite was the main gangue mineral [10]. The results indicated the possibility to increase the Fe content from 46.6% to 57%. Wheat starch was the most appropriate selective flocculant. The recovery of all minerals was very sensitive to changes in flocculation conditions, and careful control of the many process variables was required in order to achieve optimum recovery. Xu and coworkers evaluated the floatability of kaolinite in different sizes and with different chain length collectors [11]. The anomalous flotation behaviour of kaolinite has been explained based on crystal structure considerations. The results showed that fine kaolinite particles have more edges to adsorb fewer cationic collectors than that of coarse kaolinite particles, which is responsible for the poorer floatability of fine kaolinite. Dey and coworkers evaluated the concentration of Indian iron ore slime using column flotation [12]. A sample with 16% passing in 25 μm size fraction containing 58.7% Fe, 5.2% SiO₂, and 4.9% Al₂O₃ was used during the investigations in a column of 7.5 cm diameter and 3 m height. The tests of direct flotation were carried out using a pulp with 10% of solids (w/w), sodium silicate as depressant, MIBC as frother and sodium oleate as collector. A concentrate with 62% Fe and 59% yield was produced using 2.5 kg/t of collector at 0.5 cm/s of

superficial air velocity. Slimes have higher surface area, which increases the reagent consumption and they can increase flotation residence time resulting in high froth volumes [13]. Lima and coworkers evaluated the effect of the by-pass on the reverse flotation of quartz for samples with different mineralogical compositions [6]. The specular hematite sample was affected by the increase of by-pass level from 4% to 6%, on the contrary of the goethite/porous hematite sample, which was not affected when the by-pass level increased from 2% to 8%. This study showed the higher specific surface area of the specular hematite sample with 6% of by-pass can be the cause of the higher grade of SiO₂ on the concentrate, as reported in Table 2.

Table 2. Effect of the specific surface area on the flotation behavior of iron ores presenting different mineralogical compositions [6].

Mineralogical Composition	By-Pass (%)	Specific Surface Area (cm ² /g)	Fe Distribution in Concentrate	SiO ₂ in Concentrate
Specular hematite	4	1000	69.7	1.2
	6	3000	67	2.7
Goethite/porous hematite	2	1295	92.9	1
	4	1556	92.5	1.1
	8	1887	90.7	1.1

Bandini and coworkers analyzed the effect of colloidal iron ore slime on the flotation of galena and quartz particles by coatings [14]. These authors investigated the formation of iron ore slime coatings and methods for their removal, using quartz as a model for deslimed galena, since it shows similar surface electrical properties and slime particle adsorption characteristics. The use of pH control alone was ineffective in removing iron oxide slime coatings from galena or quartz. By increasing the pH to 10, both iron oxide and galena/quartz particles become negatively charged; however, there is still an energy barrier to overcome for slime detachment. Combining pH control with high shear mixing or sonication removed rapid and completely the iron ore slime coatings. Rulyov and coworkers evaluated the microflotation of particles below 1 μm. The use of 40 μm bubbles and the coagulation or flocculation of particles to reach 7 μm were necessary to increase their recovery [15]. The presence of slimes in the beneficiation plants of the Iron Ore Quadrangle in Brazil have increased even more, reaching almost 40 millions of tons per annum. Understanding the harmful effect of these slimes on the iron ore flotation is a challenging and it can be useful to develop alternatives to increase the Fe recovery on the beneficiation plants.

2. Materials and Methods

2.1. Samples

This study was carried out using eight samples, as described in Table 3

Table 3. General characteristics of the samples.

Sample	Sample Name	Mass of Solids (kg)	Source	Description
1	Iron ore slime	150	Industrial slime thickener	Iron ore slime collected on the underflow's thickener
1A	Hematite	20	Industrial slime thickener	Concentrate obtained after several stages of bench scale magnetic separation of sample 1
1B	Silicates	20	Industrial slime thickener	Tailing obtained after several stages of bench scale magnetic separation of sample 1
2A	Iron ore desliming feed with 21% SiO ₂ +74 μm	150	Industrial desliming cyclones (20° of diameter)	Iron ore desliming feed collected on 20° cyclones feed
2B	Iron ore desliming feed with 21% SiO ₂ +74 μm	150	Industrial desliming cyclones (20° of diameter)	Iron ore desliming feed collected on 20° cyclones feed
2C	Iron ore desliming feed with 21% SiO ₂ +74 μm	150	Industrial desliming cyclones (20° of diameter)	Iron ore desliming feed collected on 20° cyclones feed
3	Pure quartz	10	Minas Gerais, Brazil	Pure samples of quartz crushed by jaw and gyratory crushers and milled to >110 μm
4	Pure hematite	10	Minas Gerais, Brazil	Pure samples of hematite crushed by jaw and gyratory crushers and milled to >186 μm

Sample 1 was collected on the underflow of the thickener of an industrial beneficiation plant in the Iron Quadrangle, before the disposal on tailings dam. Samples 1A and 1B were obtained from sample 1 after three cleaning and three of scavenging stages, aiming to obtain the highest grades of Fe on the concentrate and silicates on the tailing. Sample 1 was also submitted to settling in a 2000 mL beaker, aiming to obtain settling products (underflow) with different percentage of gangue minerals, especially aluminosilicates. The sedimentation tests were carried out on the following conditions. The percentage of solids in the feed was 5%. The pulp pH was 10.5 aiming the dispersion of the pulp. Settling time after dispersion of the pulp was put at rest for 5 min. Cut-off-size during desliming was at 10 μm and the corn starch

dosages were 0, 100, 250, and 500 g/t. The obtained underflow samples were used for bench scale flotation tests with 100 g/t of collector (Etheramine Flotigam 7100 by Clariant, Muttenz, Switzerland), 500 g/t of corn starch as depressant at pH 10 and using Denver 1200 mL bench scale cell. Samples 2A, 2B, and 2C were collected on the desliming hydrocyclones feed of the same industrial beneficiation plant. The samples were collected in different days, when the% of SiO₂ on the +74 μm were 20%, 23%, and 31%, respectively. Each of these three samples were deslimed at bench scale to obtain 1.5%, 3.5%, 5.5%, and 10.0% of slimes in the flotation feed composition. These tests were done aiming at evaluating the combined effect of slimes and the distribution of SiO₂ on the +74 μm in the flotation feed. The flotation tests combining the% of SiO₂ on the +74 μm fraction and the% of slimes were done with 100 g/t of collector (Etheramine Flotigam 7100 by Clariant), 500 g/t of corn starch, and pH 10.5 in a 1200 mL Denver cell. Samples 3 and 4 are pure quartz and hematite minerals from Minas Gerais, Brazil. They were crushed using jaw and gyratory crusher and milled using ceramic ball mill to reach the size fraction approximately below 200 μm. The quartz sample was screened to obtain +74 μm for the flotation tests. The hematite sample was classified using a cyclosizer in +20 μm and -20 μm fractions. The flotability of quartz in the presence of hematite (+20 μm and -20 μm) was evaluated using 100 g/t of collector (Etheramine Flotigam 7100 by Clariant), 500 g/t of corn starch as depressant at pH 10 and using MineMet 300 mL bench scale. The proportion of coarse quartz and fine hematite was almost the same in typical desliming feed, as 80% and 20%, respectively

2.2. Characterizations

Chemical assays were done by X-ray fluorescence (XRF) by Thermo Fisher Scientific Niton XL3t XRF Analyzer (Thermo Fisher Scientific, Waltham, MA, USA), to determine Fe, SiO₂, Al₂O₃, P, Mn, CaO, MgO, and LOI. The error of chemical analysis was evaluated to 2%. Size distribution was obtained by laser sizer instrument (Malvern® Mastersizer 2000, Malvern, Malvern, UK). The mineralogical composition of sample 1 was determined using an X-ray diffraction technique and the automated scanning electron microscope (QEMSCAN® system) with a tungsten source from the FEI company (Hillsboro, OR, USA). The iDiscover software (everly Hills, CA, USA) was used for the measurements and the data processing. The PMA (Particle Mineral Analysis) analysis model was used. The QEMSCAN® was operated using a voltage acceleration of 15 kV and a current of approximately 5 nA. For the X-ray diffraction, the samples were pressed and analyzed in a PANalytical X-ray diffractometer (Empyrean model) while using a Co tube. The crystalline phases were identified and interpreted

by the High Score Plus software (Malvern Panalytical, Worchestershire, UK) and the mineralogical composition was quantified by the Rietveld method.

3. Results and Discussion

The chemical analyses and size distribution of the iron ore slime, sample 1 are shown in Table 4 and Figure 1, respectively.

Table 4. Chemical analyses of the iron ore slime (sample 1).

Fe (%)	SiO ₂ (%)	Al ₂ O ₃ (%)	P (%)	Mn (%)	LOI (%) *
45.17	28.64	3.06	0.085	0.91	3.07

* Loss on ignition.

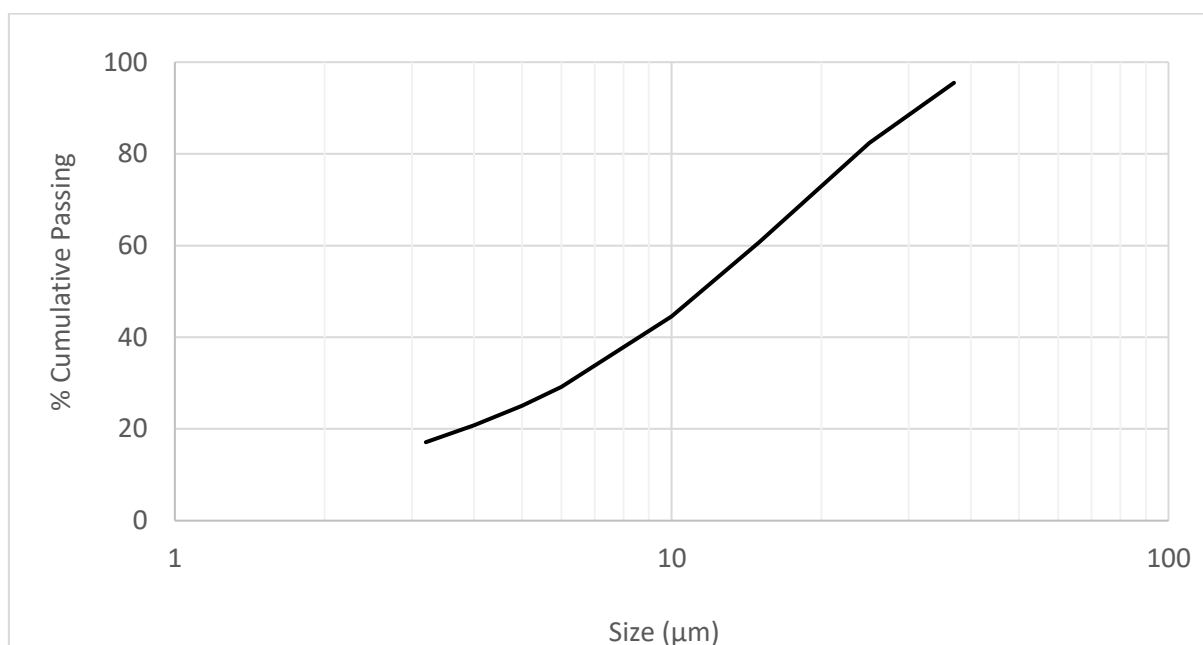


Figure 1. Particle size distribution of the iron ore slime (sample 1).

The typical iron ore slime is about 95% passing in 37 μm, 45% passing 10 μm, and 17% passing 3.2 μm. By combining the sieving analysis with the XRF results, it was possible to estimate the distribution of Fe, Si, and Al in the different size fractions, as shown in Figure 2. It was possible to observe that the majority of the iron (87%) is present in the fine particle size fractions (<20 μm), which are susceptible to report to the tailing by entrainment when performing reverse cationic flotation. At the same way, almost 91% of the Al (mainly kaolinite) is distributed in the size fraction below 20 μm, with low floatability behavior as reported by Xu and coworkers [11]. On the contrary, 58% of Si is below 20 μm

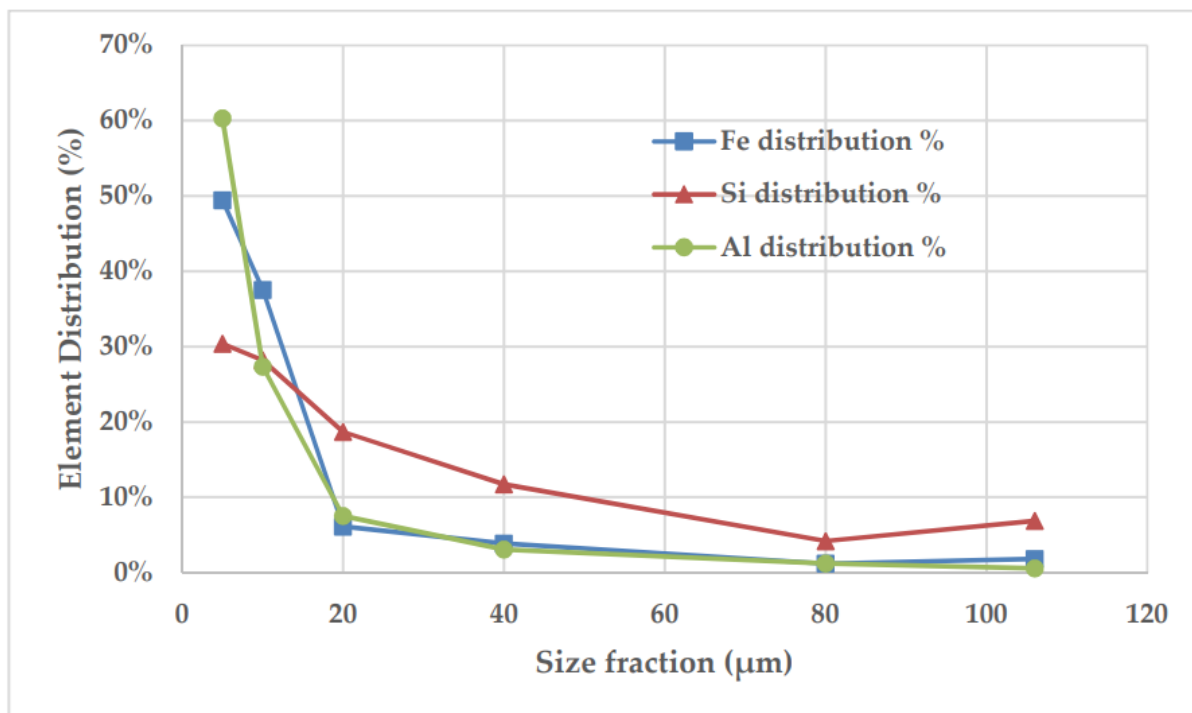


Figure 2. Distribution of Fe, Si and Al according to size fraction of the iron ore slime (sample 1).

The mineralogical analyses are reported in Figure 3, where hematite is the main iron mineral, Minerals and quartz and kaolinite are the main gangue minerals.

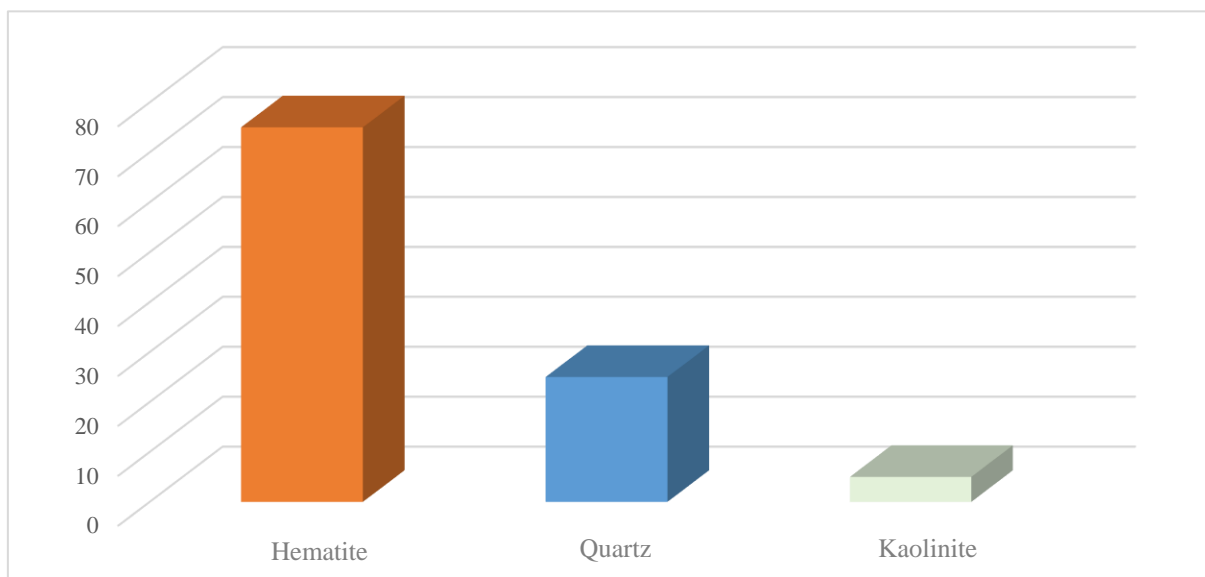


Figure 3. Mineral composition (in%) of the iron ore slime sample.

Figure 4 illustrates an image of the surface of the hematite, where it is possible to observe the presence of finely disseminated quartz inclusions that appear to be smaller than 2 μm, which can impact the selectivity of flotation.

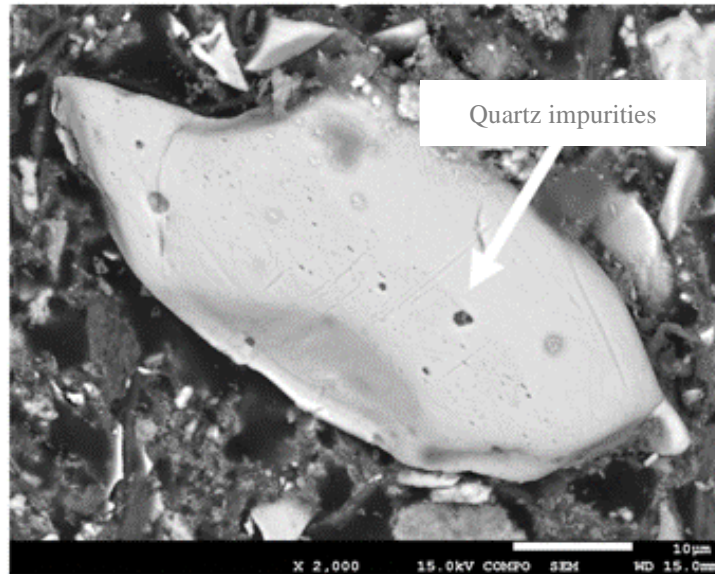


Figure 4. Selected image of the surface of a hematite with finely dispersed quartz (sample 1).

Figure 5 shows the comparative of PSD between the iron ore slime (sample 1) and the products (samples 1A and 1B) obtained after several stages of magnetic concentration and Table 5 show the comparative chemical analyses between them.

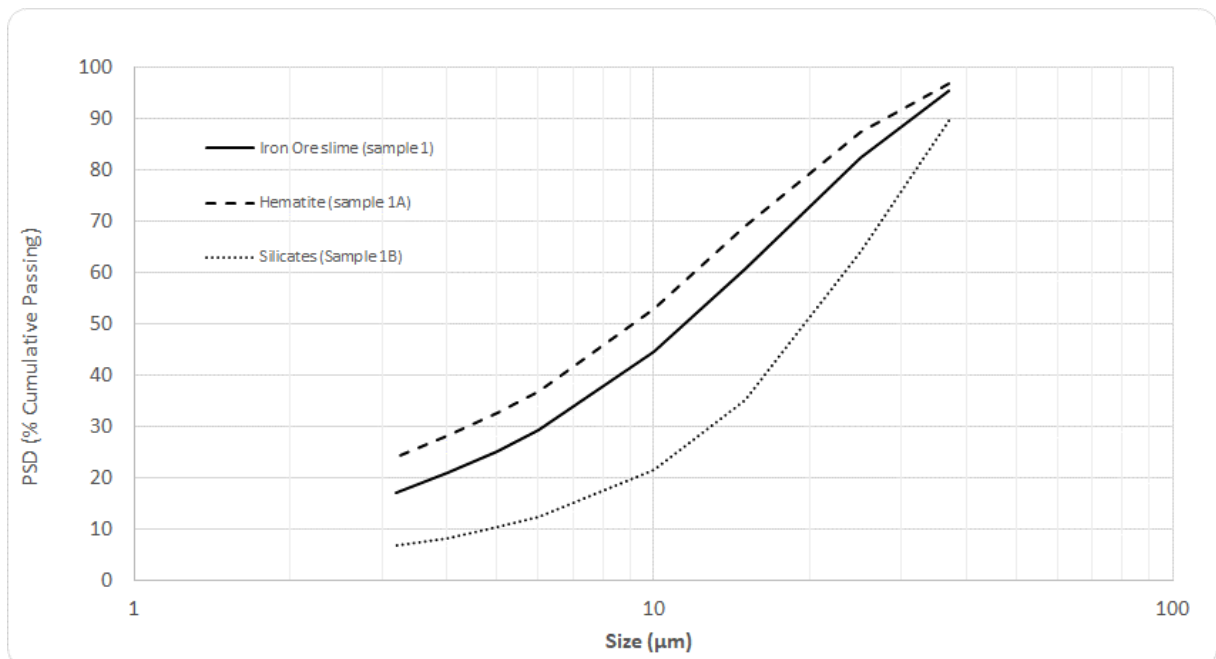


Figure 5. Comparative PSD between the iron ore slime (sample 1), hematite (sample 1A), and the silicates (sample 1B).

Table 5. Comparative chemical analyses between the iron ore slime sample, the hematite and the silicates.

ID	Mass Recovery	Fe (%)	SiO₂ (%)	Al₂O₃ (%)	P (%)	Mn (%)	LOI* (%)
Iron ore slime (sample 1)	100	45.17	28.64	3.06	0.085	0.091	3.54
Hematite (sample 1A)	55	66.07	2.57	0.98	0.061	0.057	1.87
Silicates (sample 10)	45	17.06	60.87	6.28	0.123	0.175	8.16

*Loss on ignition

The hematite of the slime (sample 1A) is much finer than the silicates (1B), in accordance with the size distribution of Figure 2. D50 of hematite is 9 μm , while d50 of the silicates is 20 μm . It was deduced that the iron oxide minerals (hematite) present on the slime sample are much finer than the gangue minerals (silicates). Moreover, after three stages of cleaning with the magnetic separator, the tailings product contains 17.06% Fe, indicating some association between gangue minerals and Fe minerals. The finer size distribution of the Fe minerals and their associations with the gangue minerals indicate the challenges and difficulties to concentrate the iron ore slimes and the maximum yielded recovery expected was evaluated as 55%. Lima and coworkers calculated the degree of entrainment for Fe in different size fractions using an empirical correlation with the water recovery for the rougher, cleaner, and recleaner industrial cells [16]. The results showed that particles smaller than 20 μm show high entrainment degree, therefore the iron oxide minerals present on the slimes can be easily lost by entrainment, as almost 80% are lower than 20 μm , as shown on the Figure 2.

Table 6 shows the results of the sedimentation tests with the iron ore slime (sample 1), indicating that the corn starch promotes the concentration of Al₂O₃ to the underflow.

When considering that kaolinite is the main aluminium oxide mineral in the iron ore slime, the increase of the Al₂O₃ content to the underflow in the presence of corn starch, can indicate its adsorption on the kaolinite surface. This behavior indicates that the presence of slimes can affect the flotation of quartz by the depression of kaolinite with the corn starch damaging the hematite depression. As the main mechanism of interaction in cationic reverse flotation of quartz is electrostatic, the lack of depression can lead the hematite to be floated by the collector.

The underflows obtained in the sedimentation tests, with different Al₂O₃ contents were submitted to standard bench scale flotation tests. The results of the tests can be seen in the Table 7, where higher percentage of Al₂O₃ on the feed (underflow) negatively affected the quality of the flotation concentrate.

Table 6. The effect of corn starch dosage on the recovery of Al_2O_3 to the underflow on the sedimentation tests with the iron ore slime (sample 1).

Corn Starch (g/t)	Recovery of Al_2O_3 to the Underflow
0	16.5
100	43.3
250	62.9
500	84.7

Table 7. Results of bench scale flotation tests with the products of the sedimentation tests of the iron ore slime (sample 1).

Al_2O_3 Concentrate%	Fe Concentrate%	SiO_2 Concentrate%
1.01	65.24	1.51
2.21	61.91	3.34
2.75	59.39	5.14
3.24	56.87	6.93

The Al sites of the kaolinite seems to interact with the starch while the Si sites can be free to interact with the collector. This behavior can reduce the floatability of quartz particles, as shown in the results of Table 7. Figure 6 shows the combined effect of the distribution of SiO_2 in the +74 μm fraction and the presence of slimes on the flotation response, regarding the % of SiO_2 in the concentrate. These tests were realized with samples 2A, 2B, and 2C (desliming feeds).

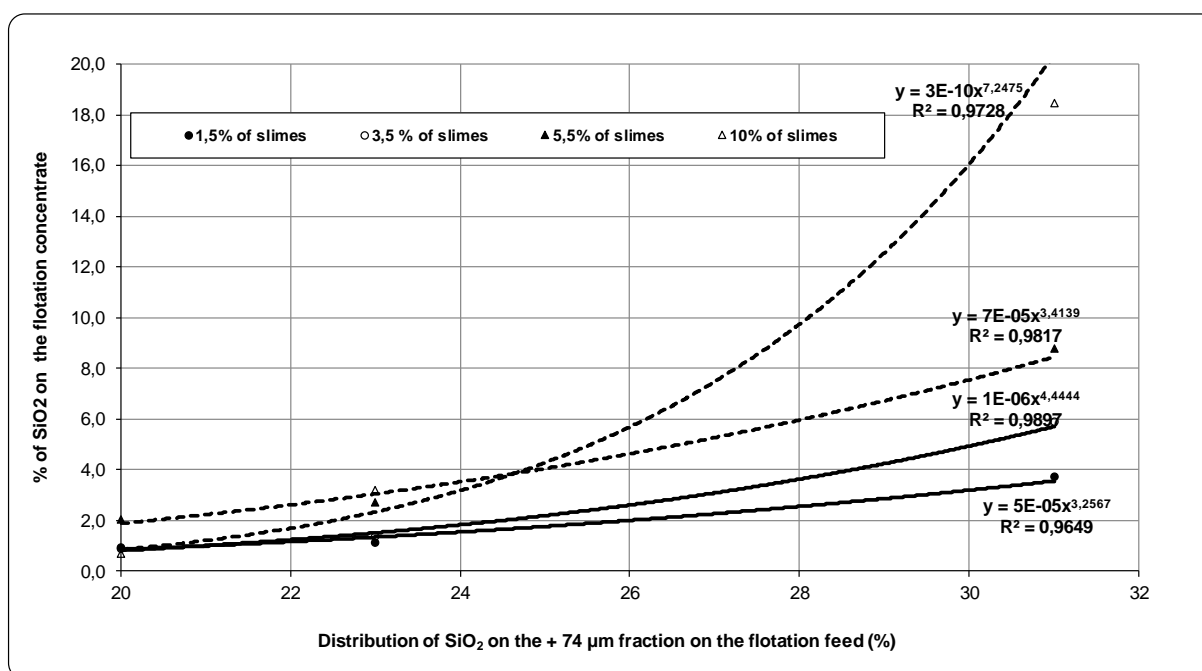


Figure 6. Combined effect of the SiO_2 distribution in the +74 μm fraction and the presence of slimes on the flotation response.

The flotation response is drastically impacted with the combination of higher SiO_2 distribution in the +74 μm fraction, even for small quantities of slimes, as indicated on the Figure 6. An increase from 1.0% to 3.0% of slimes can lead to a drop of almost 10% in the iron grade in the concentrate. The presence of slimes can adsorb part of the available collector, resulting in insufficient hydrophobicity of the coarse quartz, causing a dropback phenomenon. This behavior is in accordance with the studies conducted by Fugen and coworkers, where the presence of ultrafine particles ($\sim 10 \mu\text{m}$) caused the high consumption of reagents due the high total surface area and also a high number of these particles to adsorb the collector (when compared to the same mass of coarse particles). An excessive consumption of collector by the finer particles could lead to incomplete coverage of the coarser particles surfaces by this collector [17]. Another hypothesis is slime coating of small kaolinite particles on the coarse quartz surface inhibiting the collector adsorption or/and the interaction between quartz particles and bubbles. The mechanism of coatings can be controlled by the electrostatic interactions with the kaolinite particles because of the face-edge structure kaolinite [9]. Additionally, the coating may be enhanced by the bridging effect of the Ca^{2+} and other metallic cations [18]. The original size distributions of samples 4 and 5 (pure hematite and pure quartz) are shown in Figure 7. The flotation tests were realized with the mixtures: 80% +74 μm quartz/20% +20 μm hematite and 80% +74 μm quartz/20% -20 μm hematite.

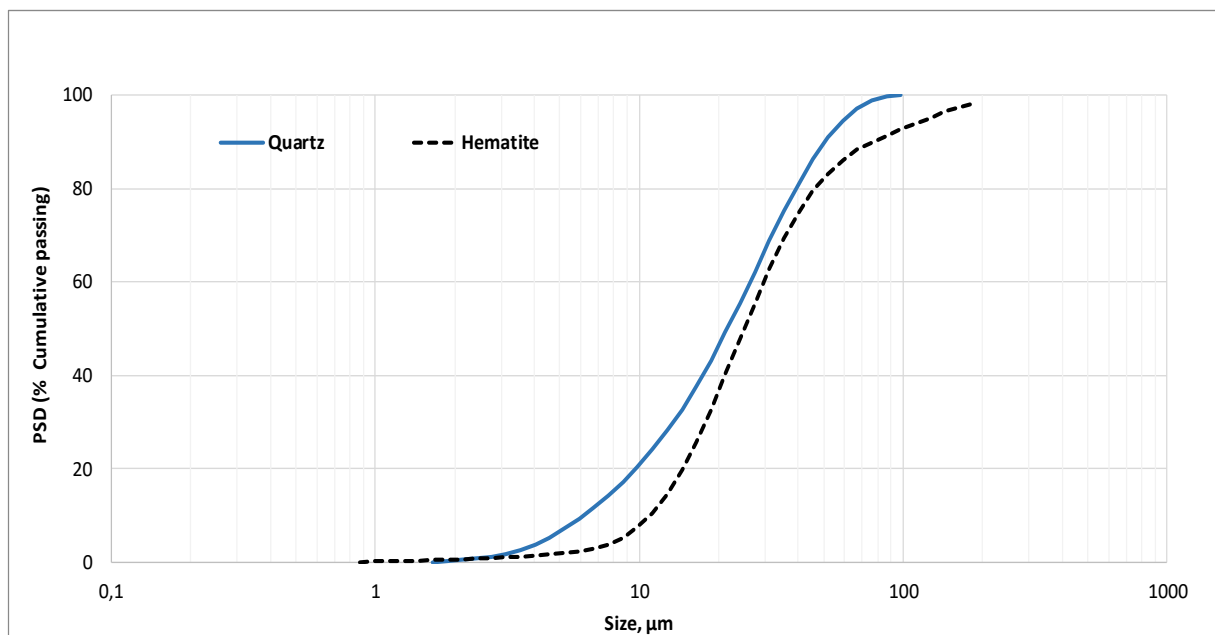


Figure 7. PSD of the pure samples of hematite and quartz (samples 4 and 5).

The harmful effect of slimes on the reverse flotation of quartz can also be observed on the results of Figure 8, where adding 20% of the -20 μm hematite reduced the floatability of

the coarse quartz particles (+74 μm) from 98% to 62%. On the other hand, the same amount of +20 μm hematite particles did not affect the floatability of these quartz particles. According to the results of Figure 4, 87% of the hematite in the slime is below 20 μm , which enhances its effect on the floatability of quartz. These ultrafine particles of hematite can adsorb a large amount of the collector, causing less hydrophobicity of the quartz particles. The other hypothesis to explain the harmful effect of the fine hematite ($-20 \mu\text{m}$) on the floatability of the coarse quartz is the slime coating, as in the study of Bandini and coworkers [14]. At pH 10.5, both particles are negatively charged, however there is still an energy barrier to overcome for slime detachment. When considering that the 2 hematite fractions showed almost the same recovery to the froth, but only the finer ($-20 \mu\text{m}$) decreased the recovery of quartz to the froth, slime coating seems to be the responsible for this harmful effect.

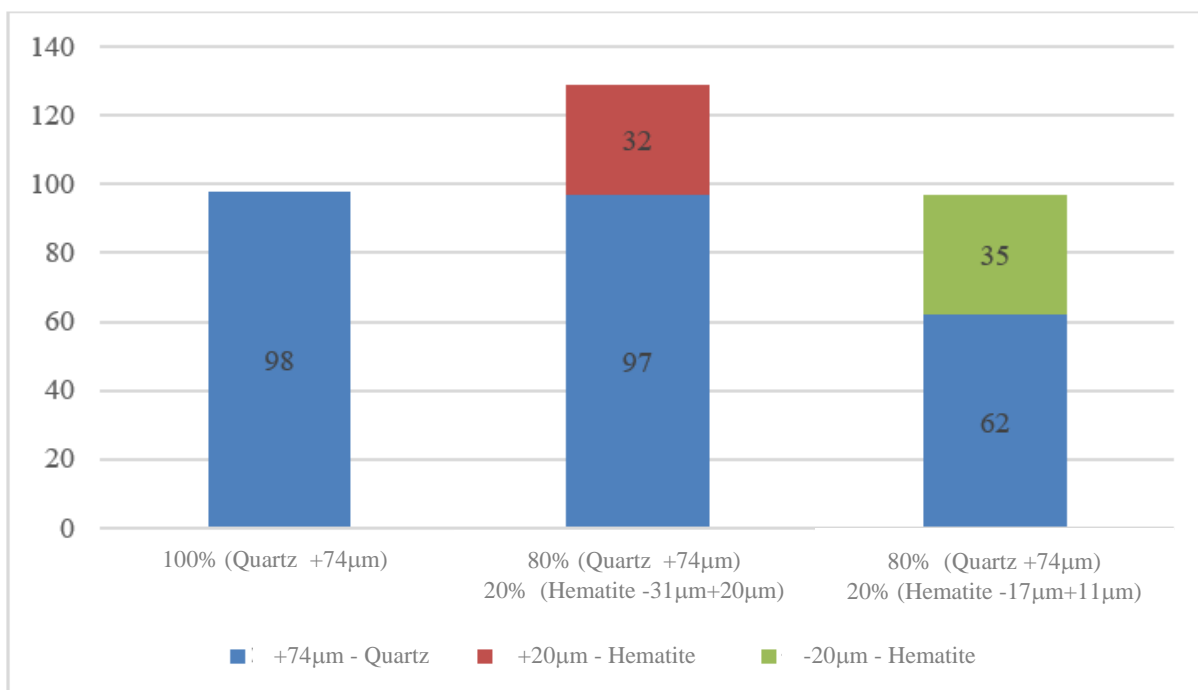


Figure 8. Effect of +20 μm and $-20 \mu\text{m}$ hematite on the floatability of +74 μm quartz (100 g/t of etheramine 7100 by Clariant, 500 g/t corn starch, and pH 10.5).

4. Conclusions

Typical slimes from the Iron Ore Quadrangle in Brazil present composition around 70% of hematite, 25% of quartz, and 5% of kaolinite as the main silicate minerals. More than 80% of the hematite and the kaolinite are below 20 μm . Some silicates appear as disseminated particles smaller than 2 μm . The addition of corn starch during sedimentation tests with desliming feed increased the kaolinite depression, which negatively affected the reverse flotation of quartz, possibly by the interaction's sites Si-amine-quartz-sites Al-depressant.

Moreover, the depressant adsorbs on this silicate minerals surfaces and enhances the harmful effect to the flotation response. The lower floatability of coarse quartz particles (+74 μm) combined with the presence of slimes, even in small quantities, drastically impacted the flotation response, which was also observed when hematite particles below 20 μm , in concentration similar to the desliming feed, reduced the floatability of coarse +74 μm sized particles of quartz from 97% to 62%. The development of new collectors without the use of traditional depressant might be an opportunity to recover the Fe minerals in the slimes. The effect of kaolinite surface sites and its implication to reagent adsorption is mandatory for a better understanding of the slime effects on cationic reverse flotation of quartz.

References

1. Filippov, L.O.; Severov, V.; Filippova, I.V. An overview of the beneficiation of iron ores via reverse cationic flotation. *Int. J. Miner. Process.* 2014, 127, 62–69. [CrossRef]
2. Lima, N.P.; Valadão, G.E.; Peres, A.E.C. Effect of amine and starch dosages on the reverse cationic flotation of an iron ore. *Miner. Eng.* 2013, 45, 180–184. [CrossRef]
3. Sahoo, H.; Rath, S.S.; Rao, D.S.; Mishra, B.K.; Das, D. Role of silica and alumina content in the flotation of iron ores. *Int. J. Miner. Process.* 2016, 148, 83–91, doi:10.1016/j.minpro.2016.01.021.
4. MA, M. Flotation mechanism of kaolinite under reverse cationic flotation conditions. In *Advances in Environmental Research*; Nova Science: New York, NY, USA, 2011; Volume 12, pp. 197–206.
5. Clemmer, J.B. Flotation of iron ore. In *Proceedings of the 8th Annual Mining Symposium*, Duluth, MN, USA, 15 January 1947.
6. Lima, N.P.; Peres, A.E.C.; Marques, M.L.S. Effect of Slimes on Iron Ores Flotation. *Int. J. Min. Eng. Miner. Process.* 2012, 1, 43–46. [CrossRef]
7. Filippov, L.O.; Filippova, I.V.; Severov, V.V. New technology for producing hematite concentrate from wastes generated in the processing of iron quartzites. *Metallurgist* 2010, 54, 268–272. [CrossRef]
8. Thella, J.S.; Mukherjee, A.K.; Srikakulapu, N.G. Processing of high alumina iron ore slimes using classification and flotation. *Powder Technol.* 2012, 217, 418–426. [CrossRef]
9. Ma, X.; Bruckard, W.J. The effect of pH and ionic strength on starch–kaolinite interactions. *Int. J. Miner. Process.* 2010, 94, 111–114. [CrossRef]

10. Weissenborn, P.K.; Warren, L.J.; Dunn, L.G. Optimisation of selective flocculation of ultrafine iron ore. *Int. J. Miner. Process.* 1994, 42, 191–213. [CrossRef]
11. Xu, L.; Hu, Y.; Dong, F.; Jiang, H.; Wu, H.; Zhen, W.; Liu, R. Effects of particle size and chain length on flotation of quaternary ammonium salts onto kaolinite. *Mineral. Petrol.* 2015, 109, 309–316. [CrossRef]
12. Dey, S.; Pani, S.; Singh, R.; Paul, G.M. Response of process parameters for processing of iron ore slime using column flotation. *Int. J. Miner. Process.* 2015, 140, 58–65. [CrossRef]
13. Fornasiero, D.; Filippov, L.O. Innovations in the flotation of fine and coarse particles. *J. Phys. Conf. Ser.* 2017, 879, 012002. [CrossRef]
14. Bandini, P.; Prestidge, C.A.; Ralston, J. Colloidal iron oxide slime coatings and galena particle flotation. *Miner. Eng.* 2001, 14, 487–497. [CrossRef]
15. Rulyov, N. Turbulent microflotation: Theory and experiment. *Colloids Surf. A Physicochem. Eng. Asp.* 2001, 192, 73–91. [CrossRef]
16. Lima, N.P.; de Souza Pinto, T.C.; Tavares, A.C.; Sweet, J. The entrainment effect on the performance of iron ore reverse flotation. *Miner. Eng.* 2016, 96, 53–58. [CrossRef]
17. Fugen, H.; Sivamohan, R. Behaviour of different particle size fractions in the flotation of calcite from wollastonite and microcline. *Miner. Eng.* 1990, 3, 257–271. [CrossRef]
18. Filippov, L.O.; Dehaine, Q.; Filippova, I.V. Rare earth (La, Ce, Nd) and rare metals (Sn, Nb, W) as by-product of kaolin production, Cornwall—Part3: Processing of fines using gravity and flotation. *Miner. Eng.* 2016, 95, 96–106. [CrossRef]

Chapter 3 - New perspectives in iron ore flotation: use of collector reagents without depressants in reverse cationic flotation of quartz

Klaydison Silva^{1,2}, Lev O. Filippov^{1*}, Alexandre Piçarra¹, Inna V. Flilippova¹, Neymayer Lima², Anna Skliar¹, Lívia Faustino^{3,4}, Laurindo Leal Filho⁴

¹ Université de Lorraine, CNRS, GeoRessources, F54000 Nancy, France

² Vale Mining Company, Iron Ore Beneficiation Development Team, Minas Gerais, Brazil

³ Vale Institute of Technology, Minas Gerais, Brazil

⁴ University of São Paulo – USP, São Paulo, Brazil

Minerals Engineering 170 (2021) 107004 <https://doi.org/10.1016/j.mineng.2021.107004>

Received 11 August 2020; Received in revised form 27 May 2021; Accepted 1 June 2021

Abstract: The reverse flotation of the iron ore with etheramine collector is significantly impacted when the iron-bearing silicates and the kaolinite are present in the silicates gangue mineral complex. This paper aims to propose a new amidoamine collector N-[3-(Dimethylamino)propyl]dodecanamide for iron ore reverse flotation with a potential of removing the iron oxides depressant. The contact angle and electrophoretic mobility measurements as well as the flotation experiments were performed on the pure quartz, kaolinite and hematite samples to compare their effect with the etheramine which is widely used as collector in reverse flotation of iron ores. Infrared spectroscopy was performed to study the adsorption of the amidoamine collector on the surface of the minerals studied. Amidoamine collector showed a significant selectivity towards quartz while the flotation of hematite and kaolinite were inhibited at pH 10 without the presence of a depressant. The high recovery of quartz to floated was explained by increased contact angle from 10° to about 50° without significantly impacting the contact angle measured on the hematite (9.4° to 17°). Steric hindrance caused by the structure of the N-[3-(Dimethylamino)propyl] dodecanamide collector on the hematite surface is the most suitable hypothesis concerning the high selectivity regarding the iron ore reverse flotation process.

Keywords: Iron ore, flotation, amidoamine, quartz, kaolinite, hematite

5. Introduction

The flotation processes performed in the main iron ore beneficiation plants located in the Iron Quadrangle region (Brazil) consist of flotation of natural fine particles (below 0.15 mm, without grinding) or flotation of all the material after grinding using ball mills (run of mine). In both cases, the flotation process adopted is a reverse cationic process with a preliminary desliming stage of flotation feed to remove materials with particle sizes below 10 μm (slimes) that are harmful to the iron ore flotation process (Filippov et al., 2014).

The reverse cationic flotation is also largely used to reduce the silica content in the iron concentrate obtained through magnetic separation. It is the most efficient upgrading process for simple systems composed of hematite/magnetite and quartz (Araujo et al., 2005; Filippov et al., 2014). However, its separation efficiency decreases when as a part of the gangue minerals there are Fe/Mg silicates. These Fe/Mg bearing gangue minerals cause a reduction in the flotation efficiency because their surface properties are similar to those of iron oxides, resulting in the non-selective action of depressants such as starch (Filippov et al., 2010; 2013).

Studies performed on the flotation of quartz with etheramines as collectors showed the efficient depression of iron oxides by starch molecules from different sources (such as corn and potato) (Araujo et al., 2005; Kar et al., 2013). However, detailed studies on reverse cationic flotation with iron ore samples from different deposits over the world (Brazil, Russia, Mexico) performed by Filippov and co-workers confirmed the inefficiency of starch when the silica content in the concentrate is controlled by Fe/Mg bearing minerals such as amphiboles, epidote, chamosite, and diopside (Filippov et al., 2010; Severov et al., 2016; Veloso et al., 2018). The main approaches for solving these issues focus on using new collector formulations (Filippov et al., 2010) or new alternative depressants such as guar gum (Turrer and Peres, 2010), humic acid (Dos Santos and Oliveira, 2007; Veloso et al., 2018), lignosulfonate, and carboxymethyl cellulose (Turrer and Peres, 2010; Veloso et al., 2020), leading to better flotation selectivity between hematite and silicates. However, the alternative depressants tested inhibited flotation of quartz owing to physical adsorption on their surfaces (Turrer and Peres, 2010). Based on Fourier transform infrared (FTIR) spectroscopy data, Severov et al., (2013) showed that starch can also adsorb on the quartz surface owing to the formation of hydrogen bonds between the hydroxyl groups of the polysaccharides and silanol groups presents on the quartz surface at pH 10. Direct adsorption studies confirmed similar adsorption densities on the surfaces of Fe-bearing silicates (pargasite) and quartz, with magnetite also showing high adsorption density (Filippov et al., 2013). However, starch adsorption on quartz and hematite is different not

merely in terms of magnitude but also in bonding strength. This is because the adsorption of the polysaccharides on the iron oxides and Fe-bearing silicates is controlled by their chemical bonding with the iron in the mineral structure (Weissenborn et al., 1995; Filippov et al., 2013); however, hydrogen bonding is the main adsorption mechanism on the quartz surface. Thus, amine collectors can replace the starch molecules on the quartz surface because of their stronger electrostatic interactions with the negatively charged quartz surface supported by lateral chain–chain interactions. Strong interactions of starch and other depressants on the Fe-bearing mineral surface through covalent bonding between the iron atoms and hydroxyl groups of the depressants lead to increased hydrophilic behaviour of such silicates when amines are used as flotation collectors. Hence, the investigations on new flotation collectors can contribute toward unlocking new iron ore resources related to primary deposits with complex gangue mineralogy (i.e., Fe-bearing silicates, kaolinite) or processing of old tailings with high degrees of alterations.

Amidoamine collectors were suggested and tested as effective agents for the flotation process, with diethylenetriamine monoamide being the most commonly used (Friedli, 1990). This type of reagent is obtained by the reaction between polyamines and organic acids. Amidoamines provide several advantages for the flotation process, i.e., selectivity and cost reduction (Friedli, 1990). In phosphate ore concentration processes, amidoamines are more tolerant toward sulphate ions. They are also inexpensive and have fewer complications due to possible overdose (Friedli, 1990). There are very few studies reporting the use of amidoamine molecules in iron ore flotation. However, they can be efficient quartz collectors in conventional iron ore reverse flotation using starch as the depressant of iron oxides.

Amidoamine-based collectors are suitable candidates for developing efficient iron ore slime flotation processes. As reported in earlier studies, iron ore slimes are generally composed of other minerals in addition to iron oxides and quartz (Lima et al., 2020). Some slimes from the Iron Quadrangle in Brazil, for example, have considerable amounts of kaolinite in their composition.

The choice of reagent is not the only factor considered for developing an iron ore slime flotation process. It is also necessary to determine the ideal hydrodynamic conditions for these processes (Fornasiero and Filippov, 2017). However, to determine the hydrodynamic conditions, it is first necessary to develop reagents that make the process viable. There are some shortcomings in the industrial flotation process with amine collectors. These shortcomings worsen the flotation indexes, resulting in low collectability, poor selectivity, large cohesive bubbles, and sensitivity to slime presence (Liu, et al., 2019).

In this study a comparison between a new amidoamine collector N-[3-(Dimethylamino)propyl]dodecanamide) with etheramine and oleate collectors in the flotation of pure minerals such as hematite, quartz and kaolinite is presented and discussed. The study was done with the focus on developing alternative routes that will allow the concentration of iron ore by flotation without a depressant reagent.

6. Materials and methods

6.1. Minerals and reagents

Pure quartz, kaolinite, and hematite mineral samples were used in this study. The kaolinite sample (Morbihan) was provided by Société Nouvelle d'Exploitation des Kaolins du Morbihan, the quartz sample was provided by Sibelco and the hematite sample was provided by Minerama.

The quartz and hematite samples were crushed using jaw and gyratory crushers. The size of hematite was reduced to flotation size ($d_{90} = 100 \mu\text{m}$) using a laboratory ball mill. To avoid surface contamination of the silicates, they were milled using a ceramic ball mill to obtain sizes below $100 \mu\text{m}$. The size distributions of the mineral samples used for this study are presented in Fig. 1.

XRD analysis results show the purity of the obtained products (Fig. 2).

The flotation performance of three collectors (etheramine, oleate, and N-[3-(Dimethylamino)propyl]dodecanamide) was evaluated through kinetic flotation tests, performed with pure mineral samples of hematite, quartz, and kaolinite and mixtures of these minerals. From this point on, the collector N-[3-(Dimethylamino)propyl]dodecanamide will be referred to as “amidoamine”.

Additionally, the reagents used are listed in Table 1.

6.2. X-Ray fluorescence (XRF) analysis

XRF analysis was performed by using a Thermo Fisher Scientific Niton XL3t XRF Analyser, with objective to analyze the percentage of elements in the products obtained during flotation. The measurements were performed using the four filters available in the analyzer, with each filter operated for 30 s (total measurement time of 120 s) and the ‘Cu-Zn’ mode selected. For representative purposes, three measurements were performed for each sample.

Fig. 3 shows the correlation between the Fe contents determined via XRF (used in this work) and the inductively coupled plasma mass spectrometry (ICP-MS) results obtained by

Service d'analyse des roches et des minéraux (SARM, Nancy, France), and the R2 value obtained.

The R2 value obtained (0.983) shows a satisfactory fit of the equation to transform Fe measurements by XRF into ICP-MS measurements. The XRF measurements have relatively small deviations from the ICP-MS results (roughly $\pm 0.5\%$). All the XRF measurements were corrected using the correlation equation given in Fig. 2.

6.3. Modified water

To simulate conditions similar to those in itabirite concentration plants in the Iron Quadrangle, mineral salts were mixed in the water. This modified water was used in the fundamental studies and flotation tests Table 2.

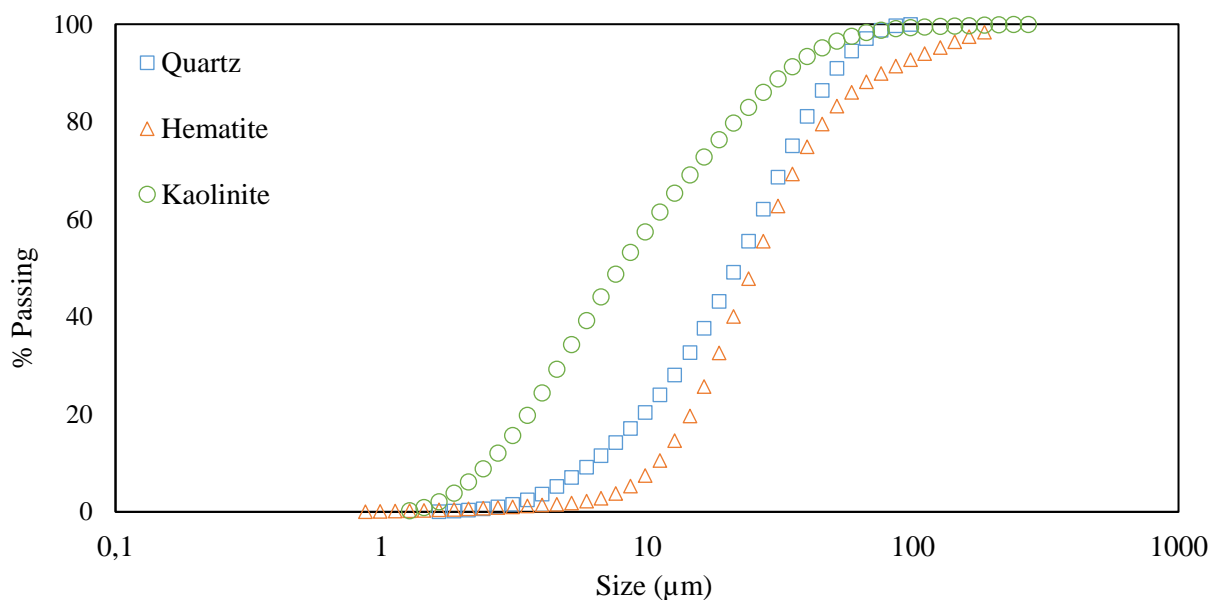


Figure 1 – Particle size distribution of pure mineral samples

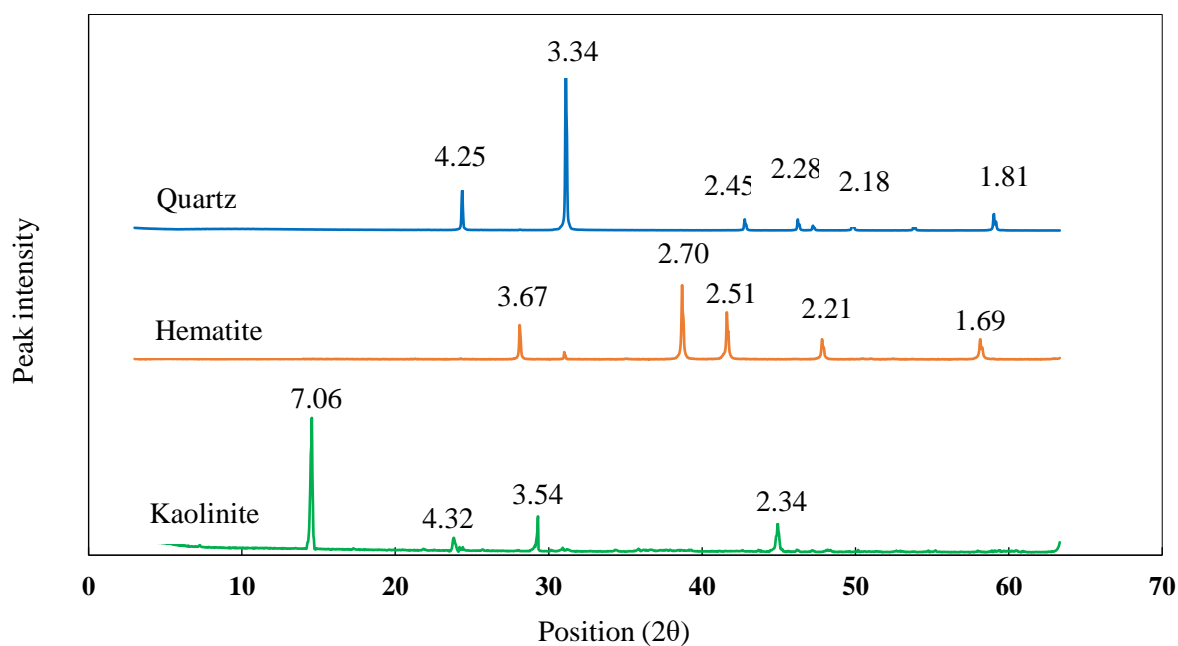


Figure 2– XRD characterization of the hematite, quartz and kaolinite samples

Table 1- Reagents used in the kinetic flotation tests.

Name	Role	Chemical formula	Provider
Corn starch	Depressant	(C ₆ H ₁₀ O ₅) _n	Sigma-Aldrich
Etheramine - Flotigam EDA	Collector	R-O-C ₂ H ₃ -(NH ₂)	Clariant
Amidoamine - N-[3-(Dimethylamino)propyl]dodecanamide	Collector	C ₁₇ H ₃₆ N ₂ O	Clariant
Oleic acid sodium salt - Oleate	Collector	C ₁₈ H ₃₃ NaO ₂	Roth
Sodium hydroxide	pH modifier	NaOH	Carlos Vela

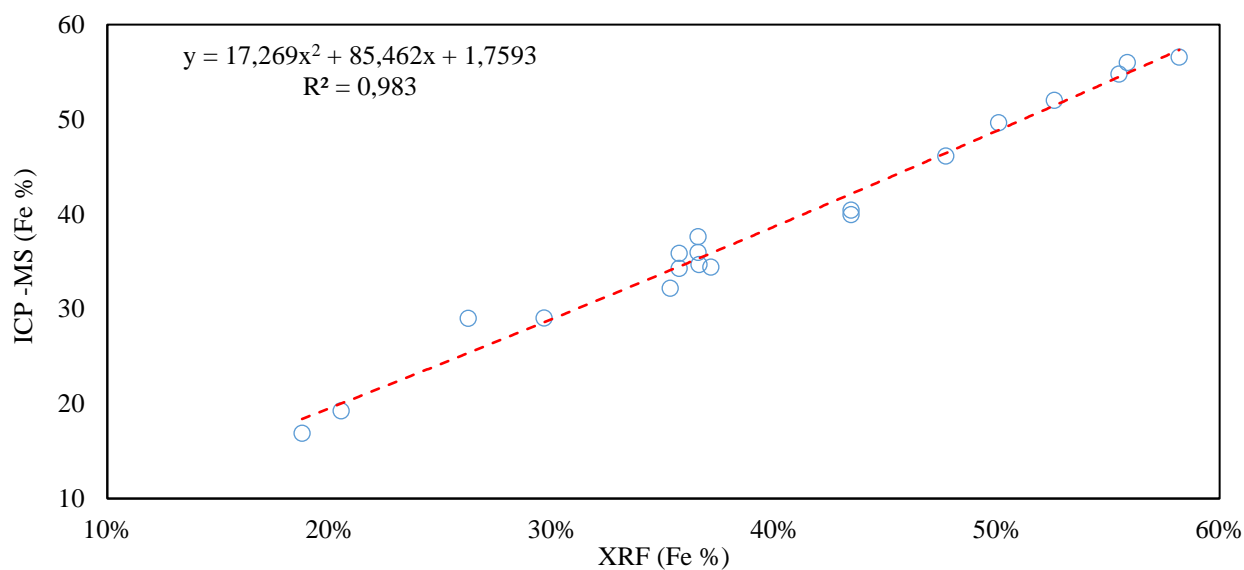


Figure 3- Correlation between Fe contents determined via XRF and ICP-MS.

Table 2 – Chemical analysis results of industrial water and salts used in the modified water

Industrial process water		Modified water used in fundamentals studies	
Element	Concentration (g/L)	Salt used	Salt concentration (g/L)
Na	9.40×10^{-2}	Na ₂ SO ₄	2.91×10^{-1}
K	1.01×10^{-3}	KCl	1.93×10^{-3}
Mn	1.42×10^{-4}	MnSO ₄ .H ₂ O	4.36×10^{-4}
Al	1.12×10^{-4}	Al ₂ (SO ₄) ₃ .18H ₂ O	1.31×10^{-3}
Fe	1.39×10^{-3}	FeCl ₃ .6H ₂ O	6.71×10^{-3}
Ca	1.16×10^{-4}	CaCl ₂ .2H ₂ O	4.25×10^{-4}
S/(SO ₄) ²⁻	$9.21 \times 10^{-2} / 1.22 \times 10^{-1}$	(SO ₄) ²⁻	4.73×10^{-2}
Ionic strength (mol/L)	4.75×10^{-3}	Ionic strength (mol/L)	3.19×10^{-3}

6.4. Contact angle measurements

Contact angle measurements using a DSA25 Shape Analyser (Krüss) for each reagent and dosage were performed.

Prior to the start of contact angle measurements, the samples of the minerals were polished and the exposed surface was carefully cleaned through immersion in aqua regia (HNO₃ 1:3 HCl, in a molar ratio) solution. Thereafter, the sample was subjected to ultrasound emissions for five minutes and intensively washed with ethanol and distilled water. Therefore, this cleaned polished mineral plate was conditioned for five minutes with the depressant, one minute with the etheramine collector, and ten minutes with the amidoamine collector. The conditioning times followed were the ones recommended by the reagent supplier, since they raise the concern that the new amidoamine collector provided was less soluble than etheramine. Consequently, a longer conditioning time was followed to ensure the adsorption efficacy. It is important to mention that even though the recommendations from the provider were followed, it was not observed any differences in the contact angle measurements when applying a conditioning time of one and ten minutes.

The pH was adjusted with sodium hydroxide or hydrochloric acid, when necessary. The contact angle measurements were performed in triplicate for each reagent, dosage, and pH analyzed, and the average values were calculated.

These measurements were performed using only etheramine (dosage of 50, 75, 100, and 200 mg/L), only amidoamine (dosage of 50, 75, 100, and 200 mg/L), etheramine with starch (75 mg/L of collector and 215 mg/L starch), and amidoamine with starch (75 mg/L of collector

and 215 mg/L starch). A reference measurement with only water was also performed. All the tests were performed at 3 different pH levels: 8, 10, and 11.

6.5. Zeta potential

Zeta potentials of hematite, quartz, and kaolinite were obtained through electrophoretic mobility measurements using a Zetasizer Nano (ZS90) system (Malvern Panalytical). The tested reagents were ether- amine, amidoamine, and corn starch. NaOH and HCl were used as pH modifiers. The pure minerals were comminuted below 37 μm and the size was reduced below 5 μm in an agate mortar. A small amount of the mineral powder was then conditioned with the reagent at a fixed concentration in a beaker and an aliquot of the supernatant solution with the mineral particles was analyzed under the following conditions:

- Without reagents
- With etheramine (75 mg/L)
- With amidoamine (75 mg/L)
- With etheramine (75 mg/L) + starch (0.25 mg/L)
- With amidoamine (75 mg/L) + starch (0.25 mg/L)

Evaluations under each of the above conditions were conducted at pH 8, 10, and 11. All zeta potential tests were performed three times for representative purposes.

6.6. Flotation

The flotation efficiency of three collectors (etheramine, oleate, and amidoamine) was evaluated through kinetic flotation tests, performed with pure mineral samples of hematite, quartz, and kaolinite and the mixture of these minerals. The reagents used are listed in Table 1. Each flotation test was performed with 30 g of mineral sample (pure or mixed) in 15% solids content in a Minimet self-aerated flotation machine with a 400 mL cell. All flotations tests were performed three times for representative purposes.

Table 3 – Test parameters for the flotation studies

Reagents	Conditioning time (min)	Dosage (g/t)	pH
Etheramine	5	300	10
Oleate	5	300	Hematite, Quartz: 10 Kaolinite: 7.5 and 10
Amidoamine	5	300	10
Starch	5	1000	10

The flotation tests using a single mineral system were performed to better understand the specific interactions of the tested reagents with a specific mineral. In the first stage of

testing, pure samples of quartz, hematite and kaolinite were floated at pH 10 and using 50, 100, 200, 300 and 400 g/t of amidoamine to determine the best dosage to perform flotation with this collector. After assessing the best dosage, the pH was varied to 11, 10, 9, 8 and 6.5 to assess the effect of pH on the collector's performance.

In the second stage of testing, pure samples of quartz were floated at pH 10 using etheramine, amidoamine, and etheramine with starch. Pure samples of kaolinite were floated using etheramine, amidoamine, etheramine with starch at pH 10, oleate at pH 7.5, and oleate at pH 10. Pure samples of hematite were floated using etheramine, amidoamine, etheramine with starch, and oleate at pH 10. The tests with the mineral mixtures (hematite-quartz; hematite-kaolinite) were performed at pH 10.

After performing the tests with pure mineral systems, the single- mineral flotation system was changed to a two-mineral system to understand the specific impacts that the presence of quartz and kaolinite could have on the flotation of hematite. The mass distributions in terms of hematite minerals and quartz were set with the objective of replicating the mass ratios of some itabirite ores from the Iron Quadrangle. Consequently, a distribution comprising 85% hematite and 15% quartz was selected to study the separation efficiency between quartz and hematite. Additionally, a mineral mixture composed of 85% hematite and 15% kaolinite was used for the two-mineral flotation system.

For the tests using etheramine, amidoamine , oleate, and starch, a conditioning time of 5 min was used. Flotation was performed at pH 10 with dosages of 300 g/t (this dosage was determined by the studies that will be shown later) for the three collector reagents and 1000 g/t for starch. However, for the tests with oleate, additional tests were conducted at pH 7.5 when studying the impacts of hematite with kaolinite.

The test parameters are described in Table 3.

6.7. Infrared measurements

Infrared spectroscopy was performed to study the adsorption of the amidoamine collector on to the surface of minerals such as hematite, quartz and kaolinite. Two types of samples were prepared for IR analysis:

- pure minerals, which were treated with water
- minerals treated with a collector solution at different collector concentrations at pH 10

Infrared (IR) spectra were measured using a laboratory Fourier transform infrared spectrometer (BRUKER IFS 55), equipped with a large-band mercury cadmium telluride (MCT) detector cooled at 77 K. Before the analysis, 2g of pure minerals (hematite, quartz and kaolinite) with a granularity of 20–40 μm was conditioned. The conditioning lasted 60 min and was performed in a 50 mL solution of distilled water, 25°C and collector at pH 10 (adjusted to pH 10 by addition of NaOH).

The total concentration of amidoamine collector was varied from 10 to $5 \cdot 10^{-3}$ Mol per litre. After agitation, the slurry was filtered, and the liquid phase was rejected. Then, the solid phase of minerals samples was washed five times with 50 mL of deionized water at pH 10, filtered and dried in a desiccator. When dried, samples were sent immediately for analysis. Sample preparation for this analysis involved mixing 50 mg of sample with 280 mg of potassium bromide (KBr). All the diffuse reflectance (DRIFT) spectra are recorded with a 2 cm^{-1} spectral resolution. Each sample was scanned 200 times, duration of the analysis was 90 s. The influence of atmospheric water was subtracted.

7. Results and discussions

7.1. Contact angle measurements

Fig. 4 shows the contact angles, on the quartz surface, obtained at pH 8, 10 and 11 using etheramine (a) and amidoamine (b) at 0, 50, 75, 100, 200 mg/L collector dosage. The contact angles measured in the presence of etheramine on the quartz surface were greater than those obtained with amidoamine at all pH values tested.

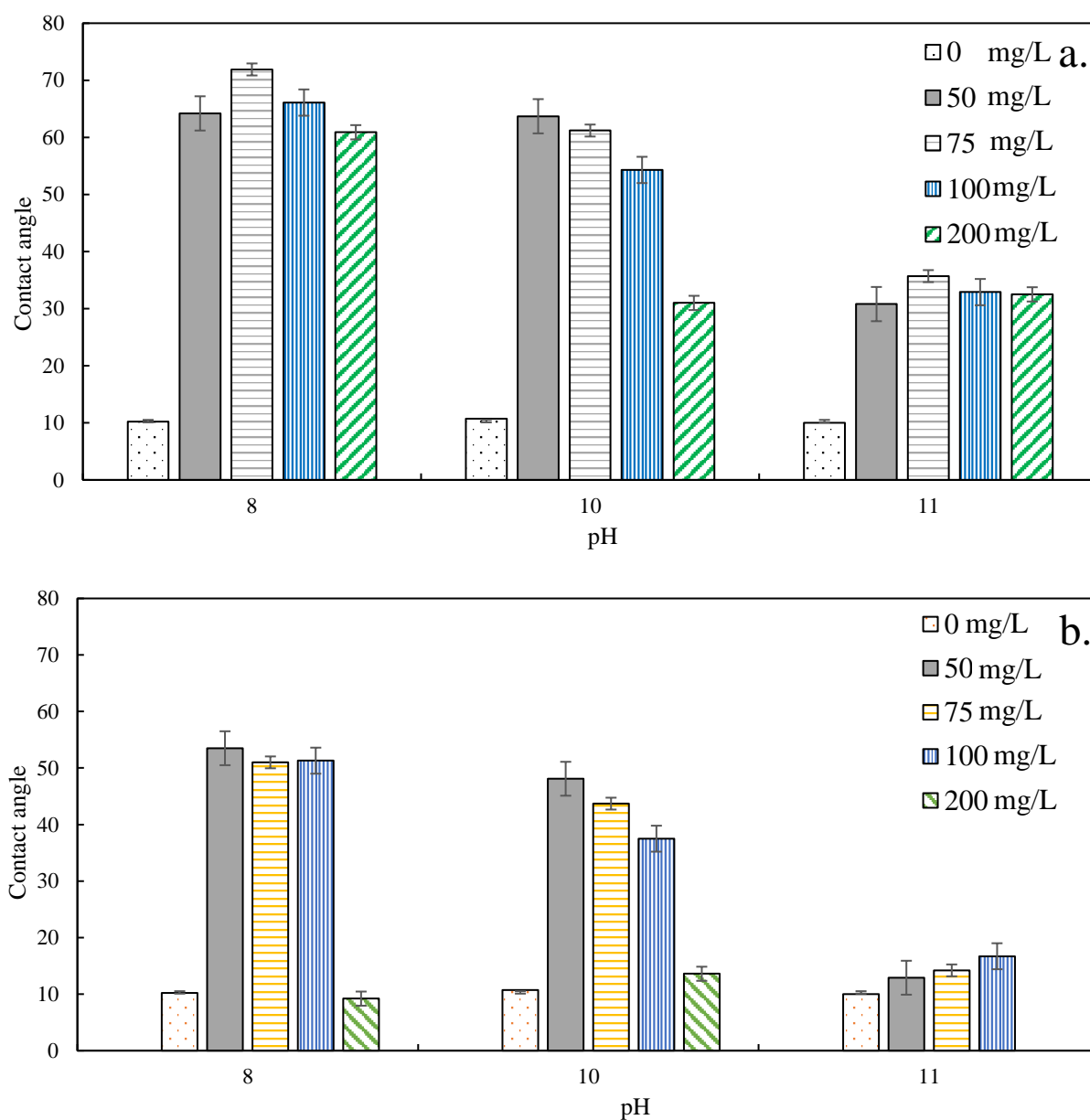


Figure 4 - Contact angle measurements on quartz with standard deviation (SD) estimated based on three experiments. (a) Obtained using aqueous solutions of etheramine. (b) Obtained using aqueous solutions of amidoamine.

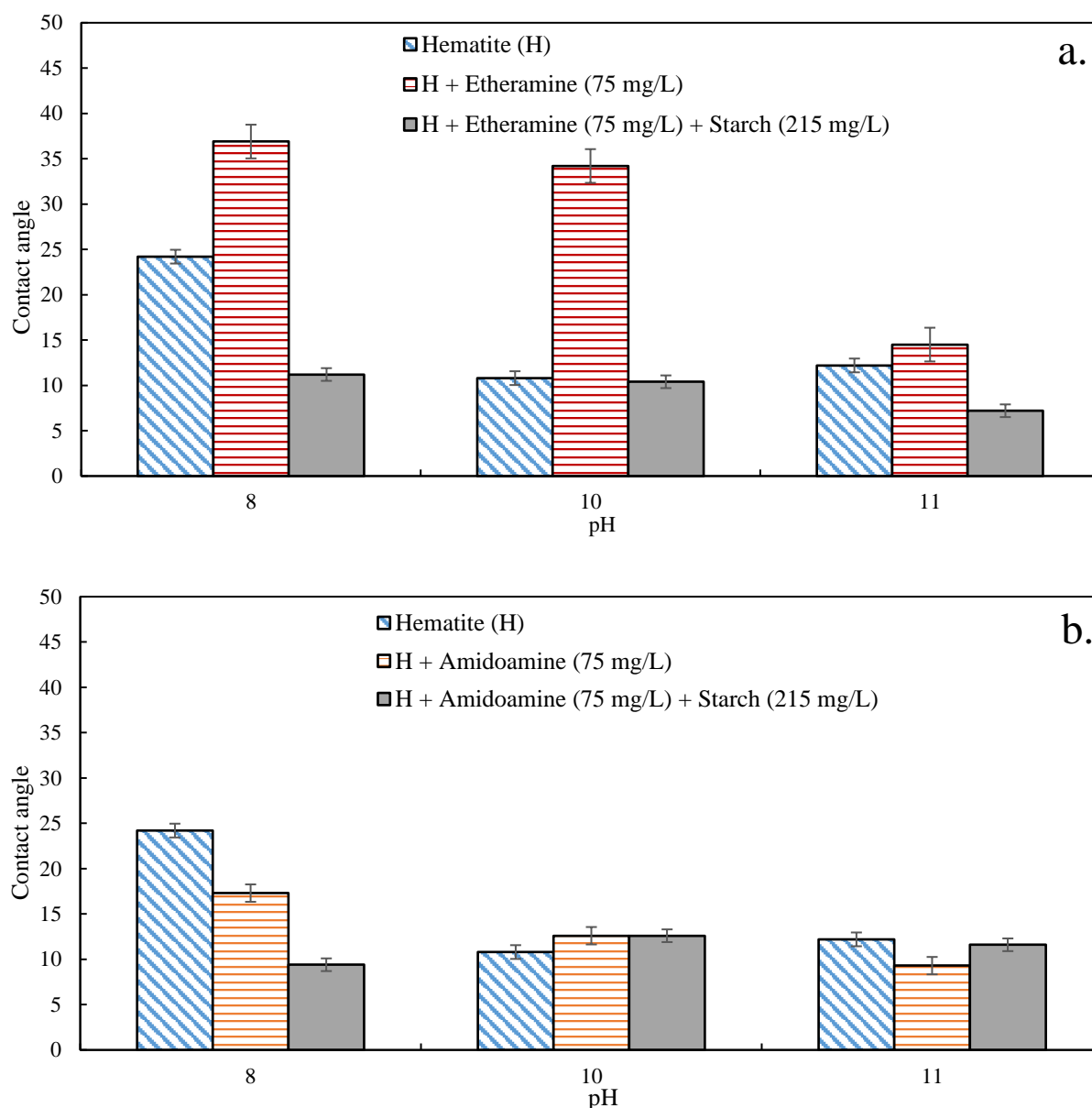


Figure 5 - Contact angle measurements on hematite with SD estimated based on three experiments. (a) Without reagents, in an aqueous solution of etheramine with and without starch. (b) Without reagents, in an aqueous solution of amidoamine with and without starch. Dosage: 215 mg/L of starch, 75 mg/L collector).

Although smaller than the contact angles for etheramine, the angles obtained with amidoamine at pH 8 and 10 showed that this collector could hydrophobise the quartz surface to promote its flotation, considering the analyzed dosages.

The adsorption of the collectors on the mineral surface is dependent on pH, therefore the values of the contact angle depend on the collector's pKa. The molecular structure of the collector is also an important factor affecting the contact angle. The favorable arrangement of adsorbent species due to the collector-collector interactions, for example, can generate different

angular distributions of the collector in the adsorption layer. Considering different collectors, with different molecular structures, different contact angles with the same pH are expected.

The results presented in the Fig. 4 and Fig. 5 allow to deduce a higher surface - hydrophobization with etheramine compared to amidoamine for all concentrations tested. The contact angle values depend on the collector concentration. On contact with water, the minerals showed a contact angle of approximately 10° . This angle increases with the introduction of the collector, towards angles that range from 31° to 72° . For both amidoamine and etheramine there was a tendency that higher dosages caused a subsequent drop in the contact angle. It was possible to observe that the optimal collector dosages were about 75 mg/L for etheramine and between 50 and 75 mg/L for amidoamine. This optimum range varies depending on the reagent structure and pH. In this case, a possible reason for the decreases in the contact angles at high collector dosages was due to the formation of a collector double layer on the mineral surface and/or micelle formation.

At pH 11, the lowest contact angles are observed for both collectors. Regarding the etheramine and its interaction with quartz at pH 11, the contact angle reduction was due to the increase in the RNH_2 molecules, which decreased the adsorption of the collector owing to the low electrostatic forces.

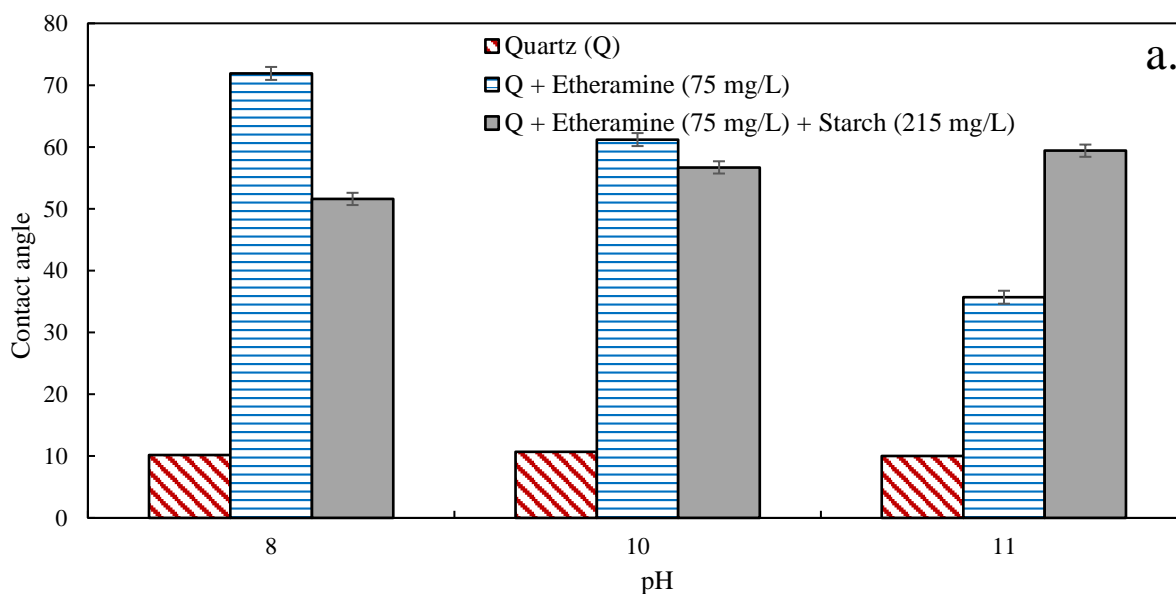
Fig. 5 presents the contact angles obtained as the result of the interactions between hematite and etheramine with and without starch (a), and the interactions between hematite and amidoamine with and without starch (b). It was observed that when using etheramine without a depressant, the contact angle obtained was between 34 and 36° (pH 8 and 10), i.e., a hydrophobicity level allowing the flotation of hematite. The contact angle decreased to 13° at pH 11 showing that at this pH, hematite was not hydrophobized enough to promote its flotation. However, when considering the results obtained in Fig. 4, which showed that the contact angle measured for both etheramine and amidoamine on quartz was also the lowest at pH 11, it can be concluded that pH 11 was not optimal to promote the selective separation between hematite and quartz. On the other hand, the contact angle on the hematite sample with amidoamine changed negligibly, remaining below 20.

The contact angles measured for the hematite conditioned in 215 mg/L of starch solution were close to 10° , indicating efficient surface hydrophilisation, which is consistent with previously reported results regarding starch adsorption on hematite surfaces (Araujo et al., 2005; Kar et al., 2013; Severov et al., 2013). A considerable distinction was observed when comparing the contact angles measured in the presence of starch and etheramine versus the angles obtained in the presence of starch and amidoamine.

At pH 8 the contact angle measured using only etheramine dropped with the addition of starch (from 37 to 11°). On a smaller scale, the same decreasing effect was observed with amidoamine upon the addition of starch, with the contact angle dropping from 17 to 9°. At pH 10, in the presence of only etheramine the contact angle measured was about 34°, with the addition of starch the angle dropped to about 10°. At the same pH, the contact angle measured using solely amidoamine was about 12°, which with the addition of starch remained at about 12°. This shows that, for etheramine, the presence of starch is crucial to impeach the hydrophobization of the hematite surface. Contrary to what was observed for etheramine, the collector amidoamine showed a similar contact angle with and without starch, especially for pH 10 and 11. This similarity indicates that starch is not required to perform a selective flotation between quartz and hematite when using amidoamine at pH 10.

Fig. 6 presents the contact angle measurements on quartz at pH 8, 10 and 11 with etheramine (a) and amidoamine (b), considering a collector dosage of 75 mg/L, with and without starch. Regarding the etheramine collector results, the contact angle of quartz at pH 8 and 10 was reduced in the presence of starch but increased at pH 11, when compared to the angles at the same collector dosage (75 mg/L) without starch.

The interaction of quartz with amidoamine after conditioning with starch showed that the contact angles increased slightly at pH 10 compared to those with no starch at the same collector dosage but dropped significantly at pH 11, as observed in Fig. 6.



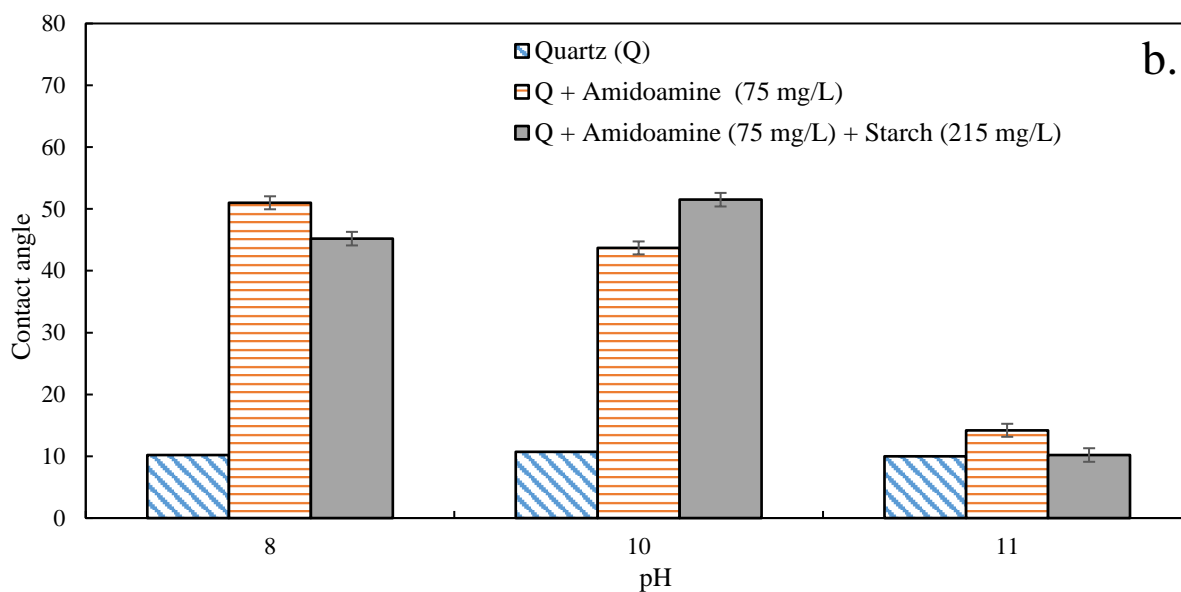


Figure 6 - Contact angles on quartz at pH 8, 10 and 11 in aqueous solutions of (a) etheramine and starch. (b) amidoamine and starch. Collector dosage: 75 mg/L. Starch dosage: 215 mg/L.

7.2. Zeta potential measurements

Surface coverage was assessed by comparing the zeta potential values upon varying pure starch dosages from zero to 215 mg/L and the resultant surface charge of hematite, quartz, and kaolinite after reagent adsorption. Starch concentrations chosen for these tests were a low one, 0.25 mg/L, and a high dosage, 215 mg/L, for adsorption comparison. The concentrations of collectors used in these tests were 75 mg/L for adsorption comparison between the standard collector etheramine and the amidoamine. The zeta potential measurements of hematite, quartz and kaolinite obtained in the presence of starch with etheramine and starch with amidoamine are shown in Figs. 7 and 8 respectively.

Fig. 7 shows that the low and the high starch dosage associated with the collector etheramine (75 mg/L) resulted in close to zero surface charges for quartz and kaolinite at pH 10 (Fig. 7 a. and b.). Diversely, for hematite the low dosage with etheramine was not sufficient to cover the hematite surface, leaving exposed negative surface charges (-15.3 mV) that were only neutralized by the higher starch dosage 215 mg/L, reversing the hematite surface charge to + 1.72 mV (Fig. 7c). By comparing Fig. 7 to Fig. 8 it can be observed that the surface charges resultant from the amidoamine adsorption onto quartz were more negative, meaning that higher dosages of this collector should be evaluated for denser surface coverage.

Similar to the contact angle studies on the quartz and hematite surface, the collector dosage selected to analyze the zeta potential was 75 mg/L. Both etheramine and amidoamine modified the surface charge of hematite, quartz, and kaolinite (Figs. 9, 10 and 11). The zeta

potential values observed for hematite and quartz agreed with previously reported results obtained using pure water and in the presence of etheramine (Filippov et al., 2010; Veloso et al., 2018).

Increases of approximately 25 and 15 mV in the positive surface charge were observed for hematite in the presence of etheramine at pH 8 and 10, respectively, when compared to the reference (hematite without reagent) (Fig. 7a). These findings are consistent with the trends and values observed by Filippov et al. (2010). The zeta potential increased by approximately 55 mV when hematite was conditioned with amidoamine at pH 8.

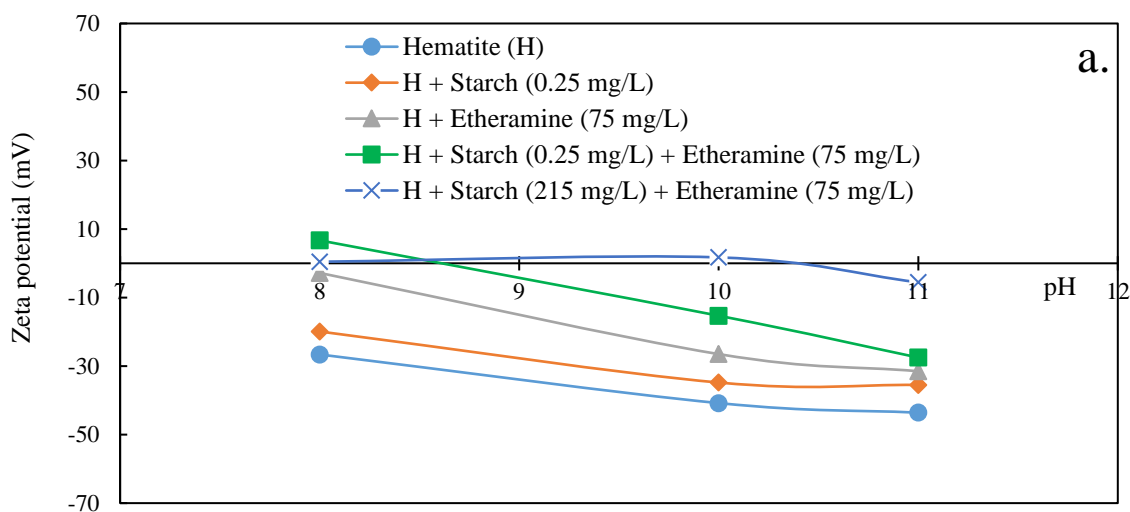
The increase in the zeta potential at pH 8 and 10 in the presence of etheramine and amidoamine for quartz and kaolinite (Fig. 10 and Fig. 11) when compared to that of the reference (without reagent) can be explained by the negative charge compensation due to the adsorption of collectors through the amine groups. However, the zeta potential increased significantly at pH 8 for amidoamine, whereas the zeta potential variation for etheramine was slightly pronounced at pH 10. The values of the zeta potentials were similar for both the collectors at pH 11. This shows that the biggest difference in the adsorption behaviour between both collectors occurs at pH 8 and 10, a similar result that was already observed and discussed based on the contact angle studies in section 3.1. The proximal values of the zeta potentials for the amine at pH 11 in all the tested minerals can be explained by the pK values close to 10.5, observed for the amine collectors (Smith and Scott, 1990). The decreased concentration of the ionic forms of the collectors decreases their adsorption on the mineral surface at an alkaline pH higher than 10.5.

The surface charge values of hematite and kaolinite in the presence of starch and etheramine are slightly higher than those obtained only using etheramine. These results confirm the different adsorption behaviours of starch on kaolinite and quartz. They corroborate the findings of Ma and Bruckard (2010), explaining that the adsorption behaviour of starch on the quartz surface cannot be extrapolated to that on kaolinite in reverse cationic flotation of iron ores. The adsorption of starch on the hematite surface is controlled by hydrogen bonding and chemical complexation (Weissenborn et al., 1995). The adsorption density of starch on the quartz surface is lower than that on the hematite surface and is controlled by hydrogen bonding (Filippov et al., 2013). Thus, depending on the hydrolysis of the surface groups, the adsorption of starch may lead to additional surface charge compensation.

Another hypothesis for this phenomenon observed in quartz with etheramine and starch could be the formation of clathrates (Aguiar et al., 2017). The complexes between starch and etheramine can lead to higher adsorption of etheramine on the quartz surface, contributing to

the reduction in the zeta potential. However, the intermolecular hydrogen bonding between the amylose chains and hydroxyl groups of the glucose molecules in starch leading to helicoid formation and then to starch–amine clathrate aggregates is observed only at higher starch concentrations. According to Khosla and Biswas (1984), free starch molecules are adsorbed at the active sites of the mineral surface until saturation is reached. In this case, starch adsorption resulting in clathrate formation will not follow the linear pattern observed in the experimental data provided by Filippov and co-workers (Filippov et al., 2013). Thus, another explanation for this phenomenon is that starch can co-absorb at the quartz–solution interface, in association with etheramine.

The presence of starch did not considerably change the zeta potential of any of the minerals with amidoamine. The results presented in this section in combination with the contact angle measurements suggest that amidoamine is a potential collector for iron ore beneficiation, specifically because it can promote the selective flotation of quartz and hematite without a depressant. The following section presents the findings of the flotation experiments performed with the pure minerals and mineral mixtures.



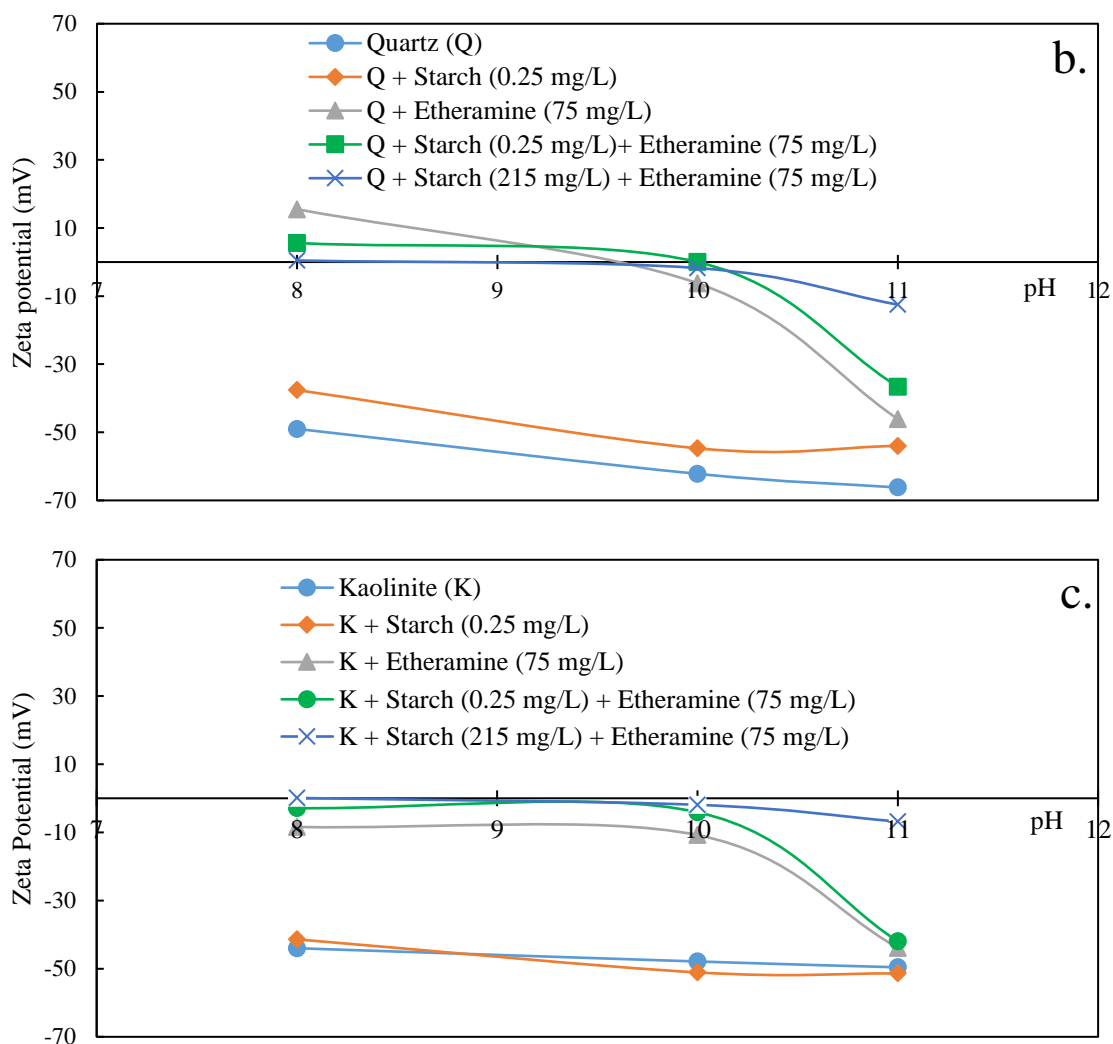
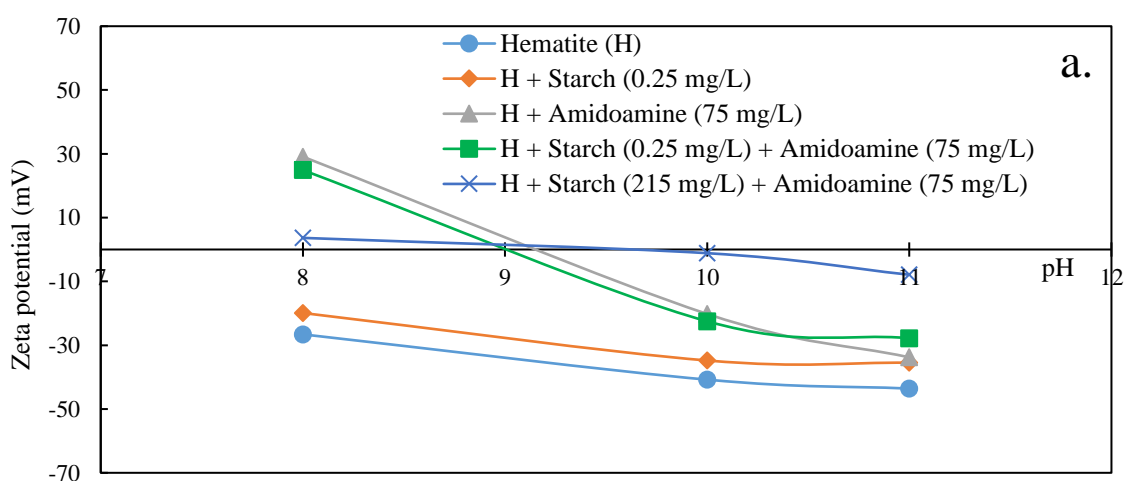


Figure 7 - Zeta potential of hematite (a), quartz (b) and kaolinite (c) with starch and etheramine.



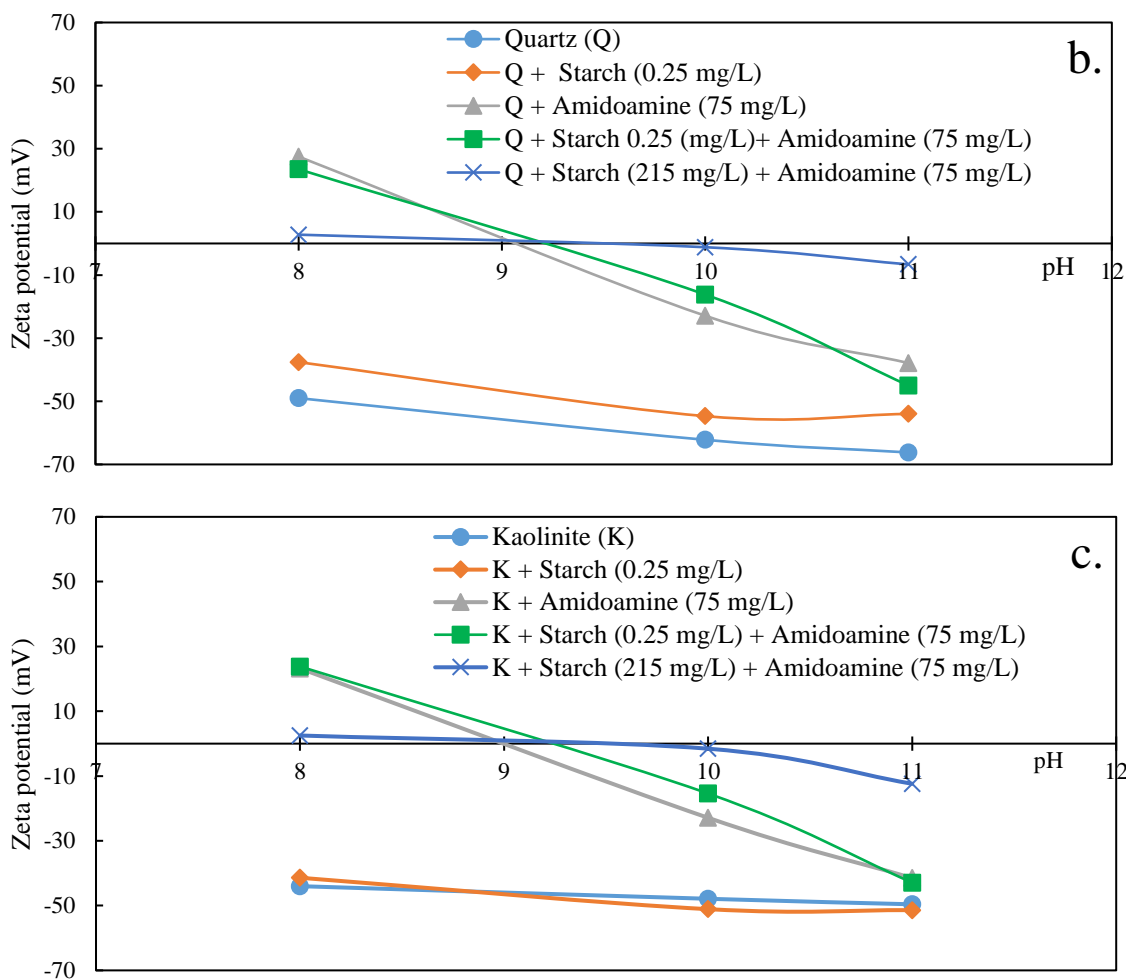
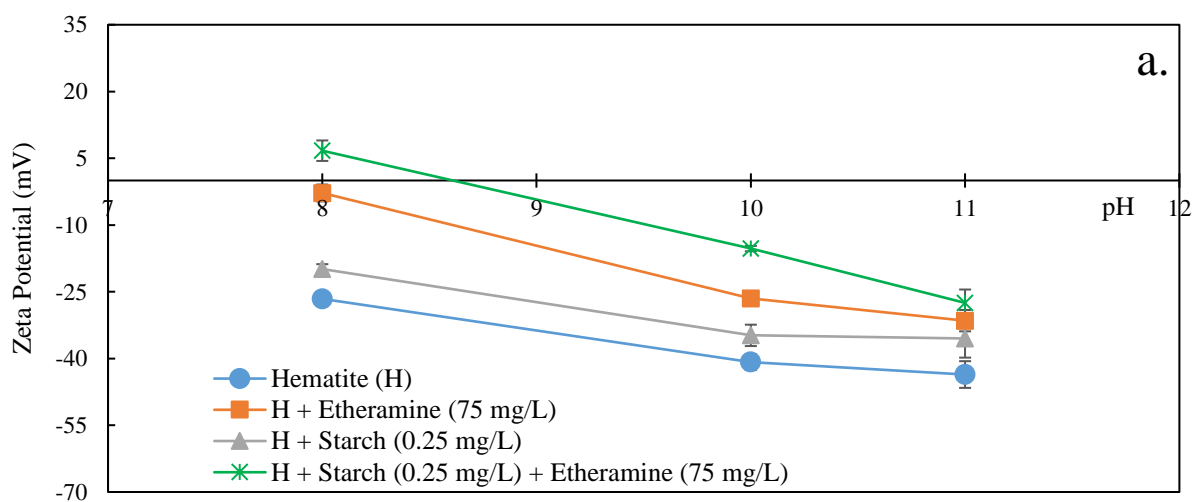


Figure 8 - Zeta potential of hematite (a), quartz (b) and kaolinite (c) with starch and amidoamine.



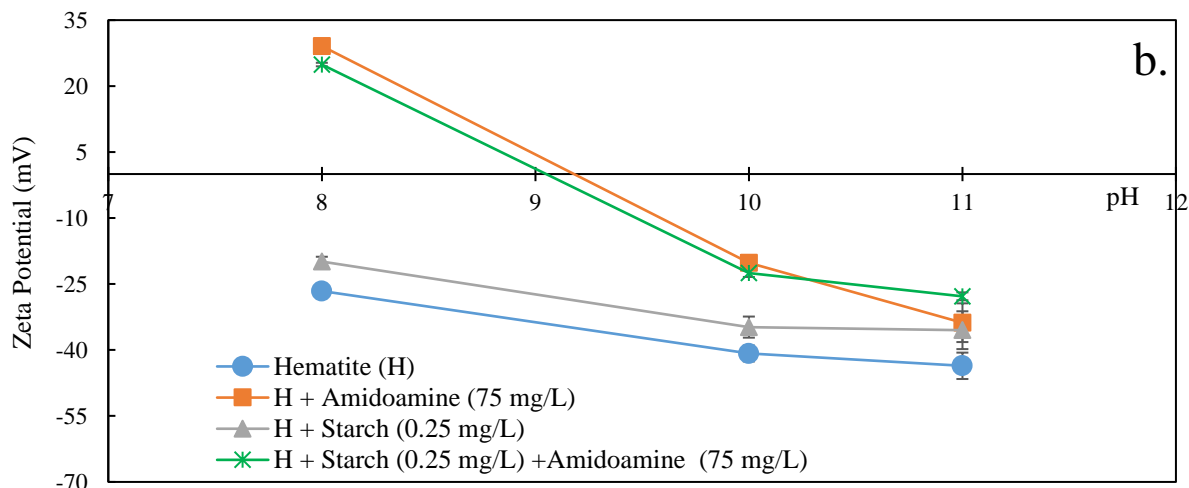


Figure 9 - Zeta potentials of hematite under different experimental conditions (SD is shown on the graph and the value varies between 0.6 and 4.4). (a) Hematite with etheramine. (b) Hematite with amidoamine.

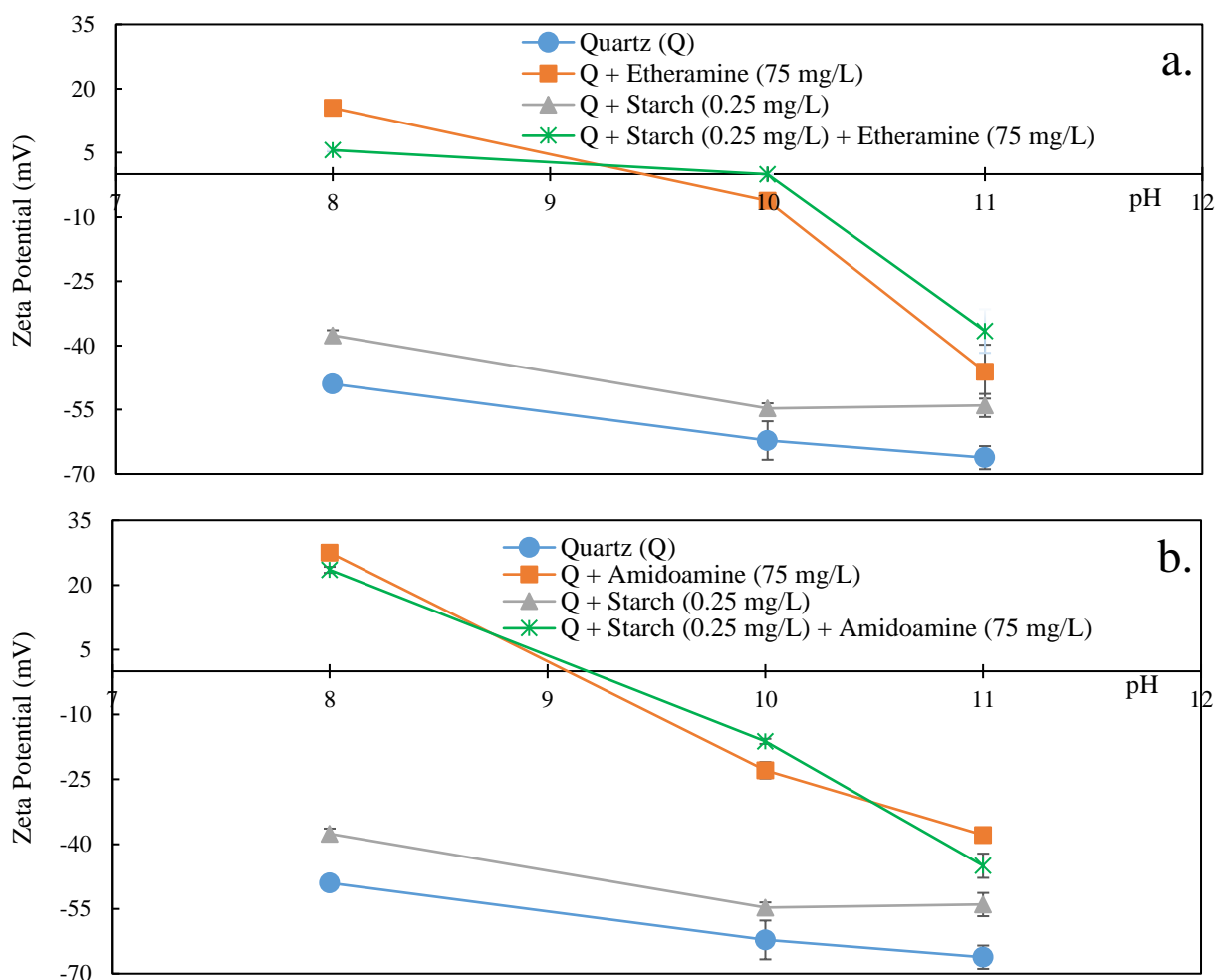


Figure 10 - Zeta potentials for quartz under different experimental conditions (SD is shown on the graph and the value varies between 0.3 and 6.3). (a) Quartz with etheramine. (b) Quartz with amidoamine.

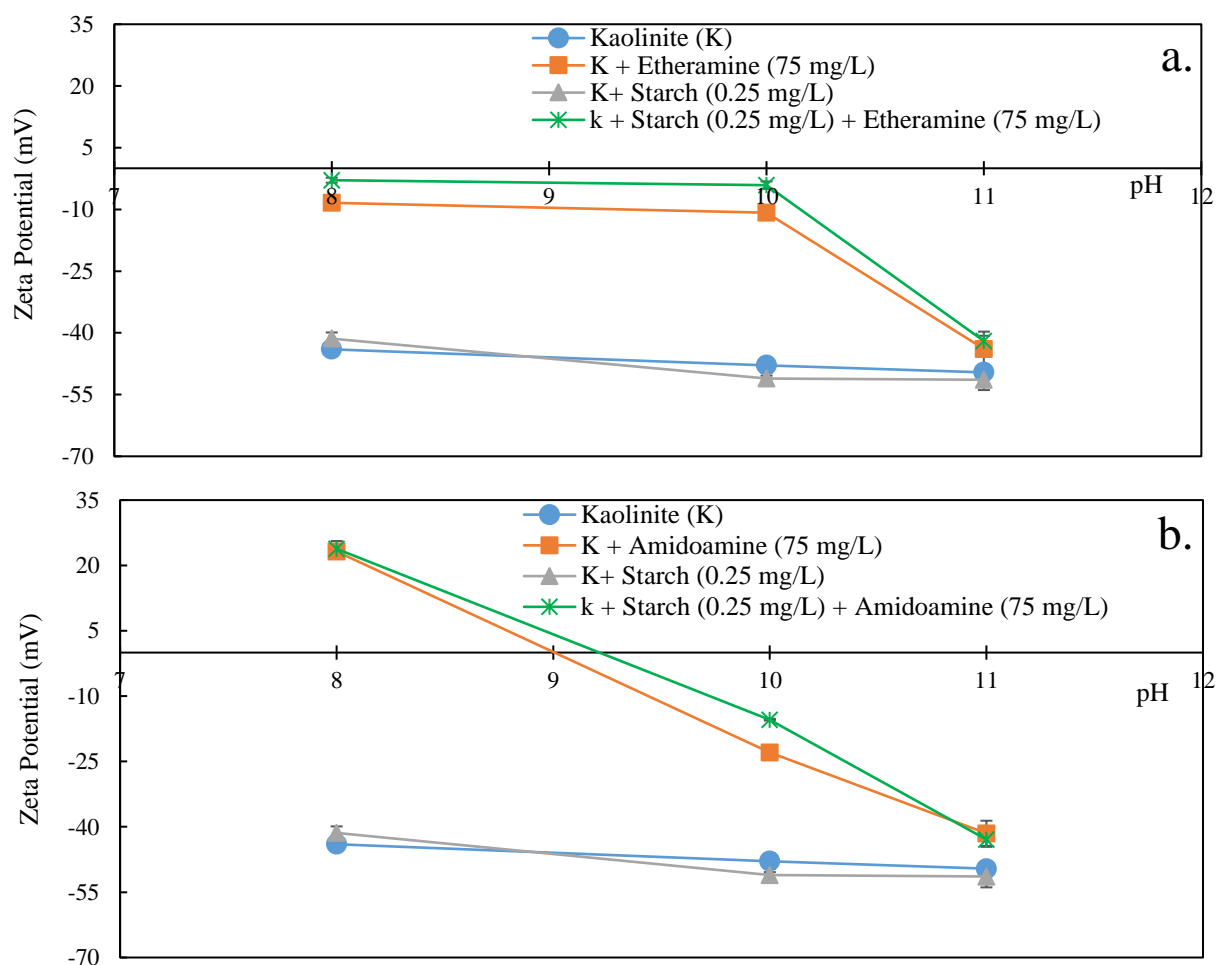


Figure 11- Zeta potential for kaolinite under different experimental conditions (SD is shown on the graph and the value varies between 0.6 and 2.9): (a) Kaolinite with etheramine. (b) Kaolinite with amidoamine.

7.3. Flotation of pure minerals

Table 4 shows the results of the flotation tests with a single mineral system: hematite, quartz, and kaolinite at pH 10 at 50, 100, 200, 300 and 400 g/t of amidoamine.

Table 4 - Recovery of hematite, quartz, and kaolinite (single mineral flotation system) to the floated fraction at pH 10 at 50, 100, 200, 300 and 400 g/t of amidoamine.

Amidoamine dosage (g/t)	Recovery to floated (%)		
	Hematite	Quartz	Kaolinite
50	0	18	0
100	0	43	0
200	1	70	0
300	1	89	1
400	12	97	10

The results showed that at the dosages of 50 and 100 g/t no hematite was recovered to the floated product. The maximum hematite recovery (12% recovery) was achieved when

dosing 400 g/t of collector. Contrarily to hematite, quartz reported to floated product at 50, 100 and 200 g/t, achieving 18, 43 and 70% recovery respectively. Kaolinite started to report to the floated product at 300 g/t, achieving 10% recovery at 400 g/t.

Based on the results presented in Table 4 and discussed above, the dosage of 300 g/t was selected to perform the future flotation studies. This dosage was selected since at 300 g/t the hematite recovery to floated product was still considerably close to 0% (app. 1% recovery) while the recovery of quartz was at 89%. In the other words, this dosage could promote a selective flotation of quartz while providing lower losses of hematite to the floated product. Table 5 shows the results of the flotation tests with a single mineral system: hematite, quartz, and kaolinite at 300 g/t of amidoamine at pH 6.5, 8, 9, 10 and 11.

Table 5 - Recovery to the froth product of hematite, quartz, and kaolinite at 300 g/t of amidoamine as a function of pH (single mineral flotation system).

pH	Recovery to floated (%)		
	Hematite	Quartz	Kaolinite
11	1	44	3
10	2	89	1
9	10	94	3
8	11	100	1
6.5	13	98	6

The results show that the recovery of quartz was higher at more low pH values. The recovery of quartz was the lowest at pH 11 (44%), increasing to 89% at pH 10, to 94% at pH 9 and to 100 % at pH 8. Hematite recovery to floated increased by about 8% when the pH value decreased from 10 to 9. Hematite reported a relatively constant recovery to the floated product (10 to 13%) at pH 9, 8 and 6.5. Kaolinite recovery was the highest at pH 6.5, with 6% recovery.

The decrease in the flotation response of the quartz at pH11 is in perfect agreement with the contact angle measurements and can be related to $pK_a \approx 8.2$ value (communicated by Clariant) when the molecular forms of collectors dominate in the solution with less adsorption capacity on the negatively charged mineral surface.

Based on the results summarized in table 5, the value of pH 10 was adopted to continue the future flotation studies because it was the pH value that reported the lowest loss of hematite to the floated product (app 1% recovery) while providing a recovery of quartz of 89%.

Hematite

The flotation kinetics curves for hematite obtained using the etheramine, etheramine with starch (reverse cationic flotation), amidoamine and oleate at pH 10 are presented in Fig. 12.

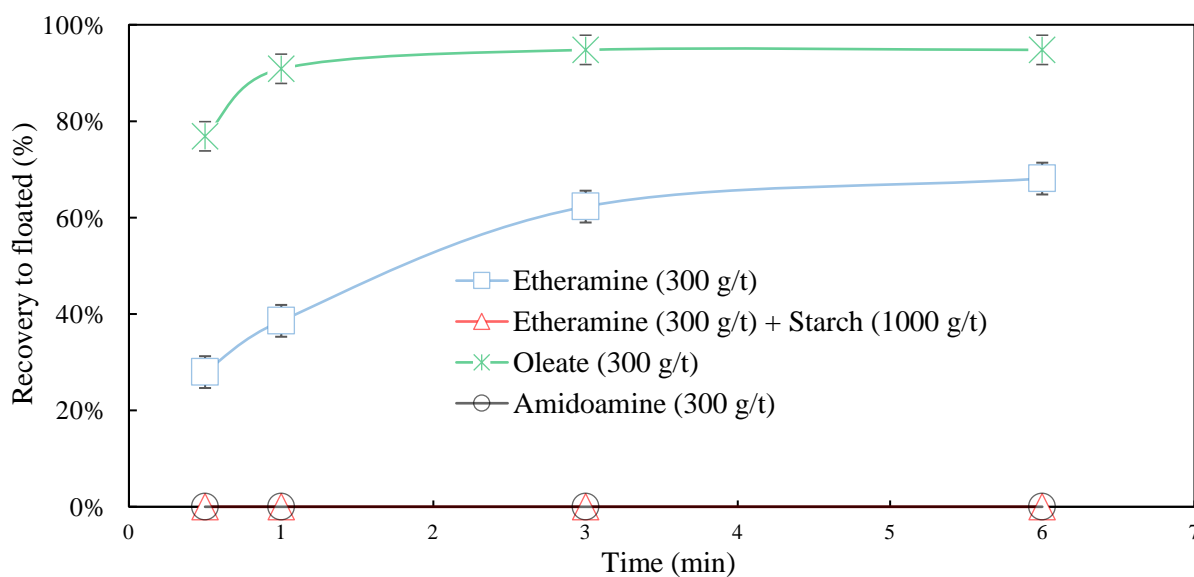


Figure 12 – Hematite recovery in bench-scale tests using etheramine, etheramine with starch, oleate and amidoamine at pH 10.

Both oleate and etheramine (without starch) promoted hematite flotation (Fig. 12). Oleate enabled greater mass recovery in the floated product for the same specific dosage at 300 g/t. The pure hematite flotation tests performed with amidoamine as the collector showed that no hematite was floated. This absence of hematite flotation is in accordance with the contact angle measurements for hematite with amidoamine. Moreover, when comparing the hematite recovery to the floated fraction by etheramine (68%) versus the recovery obtained with etheramine and starch (0%) it becomes visible that the presence of starch was essential to inhibit the flotation of hematite by etheramine, contrary to amidoamine which did not require the addition of starch to inhibit hematite flotation.

Kaolinite

The flotation kinetics curves for pure kaolinite obtained using the etheramine, etheramine with starch (reverse cationic flotation), amidoamine and oleate at pH 10 are presented in Fig. 13.

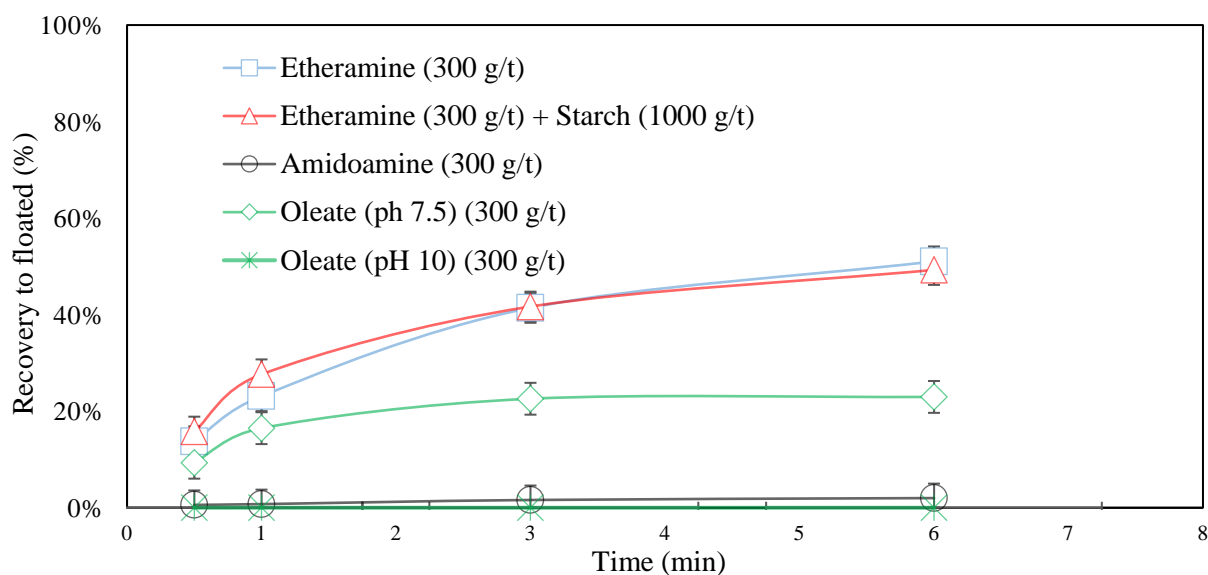


Figure 13 – Kaolinite recovery in bench-scale tests at pH 10 with etheramine, etheramine with starch, amidoamine and oleate (pH 7.5 and 10).

The etheramine floated 51% of kaolinite, a result that remained relatively unchanged upon the addition of starch. The floatability obtained when using etheramine can be explained by the high specific surface area of the kaolinite, which may require higher doses of the collector. Some studies have reported that kaolinite has characteristics that pose challenges during concentration through cationic collectors, such as amines. The kaolinite crystal system has an anisotropy that causes it to behave in a manner opposite to that of quartz in terms of the pH dependence on cationic flotation (Xu et al., 2015). The flotation of the fine kaolinite particles is also impacted by the increased number of edges to adsorb the amines in a cationic form which decreases adsorption layer density.

When varying the pH to obtain more alkaline values, the negative surface charges of the oxides and silicates are enhanced, thereby increasing the adsorption of the cationic collector and, consequently, the floatability of the mineral. Ma et al., (2009) reported that the flotation behavior of quartz cannot be extrapolated to that of kaolinite owing to the face-edge structure of kaolinite. Kaolinite is an aluminosilicate that has two different surfaces parallel to the (001) plane in its structure: a (001) plane formed from the tetrahedral sheet (SiO_4) and the second plane formed from the AlO_6 octahedron (Liu et al., 2015). At an alkaline pH, preferential adsorption occurs at the SiO_4 basal plane. Hydrophobic aggregation seems to occur owing to the chain-chain associations between collector molecules adsorbed at the SiO_4 basal plane. Consequently, the (001) planes of AlO_6 are exposed, thus reducing the floatability of kaolinite (Xu et al., 2015). The basal plane of SiO_4 exhibits a strong affinity for cationic collectors and

is responsible for kaolinite flotation, whereas the AlO_6 plane has limited interactions with cationic collectors and remains hydrophilic (Yuehua et al., 2004). Thus, preliminary conditioning with starch does not impact kaolinite flotation because of two competing phenomena: hydrogen bonding between the hydroxyl groups of starch and alumina tetrahedron and repulsion between anionic starch molecules and negatively charged basal planes of the silanol surface (Ma and Bruckard, 2010).

Oleate did not promote the flotation of pure kaolinite at pH 10. At pH 7.5, it could enable flotation of approximately 20% of the kaolinite at a dosage of 300 g/t. Owing to the anisotropic structure of kaolinite, the zeta potential on the surface of each plane varies differently in relation to the pH. The isoelectric point of the AlO_6 face is between pH 6 and 8 and the same for the SiO_4 face is observed at approximately pH 4 (Gupta and Miller, 2010). As oleate is an anionic collector, physical adsorption seems to occur at pH 7.5 because the surface charge of the AlO_6 face in kaolinite is positive. However, the mass recovery is low (23%) at a dosage of 300 g/t. At pH 10, no flotation occurred owing to physical adsorption because of the high hydroxyl ion concentration. Thus, the amidoamine at dosage of 300 g/t did not promote a significant kaolinite recovery to the floated product.

Quartz

The flotation kinetics curves for pure quartz obtained using each reagent are presented in Fig. 14.

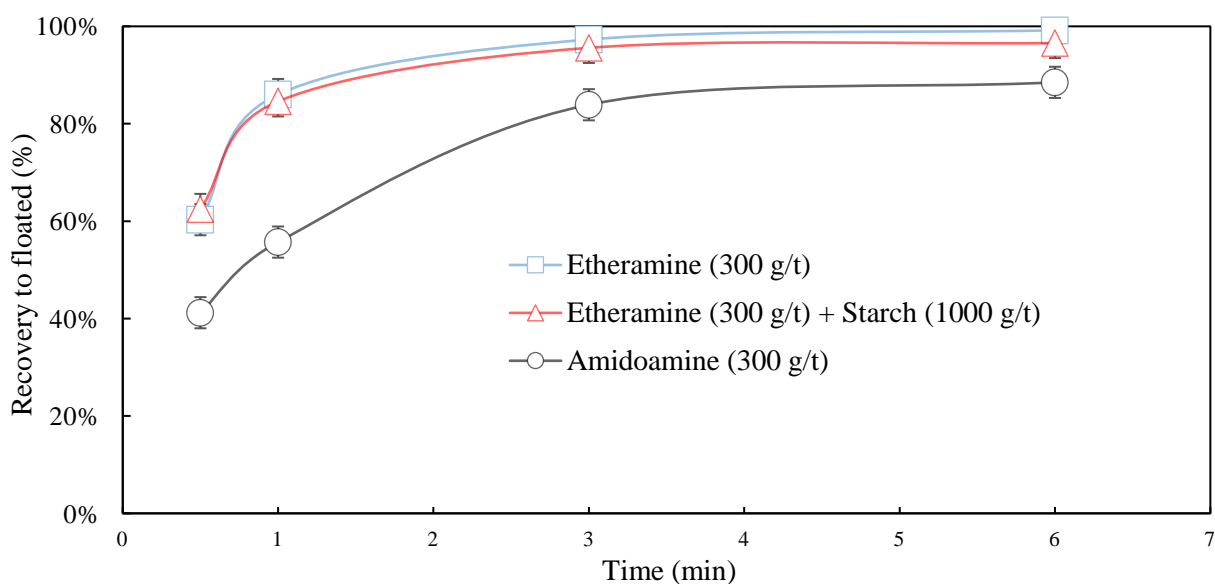


Figure 14 – Quartz recovery in bench-scale tests with etheramine, etheramine plus starch, and amidoamine.

The quartz recovery obtained when only using amine is considerably similar to the recovery obtained when using amine with starch, meaning that starch had virtually no depression effect on quartz flotation. Literature suggests that a lack of quartz depression does not mean that there is no adsorption of starch to the surface of quartz (Filippov et al., 2013). Several authors reported starch adsorption on hematite and not on quartz surface (Balajee and Iwasaki, 1969; Cooke et al., 1952; Peres and Correa, 1996). Pavlovic and Brandão (2003) showed a decrease in the floatability of quartz in the presence of starch while the flotation of hematite flotation was depressed. Moreover, the adsorption studies performed with different polysaccharides led to conclude about the starch adsorption on the hematite, quartz and other silicates (Pavlovic and Brandão, 2003; Dogu and Arol, 2004, Filippov et al., 2013). However, the starch adsorption on the quartz was difficult to confirm using the surface sensitive techniques, i.e., infrared spectroscopy. Pavlovic and Brandão (2003) suggested that the very intense IR absorption bands of quartz in the same wavenumber area where important carbohydrates bands occur makes the detection of the polysaccharides difficult. Severov et al. (2013) and Filippov et al. (2013) agreed that hydrogen bonding is difficult to confirm from the IR spectra because starch molecules are capable of forming intramolecular hydrogen bonds. However, analyzing the vibration band of the other involved groups (C-O stretch and C1/H deformation) they have proved the hydrogen bonding on the quartz from the FTIR spectra.

The amidoamine collector promoted quartz flotation. However, for the same collector dosage of 300 g/t, etheramine achieved a higher mass recovery. The mass recovery when only using etheramine was almost 100% after 6 min of flotation versus 88% recovery with amidoamine.

The results showed that at the dosages of 50 and 100 g/t no hematite was recovered to the floated product. Hematite started to report to the floated product at 200 g/t (1% recovery), with recovery reaching 12% when dosing 400 g/t of collector.

7.4. Flotation of mineral mixtures

Mixture: 85% hematite and 15% quartz

The flotation kinetics curves for the hematite–quartz mixture are presented in Fig. 15.

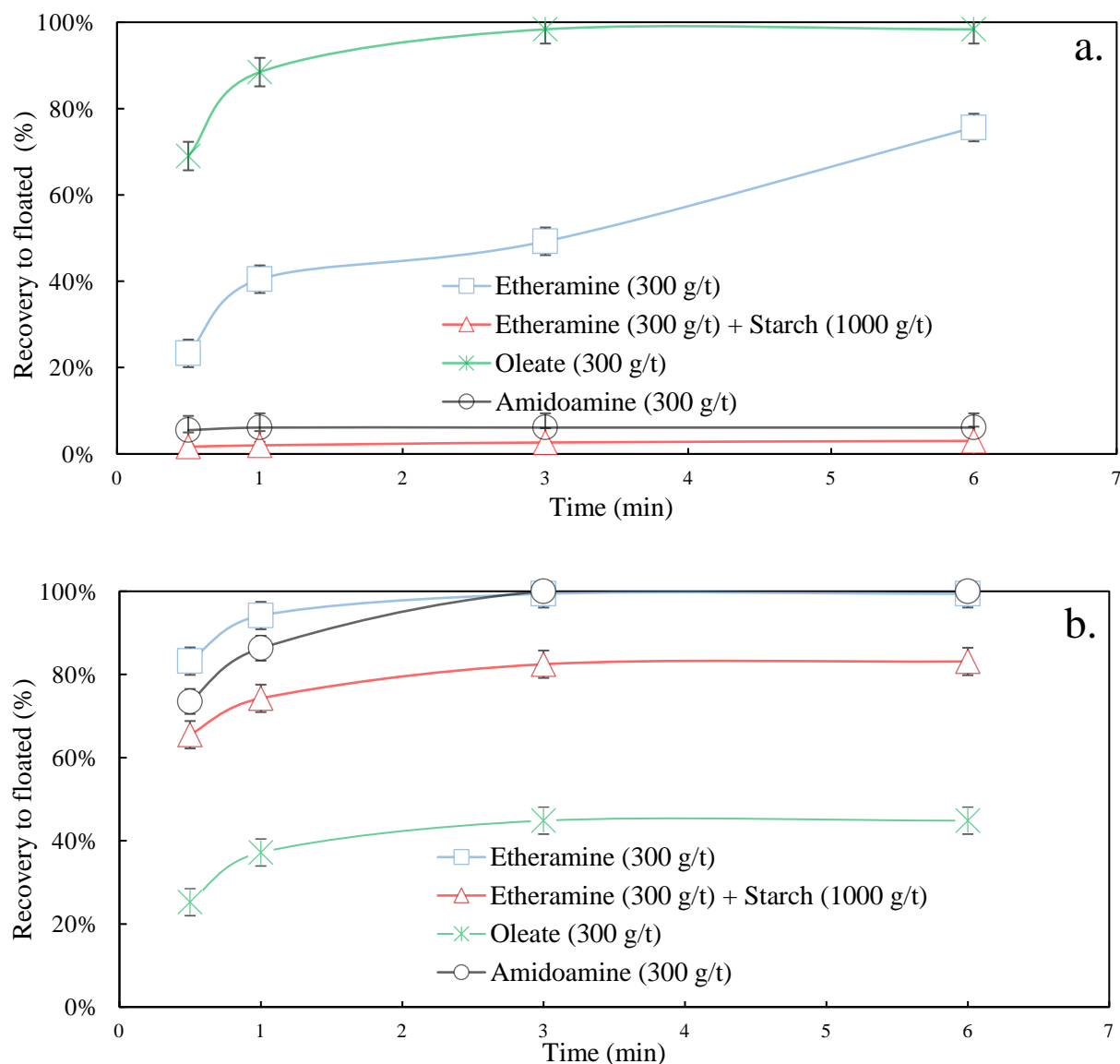


Figure 15 – Flotation test results of the hematite–quartz mixture at pH 10: (a) Hematite recovery. (b) Quartz recovery.

The results presented in Fig. 15 agree with those available in the literature (Araujo et al., 2005) indicating that a depressant is necessary for quartz during direct flotation of hematite with oleate to obtain adequate selectivity in the concentration process. For recovering approximately 100% of the hematite in the froth product with oleate, a recovery of approximately 45% was achieved for quartz as well.

Similarly, a depressant was found to be required for hematite during quartz flotation using amine collectors to achieve adequate selectivity in the concentration process. When using only etheramine almost 100% of the quartz and 50% of hematite reported to the froth product. The hematite recovery to the floated fraction by etheramine dropped to 3% upon the addition of starch.

The reverse flotation of quartz using amidoamine reported satisfactory results without the addition of starch. This collector enabled 100% recovery of quartz to the floated fraction, whereas approximately 94% of the hematite was not floated. One of the possible reasons for the rejection of approximately 6% iron content when using amidoamine in the flotation process may be due to hematite dragging in the froth during the flotation of quartz (entrainment and entrapment).

A considerable selectivity was attained by using amidoamine as collector without any depressant. The starch has an unselective flocculation effect of particles under 5 μm (Weissenborn et al., 1995). In conventional operations of iron ore beneficiation by flotation, the flotation feed is deslimed to remove the 10 μm fraction prior to flotation (Filippov et al 2014), thus the unselective flocculation effect of starch does not affect the flotation selectivity. Contrary to what occurred in this study, where the pure mineral samples used for the flotation tests were not deslimed. Therefore, it could be stated that by using amidoamine, additionally to eliminating the necessity of a depressant agent in the reverse flotation of iron ore may as well eliminate the necessity of having a desliming stage before the flotation process.

Fig. 16 shows that higher specific dosages (g/t SiO_2) of amidoamine improved the recovery of quartz, reaching 100%. The results of the flotation tests conducted for a mixture of pure minerals indicate that is possible to obtain selective flotation of quartz in the reverse approach without a depressant. However, to reach the same recovery level as that achieved using the amine collector, it is necessary to use a higher dosage of amidoamine than etheramine.

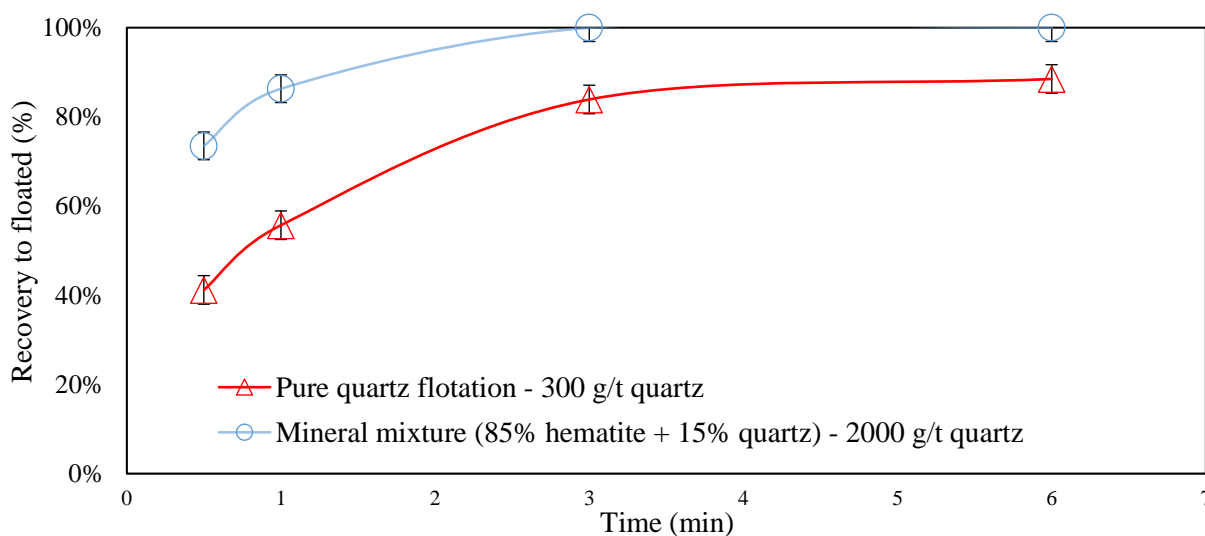


Figure 16 – Quartz recovery using amidoamine on pure quartz sample and in hematite–quartz mixture at pH 10.

Mixture: 85% hematite and 15% kaolinite

The flotation kinetics curves for the hematite–kaolinite mixture are presented in Fig. 17.

Regarding the direct flotation of hematite with oleate, at pH 10, approximately 95% hematite and (Fig. 17a) 16% kaolinite were recovered (Fig. 17b). The oleate collector showed good selectivity, indicating the possibility of direct flotation (considering the hematite/kaolinite composition) without using depressants.

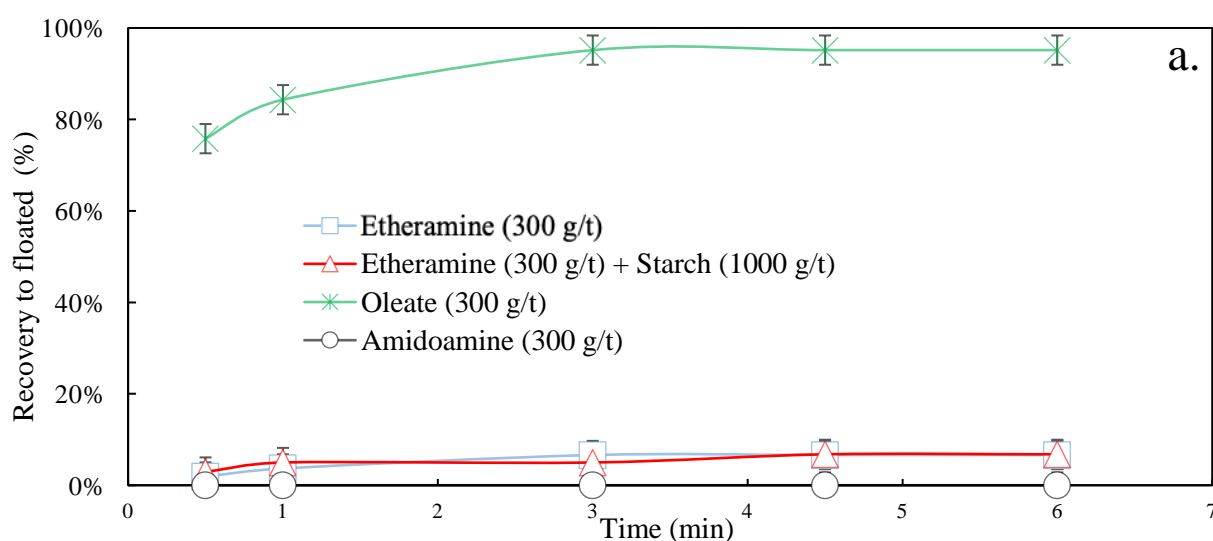
In the reverse flotation of kaolinite with etheramine without a depressant, 57% of the kaolinite mass was floated (Fig. 17b), whereas approximately 7% of hematite mass was floated (Fig. 17a). The use of starch reduced kaolinite recovery to 43% to the floated fraction (Fig. 17b), maintaining the hematite recovery at 7% (Fig. 17a).

The results obtained for the flotation of pure hematite and hematite–kaolinite mixture using the etheramine collector are shown in Fig. 18.

The recovery of iron oxide reduced from 68% to approximately 7% in the presence of 15% kaolinite. The presence of kaolinite appears to inhibit the cationic flotation of hematite by the etheramine. As mentioned previously, the SiO_4 face on kaolinite is capable of adsorbing etheramine, but the flotation of kaolinite is hampered by an anisotropy in its structure.

When compared to pure kaolinite flotation, the kaolinite recovery after 6 min of flotation showed an increase from 51% (pure kaolinite flotation) to 57% (kaolinite flotation in the hematite–kaolinite mixture), as shown in Fig. 19. However, although the total collector dosage was the same in both tests, the specific dosage of the collector (g/t kaolinite) varied from 300 g/t (pure kaolinite sample) to 2000 g/t (hematite–kaolinite mixture).

For the results obtained using amidoamine with the hematite–kaolinite mixture, the same results as those obtained in the pure mineral flotation tests were obtained; that is, the amidoamine collector did not float kaolinite and hematite at a dosage of 300 g/t.



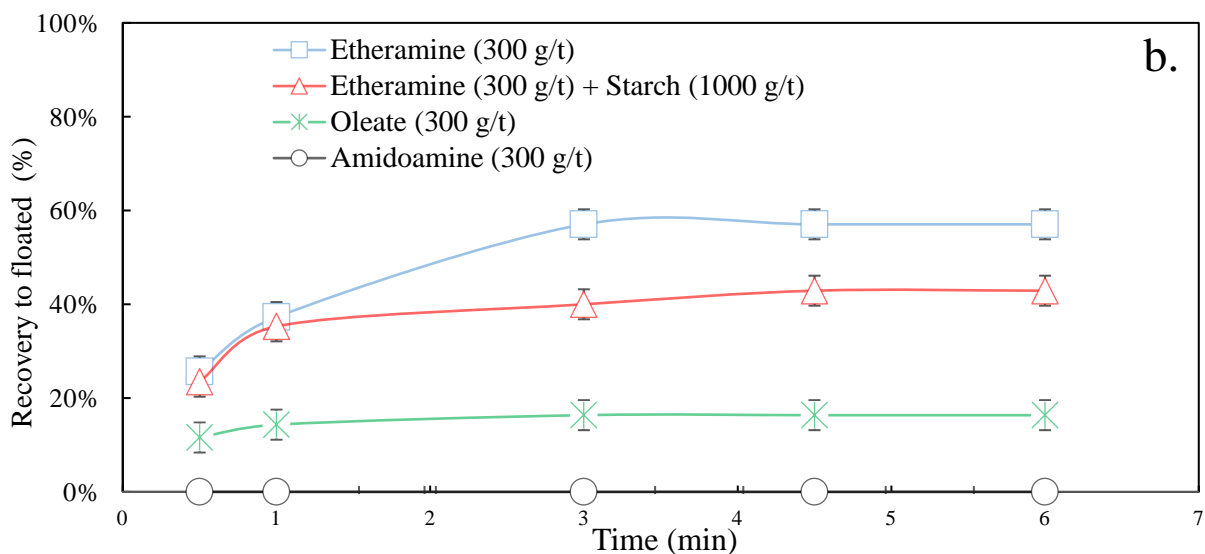


Figure 17 - Flotation recovery results of the hematite–kaolinite mixture at pH 10: (a) Hematite recovery. (b) Kaolinite recovery.

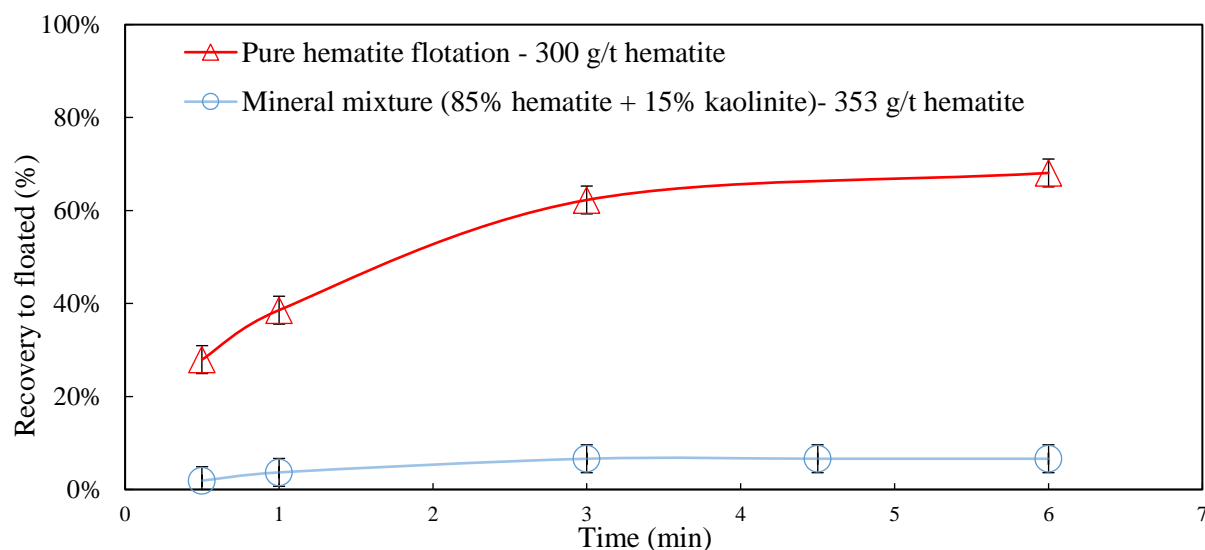


Figure 18 - Hematite recovery during flotation tests of pure hematite and hematite–kaolinite mixture using etheramine collector at pH 10.

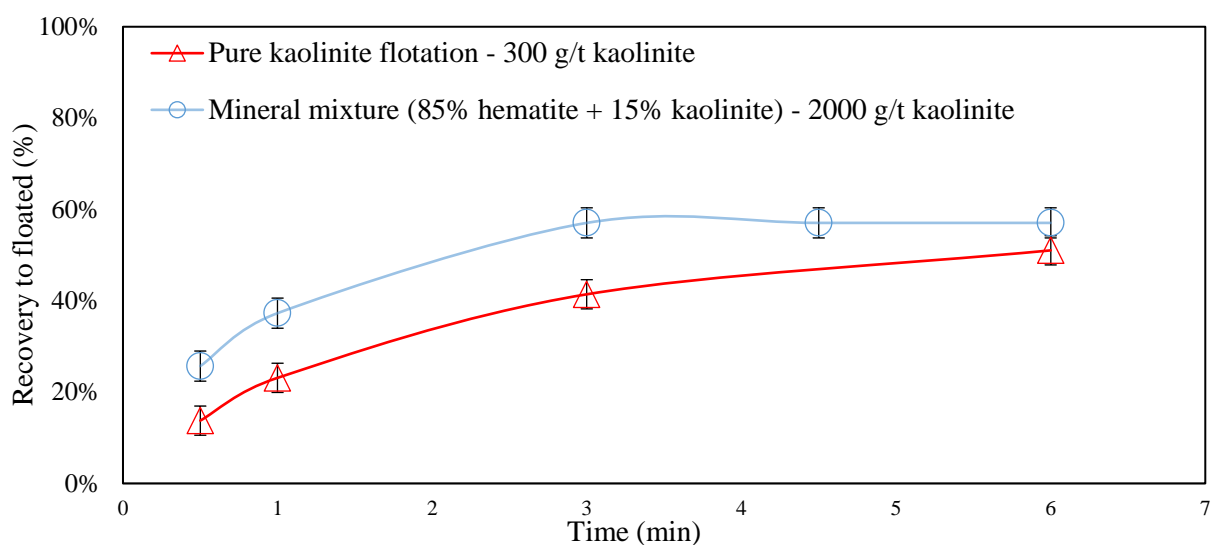


Figure 19 – Kaolinite recovery in the flotation tests using kaolinite and hematite–kaolinite mixture using etheramine collector.

7.5. Infrared measurements

Three types of samples were analyzed: 1) pure amidoamine, 2) pure minerals (hematite, quartz and kaolinite), and 3) minerals after the addition of amidoamine. Fig. 20 shows the FTIR spectra obtained for amidoamine N-[3-(Dimethylamino)propyl]dodecanamide. The FTIR spectra obtained for hematite, quartz, and kaolinite, before and after the interaction with three distinct dosages of the amidoamine collector are presented in Figs. 21, 22 and 23 respectively.

The characteristics bands (cm^{-1}) identified for the amidoamine collector (Fig. 20) were: 3307, 3081, 2921, 2852, 2814, 2763, 1640, 1548, 1466, 1377, 1263, 1042, 840, 720.

The spectra obtained for the amidoamine collector showed two main domains of absorbance (Fig. 20). The first domain is located between 2700 and 3300 cm^{-1} (Tables 6 and 7), characteristic of the C-H and NH bond vibrations. The four peaks at 2852 cm^{-1} , 2921 cm^{-1} , 2956 cm^{-1} , 2814 cm^{-1} respectively correspond to the asymmetric elongation vibrations of the group ($\nu_s(\text{CH}_2)$), ($\nu_s(\text{CH}_2)$), ($\nu_s(\text{CH}_3)$) in the hydrocarbon chain and the symmetric stretching ($\nu_s(\text{CH})$) of carbon bound to nitrogen (C-H)-N. The peaks at 3307 and 3081 cm^{-1} corresponds to the stretching and harmonic vibration of NH of amidoamine collector respectively.

The second domain is located between 1640 and 600 cm^{-1} . In this region, the FTIR spectra showed a strong absorption band at 1640 cm^{-1} , which is characteristic of C = O amide. The peak 1548 correspond to the angular deformation of NH while the peak at 1466 cm^{-1} to asymmetric bending of CH_3^+ scissoring (in-plane symmetric bending) of CH_2 and 1377 cm^{-1} - symmetric bending of CH_3 .

After interaction with amidoamine, new bands at around 2921 and 2852 cm^{-1} for kaolinite, around 2923 and 2852 cm^{-1} for quartz and 2923 and 2852 cm^{-1} for hematite were assigned to the stretching bands of $-\text{CH}_3$ and $-\text{CH}_2$ groups in amidoamine when the concentration of the collector increases (Table 7). The bending and stretching vibration of N–C bonds of amidoamine appeared at 1466 cm^{-1} for kaolinite and 1466 cm^{-1} for quartz, respectively.

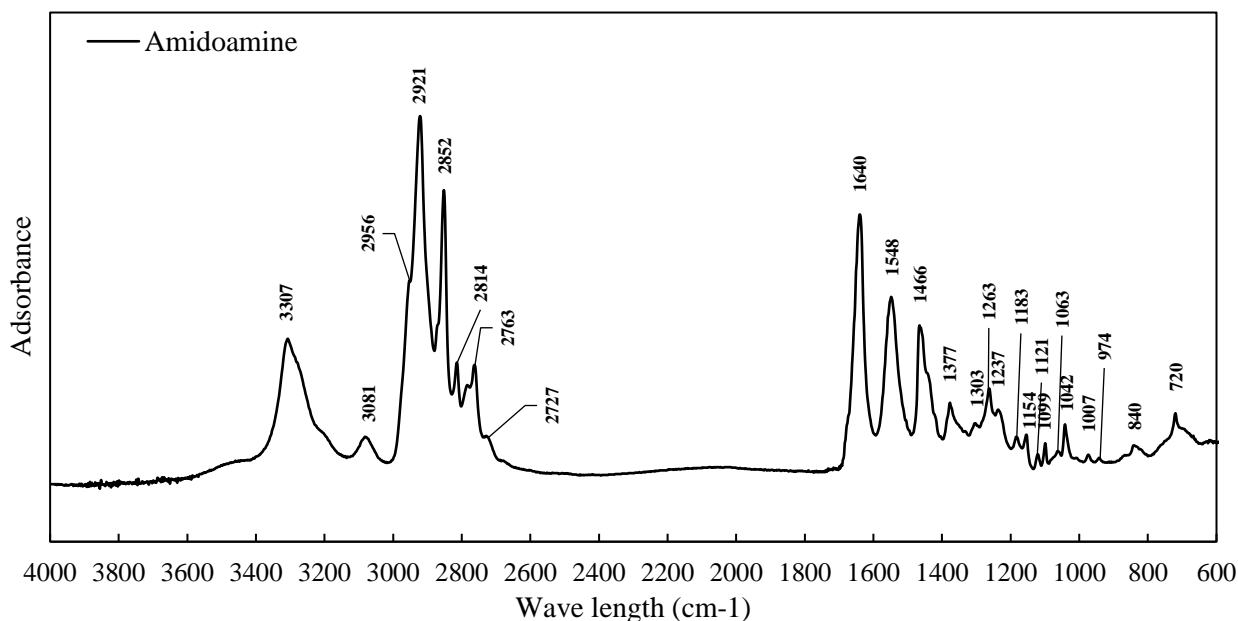


Figure 20 - The FTIR spectra obtained for the amidoamine N-[3-(Dimethylamino)propyl] dodecanamide collector.

Table 6. Peaks and corresponding groups in the 2 800 and 3300 cm^{-1} domain

ID	FTIR data (cm^{-1})				
		Symmetric stretching of (CH_2)	Asymmetric stretching of (CH_2)	Asymmetric stretching of (CH_3)	Symmetric stretching of (CH)
Group	($\nu(\text{NH})$)	($\nu_s(\text{CH}_2)$)	($\nu_{as}(\text{CH}_2)$)	($\nu_{as}(\text{CH}_3)$)	($\nu_s(\text{CH}_2)$)
Wave number (cm^{-1})	3307	2852	2921	2 956	2814

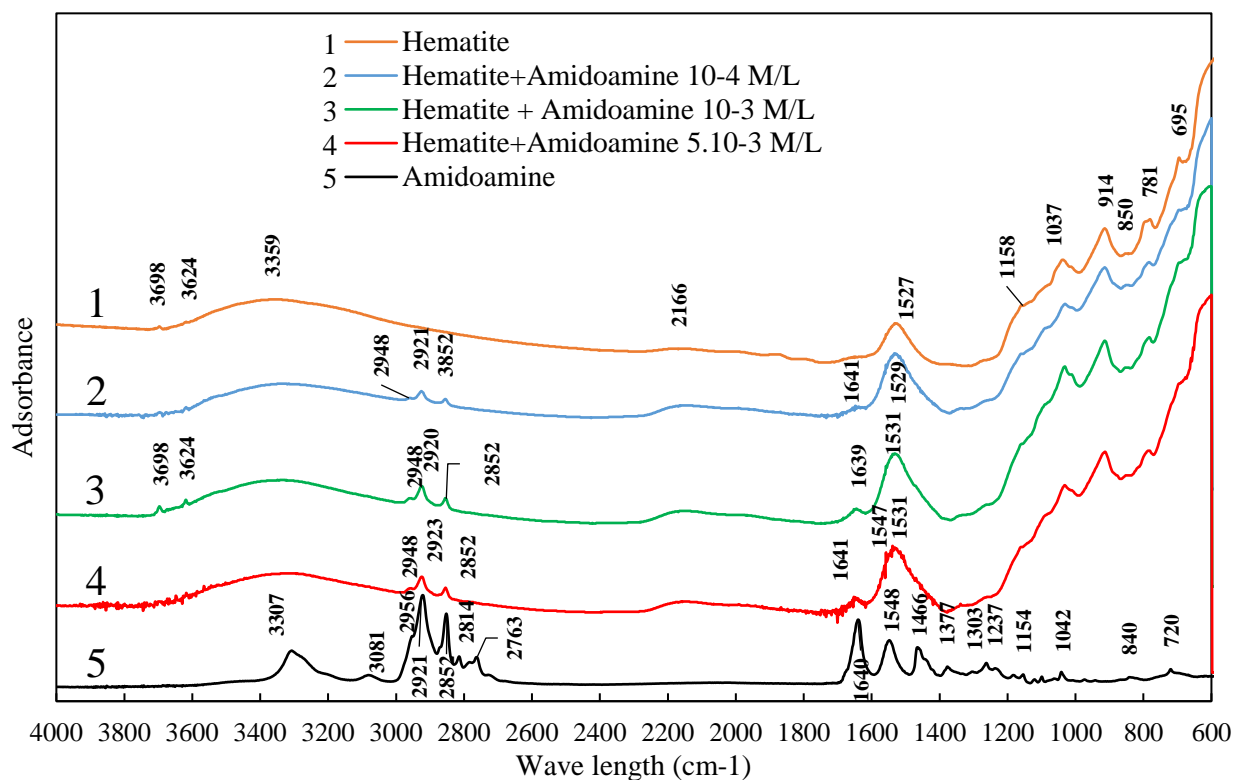


Figure 21 - FTIR spectra of hematite before (1) and after interaction with amidoamine (2, 3, and 4).

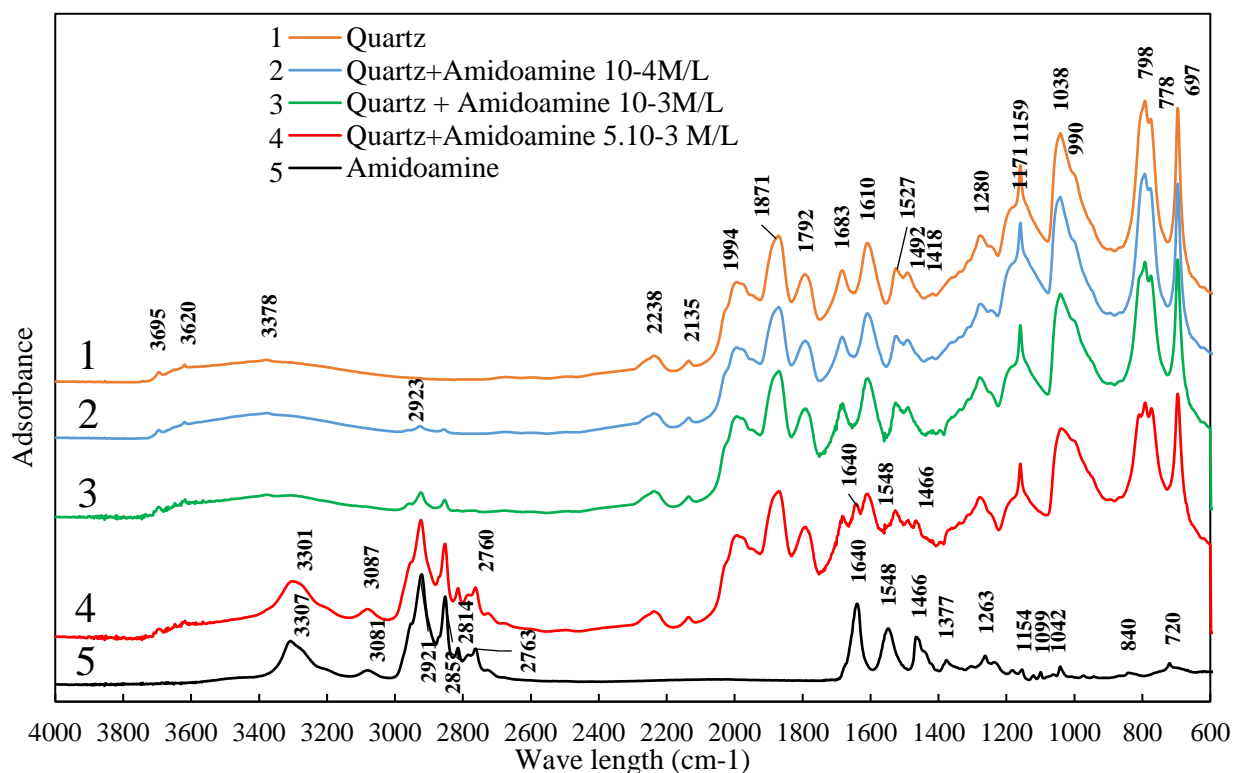


Figure 22 - FTIR spectra of quartz before (1) and after interaction with amidoamine (2, 3, and 4).

values where both two mineral surfaces display negative charges. Fig. 24 shows the amidoamine N-[3-(Dimethylamino)propyl]dodecanamide chemical structure.

The amidoamine N-[3-(Dimethylamino)propyl]dodecanamide molecule structure has a bond between the methyl and amine groups in the hydrophilic head of this reagent, which significantly increases the volume of the polar head in comparison with those of more conventional cationic collectors such as etheramine and makes this molecule more susceptible to steric hindrance effects (Fig. 24).

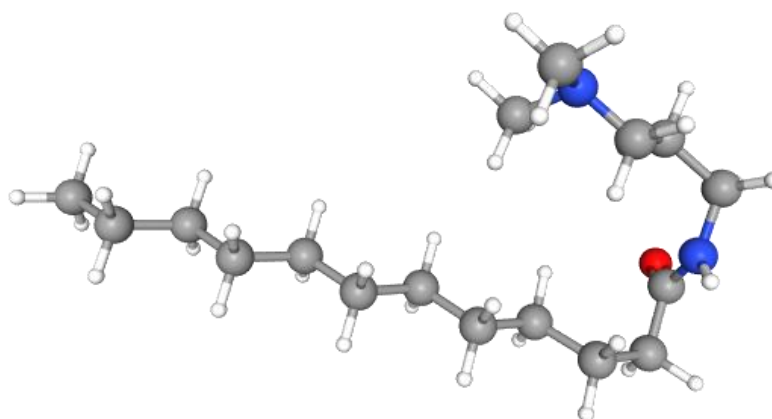


Figure 24 - Chemical structure of N-[3-(Dimethylamino)propyl]dodecanamide (Copied from PubChem, 2020).

As mentioned by Chen et al., (2017), surfactants initially adsorb on mineral surfaces through electrostatic interaction as individual ions; further, with the increase in the coverage of the surfactant on the mineral surface, steric hindrance gradually occurs. Liu et al., (2019) used surface tension measurements, molecular dynamics simulations and density functional theory to investigate the effects of introducing an isopropanol substituent in amine collectors. The results showed that introducing this isopropanol substituent in dodecyl amine weakened the electrical properties of the polar groups and increased the cross-sectional size of these groups. Similar effects were demonstrated and reported previously by Filippov and co-workers when an aliphatic iso-alcohol reagent was used in combination with anionic collectors for calcium minerals flotation (Filippov et al., 2006; Filippova et al., 2014; Filippov et al., 2019) and with cationic collectors for reverse iron ore and silicates flotation (Filippov et al., 2010; Filippov et al., 2012, Filippov, 2017). The results obtained in our work agree with the effect demonstrated by Liu et al. on the reverse flotation of quartz and hematite in relation to the performance of a collector with high steric hindrance (Liu et al., 2020). The results reported show that the increase in the steric hindrance improves the selectivity in relation to the cationic reverse flotation of these minerals.

The infrared spectra presented in Figs. 21 to 23 showed no difference in the adsorption behavior of the amidoamine collector at a low concentration of 10^{-4} M/L, what is consistent with the zeta potential measurements (Fig. 8).

The intensity of peaks related to the stretching bands of CH₃ and CH₂ is the same or slightly higher on the hematite than in quartz and kaolinite. However, the peaks intensity increases significantly on the quartz and kaolinite for the concentration of $5 \cdot 10^{-3}$ M/L of the collector (Figs. 22 and 23), pointing to a higher quantity of adsorption of the collector on silicate minerals, such does not occur for hematite (Fig. 21). This difference in adsorption behavior is responsible for the selective flotation of quartz from hematite.

For quartz and kaolinite, the more intense peaks may be explained by the specific adsorption on the more negatively charged silicate minerals surface defined by the silica tetrahedron.

Since for this amidoamine collector the structure of the adsorption layer is controlled by the collector concentration, there is a hindrance effect for hematite. Such hindrance effects can be caused by characteristic as for example, molecular arrangements or interactions promoted by hydrogen bonding and/or electrostatic forces.

An increase in collector concentration leads to the increased quartz recovery due to the increased quantity of the collector deduced from the higher peak intensity (Fig. 16), while the flotation of hematite does not occur or is very low (Fig. 15a). However, the flotation behavior of kaolinite is similar to those of hematite while the CH₃ and CH₂ peaks intensity is similar to the spectrum of quartz. The high specific surface area coupled with double sheet structure may be an explanation for this behavior (Ma and Bruckard, 2010; Xu et al., 2015).

8. Conclusions

Contact angle measurements showed no significant hydrophobization of the hematite surface with N-[3-(Dimethylamino)propyl] dodecanamide, despite the zeta potential studies showed a certain level of adsorption of this amidoamine on the hematite surface. The flotation studies corroborated with the interpretation made from the contact angle measurements by showing a low floatability for hematite and kaolinite while a total flotation of the quartz was observed.

The infrared spectroscopy results showed that an increase in amidoamine concentration did not result in a significant variation in peak intensity (stretching bands of CH₃ and CH₂) for hematite while the peaks intensity on the quartz and kaolinite were increased significantly.

The most adequate hypothesis for the mechanism responsible for the selective flotation of quartz with N-[3-(Dimethylamino)propyl]dodecanamide (without starch) is a hindrance effect due to the intermolecular interactions controlled by the collector concentration.

The new amidoamine collector was able to promote a selective flotation of quartz from hematite without a depressant agent, such as starch. Therefore, this reagent can be an advantageous alternative to conventional amines, currently used in reverse cationic flotation of iron ores.

Understanding the adsorption mechanism of this specific amido- amine may contribute to the development of a new class of collecting reagents, more effective for reverse iron ore flotation, reducing or eliminating the need for the depressant reagent, also contributing to a decrease of iron loss to tailings.

Credit authorship contribution statement

Klaydison Silva: Conceptualization, Resources, Investigation, Data curation, Validation, Writing - original draft, Writing - review & editing. Lev O. Filippov: Conceptualization, Resources, Validation, Supervision, Funding acquisition, Project administration, Writing - original draft, Writing - review & editing. Alexandre Piçarra: Investigation, Data curation, Validation, Writing - original draft, Writing - review & editing. Inna V. Filippova: Data curation, Validation. Neymayer Lima: Methodology, Investigation. Anna Skliar: Investigation. Lívia Faustino: Methodology, Investigation, Data curation. Laurindo Leal Filho: Conceptualization, Resources, Methodology.

Declaration of Competing Interest

The authors declare that they have no known competing financial interests or personal relationships that could have appeared to influence the work reported in this paper.

Acknowledgments

This paper was supported by VALE S.A in the context of developing new beneficiation routes for iron ore. The support of Clariant, Brazil as a partner in this project is deeply appreciated. The technical support from the Steval staff at GeoResources, University of Lorraine, is greatly acknowledged.

References

- Aguiar, M., Furtado, R., Peres, A., 2017. Seletividade na flotação catiônica reversa de minério de ferro. *Holos* 24 (11), 126–135.
- Araujo, A.C., Viana, P.R.M., Peres, A.E.C., 2005. Reagents in iron ores flotation. *Miner. Eng* 18 (2), 219–224. <https://doi.org/10.1016/j.mineng.2004.08.02>.

Balajee, S.R., Iwasaki, I., 1969. Adsorption mechanism of starches in flotation and flocculation of iron ores. *Trans. AIME* 244, 401–406.

Chen, P., Hu, Y., Gao, Z., Zhai, J., Fang, D., Yue, T., Zhang, C., Sun, W., 2017. Discovery of a novel cationic surfactant: tributyltetradecyl-phosphonium chloride for iron ore flotation: From prediction to experimental verification. *Minerals*. 7, 240. <https://doi.org/10.3390/min7120240>.

Cooke, S.R.B., Schultz, N.F., Lindroos, E.W., 1952. The effect of certain starches on quartz and hematite suspensions. *Trans. AIME* 193, 697–698.

Dogu, I., Arol, A.I., 2004. Separation of dark-colored minerals from feldspar by selective flocculation using starch. *Powder Technol.* 139, 258–263.

Dos Santos, I.D., Oliveira, J.F., 2007. Utilization of humic acid as a depressant for hematite in the reverse flotation of iron ore. *Miner. Eng.* 20, 1003–1007. <https://doi.org/10.1016/j.mineng.2007.03.007>.

Filippov L.O., Filippova I.V., 2006. Synergistic effects in mix collector systems for non-sulfide mineral flotation. *Proc. of XXIII Int. Min Proc. Congress, Istanbul, Turkey, 3-8 September 2006* (Eds. Onal G. et al) pp. 631-634.

Filippov, L., Filippova, I., Severov, V., 2010. The use of collectors mixture in the reverse cationic flotation of magnetite ore. The role of Fe-bearing silicates. *Miner. Eng.* 23, 91–98. <https://doi.org/10.1016/j.mineng.2009.10.007>.

Filippov, L., Duverger, A., Filippova, I., Kasaini, H., Thiry, J., 2012. Selective flotation of silicates and Ca-bearing minerals : the role of non-ionic reagent on cationic flotation. *Minerals Engineering* 36–38 (10), 314–323.

Filippov, L., Severov, V., Filippova, I., 2013. Mechanism of starch adsorption on Fe-Mg- Al-bearing amphiboles. *Int. J. Miner. Process.* 123, 120–128. <https://doi.org/10.1016/j.minpro.2013.05.010>.

Filippov, L., Severov, V., Filippova, I., 2014. An overview of the beneficiation of iron ores via reverse cationic flotation. *Int. J. Miner. Process.* 127, 62–69. <https://doi.org/10.1016/j.minpro.2014.01.002>.

Filippov, L.O., Filippova, I.V., Lafhaj, Z., Fornasiero, D., 2019. The role of a fatty alcohol in improving calcium minerals flotation with oleate. *Colloids and Surfaces A: Physicochemical and Engineering Aspects* 560, 410–417.

Filippova, I.V., Philippov, L.O., Duverger, A., Severov, V.V., 2014. Synergetic effect of a mixture of anionic and nonionic reagents: Ca mineral contrast separation by flotation at neutral pH. *Minerals Engineering* 66–68, 135–144.

Filippov L. O. Flotation process for recovering feldspar from a feldspar ore., 2017. US Patent 9,675,980.

Fornasiero, D., Filippov, L.O., 2017. Innovations in the flotation of fine and coarse particles. *J. Phys. Conf. Ser.* 879, 012002 <https://doi.org/10.1088/1742-6596/879/1/012002>.

Friedli, F.E., 1990. Amidoamine surfactants. In: *Cationic Surfactants - Organic Chemistry (Surfactant Science Series; v34)*. Marcel Dekker Inc., New York, pp. 52–83.

Gupta, V., Miller, J., 2010. Surface force measurements at the basal planes of ordered kaolinite particles. *J. Colloid. Interface Sci.* 344 (2), 362–371. <https://doi.org/10.1016/j.jcis.2010.01.012>.

Kar, B., Sahoo, H., Rath, S.S., Das, B., 2013. Investigations on different starches as depressant for iron ore flotation. *Miner. Eng.* 49, 1–6. <https://doi.org/10.1016/j.mineng.2013.05.004>.

Khosla, N.K., Biswas, A.K., 1984. Mineral–collector–starch constituent interactions. *Colloids Surf.* 9 (3), 219–235.

Lima, N., Silva, K., Souza, T., Filippov, L., 2020. The Characteristics of Iron Ore Slimes and Their Influence on the Flotation Process. *Minerals.* 10, 675. <https://doi.org/10.3390/min10080675>.

Liu, W., Liu, W., Zhao, Q., Shen, Y., Wang, X., Wang, B., Peng, X., 2020. Design and flotation performance of a novel hydroxy polyamine surfactant based on hematite reverse flotation desilication system. *Journal of Molecular Liquids* 301, 1–9. <https://doi.org/10.1016/j.molliq.2019.112428>.

Liu, J., Wang, X., Lin, Ch.-L., Miller, J.D., 2015. Significance of particle aggregation in the reverse flotation of kaolinite from bauxite ore. *Minerals Engineering* 78, 58–65. <https://doi.org/10.1016/j.mineng.2015.04.009>.

Liu, W., Peng, X., Liu, W., Wang, X., Zhao, Q., Wang, B., 2019. Effect mechanism of the isopropanol substituent on amine collectors in the flotation of quartz and magnesite. *Powder Technol.* 360, 1117–1125. <https://doi.org/10.1016/j.powtec.2019.10.060>.

Ma, X., Bruckard, W.J., 2010. The effect of pH and ionic strength on starch–kaolinite interactions. *Int. J. Miner. Process.* 94, 111–114. <https://doi.org/10.1016/j.minpro.2010.01.004>.

Nakhaei, F., Irannajad, M., 2017. Reagents types in flotation of iron oxide minerals: A review. *Mineral Processing and Extractive Metallurgy Review* 39 (2), 89–124. <https://doi.org/10.1080/0882750017.1391245>.

Pavlovic, S., Brandão, P.R.G., 2003. Adsorption of starch, amylose, amylopectin and glucose monomer and their effect on the flotation of hematite and quartz. *Minerals Engineering* 16, 1117–1122.

Peres, A.E.C., Correa, M.I., 1996. Depression of iron oxides with corn starches. *Minerals Engineering* 9 (12), 1227–1234.

PubChem, 2020, Compound. Lauramidopropyldimethylamine. <https://pubchem.ncbi.nlm.nih.gov/compound/lauramidopropyldimethylamine> (Accessed 17th of December, 2020).

Severov, V.V., Filippova, I.V., Filippov, L.O., 2013. Floatability of Fe-bearing silicates in the presence of starch: adsorption and spectroscopic studies. *J. Phys. Conf. Ser.* <https://doi.org/10.1088/1742-6596/416/1/012017>.

Severov, V.V., Filippov, L.O., Filippova, I.V., 2016. Relationship between cation distribution with electrochemical and flotation properties of calcic amphiboles. *Int J Mineral Processing* 147, 18–27.

Smith, R.W., Scott, J.L., 1990. Mechanisms of dodecylamine flotation of quartz. *Mineral Processing and Extractive Metallurgy Review* 7 (2), 81–94. <https://doi.org/10.1080/08827509008952667>.

Turrer, H.D.G., Peres, A.E.C., 2010. Investigation on alternative depressants for iron ore flotation. *Miner. Eng.* 23, 1066–1069. <https://doi.org/10.1016/j.mineng.2010.05.009>.

Veloso, C.H., Filippov, L.O., Filippova, I.V., Ouvrard, S., Araujo, A.C., 2018. Investigation of the interaction mechanism of depressants in the reverse cationic flotation of complex iron ores. *Minerals Engineering* 125, 133–139.

Veloso, C.H., Filippov, L.O., Filippova, I.V., Ouvrard, S., Araujo, A.C., 2020. Adsorption of polymers onto iron oxides: Equilibrium isotherms. *J Mater Res Technol* 9 (1), 779–788.

Weissenborn, P., Warren, L., Dunn, J., 1995. Selective flocculation of ultrafine iron ore. 1. Mechanism of adsorption of starch onto hematite. *Colloid. Surf. A: Physicochem. Eng. Asp.* 99, 11–27. [https://doi.org/10.1016/0927-7757\(95\)03111-P](https://doi.org/10.1016/0927-7757(95)03111-P).

Xu, L., Hu, Y., Dong, F., Jiang, H., Wu, H., Zhen, W., Liu, R., 2015. Effects of particle size and chain length on flotation of quaternary ammonium salts onto kaolinite. *Mineral. Petrol.* 109, 309–316. <https://doi.org/10.1007/s00710-014-0332-8>.

Yuehua, H., Wei, S., Haipu, L., Xu, Z., 2004. Role of macromolecules in kaolinite flotation. *Miner. Eng.* 17, 1017–1022. <https://doi.org/10.1016/j.mineng.2004.04.012>.

Chapter 4 - Comparison Between Etheramine and Amidoamine (N-[3-(dimethylamino)propyl]dodecanamide) Collectors: Adsorption Mechanisms on Quartz and Hematite Unveiled by Molecular Simulations

Klaydison Silva¹, Lucas A. Silva³, Alexandre M. Pereira³, Leonardo C. Bastos³, Julio C. G. Correia³, Alexandre Piçarra², Leandro Bicalho⁴, Neymayer Lima¹, Lev Filippov^{2*}

¹ VALE S.A. - Mineral Processing Development Department - Av. Dr. Marco Paulo Simon Jardim, 3580 Bairro Piemonte, Nova Lima CEP 34.006-200, MG, Brazil

² Université de Lorraine, CNRS, GeoRessources, F54000 Nancy, France

³ Centre for Mineral Technology (CETEM), Molecular Modeling Laboratory - Av. Pedro Calmon, 900, Ilha da Cidade Universitaria, CEP 21941-908, Rio de Janeiro, RJ, Brazil

⁴ Clariant, Av. Portugal, 3899 - Itapoã, Belo Horizonte - MG, 31710-400

Minerals Engineering 180 (2022) 107470; <https://doi.org/10.1016/j.mineng.2022.107470>

Received 28 September 2021; Received in revised form 21 February 2022; Accepted 22 February 2022

Abstract: This work describes, at a molecular level, the adsorption differences between etheramine and amidoamine N-[3-(dimethylamino)propyl]dodecanamide, a conventional silicate collector and one not yet used in industrial iron ore flotation, respectively. The molecular dynamics simulations showed that the adsorption of this amidoamine on the quartz surface, regarding the quartz-hematite system, tends to be more selective than etheramine. The explanation for this behavior is related to the combination of the water coordination at hematite-(D2) surface and the bulky head group of the amidoamine. Regarding the neutral molecules of etheramine and amidoamine, the coordination of water on the surface of hematite-(D2) acts as a shield, making it difficult for collector adsorption. In relation to protonated collector molecules, the combination of the amidoamine head group (with methyl bonded to nitrogen in the tertiary amine) with the water on the hematite-(D2) surface causes steric hindrance, impairing the amidoamine adsorption, while the etherammonium cations manage to adsorb on this hematite surface anyway. Also, the amide group favors hydrogen-bonding between collectors in the adsorption layer, which brings stability to the layer.

Keywords: iron ore; flotation; amidoamine; molecular dynamics; adsorption mechanism; hydrogen bonding; etheramine; adsorption layer arrangement.

1. Introduction

1.1. Nomenclatures and abbreviations

In this study, the following nomenclatures / abbreviations were adopted:

- CC – Collector-collector
- CM – Collector-mineral
- CMD – Classical Molecular Dynamics
- D1 – Domain 1
- D2 – Domain 2
- ECC – Collector-collector interaction energy
- ECM – Collector-mineral interaction energy
- HB – Hydrogen Bond
- H – Hematite
- Q – Quartz
- MD – Molecular Dynamics
- STD – Standard Deviation
- Etheramine – 3-dodecoxypropan-1-amine, also known as Laurixamine.
- Amidoamine – N-[3-(dimethylamino)propyl]dodecanamide, also known as Lauramidopropyl dimethylamine

1.2. Development of new more selective collectors in the iron ore flotation

The cationic reverse flotation of quartz is one of the most common techniques for the concentration of iron ores by flotation (Araujo et al., 2005; Filippov et al., 2014). The first applications of reverse cationic flotation relied upon the usage of fatty amines, later replaced by the more efficient etheramines. The adsorption mechanism involved in the cationic flotation of quartz is governed by electrostatic interactions between the mineral surface and the collector's polar head. Since this type of flotation was adopted in the iron ore plants, no significant advances were observed in the reverse cationic flotation and, to obtain selectivity in the process containing quartz and hematite, polysaccharides as depressants for iron-containing minerals are used (Filippov et al., 2014).

The two main reasons for iron loss to the froth in reverse cationic flotation are the entrainment (hydrodynamic dragging) and true flotation. Loss by true flotation is majorly attributed to failures in the conditioning processes of the target iron minerals by starch (Nykänen et al., 2020).

The separation efficiency in iron ore flotation decreases when part of the gangue minerals is composed by Fe/Mg bearing silicates. This loss of selectivity occurs because these gangue minerals have surface properties similar to iron oxides in the cationic flotation process, making the depressants non-selective (Filippov et al., 2010; Filippov et al., 2013; Severov et al., 2013; Veloso et al., 2018). Thus, the development of more selective collectors, capable of reducing or eliminating the need for the use of depressant reagents, can contribute to increase the metallurgical recovery and the quality of the product in the current beneficiation plants and in new projects aimed at more complex ores.

Studies have been carried out to develop new more selective collectors for iron ore flotation. Huang et al. (2014) investigated the adsorption mechanism of a Gemini surfactant, ethane-1,2-bis(dimethyl-dodecyl-ammonium bromide) (EBAB) for the reverse cationic flotation separation of quartz from magnetite. According to the authors, the EBAB presented a stronger collecting power than the conventional monomeric surfactant dodecylammonium chloride (DAC) and a superior selectivity towards quartz. Liu et al. (2020a) synthesized a N,N-dimethyl-N'-(2-hydroxyethyl)-N'-dodecyl-1,3-propanediamine (DMPDA) with the objective of designing a hydroxyl-containing polyamine cationic surfactant to enhance the separation efficiency between hematite and quartz by reverse flotation. The results showed that the introduction of the hydroxyl group could enhance the surface activity of the collector and the selective adsorption on the desired mineral surface. The flotation tests showed that DMPDA had a higher selectivity than dodecylamine.

1.3. The quartz and hematite mineral surfaces.

Quartz and hematite's symmetry do not present a perfectly weaker plane, so they cleave in many different positions. The planes (100) or (010) and (101) of quartz and (001) of hematite are usually considered the most common. These facets present yet different possible terminations (Liu et al., 2014; Lützenkirchen et al., 2015).

Hematite (001) possesses mainly two coexistent distinct surface stoichiometries which differ mainly by the exposed atoms (Kiejna and Pabisiak, 2013; Lützenkirchen et al., 2015; Tanwar et al., 2009; Trainor et al., 2004). When the surface presents an oxygen termination it is called Domain 1 (D1), often represented by (O3-Fe-Fe-R); it has an analogue crystal structure to that of the alumina face of kaolinite, characterized by doubly coordinated hydroxyl ions. When the surface presents an iron termination it is called Domain 2 (D2), that when exposed to the environment is immediately coordinated by water. This surface is often represented by (O3-Fe-O3-R) or (Fe-O3-Fe-R). The literature emphasizes their difference in pH response, while

the D2 surface develops charges, the D1 surface is almost inert in a wide range of pH values (Lützenkirchen et al., 2015).

Liu et al. (2014) studied the acid-base characteristics of quartz. The (100) surface of quartz has two possible terminations denoted Alpha (α) and Beta (β). The α termination contains only Q2 Si and therefore, geminal silanols. The β termination contains Q3 Si, and vicinal silanols. Each type of silanol has a different pKa value, so that as pH increases, the silanols on the (100)- β surface first dissociate, and then the germinal silanols on the (100)- α surface and the silanols on (101) facets.

1.4. Amidoamine Flotisor 5530

Amidoamines are substances that contain one or more amide groups as well one or more amine functions (Friedli, 1990). The amidoamine studied in this work is the Flotisor 5530, designed by Clariant, synthesized from vegetable sources.

Araujo et al. (2020) studied the flotation performance of the amidoamine (Flotisor 5530) in the reverse rougher flotation of iron bearing slimes assisted by high intensity conditioning (HIC) using a column flotation. Matiolo et al. (2020) performed column flotation tests of iron ore slimes using the same amidoamine collector than Araújo et al., (Flotisor 5530), without starch. The results presented by the Matiolo et al. showed that it was possible, by only using Flotisor 5530 (200 g/t), at pH 10.5, to achieve a final concentrate containing 62.3% Fe, 3.3% SiO₂ and Fe recovery up to 93.2% (feed with 45.2% Fe, 28.6% SiO₂). The addition of starch (1152 g/t) did not significantly alter the results obtained when only dosing Flotisor 5530. With the addition of starch, the concentrate obtained had a Fe and SiO₂ grade of 62.5% and 4.7%, respectively. These results show that, contrary to conventional amines, the studied amidoamine collector (Flotisor 5530), concerning the iron ore slimes flotation, did not require the action of an iron depressant such as starch to inhibit iron loss by true flotation (Matiolo et al., 2020; Filippov et al., 2021). The authors also showed that the results obtained with amidoamine are competitive with those obtained by the conventional reverse cationic route (amine with iron depressant). When using etheramine and starch the best concentrate grade obtained was 59.2% Fe, 5.8% SiO₂ with a recovery of 71.5% Fe.

The works presented by these authors show the possibility to concentrate iron ore slimes, without the employment of depressant agent to inhibit the flotation of target iron oxide minerals but did not aim to explain the interaction mechanism between the amidoamine collector with the minerals present in the samples (e.g., interactions with hematite and quartz). In other words, there is a knowledge gap in terms of the mechanism of adsorption of this

collector and the reason for its selectivity. To tackle this knowledge gap, molecular simulations were done and presented in this study with the goal of explaining the differences between a more conventionally used silicate collector (etheramine) and the amidoamine Flotisor 5530, to contribute to the understanding of the mechanism of adsorption of each type of collector. Hydrogen bonds, interaction energies and spatial arrangement of these collectors, both at infinite dilution adsorption and in adsorption layers were analyzed to understand the causes, at a molecular level, of the selective iron ore slimes flotation performance of the reported amidoamine.

The main molecule that constitutes the reagent Flotisor 5530 is Lauramidopropyl dimethylamine, better known as N-[3-(dimethylamino)propyl]dodecanamide (molecular formula $C_{17}H_{36}N_2O$) and its chemical structure model is shown in Fig. 1. Budenberg (2016) studied the use of amidoamines in iron ore flotation, but these studies were carried out with starch and were not intended to develop a new depressantless flotation process, but rather to find new collectors in conventional iron ore flotation. The studies were carried out with ore from the Alegria mine, in the Iron Quadrangle region (Brazil). One of the amidoamines tested was N-[3-(dimethylamino)propyl]dodecanamide. Bench scale flotation test results using this amidoamine were very similar to those obtained with a standard reagent (ether monoamine), but the amidoamine dosage was higher than the standard collector to obtain similar results.

Silva et al. (2021a) performed a fundamental work on the use of the amidoamine N-[3-(dimethylamino)propyl]dodecanamide as quartz collector for iron ore reverse flotation, without depressant. The authors investigated, by FTIR analysis, the adsorption of this collector on the quartz, hematite and kaolinite surfaces and they found that, the adsorption on the hematite surface is controlled by a hindrance effect that impairs this collector adsorption. The selectivity behavior was also demonstrated by contact angle measurements and pure minerals bench scale flotation tests carried out by the authors.

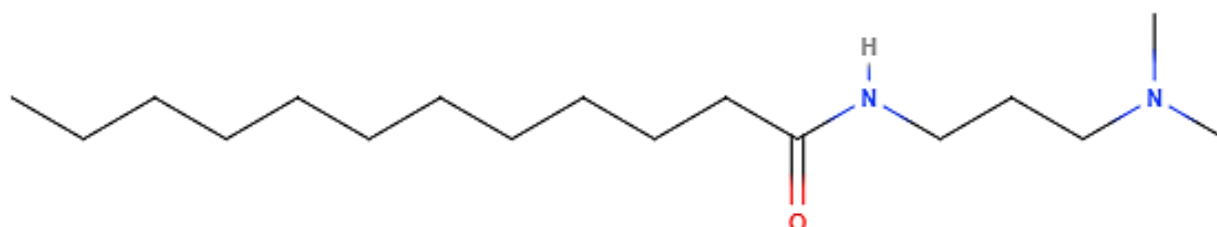


Figure 1 – Chemical structure of N-[3-(dimethylamino)propyl]dodecanamide (Pubchem, 2021).

1.5. Molecular modeling.

The different minerals and surface terminations present different types of surficial groups, crystal structure, charging states and molecular surface roughness. These characteristics can help explain the action of flotation reagents (Cao et al., 2021; Leal Filho et al., 2000; Liu et al., 2021a,b). This can be well evaluated by using computational methods. Molecular modeling has been extensively used in recent years for the understanding of key mechanisms of mineral related processes. The different computational approaches can prove very impacting for determining all sorts of bulk and interfacial phenomena (Foucaud et al., 2019). Molecular Dynamics (MD) is a computational simulation method which describes the solution of Newton's equations of motion for a set of molecules (Allen and Tildesley, 2017). The equations are numerically integrated into small time intervals and the forces of interaction between the particles are calculated. In classical molecular dynamics (CMD), these interactions come from expressions called force fields, which define the energetic potential in the particle system. All sorts of energetic, dynamic and structural information can be obtained from the results of such simulations. Many studies in recent literature have used such techniques to investigate flotation-related phenomena with success (Filippov et al., 2018; Foucaud et al., 2019, 2018; Leal Filho et al., 2000; Liu et al., 2020b; Rai et al., 2011) and this field of literature has been growing exponentially (Foucaud et al., 2019; Silva et al., 2021b). Among the most important adsorption properties that can be measured in MD simulations are hydrogen bonding, spatial arrangement and interaction energies.

2. Methodology

2.1. Measurement of the pKa

The pH point at which the concentration of ionic and molecular species is equal defines the pKa value. This work aims to explain the main adsorption mechanism for the amidoamine Flotisor 5530 at pH close to 8.5 and to 10.5, therefore it is necessary to determine the pKa for this reagent to know the species predominant at each pH studied.

The pKa value for the etheramine was evaluated by Filippov and co-workers to be slightly lower than for primary amine but close to 10 (Severov et al., 2016).

The pKa of amidoamine was determined using the methodology proposed by Mhonde (2016). Thus, potentiometric acid-base titrations of the collector solution with a NaOH titrant solution were performed and the curve of the first derivative (Δ Volume of NaOH/ Δ pH) was

plotted by pH (Fig. 2). The point on the pH axis with the highest peak on this curve represents the approximate pKa value.

The pKa measurements of Flotisor 5530 were performed in triplicate and the average value obtained was 8.2. Therefore, at pH 10.5, the molecular (neutral) species are predominant for this reagent, while at pH 8.5 the speciation is close to 50% neutral and 50% cationic (protonated).

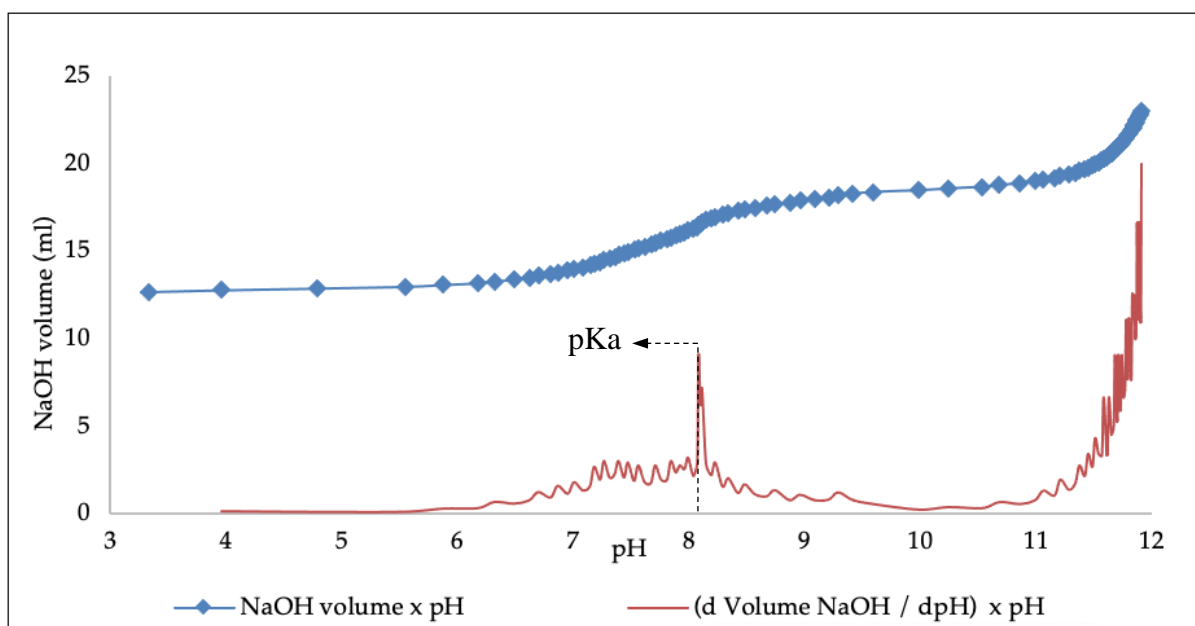


Figure 2 – Determination of pKa for the Flotisor 5530 amidoamine. Average value (3 measurements) for the peak of the first derivative shows pKa ~ 8.2.

2.2. Systems Modeling

The chemical structures of the collectors were drawn and pre-optimized in Avogadro (Hanwell et al., 2012). As said before, the amidoamine studied here is N-[3-(dimethylamino)propyl]dodecanamide (molecular formula $C_{17}H_{36}N_2O$) and the etheramine is 3-dodecoxypropan-1-amine (molecular formula $C_{15}H_{33}NO$). Minerals' unit cells and general information were obtained from Crystallography Open Database (COD) (2020), Mineralogy Database (2020) or Mindat.org-Mines (2020). Fig. 3 shows the crystal structures of Hematite (H) (Blake et al., 1966) and Quartz (Q) (Levien et al., 1980). The cells were then multiplied and cleaved as described in Fig. 3(e) and 3(f). The resulting mineral supercells were designed to present at least 24 Å in each edge (the double of the used non-bonded cutoff, respecting the minimal imaging convention). Hematite (a 26.16 Å, b 25.18 Å, c 27.44 Å) and quartz (a 24.55 Å, b 27.01 Å, c 25.51 Å) supercells' cleavage resulted in surfaces of virtually equal surface area, 6.59 and 6.63 nm² respectively, as intended for better comparison. The c crystallographic

parameter determined the slab thickness to expose the corresponding surfaces. The structures of the collectors are also shown Fig. 3.

Two studies were conducted in parallel to tackle two fundamental aspects of collector action (Fig. 4), which are, physically speaking: the adsorption of collectors at minerals surfaces and the development of a stable adsorption layer. At the first stage, called Study 1, a single collector molecule/cation was simulated at the solid-liquid interface to measure collector-surface affinity at varying degrees of surface charging, varying from neutral to 25% ionized which is based on the observation that quartz is approximately at this ionization degree at a pH close to 10.5 (Emami et al., 2014; Lowe et al., 2018). These simulations account for the different microstates these mineral surfaces can present, since not always the surface charge developed with pH will be perfectly homogenous across the surface domains.

At the second stage, called Study 2, 30 reagent molecules/cations were assembled over the mineral surface to study the stability of the adsorption layer. Protonation states were defined in such a way to simulate pH close to 8.5 and 10.5. This number of molecules/cations was chosen after tests because it is close enough to a state of a perfect adsorption monolayer of classic surfactants (Dynarowicz-Latka et al., 2001; Ganguly et al., 1997; Wood et al., 2016). Thus, in order to understand the predominant adsorption mechanism for each type of reagent, for the sake of simplicity, amidoamine was considered only in the neutral state at pH 10.5 and at 50%/50% neutral/cation proportion at pH 8.5, while etheramine was considered fully protonated at pH 8.5 and a mixture of 50% neutral and 50% cationic at pH 10.5, since amines in general have a higher pKa (Scott and Smith, 1991) than amidoamine studied in this work (8.2).

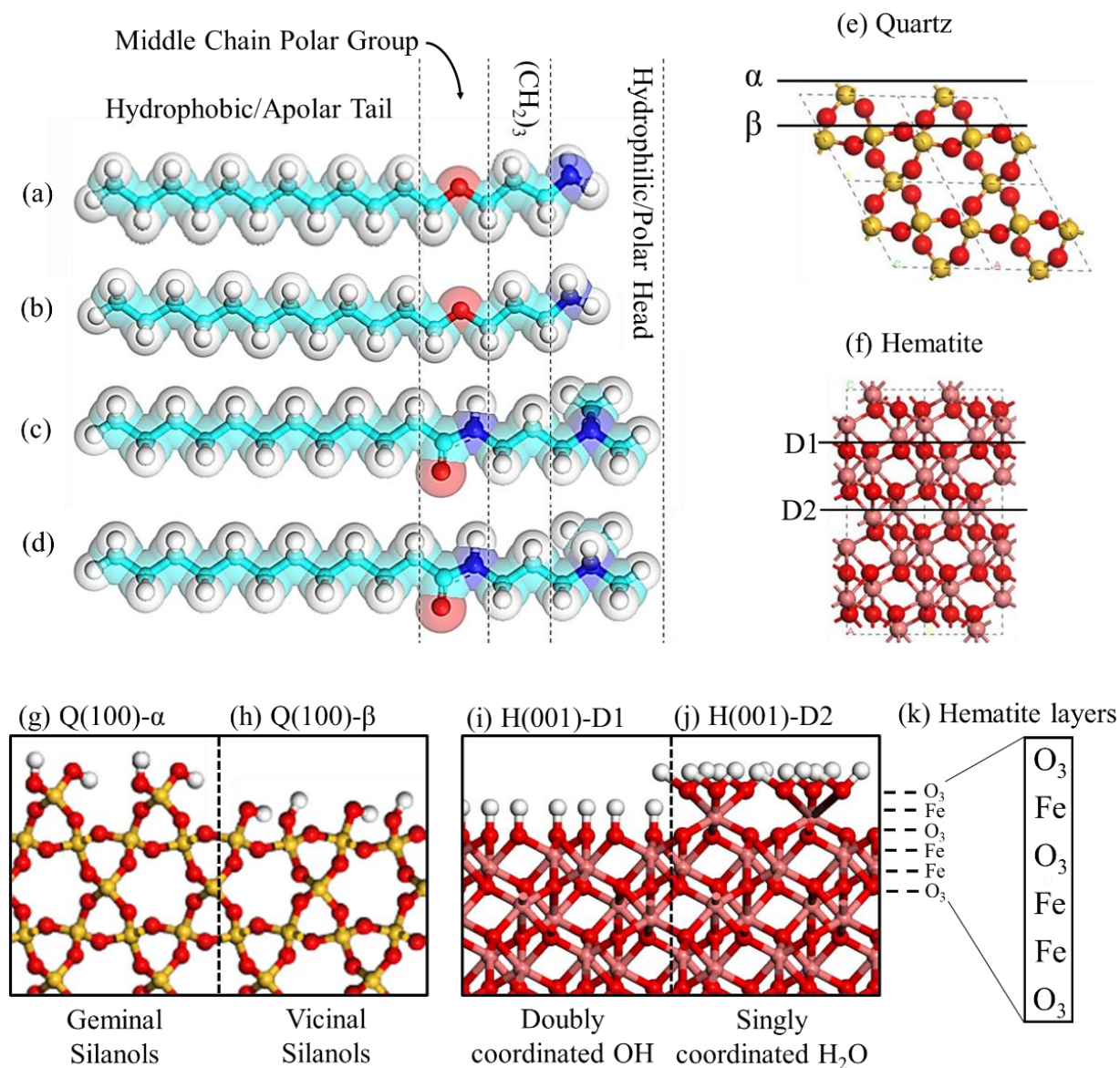


Figure 3 – Molecular and crystal structures of: (a) Etheramine, (b) Etherammonium, (c) Amidoamine, (d) Protonated Amidoamine (e) Quartz unit cell, (f) Hematite unit cell, (g) Quartz (100)- α surface, (h) Quartz (100)- β surface, (i) Hematite (001)-D1 surface, (j) Hematite (001)-D2 surface (k) Order of hematite layers. Atom color code: hydrogen - white, oxygen - red, nitrogen - blue, carbon - cyan, silicon - yellow, iron - pink.

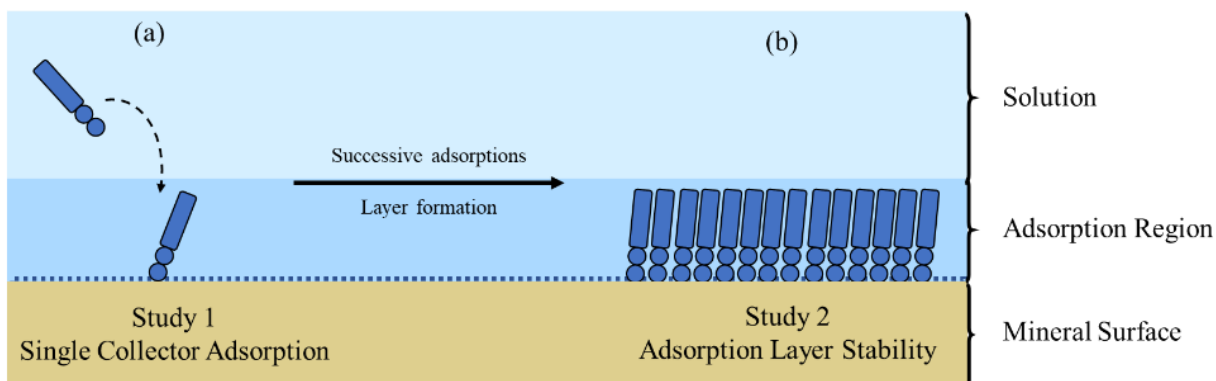


Figure 4 – Scheme of the two types of studies conducted and their physical meaning: (a) Study 1- Single collector adsorption at the mineral interface; (b) Study 2 - Stability of the adsorption layers.

Rectangular boxes were modeled under 3D periodic boundary conditions (PBC). The mineral surfaces, collector molecules/cations, 1000 water molecules and Na^+ and Cl^- counter ions, when needed, were assembled into the simulation systems using GEMS-Pack (Silva and Correia, 2020) and PACKMOL (Martínez et al., 2009). Fig. 5 shows the general scheme of the interfacial systems.

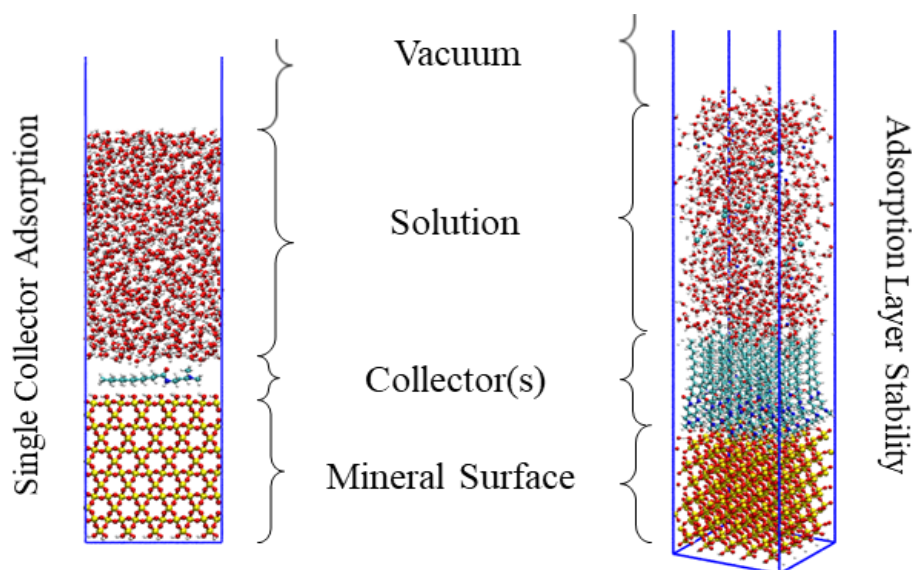


Figure 5 – General schemes for the two types of systems used in MD simulations.

2.3. Molecular Dynamics Simulations

The SPC (Berendsen et al., 1987), CVFF (Dauber-Osguthorpe et al., 1988) and CLAYFF (Cygan et al., 2004; Kerisit, 2011) force fields were used to model these interfacial systems. They use an energy expression based on intramolecular bonded terms (bonds, angles, dihedrals) and non-bonded terms (electrostatics and van der Waals); these are described by Equations 1–3:

$$E_{total} = E_{coulombic} + E_{vdW} + E_{intramolecular} \quad (1)$$

Where E_{total} is the total potential energy, $E_{coulombic}$ is the electrostatic energy, E_{vdW} is the Van der Waals energy and $E_{intramolecular}$ is the sum of intramolecular energy terms. The electrostatic energy is given by Coulomb's law:

$$E_{coulombic} = \frac{e^2}{4\pi\epsilon_0} \sum_{i \neq j} \frac{q_i q_j}{r_{ij}} \quad (2)$$

Where r_{ij} is the distance between atoms i and j , q_i and q_j are their atomic charges, e is the electron charge, ϵ_0 is the dielectric permittivity of vacuum. The Van der Waals energy is given by the conventional Lennard Jones potential, which is composed of a short-range nuclear repulsion term and an attractive London dispersion term:

$$E_{vdW} = \sum_{i \neq j} D_{0,ij} \left[\left(\frac{R_{0,ij}}{r_{ij}} \right)^{12} - 2 \left(\frac{R_{0,ij}}{r_{ij}} \right)^6 \right] \quad (3)$$

Where $D_{0,ij}$ and $R_{0,ij}$ are the energy and distance parameters of the Lennard Jones potential. Standard Lorentz-Berthelot combination rules, 12 Å cutoff for Lennard Jones interactions and PPPM method for long range electrostatics were used. The CLAYFF model does not include specific typing and charges for ionized mineral groups. As such, a specific strategy was needed to describe the states of surface deprotonation. For this, the following methodology was used: when deprotonating an OH group (removing H atom), a charge deficiency of -0.425 is created, and it is necessary to complete this negative charge with -0.575 to reach the charge of -1.00e. That extra charge was then redistributed between the deprotonated O- and the two closest neighboring bonded atoms. This strategy was based on that of Butenuth et al. (2012), who studied deprotonated silica surfaces, with the difference of redistributing the charge in a weighted way among neighboring atoms. Here, for simplicity, the redistribution was homogeneous, similar to the methodology of Garley et al., (2019), in which they redistributed charges of neighboring oxygen according to ion substitution).

Molecular dynamics simulations were carried out using LAMMPS (Plimpton, 1997). The simulations were performed in the canonical ensemble NVT (constant number of particles, volume and temperature) at 298 K using the Nosé-Hoover thermostat (Evans and Holian, 1985). The SHAKE algorithm (Ryckaert et al., 1977) was used to freeze bonds to hydrogens and the water and hydroxyl angles. This procedure enables increasing the time step dt from 1 fs to 2 fs.

A total simulation time of 6 ns (3×10^6 steps) for Study 1 and of 8 ns (4×10^6 steps) for Study 2 were used by means of the following protocol:

- **Minimization:** optimization of the initial geometry to relax to a point of minimum local energy. A cascade of methods in the form Steepest Descent → Conjugate Gradients → Newton → Steepest Descent was used, starting from a convergence criterion of 1.0×10^{-10} and ending at 1.0×10^{-20} , for forces and energies.
- **Thermalization:** First stage of molecular dynamics; a temperature ramp takes the system gradually from 150 K to the target temperature of 298 K over 2000 ps (106 steps).
- **Equilibration:** The system adapts to the objective temperature and relaxes, coming into equilibrium for another 2000 ps.
- **Production:** After equilibration, another 2000 ps (Study 1) or 4000 ps (Study 2) of simulation were used to sample the properties to be measured.

2.4. Analysis

Avogadro (Hanwell et al., 2012), VMD (Humphrey et al., 1996), TRAVIS (Brehm et al., 2020; Brehm and Kirchner, 2011) and in-house scripts (developed by CETEM/Labmol - Molecular Modeling Laboratory) were used for visualization, manipulation, and further analyses. The analysis methodology was based on the evaluation of collector-mineral interaction energies (E_{CM}), collector-collector interaction energies (E_{CC}), 1-D concentration profiles perpendicular to the surface, $\rho(z)$, hydrogen bond (HB) analysis and angular distribution of adsorbed collectors.

For Study 1, the interaction energies were used to calculate selectivity indexes of the form E_{QTZ}/E_{HEM} and $(E_{QTZ} - E_{HEM})/E_{QTZ}$. It was evaluated a general average case, using the average of E_{CM} for each collector with hematite (E_{HEM}) and quartz (E_{QTZ}) and also worst and best-case scenarios, in which the values of E_{QTZ} and E_{HEM} were chosen from four groups, respective to the four types of surfaces, namely Q (100)- α , Q (100)- β , H (001)-D1 and H (001)-D2. In best-case scenarios the lowest (more negative, more favorable) average value of E_{CM} out of Q (100)- α and Q (100)- β , and the highest value between H (001)-D1 and H (001)-D2 were chosen. In the worst-case scenarios, the highest value for quartz was used together with the lowest value of hematite. This was done separately for the cases of pH ~ 10.5 and pH ~ 8.5.

3. Results

3.1. Study 1 - Single collector adsorption

It is noticeable that some of the collectors were transferred to the liquid-vapor interface, even though they were placed at the solid-liquid adsorption position a priori. This result shows that, for these cases, the adsorption on the mineral has a weak driving force, so that it does not persist even though it was forced at first. The cases in which such a phenomenon occurred were for neutral etheramine at quartz (100)- β – (0e), quartz (100)- α – (-1e) and hematite (001)-D2 – (0e) as shown by Figure 6-a-c.

It is possible to infer, at least qualitatively, that etheramine in neutral form, in general, tends to be more at the liquid-vapor interface than in solution or at the solid-liquid interface. Such result is in line with a classic flotation heuristic that says that operational pH \cong collector's pK_a is optimal because the cationic half acts as collector, while the neutral half acts as frother (Drzymala and Kowalczyk, 2018; Kapiamba and Kimpiab, 2021; Matos et al., 2021; Zhou et al., 2019). This aspect related to the liquid-vapor interface can be further explored in relation to the frothing properties of collector reagents.

Table 1 presents the measured E_{CM} values. Neutral surfaces adsorb the collectors weakly, showing unstable attraction for neutral collectors mainly. On the other hand, the cationic collectors show repulsion by neutral hematite (001)-D2 and quartz (100)- α , which can be explained by the fact that the outermost layer of these surfaces is dominated by positive partial charges, Fe in hematite and H and Si in quartz. Also, the collectors in cationic form display high similarity in the E_{CM} values regarding the neutral surfaces, what indicates that their net +1 charge is the dominant factor in such interactions.

The results showed that amidoamine-quartz interaction energies are more favorable than those of amidoamine-hematite, with a value of 0 for H (001)-D1. As already mentioned, the D1 surface is almost inert in a wide range of pH values, thus the collectors have low to no tendency to adsorb at hematite-D1. Lützenkirchen et al. (2015) observed that D1 increases with sample aging in aqueous solution, in a way that for fresh hematite samples, the proportion of D1 and D2 is similar and close to 50%. With aging, D1 becomes dominating. The authors observed values of PZC close to 6.5 for fresh samples and 9 for aged samples.

Amidoamine, in neutral form, shows more attraction for surfaces than neutral etheramine, mainly for quartz surfaces. Charged surfaces strongly adsorbed the protonated collectors, as expected, by the electrostatic driving force. Their main adsorption configurations are shown in Fig. 6 d-i. This fact is even more evident in the simulated systems with higher

surface ionization. Table 2 shows selectivity indexes calculated in different ways. Even for worst case scenarios, amidoamine shows the highest selectivity.

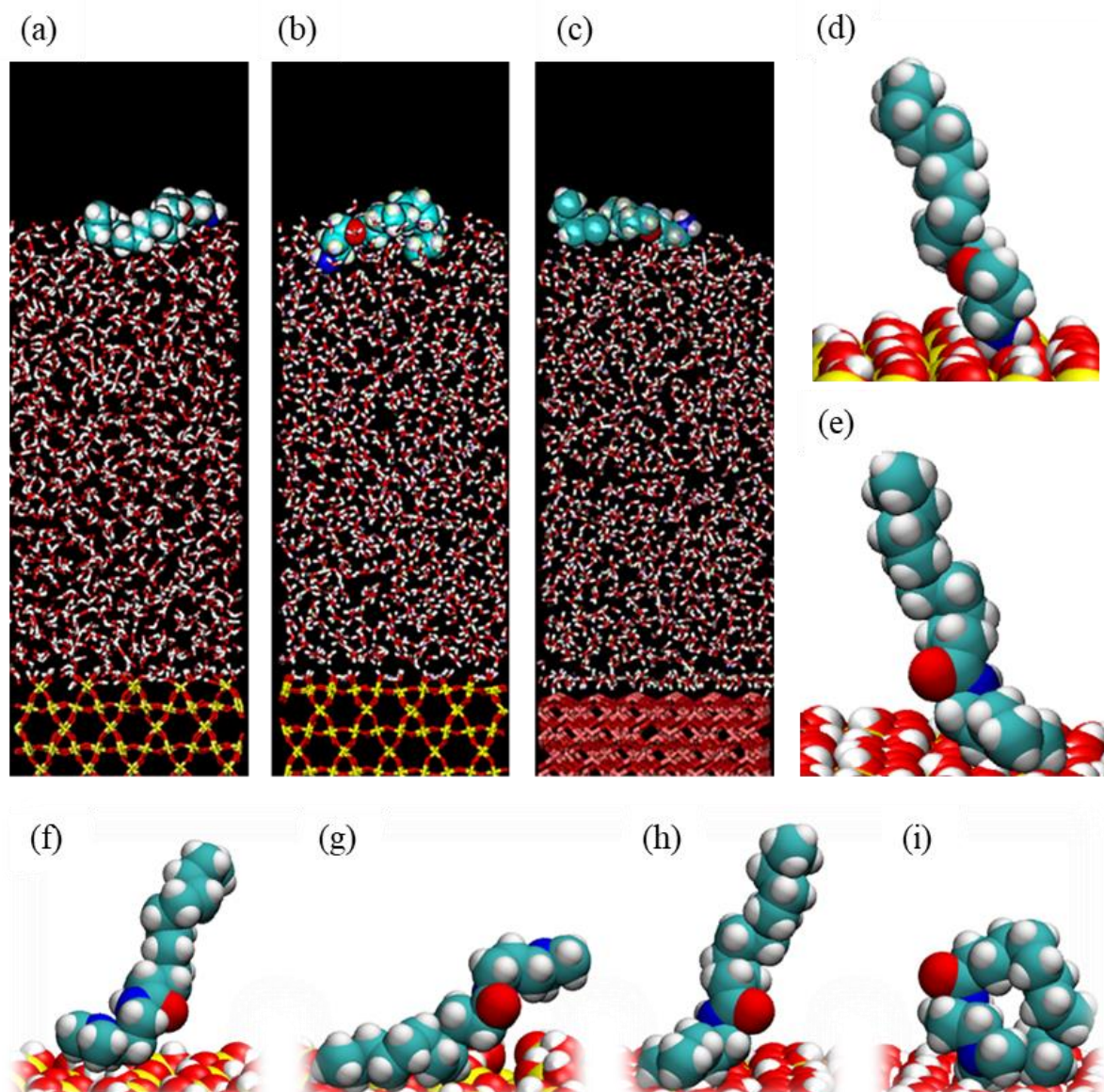


Figure 6 – Most important adsorption modes identified in Study 1. Adsorption of neutral etheramine at the liquid-vapor interface in the systems with (a) Quartz (100)- α ; (b) Quartz (100)- β ; (c) Hematite (001)-D2. Main adsorption mode of the cations, strongly attached by the charged head-group: (d) Etherammonium; (e) Amidoammonium. Main observed adsorption modes of amidoamine onto quartz: (f) Attached by the head, amino and amide polar regions in contact with water; (g) Attached by hydrocarbon chain; (h) Attached by the head with amino group interacting with the surface (hydrogen bond or electrostatics, if protonated); (i) Attached by both ends, coiled around itself minimizing hydrocarbon-water contact area.

Table 1 – Collector-Mineral interaction energies (kcal/mol) related to Study 1

Surface	Charge	Amidoamine	Amidoammonium	Etheramine	Etherammonium
Quartz (100)- α	0e	-1.40 \pm 1.78	3.51 \pm 3.11	-0.33 \pm 0.85	3.90 \pm 1.93
	-1e	-0.15 \pm 0.98	-39.31 \pm 12.98	0.00 \pm 0.28	-82.83 \pm 24.96
	-4e (\approx pH 8,5)	-1.46 \pm 3.52	-187.39 \pm 44.36	-	-61.90 \pm 32.61
	-6e (\approx pH 10,5)	-3.97 \pm 7.37	-	0.27 \pm 3.70	-393.13 \pm 118.61
Quartz (100)- β	0e	-1.40 \pm 1.52	-6.47 \pm 1.37	0.00 \pm 0.00	-6.61 \pm 2.12
	-1e	-2.26 \pm 4.00	-65.22 \pm 17.38	-0.83 \pm 1.40	-99.20 \pm 42.47
	-4e (\approx pH 8,5)	-3.70 \pm 6.11	-343.95 \pm 38.38	-	-199.50 \pm 55.38
	-6e (\approx pH 10,5)	-4.78 \pm 6.69	-	-0.36 \pm 3.10	-570.12 \pm 15.46
Hematite (001)-D2	0e	-0.08 \pm 0.23	8.17 \pm 1.74	0.00 \pm 0.01	9.55 \pm 1.31
	-1e	0.02 \pm 1.01	-32.17 \pm 21.72	-0.33 \pm 0.72	-143.90 \pm 6.10
	-2e (\approx pH 8,5)	-0.38 \pm 2.39	-129.03 \pm 40.23	-	-283.04 \pm 10.48
	-4e (\approx pH 10,5)	-1.31 \pm 3.35	-	-0.38 \pm 1.00	-215.16 \pm 36.26
Hematite (001)-D1	0e	0.00 \pm 0.11	-1.42 \pm 0.28	-0.67 \pm 1.01	-1.43 \pm 2.18

Table 2 – Selectivity of the collectors from different metrics related to Study 1.

pH 10,5	Selectivity Metric	Amidoamine	Etheramine	Etherammonium
		average (E_{QTZ})	-2.33	-0.21
	average (E_{HEM})	-0.34	-0.35	-87.74
$\frac{E_{QTZ}}{E_{HEM}}$	average	6.79	0.6	2.18
	best case	∞	1.68	157.56
	worst case	4.03	0.03	1.35
$\frac{E_{QTZ} - E_{HEM}}{E_{QTZ}}$	average	0.85	-0.66	0.54
	best case	1.00	0.4	0.99
	worst case	0.75	-32.5	0.26
pH 8,5	Selectivity Metric	Amidoamine	Amidoammonium	Etherammonium
		average (E_{QTZ})	-1.73	-106.47
	average (E_{HEM})	-0.11	-38.61	-104.70
$\frac{E_{QTZ}}{E_{HEM}}$	average	15.75	2.76	0.71
	best case	∞	97.74	71.17
	worst case	6.85	1.46	0.34
$\frac{E_{QTZ} - E_{HEM}}{E_{QTZ}}$	average	0.94	0.64	-0.41
	best case	1.00	0.99	0.99
	worst case	0.85	0.31	-1.96

It is worth noting that, the amidoamine in neutral form interacts favorably with quartz and that behavior is increased with higher surface ionization. Such behavior seems contradictory since there is no net charge electrostatic driving force. In fact, if electrostatics were to play an important role, would be by repulsion, since the strongest partial charges of the amidoamine are in its carbonyl and tertiary amino groups, both of negative sign (-0.38 in O and - 0.66 in N). Furthermore, such groups are highly hydrophilic, and do not favor from leaving their water coordination to coordinate to the surface hydroxyls most of the time. We can only infer that the main force that drives the neutral amidoamine binding to quartz is the van der Waals force. In fact, by inspecting the trajectory results, we observed in the adsorption modes shown in Fig. 6- f-i that most of the amidoamine-quartz contact is made by the hydrocarbon portion, especially the methyl groups of the amidoamine head as in Fig. 6-f.

3.2. Study 2 - Adsorption Layer Stability

Interaction Energies

The results show that, while E_{CM} is stronger for etheramine, E_{CC} favors neutral amidoamine and is highly repulsive for the cases presenting cationic species. Since the adsorption layer of etheramine is composed of neutral molecules and cations at pH ~ 10.5 and mainly of cations at pH ~ 8.5, the latter repel each other, while for neutral amidoamine (pH ~ 10.5) they attract each other not only by vdW tail-tail interactions, but mostly because of amide groups HBs as shown later in the text. Even at pH ~ 8.5, in which there is 50% cationic amidoamine, the collector-collector repulsion is weaker in quartz than it is for etherammonium.

As already observed in the previous section, etherammonium, followed by protonated amidoamine, binds better to the negatively charged quartz surfaces because of electrostatic attraction, and this also reflected in the E_{CM} interaction energy calculated in this section.

An important observation is that protonated amidoamine interacts less intensely with hematite and more strongly with quartz than the etherammonium. This may be related to a steric hindrance due to the combination of the bulky group of the amidoamine head with the coordinating water on hematite-(D2) surface, as will be shown in following sections. Table 3 shows the summary of these interaction energies, which account for the total interaction energy (coulomb and vdW).

Table 3 - Summary of ECM and ECC related to Study 2.

pH	Collector	Mineral	ECC (Kcal/mol)	ECM (Kcal/mol)
10,5	Amidoamine	H(001)-D2	-27.924 ± 15.263	-172.0388 ± 11.953
		Q(100)- α	-31.808 ± 17.275	-260.6884 ± 18.171
		Q(100)- β	-19.351 ± 18.457	-253.9323 ± 20.007
	Etheramine/ ammonium	H(001)-D2	14092.98 ± 93.577	-7066.345 ± 54.684
		Q(100)- α	13116.82 ± 86.804	-11586.122 ± 57.840
		Q(100)- β	12842.23 ± 75.085	-11075.459 ± 58.580
8,5	Amidoamine/ ammonium	H(001)-D2	13661.86 ± 354.95	-2940.19 ± 53.06
		Q(100)- α	7340.62 ± 89.34	-4000.59 ± 46.71
		Q(100)- β	7528.13 ± 71.16	-3974.27 ± 46.28
	Etherammonium	H(001)-D2	31923.03 ± 224.06	-10870.07 ± 60.33
		Q(100)- α	32049.05 ± 245.56	-12313.70 ± 79.07
		Q(100)- β	27952.96 ± 252.25	-11244.90 ± 63.60

1D Atomic Concentration Profiles

Figure 7 shows the concentration profiles along the surface normal vector, $\rho(z)$ (direction z). They show that etheramine/ammonium adsorb by the charged polar head, as expected. It also shows that there is inversion of these collectors at the adsorption layer. Etheramine population is majorly inverted at Quartz (100)- α and display less inversion at the other surfaces.

Etherammonium, on the other hand, displays significative inversion in all cases, and this phenomenon is more pronounced for hematite cases, as seen by the height and width of the peaks (red and dark red curves). An important finding is that amidoamine also adsorbs mostly by the head, not the amide group. That is actually consistent with the fact that the dominating character of the amide group is associated with the highly electronegative carbonyl group.

It is noticeable that both quartz surfaces show similarity between their peaks of collector's head group at pH ~ 10.5 (dark blue and dark red curves), both high and near peaks, while hematite (100)-D2 shows a difference of ~ 3.5 Å between etherammonium and amidoamine head peaks. This difference is due to a shielding effect promoted by hematite's coordination water groups at the surface that hinder the approximation of weak adsorbates and even of charged amidoamine.

Quartz (100)- α shows the broadest headgroup peaks which is probably related to its more irregular surface, denying homogeneous surface accessibility to the collectors.

For the results of pH \sim 8.5, we can note that protonated amidoamine also presents significative inversion. The peaks of their protonated head group (dark green curve) are more distant to the surface than etherammonium headgroup at hematite D2, but closer at both quartz surfaces. Once more, coordinating water shields amidoamine, even in cationic form, mostly because its head group is too large to penetrate the water layer.

The head groups peak followed by the middle chain groups peak represents a more organized adsorption layer. This is observed in all cases for neutral and protonated amidoamine and for etherammonium. For etheramine, the head and middle group profiles are overlapping (yellow and dark yellow curves), which indicate a very disordered structure and the formation of hydrogen bonds between the ether and amine groups in the middle of the adsorption layer, as will be shown further in the text.

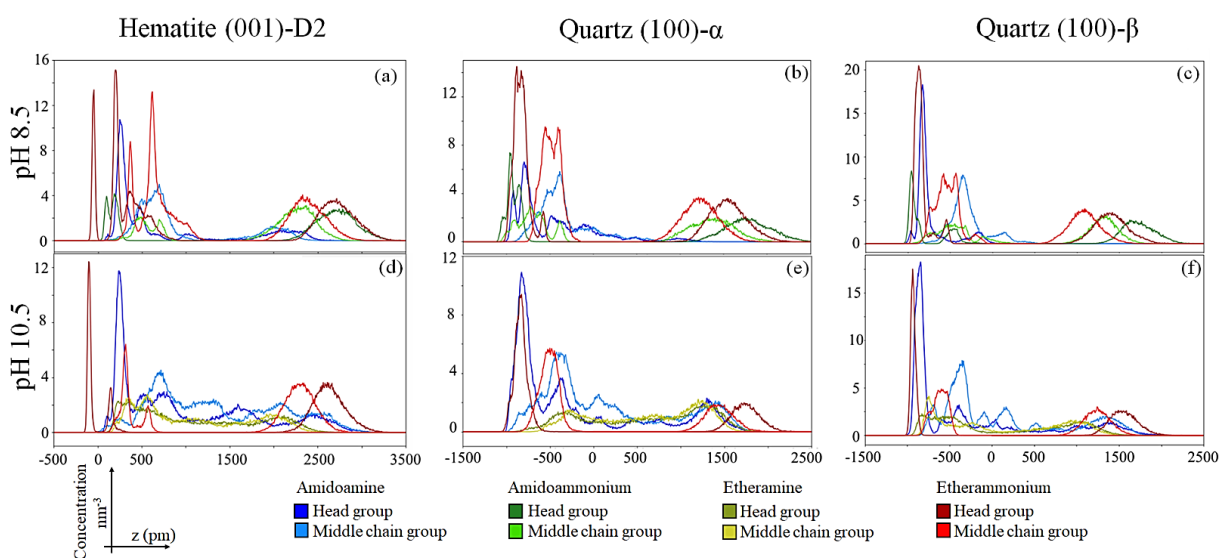


Figure 7 – 1D atom concentration profiles of the adsorption layers (distance values distribution from the head and middle group of collectors to mineral surfaces).

Surface Normal Angle Profiles

The angular distribution profiles in Figure 8 show that amidoamine is much closer to an angle perpendicular to the surface than etheramine since it is closer to 0, distancing from the surface normal vector.

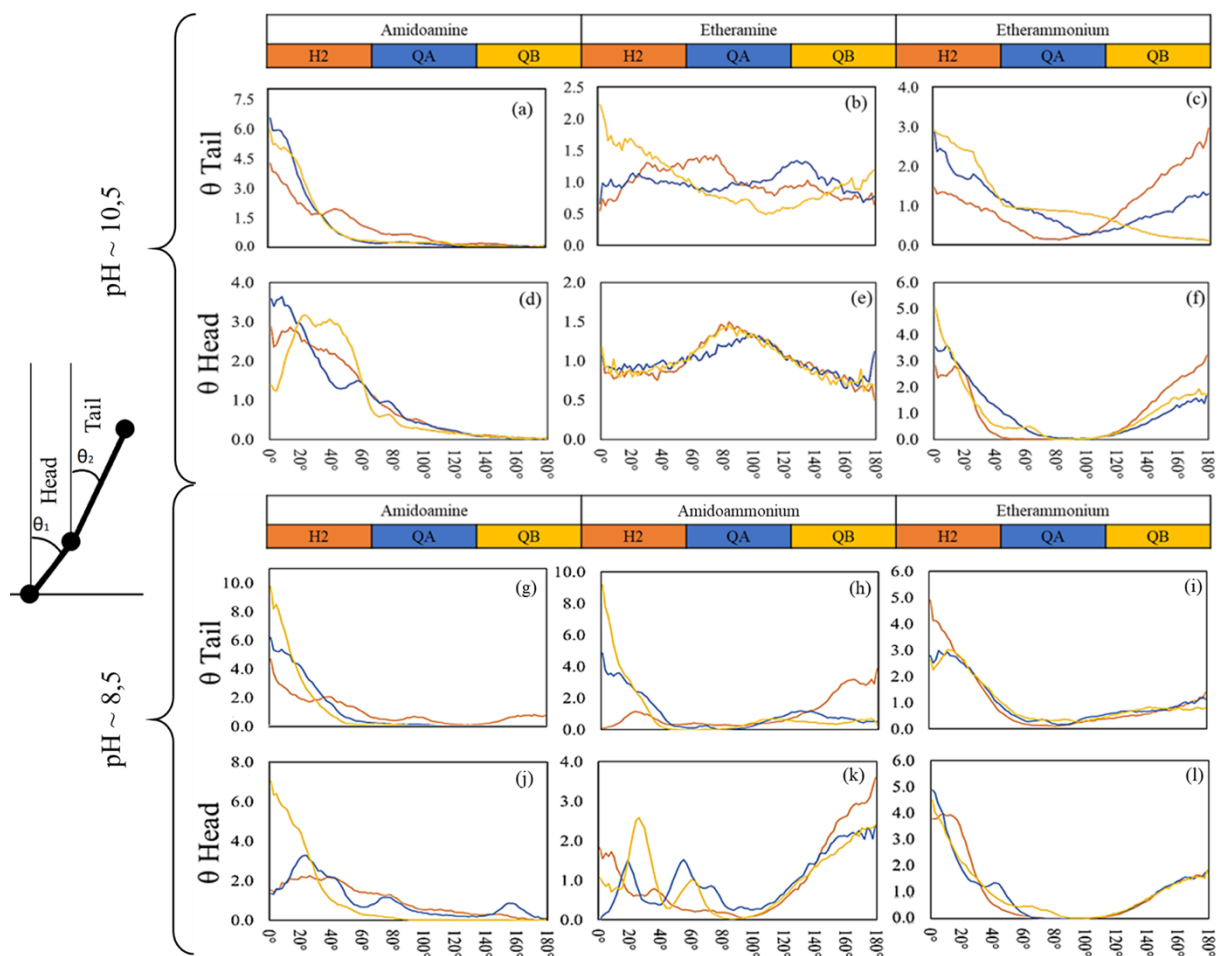


Figure 8 – Collectors' angle distribution (occurrence x angle). Brown: H2 – Hematite (001)-D2 ; Blue: QA – Quartz (100)- α ; Yellow: QB - Quartz (100)- β .

The neutral etheramine shows a very dispersed profile, while the cationic form presents an inversion, part of the cations is pointing towards the surface and part towards the solution. That behavior is seen for all cationic species. The disorganization of neutral etheramine entails less adsorption layer stability while the inversion of etherammonium generates a less hydrophobic character, two factors that hinder flotation. Neutral amidoamine profiles display much less dispersion and virtually no inversion.

Summarizing, by comparing the systems with 50/50 % of neutral/cation population (etheramine/etherammonium at pH 10,5 and amidoamine/amidoammonium at pH 8,5), we see that both collectors display significative inversion in their protonated form, but in neutral form, etheramine tends to be dispersed in very disorganized way, while amidoamine is organized and present low dispersion and almost no inversion.

Hydrogen Bonds

The hydrogen bond (HB) analysis shows that the amide group is responsible for establishing a stable HB network between the amidoamine molecules. While the tertiary amine head points toward the surface, the amide group, far by three carbons, connect to one another. The amide hydrogen donates to the next molecule's amide oxygen, creating a continuous and organized framework. It stands out that etheramine/ammonium forms many HBs, but they are either at the mineral surface or at the solution interface, while amidoamine's HBs are mostly inside the collector layer. Fig. 9 shows the hydrogen bond structure in the simulated systems and Table 4 shows the HB counts.

Table 4 – Hydrogen bond count between collector-collector and collector-mineral.

pH	Mineral Surface	Collector	CC	CM
10,5	Hematite (001)-D2	Amidoamine	13.26 ± 4.64	0.27 ± 0.62
		Etheramine/ammonium	11.12 ± 5.42	29.16 ± 4.70
	Quartz (100)- α	Amidoamine	10.36 ± 5.33	8.84 ± 2.77
		Etheramine/ammonium	13.34 ± 5.82	69.55 ± 10.46
	Quartz (100)- β	Amidoamine	14.64 ± 4.21	2.21 ± 1.34
		Etheramine/ammonium	13.38 ± 5.98	87.40 ± 10.79
8,5	Hematite (001)-D2	Amidoamine/ ammonium	13.86 ± 4.45	0.00 ± 0.03
		Etherammonium	7.23 ± 4.24	32.68 ± 3.71
	Quartz (100)- α	Amidoamine/ ammonium	13.34 ± 4.16	8.81 ± 2.66
		Etherammonium	10.29 ± 5.25	132.91 ± 9.46
	Quartz (100)- β	Amidoamine/ ammonium	12.86 ± 4.57	1.40 ± 1.14
		Etherammonium	13.83 ± 6.25	106.41 ± 10.17

It is noteworthy that etheramine, especially when protonated, is a better HB donor than amidoamine. In fact, it forms more hydrogen bonds than the amidoamine molecules, but the crucial difference is that all HB donor potential is in the polar head, which is responsible for adhering to the surface. The etheramine topological equivalent functional group of the amide in amidoamine is the ether group, which is a HB acceptor that actually forms HBs with amine headgroups. But this HBs are not beneficial, since they require the amine/ammonium headgroups to be away from the surface, contributing to layer disorganization and inversion, as can be seen in Fig. 9. Also, as the adsorption layers form, there starts to exist a neighborhood of ether groups, which have negative partial charge and repel each other. Contrastingly, for amido-

amine, as the layers start to form, the amide groups form HB to each other, creating the exact opposite type of interaction.

It is noticeable that surface OH groups act as HB donor to amidoamine head group nitrogen, which acts as HB acceptor. For etheramine/ ammonium, it is mainly the opposite, the head group acts more as HB donor and the minerals as HB acceptors. This behavior is noticeable when comparing Fig. 9-b and Fig. 9-e.

Quartz (100)- α surface entraps more water, especially with etheramine/ammonium. This entrained water finds easier access because of this surface's higher roughness and irregular topography. This water seeks to balance the high electrostatics in the interface.

Fig. 9-c and Fig. 9-f show perfectly the already mentioned effect of coordination water at hematite (001)-D2 surface. Such layer of chemically bound water shields the surface from the adsorption of neutral collectors. It is noticeable how far and disorganized are amidoamine molecules from the surface. On the other hand, because of the electrostatic driving force, the etherammonium can penetrate this layer and bind to some surface sites.

Figure 9 also shows the aforementioned inversion of etherammonium and protonated amidoamine at pH \sim 8.5. Also, it can be seen that even with the electrostatic driving force, protonated amidoamine has difficulties in penetrating hematite's coordinating water layer, mostly because of the steric hindrance due its bulky head group.

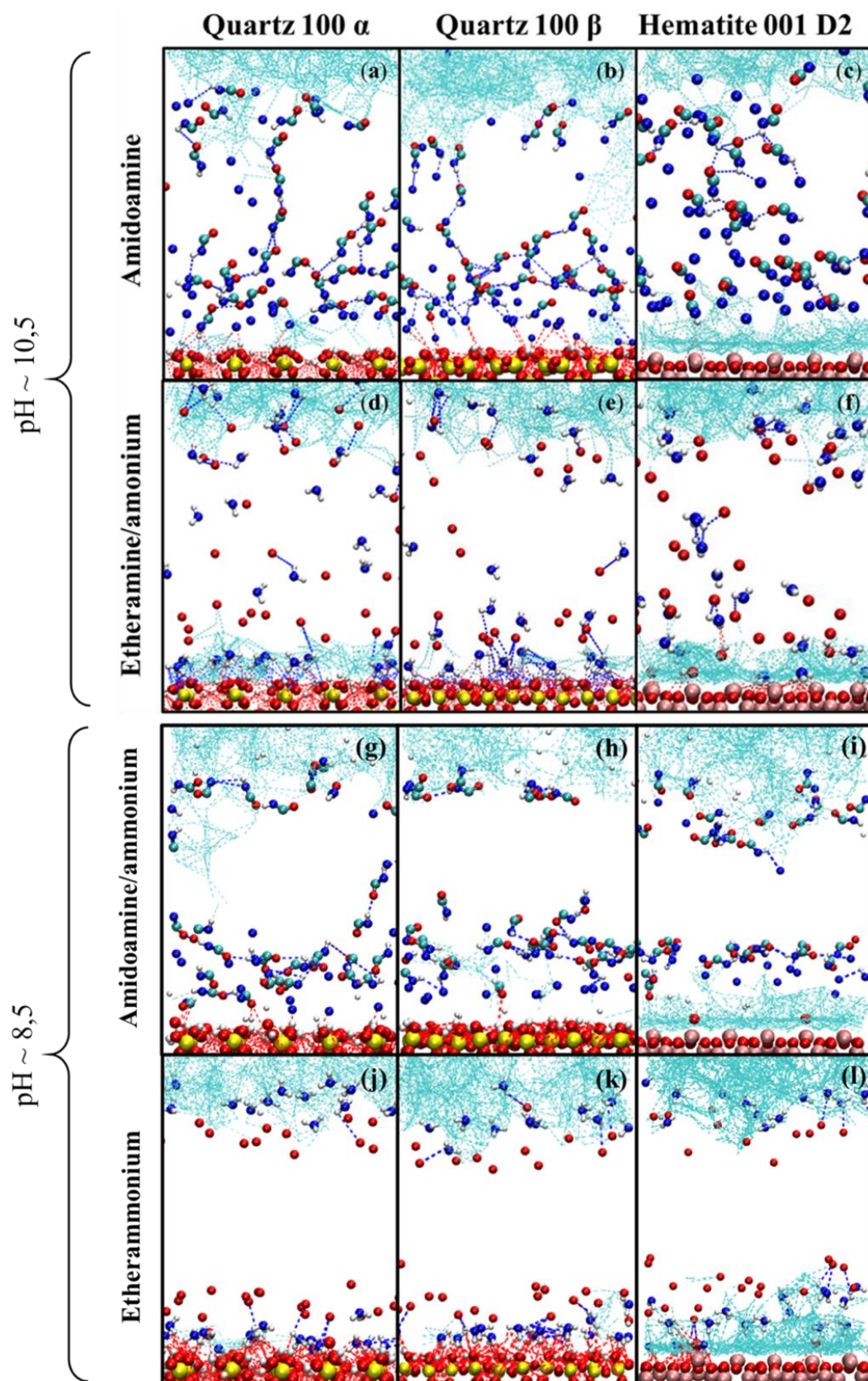


Figure 9 – Snapshots of the hydrogen bonds observed in the simulation systems. For clarity, only the collectors' hydrogen bonding functional groups are shown, as well as surface atoms. Hydrogen bonds color code by HB donor: water - cyan; non-water: oxygen - red, nitrogen - blue. Atom color code: hydrogen - white, oxygen - red, nitrogen - blue, carbon - cyan, silicon - yellow, iron - pink.

4. Conclusion

The molecular dynamics simulations showed the adsorption difference between etheramine and amidoamine.

The single collector adsorption simulations showed that amidoamine has a much higher affinity for quartz than for hematite, indicating selectivity.

The amidoamine N-[3-(dimethylamino)propyl]dodecanamide, in the neutral state (pH 10.5), presents sufficient mineral-collector interaction energy to start the adsorption process on the quartz surface. The amide group in this collector structure plays important role for the hydrogen bonding stabilization of the adsorption layer, thus the collector-collector interaction energy contributes to organize the amidoamine on the quartz surface.

The etheramine ether middle chain groups repel each other and cannot link themselves by hydrogen bonds at pH 10.5. To form HB and stabilize the adsorption layer, the amine/ammonium headgroups must escape the surface plane to act as HB donors for ether, and as such lose the same interaction, they would otherwise be developing with the surface atoms. Thus, the etheramine does not have the same ability to organize itself on the mineral's surface, presenting much higher levels of inversion and disorganization, with the head facing the opposite direction of the mineral surface, towards the solution.

The selectivity behavior for the quartz-hematite system flotation with amidoamine can be explained by the combination of the "shield" formed by the coordinating water molecules on the surface D2 of the hematite with the large molecular volume of amidoamine head group, due the methyl bonded to nitrogen in the tertiary amine, generating steric hindrance and impairing the adsorption on hematite-(D2) surface, even considering the protonated amidoamine (pH 8,5).

In relation to etheramine, the neutral collector adsorption is impaired by the coordinating water on the hematite-(D2) surface, but the protonated molecule (etherammonium) can penetrate and bind on this surface due the electrostatic driving force.

Hematite-D1 barely shows any collector affinity when comparing to the other surfaces.

These simulation results contribute to explain the results obtained by authors such as Matiolo et al. (2020) when adopting the amidoamine N- [3-(dimethylamino)propyl] dodecanamide as collector in iron ore slimes flotation, at pH 10.5 without a depressant and Silva et al. (2021a) when demonstrating, by FTIR, the hindrance effect related the adsorption of this collector on the hematite.

Furthermore, the properties of the froth generated by this amidoamine and its effect on flotation also need to be investigated in further studies.

Changes in mineral surface characteristics due to aging and/or different textures contribute to explain some experimental behaviors, such as obtaining different degrees of recovery and selectivity in flotation in relation to the size distribution or lithology of iron ore, for example. Therefore, it is also recommended that further simulations and analyses be conducted to explore collector-collector interactions and collector adsorption behavior in other mineral planes, regarding the system quartz-hematite, mainly for hematite surfaces.

Acknowledgements

This paper was supported by VALE S.A in the context of developing beneficiation routes for iron ore slimes. The support of LABMOL/CETEM (Centre for Mineral Technology) is also acknowledged. The support of GeoRessources Laboratory, University of Lorraine, is greatly acknowledged. The support of Clariant, Brazil is deeply appreciated.

References

- Allen, M.P., Tildesley, D.J., 2017. Computer simulation of liquids, second ed. Oxford University Press, Oxford.
- Araujo, A.C., Viana, P.R.M., Peres, A.E.C., 2005. Reagents in iron ores flotation. *Miner. Eng.* 18 (2), 219–224. <https://doi.org/10.1016/j.mineng.2004.08.023>.
- Araujo, V.A., Lima, N., Azevedo, A., Bicalho, L., Rubio, J., 2020. Column reverse rougher flotation of iron bearing fine tailings assisted by HIC and a new cationic collector. *Miner. Eng.* 156, 106531. <https://doi.org/10.1016/j.mineng.2020.106531>.
- Berendsen, H.J.C., Grigera, J.R., Straatsma, T.P., 1987. The missing term in effective pair potentials. *J. Phys. Chem.* 91 (24), 6269–6271. <https://doi.org/10.1021/j100308a038>.
- Blake, R.L., HessevicK, R.E., Zoltai, T., Finger, L.W., 1966. Refinement of the Hematite Structure. *Am. Mineral.* 51, 123–129.
- Brehm, M., Kirchner, B., 2011. TRAVIS - A free analyzer and visualizer for monte carlo and molecular dynamics trajectories. *J. Chem. Inf. Model.* 51 (8), 2007–2023. <https://doi.org/10.1021/ci200217w>.
- Brehm, M., Thomas, M., Gehrke, S., Kirchner, B., 2020. TRAVIS—A free analyzer for trajectories from molecular simulation. *J. Chem. Phys.* 152 (16), 164105. <https://doi.org/10.1063/5.0005078>.

Budenberg, G., 2016. Síntese de coletores para flotação de minério de ferro. Dissertação de Mestrado, Escola de Engenharia de Lorena, Universidade de São Paulo, Lorena. <https://doi.org/10.11606/D.97.2017.tde-20112017-12415>.

Butenuth, A., Moras, G., Schneider, J., Koleini, M., Köppen, S., Meißner, R., Wright, L.B., Walsh, T.R., Ciacchi, L.C., 2012. Ab initio derived force-field parameters for molecular dynamics simulations of deprotonated amorphous-SiO₂/water interfaces. *Phys. Status Solidi Basic Res.* 249, 292–305. <https://doi.org/10.1002/pssb.201100786>.

Cao, Y., Tong, X., Xie, X., Song, Q., Zhang, W., Du, Y., Zhang, S., 2021. Effects of grinding media on the flotation performance of cassiterite. *Miner. Eng.* 168, 106919. <https://doi.org/10.1016/j.mineng.2021.106919>.

Crystallography Open Database [WWW Document], 2020. URL <http://www.crystallography.net/cod/>.

Cygan, R.T., Liang, J.-J., Kalinichev, A.G., 2004. Molecular Models of Hydroxide, Oxyhydroxide, and Clay Phases and the Development of a General Force Field. *J. Phys. Chem. B* 108 (4), 1255–1266. <https://doi.org/10.1021/jp0363287>.

Dauber-Osguthorpe, P., Roberts, V.A., Osguthorpe, D.J., Wolff, J., Genest, M., Hagler, A. T., 1988. Structure and energetics of ligand binding to proteins: Escherichia coli dihydrofolate reductase-trimethoprim, a drug-receptor system. *Proteins Struct. Funct. Genet.* 4 (1), 31–47. <https://doi.org/10.1002/prot.340040106>.

Drzymala, J., Kowalczyk, P., 2018. Classification of Flotation Frothers. *Minerals* 8 (2), 53. <https://doi.org/10.3390/min8020053>.

Dynarowicz-Iatka, P., Dhanabalan, A., Oliveira, O.N., 2001. Modern physicochemical research on Langmuir monolayers. *Adv. Colloid Interface Sci.* 91 (2), 221–293. [https://doi.org/10.1016/S0001-8686\(99\)00034-2](https://doi.org/10.1016/S0001-8686(99)00034-2).

Emami, F.S., Puddu, V., Berry, R.J., Varshney, V., Patwardhan, S.V., Perry, C.C., Heinz, H., 2014. Force Field and a Surface Model Database for Silica to Simulate Interfacial Properties in Atomic Resolution. *Chem. Mater.* 26 (8), 2647–2658. <https://doi.org/10.1021/cm500365c>.

Evans, D.J., Holian, B.L., 1985. The Nose-Hoover thermostat. *J. Chem. Phys.* 83 (8), 4069–4074. <https://doi.org/10.1063/1.449071>.

Filippov, L.O., Filippova, I.V., Severov, V.V., 2010. The use of collectors mixture in the reverse cationic flotation of magnetite ore: The role of Fe-bearing silicates. *Miner. Eng.* 23 (2), 91–98. <https://doi.org/10.1016/j.mineng.2009.10.007>.

Filippov, L.O., Severov, V.V., Filippova, I.V., 2013. Mechanism of starch adsorption on Fe-Mg-Al-bearing amphiboles. *Int. J. Min. Process.* 123 (10), 120–128. <https://doi.org/10.1016/j.minpro.2013.05.010>.

Filippov, L.O., Foucaud, Y., Filippova, I.V., Badawi, M., 2018. New reagent formulations for selective flotation of scheelite from a skarn ore with complex calcium minerals gangue. *Miner. Eng.* 123, 85–94. <https://doi.org/10.1016/j.mineng.2018.05.001>.

Filippov, L.O., Severov, V.V., Filippova, I.V., 2014. An overview of the beneficiation of iron ores via reverse cationic flotation. *International Journal of Mineral Processing* 127, 62–69. <https://doi.org/10.1016/j.minpro.2014.01.002>.

Filippov, L.O., Silva, K., Piçarra, A., Lima, N., Santos, I., Bicalho, L., Filippova, I.V., Peres, A., 2021. Iron ore slimes flotation tests using column and amidoamine collector without depressant. *Minerals* 11 (7), 699. <https://doi.org/10.3390/min11070699>.

Foucaud, Y., Badawi, M., Filippov, L., Filippova, I., Lebègue, S., 2019. A review of atomistic simulation methods for surface physical-chemistry phenomena applied to froth flotation. *Miner. Eng.* 143, 106020. <https://doi.org/10.1016/j.mineng.2019.106020>.

Foucaud, Y., Lebègue, S., Filippov, L.O., Filippova, I.V., Badawi, M., 2018. Molecular Insight into Fatty Acid Adsorption on Bare and Hydrated (111) Fluorite Surface. *J. Phys. Chem. B* 122 (51), 12403–12410. <https://doi.org/10.1021/acs.jpcc.8b08969>.

Friedli, F., 1990. Amidoamine Surfactants. In: Richmond, J. (Ed.), *Cationic Surfactants - Organic Chemistry (Surfactant Science Series; V34)*. Marcel Dekker Inc., New York, pp. 52–83.

Ganguly, P., Paranjape, D.V., Rondelez, F., 1997. Role of tail-tail interactions versus head-group/subphase interactions in the pressure-area isotherms of fatty amines at the air-water interface. 1. Influence of subphase acid counterions. *Langmuir* 13 (20), 5433–5439. <https://doi.org/10.1021/la960981m>.

Garley, A., Hoff, S.E., Saikia, N., Jamadagni, S., Baig, A., Heinz, H., 2019. Adsorption and Substitution of Metal Ions on Hydroxyapatite as a Function of Crystal Facet and Electrolyte pH. *J. Phys. Chem. C* 123 (27), 16982–16993. <https://doi.org/10.1021/acs.jpcc.9b02808>.

Hanwell, M.D., Curtis, D.E., Lonie, D.C., Vandermeersch, T., Zurek, E., Hutchison, G.R., 2012. Avogadro: an advanced semantic chemical editor, visualization, and analysis platform. *J. Cheminform.* 4, 17. <https://doi.org/10.1186/1758-2946-4-17>.

Huang, Z., Zhong, H., Wang, S., Xia, L., Zou, W., Liu, G., 2014. Investigations on reverse cationic flotation of iron ore by using a Gemini surfactant: Ethane-1,2-bis(dimethyl-dodecylammonium bromide). *Chem. Eng. J.* 257, 218–228. <https://doi.org/10.1016/j.cej.2014.07.057>.

Humphrey, W., Dalke, A., Schulten, K., 1996. VMD – Visual Molecular Dynamics. *J. Mol. Graph.* 14 (1), 33–38.

Kapiamba, K.F., Kimpiab, M., 2021. The effects of partially replacing amine collectors by a commercial frother in a reverse cationic hematite flotation. *Heliyon* 7 (3), e06559. <https://doi.org/10.1016/j.heliyon.2021.e06559>.

Kerisit, S., 2011. Water structure at hematite-water interfaces. *Geochim. Cosmochim. Acta* 75 (8), 2043–2061. <https://doi.org/10.1016/j.gca.2011.01.026>.

Kiejna, A., Pabisiak, T., 2013. Mixed termination of hematite (α -Fe₂O₃)(0001) surface. *J. Phys. Chem. C* 117 (46), 24339–24344. <https://doi.org/10.1021/jp406946s>.
Leal Filho, L.S, Seidl, P.R., Correia, J.C.G., Cerqueira, L.C.K., 2000. Molecular modelling of reagents for flotation processes. *Miner. Eng.* 13 (14–15), 1495–1503. [https://doi.org/10.1016/S0892-6875\(00\)00133-3](https://doi.org/10.1016/S0892-6875(00)00133-3).

Levien, L., Prewitt, C.T., Weidner, D.J., Prewitt, C.T., Weidner, D.J., 1980. Structure and Elastic Properties of Quartz at Pressure. *Am. Mineral.* 65, 920–930.
Liu, D., Zhang, G., Liu, J., Pan, G., Chen, Y., Wang, M., 2021a. Studies on the surface oxidation and its role in the flotation of mixed Cu-Ni sulfide ore. *Powder Technol.* 381, 576–584. <https://doi.org/10.1016/j.powtec.2020.12.038>.

Liu, J., Xie, R., Zhu, Y., Li, Y., Liu, C., 2021b. Flotation behavior and mechanism of styrene phosphonic acid as collector on the flotation separation of fluorite from calcite. *J. Mol. Liq.* 326, 115261. <https://doi.org/10.1016/j.molliq.2020.115261>.

Liu, W., Liu, W., Zhao, Q., Shen, Y., Wang, X., Wang, B., Peng, X., 2020a. Design and flotation performance of a novel hydroxy polyamine surfactant based on hematite reverse flotation desilication system. *J. Mol. Liq.* 301, 112428. <https://doi.org/10.1016/j.molliq.2019.112428>.

Liu, W., Peng, X., Liu, W., Wang, X., Zhao, Q., Wang, B., 2020b. Effect mechanism of the isopropanol substituent on amine collectors in the flotation of quartz and magnesite. *Powder Technol.* 360, 1117–1125. <https://doi.org/10.1016/j.powtec.2019.10.060>.

Liu, X., Cheng, J., Lu, X., Wang, R., 2014. Surface acidity of quartz: Understanding the crystallographic control. *Phys. Chem. Chem. Phys.* 16 (48), 26909–26916.

Lowe, B.M., Skylaris, C.-K., Green, N.G., Shibuta, Y., Sakata, T., 2018. Calculation of surface potentials at the silica-water interface using molecular dynamics: Challenges and opportunities. *Jpn. J. Appl. Phys.* 57 (4S), 04FM02. <https://doi.org/10.7567/JJAP.57.04FM02>.

Lützenkirchen, J., Heberling, F., Supljika, F., Preocanin, T., Kallay, N., Johann, F., Weisser, L., Eng, P.J., 2015. Structure-charge relationship - The case of hematite (001). *Faraday Discuss.* 180, 55–79. <https://doi.org/10.1039/c4fd00260a>.

Martínez, L., Andrade, R., Birgin, E.G., Martínez, J.M., 2009. PACKMOL: A package for building initial configurations for molecular dynamics simulations. *J. Comput. Chem.* 30 (13), 2157–2164. <https://doi.org/10.1002/jcc.21224>.

Matiolo, E., Couto, H.J.B., Lima, N., Silva, K., de Freitas, A.S., 2020. Improving recovery of iron using column flotation of iron ore slimes. *Miner. Eng.* 158, 106608. <https://doi.org/10.1016/j.mineng.2020.106608>.

Matos, V.E., Nogueira, S.d.C.S., Kowalczyk, P.B., Silva, G.R.d., Peres, A.E.C., 2021. Differences in Etheramines Froth Properties and the Effects on Iron Ore Flotation. Part I: Two-Phase Systems. *Miner. Process. Extr. Metall. Rev.* 43 (2), 209–216. <https://doi.org/10.1080/08827508.2021.1875461>.

Mhonde, N.P., 2016. Investigating collector and depressant performance in the flotation of selected iron ores. University of Cape Town. MSc thesis.

Mindat.org - Mines, Minerals and More [WWW Document], 2020. Hudson Inst. Mineral. URL <http://webmineral.com>.

Mineralogy Database [WWW Document], 2020. URL <http://webmineral.com>.

Nykänen, V.P.S., Braga, A.S., Pinto, T.C.S., Matai, P.H.L.S., Lima, N.P., Leal Filho, L.S., Monte, M.B.M., 2020. True flotation versus entrainment in reverse cationic flotation for the concentration of iron ore at industrial scale. *Miner. Process. Extr. Metall. Rev.* 41 (1), 11–21. <https://doi.org/10.1080/08827508.2018.1514298>.

Plimpton, S., 1995. Fast Parallel Algorithms for Short-Range Molecular Dynamics. *J. Comput. Phys.* 117 (1), 1–19.

Pubchem, 2021. Compound. Lauramidopropyldimethylamine. [WWW Document]. URL <https://pubchem.ncbi.nlm.nih.gov/compound/lauramidopropyldimethylamine> (accessed 12.27.20).

Rai, B., Sathish, P., Tanwar, J., Pradip, Moon, K.S., Fuerstenau, D.W., 2011. A molecular dynamics study of the interaction of oleate and dodecylammonium chloride surfactants with complex aluminosilicate minerals. *J. Colloid Interface Sci.* 362 (2), 510–516. <https://doi.org/10.1016/j.jcis.2011.06.069>.

Ryckaert, J.-P., Ciccotti, G., Berendsen, H.J.C., 1977. Numerical integration of the cartesian equations of motion of a system with constraints: molecular dynamics of n- alkanes. *J. Comput. Phys.* 23 (3), 327–341. [https://doi.org/10.1016/0021-9991\(77\)90098-5](https://doi.org/10.1016/0021-9991(77)90098-5).

Severov, V.V., Filippova, I.V., Filippov, L.O., 2013. Floatability of Fe-bearing silicates in the presence of starch: Adsorption and spectroscopic studies. *J. Phys. Conf. Ser.* 416, 012017. <https://doi.org/10.1088/1742-6596/416/1/012017>.

Scott, J.L., Smith, R.W., 1991. Diamine Flotation of Quartz. *Minerals Engineering* 4 (2), 141–150. [https://doi.org/10.1016/0892-6875\(91\)90030-Y](https://doi.org/10.1016/0892-6875(91)90030-Y).

Severov, V.V., Filippov, L.O., Filippova, I.V., 2016. Relationship between cation distribution with electrochemical and flotation properties of calcic amphiboles. *Int J Mineral Processing* 147, 18–27.

Silva, K., Filippov, L.O., Piçarra, A., Filippova, I.V., Lima, N., Skliar, A., Faustino, L., Filho, L.L., 2021a. New perspectives in iron ore flotation: Use of collector reagents without depressants in reverse cationic flotation of quartz. *Miner. Eng.* 170, 107004. <https://doi.org/10.1016/j.mineng.2021.107004>.

Silva, L.A., Garrot, T.G., Pereira, A.M., Correia, J.C.G., 2021b. Historical perspective and bibliometric analysis of molecular modeling applied in mineral flotation systems. *Miner. Eng.* 170, 107062. <https://doi.org/10.1016/j.mineng.2021.107062>.

Silva, L.A., Correia, J.C.G., 2020. GEMS-Pack: A Graphical User Interface for the Packmol Program. *J. Chem. Inf. Model.* 60 (2), 439–443. <https://doi.org/10.1021/acs.jcim.9b00740><https://doi.org/10.1021/acs.jcim.9b00740.s001><https://doi.org/10.1021/acs.jcim.9b00740.s002>.

Tanwar, K.S., Petitto, S.C., Ghose, S.K., Eng, P.J., Trainor, T.P., 2009. Fe(II) adsorption on hematite (0 0 0 1). *Geochim. Cosmochim. Acta* 73 (15), 4346–4365. <https://doi.org/10.1016/j.gca.2009.04.024>.

Trainor, T.P., Chaka, A.M., Eng, P.J., Newville, M., Waychunas, G.A., Catalano, J.G., Brown, G.E., 2004. Structure and reactivity of the hydrated hematite (0001) surface. *Surf. Sci.* 573 (2), 204–224. <https://doi.org/10.1016/j.susc.2004.09.040>.

Veloso, C.H., Filippov, L.O., Filippova, I.V., Ouvrard, S., Araujo, A.C., 2018. Investigation of the interaction mechanism of depressants in the reverse cationic flotation of complex iron ores. *Minerals Engineering* 125, 133–139. <https://doi.org/10.1016/j.mineng.2018.05.031>.

Wood, M.H., Casford, M.T., Steitz, R., Zorbakhsh, A., Welbourn, R.J.L., Clarke, S.M., 2016. Comparative Adsorption of Saturated and Unsaturated Fatty Acids at the Iron Oxide/Oil Interface. *Langmuir* 32 (2), 534–540. <https://doi.org/10.1021/acs.langmuir.5b04435>.

Zhou, X., Tan, Y.H., Finch, J.A., 2019. Frothing Properties of Amine/Frother Combinations. *Mining. Metall. Explor.* 36 (1), 81–88. <https://doi.org/10.1007/s42461-018-0034-6>.

Chapter 5 - Improving recovery of iron using column flotation of iron ore slimes

Elves Matiolo¹; Hudson Jean Bianquini Couto¹; Neymayer Lima²; Klaydison Silva² and Amanda Soares de Freitas¹

¹ Centro de Tecnologia Mineral (CETEM/MCTIC), Serviço de Processamento Mineral (SEPMI) – Rio de Janeiro - Brazil

² VALE – Desenvolvimento de projetos de tratamento de minérios – Belo Horizonte – Brazil

Minerals Engineering 158 (2020) 106608 <https://doi.org/10.1016/j.mineng.2020.106608>

Received 6 May 2020; Received in revised form 17 August 2020; Accepted 20 August 2020

Abstract: In general, the industrial flowsheets for the beneficiation of itabirite iron ores from the Quadrilátero Ferrífero (Minas Gerais state) in Brazil involves grinding, desliming, magnetic separation and cationic reverse flotation using both mechanical and columns flotation cells. At Brazilian plants, it is estimated that Fe losses generated at the slimes stage range between 8% reaching values higher than 20%. Slimes generated at hydrocyclone containing particle sizes of approximately 99% < 45 µm, 25% > 10 µm, 45% < 5 µm and 15% < 1 µm, 3% of solids by weight and between 35% and 45% of Fe grade. This work aims at evaluating the technical feasibility of concentration of two slimes samples from two different plants in operation at the Quadrilátero Ferrífero using the column flotation technology without prior desliming. Despite the similarity in terms of mineralogy, grade and particle size distribution, the flotation results indicate a very distinct behavior considering similar process conditions, including variables such as collector type and dosage, depressant dosage, pH and circuit configuration. Concentrate containing an Fe grade higher than 60%, 4% SiO₂ and 3.1% Al₂O₃ with an Fe recovery up to 75% in rougher column flotation it was obtained from Sample 1 with 45.2% Fe, 28.6% SiO₂ and 3.1% Al₂O₃, when a collector type amidoamine (Flotisor 5530) was used in substitution of a conventional amine collector. On the other hand, it was not possible to obtain a final concentrate containing an Fe grade higher than 55% from Sample 2 with 39.6% Fe, 33.4% SiO₂ and 5.1% Al₂O₃, using both types of collectors (amidoamine and amine) even when applying different types of column flotation circuits (rougher or rougher/cleaner). Based on literature review and the results obtained in this study, it can be observed the non-existence of a standard solution for an efficient slimes processing in the iron ore industry. Considering flotation as the most suitable technology for the treatment of such type of material, future research should focus

on a deep fundamental study of the collector-depressant mechanism interaction with the iron-bearing and gangue minerals, especially in those ores with a high amount of alumina-containing minerals. Considerations about the effect of bubble generator device to flotation columns and its impact on the metallurgical performance are also discussed regarding to application at industrial scale to slimes concentration.

1. Introduction

Froth flotation has been established as an efficient method to remove impurities from iron ore in half a century's practice around the world. Reverse cationic flotation is currently the most widely used flotation route (Houot, 1983; Araujo et al., 2005; Ma et al., 2011; Ma, 2012; Filippov et al., 2014). Brazil is the third largest producer of iron ore concentrates, yielding in 2017 around 453 million with 63.7% average iron grade (ANM, 2018) from which 60% are estimated to be produced by the froth flotation technology. According to Lima et al. (2005), the most common route used by far for flotation of Brazilian itabirite ores was cationic reverse flotation, where quartz is recovered from the froth and iron oxides remaining in the pulp phase.

The typical feed to a flotation system in the iron ore industry consists of particles in the size range between 10 μm and 300 μm . The slimes fraction ($< 10 \mu\text{m}$) is removed using hydrocyclones prior to flotation and the top size is limited to 5–10% greater than 150 μm . Flotation is performed in circuits consisting of mechanical cells, columns, or a combination of both types (Lima et al., 2016). Etheramines are employed as quartz collectors and gelatinized corn starch used as iron oxides depressants (Araujo et al., 2005). The reverse cationic flotation route was developed by the USBM in Minnesota and the importance of desliming before the reverse cationic flotation of iron ores was reported by Clemer in the 40s (Clemmer, 1947). A high grade of fines increases the required cationic collector dosage and reduces the selectivity. However, iron metal losses in the desliming stage are very high which is a problem observed in iron ores treatment in India (Thella et al., 2010, 2012; Rao et al., 2011; Singh et al., 2014; Dey et al., 2015), Brazil (Rocha et al., 2010; Sales, 2012; Castro and Peres, 2013) and Russia (Filippov et al., 2010). In Brazil, the generation of iron ore slimes is estimated to be 20–40% by weight of the total iron ore mined. Taking into account the present magnitude of the iron ore slimes generated annually and accumulated over the years, it can be considered a national resource in the iron and steel industries if properly beneficiated using innovative technology. Table 1 summarizes the main technological and scientific studies focused on recovery of iron bearing minerals from slimes.

The main alternatives to treat the slimes fraction include selective flocculation (Tammishetti et al., 2017; Kumar and Mandre, 2016, 2017; Panda et al., 2018), a combination of hydrocyclones and froth flotation (Thella et al., 2010, 2012; Ma et al., 2011, 2009; Rao et al., 2011; Castro and Peres, 2013; Lima et al., 2016; de Praes et al., 2013; Dey et al., 2015) and a combination of hydrocyclones and magnetic separation (Jena et al., 2015; Rao et al., 2016). Kumar and Mandre (2016) evaluated the selective flocculation to treat iron ores slimes applying polyacrylamine and guar gum as a flocculant and sodium hexametaphosphate as a dispersant. The results indicated that selective flocculation enhanced the Fe grade from 58.2% to 64.6% and an Fe recovery of 66.3% using polyacrylamine as a flocculant whereas when guar gum was used the iron grade was 63.2%, achieving a recovery of around 68%. Panda et al. (2018) carried out a study on the application of the selective flocculation process for the beneficiation of synthetic mixtures of iron ore and kaolinite as well as iron ore tailings. Results showed that it was possible to achieve 65.78% of Fe, with 2.65% Al_2O_3 and 3.66% SiO_2 in the concentrate using a synthetic mixture feed and more than 60% of Fe was obtained from natural iron ore tailings. In Brazil, a great number of researchers and engineers have been making efforts towards iron ore slimes concentration. Rocha et al. (2010) carried out studies with slimes samples with the currently produced slimes as well as slimes that will be generated in the future. It was observed that a reverse cationic column flotation process using a high depressant dosage was selective, yielding high grade concentrates with low impurity grades at high levels of iron recovery. For the future ROM, results indicated that high collector dosages were not required. At 1000 g/t starch and 30 g/t amine dosages, an ultrafine concentrate was achieved at a silica grade under 1% and a silica + alumina grade under 2%, adequate for making direct reduction pellets. The mass and iron metallurgical recoveries reached, respectively, 41.7% and 80.5% in the flotation stage, and 17.9% and 33.4% in the global desliming and flotation process. The high process selectivity yielded tailings assaying 12% iron in a single rougher stage. The controlled use of wash water was essential for the removal from the froth of entrained fine iron minerals particles. The beneficiation of iron ore slime in the Brazilian scenario is a challenging task as it contains a significant amount of silicates, goethite and clay minerals (kaolinite and gibbsite) (Lima and Abreu, 2019). The iron ore slime could be a material generated during the desliming stage (overflow) containing particle sizes of approximately 99% < 45 μm , 25% > 10 μm , 45% < 5 μm and 15% < 1 μm , 3% of solids by weight and between 35% and 45% of Fe. The high surface area and high impurity content associated with this particle size class make it difficult to treat by a conventional flotation equipment (Sivamohan, 1990, Lima et al., 2016). Primary etheramines and etherdiamines have been the dominant collectors for the flotation of

iron ore since their introduction in the 6s (Houot, 1983; Araujo et al., 2005). Quartz is floated with etheramines ($R-(OCH_2)_3-NH_2$) partially neutralized with acetic acid. The degree of neutralization is an important parameter. If on the one hand higher degrees enhance the collector solubility, on the other hand they impair the flotation performance). Most etheramines are currently supplied with neutralization degrees in the range between 25% and 30%. The flotation performance of certain iron ore types is enhanced with the use of ether diamines in combination with ether monoamines (Araujo et al., 2005). Desliming is mandatory to remove particles with size $< 30 \mu m$ prior to reverse cationic flotation with amines to achieve adequate separation between iron-bearing and gangue minerals (Houot, 1983; Araujo et al., 2005; Ma, 2012; Filippov et al., 2014). Although a concentrate with an Fe grade higher than 58% was obtained with the use of amines in the flotation of slime Sample 1, the iron recovery was lower in comparison with the one obtained with the amidoamine collector. There is not a large number of studies regarding the application of amidoamine collectors in the literature. Wittelsheim et al. (1967) patented a collector composition especially suitable for the coarse flotation of sylvinitic comprising: (A) at least about 90 percent by weight of a primary aliphatic amine of 16–18 carbon atoms, or water-soluble salts thereof; and (B) about 0.5–10 percent by weight of a primary aliphatic amide of 10–20 carbon atoms. In order to obtain the very best results, it is recommended the use of amine collectors containing a major proportion of primary saturated amines and a very low proportion of secondary or tertiary amines and unsaturated amines with respect to the total amine content. Thus, a particularly efficient collector composition can be prepared by adding the amide to an amine reagent containing more than 90 percent, and preferably more than 95 percent primary amines with respect to the total quantity. Also, the amidoamine collectors can be used with the various conventional auxiliary reagents generally employed in flotation operations: depressants, such as starch, guar flour, proteins, cellulose derivatives, etc.; frothers, such as pine oil, methylisobutylcarbinol and analogs thereof; pH regulators; flocculators; and/or dispersants. In Brazil, the first application of amidoamine applied to flotation was reported by Souza et al. (2015, 2016) where the authors used this collector for kaolinite flotation from a manganese ore. The process was composed of desliming ($-10 \mu m$), followed by reverse cationic flotation of kaolinite (rougher, scavenger) at pH ~ 5 . Results indicated that the reverse cationic flotation in the acid medium, when utilizing amidoamine as a collector and in the presence of a silicate activator and a dispersing agent, could be a possible route for the concentration of tailings that had previously been deslimed at $10 \mu m$. Both fundamental and applications studies of amidoamine collectors and the results obtained on the treatment of this sample represent an exception.

Considering flotation as the most suitable technology for the treatment of such type of material, future research should focus on a deep fundamental study of the collector-depressant mechanism interaction with the iron-bearing and gangue minerals, especially in those ores with a high amount of alumina-containing minerals. The application of column flotation makes it possible to extend the size range of particles that can be treated by flotation to about 5–10 μm (Wyslouzil, 2009). Therefore, this work aims at evaluating the technical feasibility of concentration of two slimes samples from two different processing plants in operation in the Brazilian southern system (Minas Gerais state) using the column flotation technology. In contrast with the established methods of iron ore beneficiation, where classification by hydrocyclone is mainly used to remove ultrafine as tailings, the method described in this paper allows a high proportion of ultrafine to be recovered via column flotation without prior separation.

Table 1. Main studies focused on the iron ore slimes treatment

Process employed	References	Sample Characterization	Main features	Main Results and Conclusions
	Tammishetti et al., (2017)	The slime sample is from the hydrocyclone overflow (COF), that is, the tailings of the beneficiation. 90% of the total slime is presented in the size fraction below 42 μm . XRD: hematite, goethite, gibbsite, kaolinite and quartz.	Pilot plant trials of a selective flocculation separation process. It was used a natural polymeric flocculant: corn starch and guar gum. - pH was adjusted at 10.5-11.5 using caustic lye;	Results indicated that it was possible to produce a concentrate assaying 65.3% Fe and 2.5% Al_2O_3 with a yield of 80.4% from a sample containing 60.3% Fe and 4.8% alumina. The corresponding tails contained less than 39.7% Fe. For a leaner grade slime sample assaying 53.4% Fe and 7.3% Al_2O_3 , the corresponding concentrate grade was 63.5% Fe and 3.1% Al_2O_3 , tailings grade 35.7% Fe and the yield achieved during the plant trials was 63.5%.
Flocculation	Kumar and Mandre (2017)	Iron ore slimes sample was collected from a slime pond at Kiriburu iron ore processing plant, Jharkhand, India. XRD: hematite, goethite and limonite, quartz, kaolinite, gibbsite and magnetite. The sample contains 58.24% Fe, with 4.72% SiO_2 , 3.47% Al_2O_3 , and had 5.18% LOI.	The beneficiation of iron ore slimes by selective flocculation was studied. Polyacrylamide (PAM) and guar gum were used as a flocculant, along with sodium hexametaphosphate (SHMP) as a dispersant.	The selective flocculation tests showed: A maximum grade of 64.6% Fe at a recovery of 66.33% was obtained with 0.09 mg/g PAM at pH 10 and 0.5 kg/t sodium hexametaphosphate. A maximum grade of 63.20% Fe at a recovery of 68.04% was obtained with 0.21 mg/g guar gum at pH of 10 and a dispersant dose of 0.5 mg/g.
Flocculation	Kumar and Mandre (2016)	The tailing samples used were collected from tailing pond of iron ore washing plant of Kiriburu mines, India. XRD: hematite, goethite and quartz and kaolinite The sample contains 58.24% Fe, with 4.72% SiO_2 , 3.47% Al_2O_3 , and had 5.18% LOI.	The beneficiation of iron ore tailings by selective flocculation was studied. Starch and guar gum were used as flocculant, along with sodium hexametaphosphate (SHMP) as a dispersant.	The selective flocculation process showed that the Fe grade could be enhanced from 58.24 to 65.32 % Fe using starch as a flocculant with a recovery of 62.08 %. However, 63.2 % Fe with a recovery of 68.04 % was obtained using guar gum as the flocculant.

Process employed	References	Sample Characterization	Main features	Main Results and Conclusions
Mechanical Flotation Cells	Thella et al., (2012)	About 70% of the total slime is present in the size fraction below 25 μm . - 80% of the total slime is presented in the size fraction below 45 μm . Head slime contains 54.93% Fe, 7.45% SiO_2 and 6.62% Al_2O_3 .	A combination of two stage of hydrocyclones and froth flotation tests at mechanical cells were performed with high alumina iron ore slimes targeting to recover Fe values with low alumina and silica grade.	Flotation results indicated that it was possible to achieve a final concentrate of 64.46% Fe, 2.66% Al_2O_3 , and 2.05% SiO_2 with Fe recovery of 69.03% in flotation stage and 34.13% with respect to the initial feed obtained with reverse cationic flotation.
Mechanical Flotation Cells	Ma et al., (2011)	Feed: d_{80} : 109 μm ; 40.4% Fe, 39.0% SiO_2 , 1.39% Al_2O_3 . XRD: hematite, with impurities including quartz, kaolinite, talc and muscovite. Cyclone underflow: d_{80} : 129 μm ; 39.6% Fe, 41.4% silica, 0.64% Al_2O_3 .	Reverse cationic flotation tests were conducted at pH 10.5 and reverse anionic flotation tests were performed at pH 11.5 in batch scale flotation tests. Reagents: Starch (depressant) and collector (sodium oleate, EDA C and EDA 3C). The effects of desliming the sample prior to the flotation tests were investigated.	Superior performance of reverse anionic flotation was achieved for ultrafine particles (<10 μm), ranging 58% of Fe recovery. Reverse cationic flotation performed better with samples containing coarse particles (>210 μm), ranging 90% of Fe recovery. Without desliming, in reverse cationic flotation at 1500g/t starch dosage, the concentrate grade achieved 67.86% Fe and 50.35% of Fe recovery; and, in reverse anionic flotation at 2000g/t starch dosage, the concentrate grade achieved 55.79% Fe and 72.36% of Fe recovery.
	Rao et al., (2011)	Iron ore slimes with about 77% of mass passant in 37 μm (P_{80} =42.0 μm). The sample assaying 54.44wt% Fe, 6.72wt% SiO_2 , and 6.80wt% Al_2O_3 .	The recovery of iron from the screw classifier overflow slimes by direct flotation was studied. The effectiveness of sodium silicates with different silica-to-soda mole ratios as depressants for silica and silicate- bearing minerals was investigated.	The concentrate of 58.9wt% Fe, 4.7wt% SiO_2 , and 5.3wt% Al_2O_3 with the weight recovery of 38.7% and the metal recovery of 41.1% could be obtained, when Na_2SiO_3 with a silica-to-soda mole ratio of 2.2 was used as a depressant at a feed rate of 0.2 kg/t.

Process employed	References	Sample Characterization	Main features	Main Results and Conclusions
	Thella et al., (2010)	Iron ore slime from Joda, India. D ₅₀ : 25 µm. Feed: 58.3 % Fe and 4.8% SiO ₂ and 3.4% Al ₂ O ₃ . BSE – (SEM-EDS): Hematite, goethite, kaolin, gibbsite and quartz.	Flotation tests were performed at mechanical flotation cell. Reverse cationic flotation was carried out to float silica and alumina gangue using amine based cationic collector and potato starch was used as a depressant, sodium hydroxide was used as a pH regulator. In direct flotation, fatty acid as a collector and pine oil as a frother were used.	The optimum results found were iron concentrate of 63% Fe and 2.3% alumina. The optimum conditions for the anionic flotation with fatty acid was 9.5 pH and 4 kg/t of collector dosage. It was found from design of experiments that collector concentration and pH played a vital role in flotation performance.
	Castro and Peres, (2013)	Iron ore slimes (underflow) from itabirite ore desliming in hydrocyclone (101.6 mm in diameter) from Samarco.	Reverse cationic flotation tests were conducted at mechanical cells. Reagents: cassava starch as a depressant and etherdiamine and ethermonoamine mixtures as collectors.	The best result was cassava starch dosage 1250 g/t, etherdiamine individually dosed at 450 g/t, and pH 10.5, yielding values of 1.2% for silica grade in the concentrate and 50.2% for the metallic recovery.
Mechanical Flotation Cells	Lima et al., (2016)	Itabirite ore	To evaluate the performance in each flotation stage and to investigate the influence of entrainment on hematite losses in iron ore reverse flotation. Cell hydrodynamic measurements were also carried out during the survey.	Results indicated a strong correlation between water recovery and hematite losses, especially for fine particles (<45 µm). A potential alternative to reduce hematite losses through entrainment and to increase quartz removal was to modify the traditional circuit design to treat rougher and cleaner/recleaner tails in different stages. It was also showed that the scavenger residence time must be matched to the quartz floatability.

Process employed	References	Sample Characterization	Main features	Main Results and Conclusions
	Ma et al., (2009)	kaolinite sample, from Georgia, USA, containing 93.0% kaolinite and 7.0% illite. d_{80} : 7 μm ., was provided by Ward's Natural Science Establishment	The effect of amine collector type, pH, and ionic strength on the flotation behavior of kaolinite was investigated in laboratory batch cationic flotation tests. Flotigam EDA 3 (Clariant), an ether monoamine, and Flotigam 2835-2L (Clariant), an ether diamine, were used as collectors for kaolinite	For both collectors, flotation recovery decreased with increasing pH, in contrast to the general trend for the cationic flotation of oxides in which recovery increases with pH. The pH dependence of kaolinite flotation is also opposite to that of oxides, with lower flotation recovery obtained at higher pH. In contrast to oxides, the flotation recovery of kaolinite increases with ionic strength. It is proposed that the screened zeta potential of kaolinite particles in a high ionic strength environment causes random aggregation of kaolinite particles exposing hydrophobic (001) silica plane in the presence of etheramines.
Flotation Columns	Praes et al., (2013)	Feed sample: 35.9% Fe, and 42.8% SiO_2 . Below 37 μm : 66.2% of the mass and 40.1% of the Fe content.	Column flotation tests were performed with iron ore slimes. The column having 5.1 cm in diameter and a total height of 6.0 meters was used. The %s in the conditioning phase and in the column feeding were kept at 35% and 25%, respectively. The pH adjustment was made with sodium hydroxide.	Corn starch remained a selective reagent for its cost/benefit equation results. Aimed results were achieved with a circuit of only one rougher flotation column, given satisfactory results, where a concentrate with Fe over 66.0% and SiO_2 below 1.0% was obtained.
	Dey et al., (2015)	Feed sample: 58.7% Fe, 5.2% SiO_2 and 4.9% Al_2O_3 . Feed size: 28.7% retained in 100 μm , 84% retained in 25 μm . XRD: hematite, goethite and the gangue being gibbsite	Desliming + column flotation was performed targeting the effect of froth height, superficial air velocity, and collector dosage on recovery of mass and grade of Fe in the processing of iron ore slime using column flotation.	In column flotation, the effect of superficial air velocity was more dominant than collector dosage for recovery at low froth height. Deslimed feed improved the metallurgical performance with high recovery and grade. Recovery of the concentrate could be improved to 63% with a grade of 64.3% Fe, 1.9% silica and 2.2% alumina.

Process employed	References	Sample Characterization	Main features	Main Results and Conclusions
Magnetic separation	Jena et al., (2015)	Iron ore slime sample contained 56.2% Fe, 5.1% SiO ₂ , 6.9% Al ₂ O ₃ , and 7.2% LOI. The sample was separated into two different sizes of > 0.500 mm and < 0.500 mm size for beneficiation. XRD: hematite, goethite and the main gangue being kaolinite.	Characterization studies of iron ore slime carried out by XRD, SEM-EDS, FESEM, and QEMSCAN were discussed. Beneficiation studies were also carried out using hydrocyclone and magnetic separation techniques.	Hematite, goethite, kaolinite, and quartz were the associated mineral phases. Iron-bearing minerals were not fully liberated from the aluminates and silicates. The beneficiation studies on slimes revealed that the sample responded positively to hydrocyclone and magnetic separation techniques. It was possible to produce an overall iron concentrate containing 62.3% Fe with 70.7% weight recovery.
Magnetic separation	Rao et al., (2016)	Iron ore slimes sample from Donimalai iron ore mine tailing dam assayed 49.40% Fe, 13.51% SiO ₂ , 8.44% Al ₂ O ₃ , and 5.16% LOI; 80% feed was passing through 35µm. XRD: hematite, goethite and the main gangue being quartz, kaolinite, ferruginous clay	The test scheme involved desliming by using hydrocyclone and subjecting the hydrocyclone underflow to wet high intensity magnetic separator (WHIMS). WHIMS concentrate was the final concentrate. The test scheme involved optimization of parameters of hydrocyclone for desliming and WHIMS operation.	Underflow deslimed: 57% Fe, 8.7% SiO ₂ and 5.69% Al ₂ O ₃ with weight recovery of 65.09%. It was possible to obtain final WHIMS concentrate assaying: - 67.40 % Fe, 1.12 % SiO ₂ , 1.30 % Al ₂ O ₃ and 1.22 % LOI with an iron recovery of 58.2 %. - 65.93 % Fe, 1.45 % SiO ₂ , 1.94 % Al ₂ O ₃ and 1.56 % LOI with and iron recovery of 60.3 %.

2. Experimental

2.1. Slimes samples

The two slimes samples tested in this work were provided by Vale SA and were collected at two different plants in the Quadrilátero Ferrífero (Minas Gerais state). Both Sample 1 and Sample 2 were collected from the underflow of the thickener, which was around 2 tons (dry basis) of the slime in pulp with 35% solid grade by weight (Sample 1) and 25% solid grade by weight (Sample 2).

2.2. Samples characterization

Both the pulp sample corresponding to the process feed and some selected samples of the flotation generated in the study were sent for physical characterization (particle size distribution), chemical characterization for oxide quantification and mineralogical characterization. The particle size distribution of the study samples was determined by the laser diffraction technique, also known as light scattering, at CETEM's technology characterization sector - SCT. A Malvern model Mastersizer 2000 SM equipment capable of analyzing particles in the diameter range 0.1–1000 was used for this purpose. Chemical analyzes were performed using the X-ray Fluorescence technique at Vale's chemical analysis laboratories. Determinations were performed for the following oxides: Fe, SiO₂, P, Al₂O₃, Mn, TiO₂, CaO and MgO. XRD analysis by the powder method was performed on a Bruker-D4 Endeavor equipment under the following operating conditions: CoK β radiation (40 kV/40 mA), 0.02° 2 θ measure, 184 s count time per step drift LynxEye linear position-sensitive detector collected from 5 to 105° 2 θ . Qualitative interpretation of the spectrum was performed by comparison with standards contained in the PDF04 + database (ICDD, 2014) using a Bruker Diffrac Plus software.

The total acquisition time of each spectrum for this work step was approximately 90 min. Quantitative analyzes from X-ray data were calculated by the total multiphase spectrum refinement method (Rietveld method) using a Bruker AXS Topas software, v.5. The crystal structure information of the refined phases came from the Bruker AXS database, the Inorganic Crystal Structure Database (FIZ Karlsruhe), and the Crystallographic Open Database (COD). Goethite data were modified to calculate Fe-Al isomorphic substitution according to the formula of Schulze (1984) implemented by (Knorr and Neumann, 2012) as part of the refinement. The chemical analyses for both samples showed that the Fe grade was around 40–45%. In terms of the major contaminants, SiO₂ and Al₂O₃ stood out, with grades of 27% and

3% for Sample 1 and 33% and 5% for Sample 2, respectively (Table 2). The main mineral phases in the samples were hematite (around 51–55%), goethite with 6–13% grade and quartz with around 28% (Table 3). As observed in Fig. 1 the particle size distribution of both slimes samples was almost the same. The particle size distribution of slime Sample 1 showed that the characteristics for diameters D32, D10, D50, and D90 were, respectively, 4.5 μm , 2 μm , 10 μm , and 34 μm , whereas for Sample 2 the values were D32 = 4.7 μm , D10 = 1.9 μm , D50 = 11 μm , and D90 = 38 μm (Fig. 1).

Table 2. Chemical analyses of the slime samples

Sample	Fe	SiO ₂	P	Al ₂ O ₃	Mn	TiO ₂	CaO	MgO
1	45.2	28.6	0.09	3.1	0.09	0.13	0.05	0.06
2	39.6	33.4	0.09	5.1	0.4	0.10	0.20	0.70

Table 3. Mineralogical composition of the slime samples

Sample	Hematite	Goethite	Quartz	Kaolinite	Others
1	51.5	13.3	27.9	4.6	2.7
2	54.6	6.4	28.9	6.4	3.7

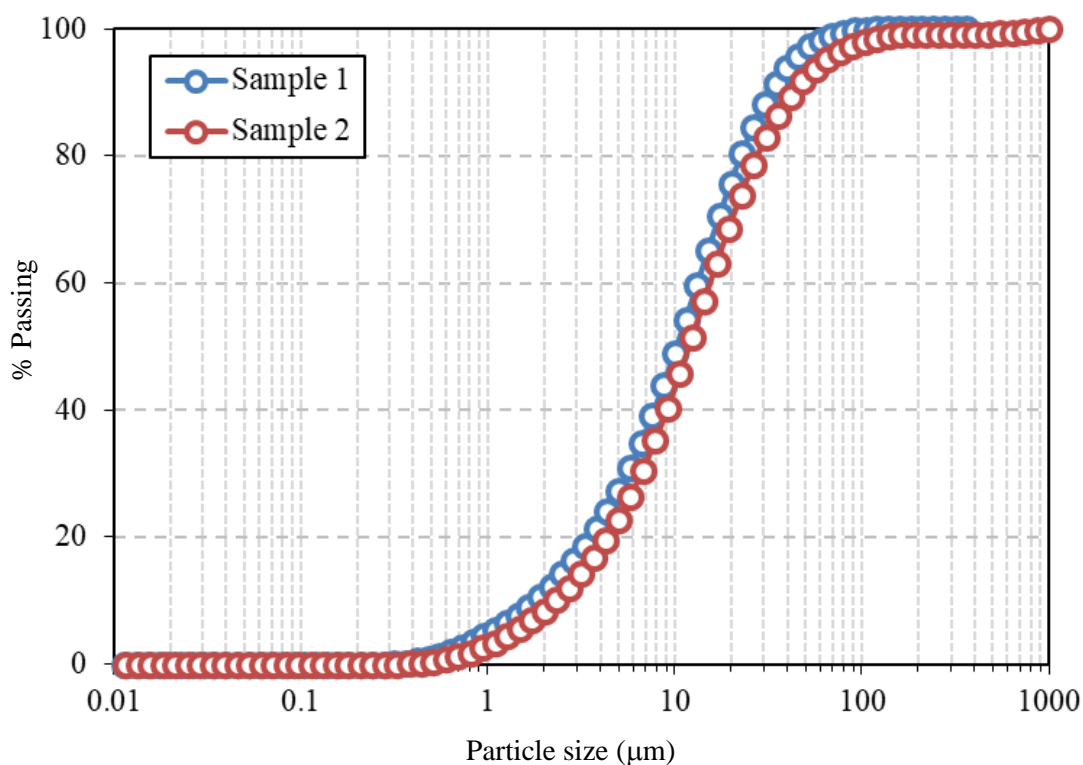


Figure 1. Particle size distribution of the iron ore slime samples 1 and 2

2.3. Flotation studies

The flotation studies were carried out without the application of the previous desliming operation. For each slime sample, experiments were performed in different scales.

Sample 1:

- Rougher flotation studies in column with an internal diameter of 2 inches (height of 6.0 meters).
- Rougher flotation studies in column with an internal diameter of 6 inches (height of 6.0 meters).

Sample 2:

- Rougher flotation studies in column with an internal diameter of 3 inches (height of 2.0 meters).
- Rougher/cleaner flotation studies in column with an internal diameter of 6 inches and 4 inches, respectively (height of 6.0 meters).

This topic describes the experimental procedure employed in flotation studies for both slime samples at the different scales tested and the description of the reagents used in the flotation process.

Reagents

Table 4 shows the reagents list, fabricant, function, and mode of application used for column flotation studies in both samples (1 and 2). Flotisor 5530 and Flotigam EDA-C were used as collectors, both supplied by Clariant. Gelatinized corn starch was used as the hematite depressant, with a starch/NaOH ratio of 1:10 and a reaction time of 10 min, in a solution with concentration at 20% w/w. After the collector preparation and gelatinization, both reagents were diluted in distilled water, producing 1–2% w/w solutions. For the pH adjustment, a 1% NaOH solution was used. Tap water from the city of Rio de Janeiro's supply network was used to attain the correct percentage of pulp solids in the flotation studies.

Table 4. List of reagents, manufacturer, function and method of application used for column flotation studies

Reagent	Fabricant	Function	Application
Flotisor 5530	Clariant	Collector	Solution 0.1% to 0.2%.
EDA-C	Clariant	Collector	Solution 0.1% to 0.3%.
Corn starch	Vale	Depressant	After gelatinization with NaOH (Solution 0.1-2.0%)
NaOH	VE TEC	Corn starch gelatinization and pH adjustment	Solution 0.1-1%

Sample 1 - Column flotation 2"

Fig. 2 shows the schematic flowsheet considering the flotation stages for iron concentration from slime Sample 1 and Fig. 3 shows a general view of the columns at CETEM's pilot plant (ERIEZ, Delta, Canada). The feed of the flotation circuit is composed of pulp with a solids content of 34 to 36% by weight. The rougher flotation trials were performed using a column with an internal diameter of 2 in. and a height of 6.0 m. The effective volume of the column was 13 L. The solid feed rate in the circuit was 7–8 kg/h dry basis. From the storage tank, the pulp was pumped into a cylindrical tank where it was conditioned with the gelatinized corn starch depressant (when it was applied) with a dosage ranging from 500 up to 1100 g/t. After conditioning with the depressant, the pulp was conditioned with the collector (EDA-C and Flotisor 5530) in a cylindrical tank and the pH was adjusted (between 8.5, 9.5 and 10.5) with NaOH. The EDA-C dosages ranged around 100 g/t and Flotisor 5530 ranged from 50 up to 190 g/t. The mean residence time for conditioning was 10 min for the depressant and around 20 min for the collector. After conditioning, the pulp was diluted to 20% solids by weight and fed in the rougher column.

The froth obtained in the rougher was discharged as final tailings, and the sink stream from the rougher was a final iron concentrate. Bubbles were generated with controlled pressure and flow via a forced air passage in a porous tube at the bottom of the 2" columns. The pulp/froth interface was controlled by a level sensor that was connected to the tailings pump and the wash water and air flow rate were controlled by a flow meter. The residence time was 12–18 min and the height of the foam layer in all tests ranged from 40 to 50 cm, and it was controlled by varying the tailings discharge flowrate. The superficial velocity of the air was 1.15 cm/s and the wash water was 0.49 cm/s.

After reaching the stationary stage (60–90 min), samples from the rougher tailings and rougher concentrate were collected simultaneously for 3–5 min for mass and metallurgical balances. The samples were flocculated and dried in an oven for 24 h at 80 °C and then weighed, disaggregated, and separated in aliquots for chemical analysis by X-ray fluorescence spectroscopy to determine the metallurgical balance.

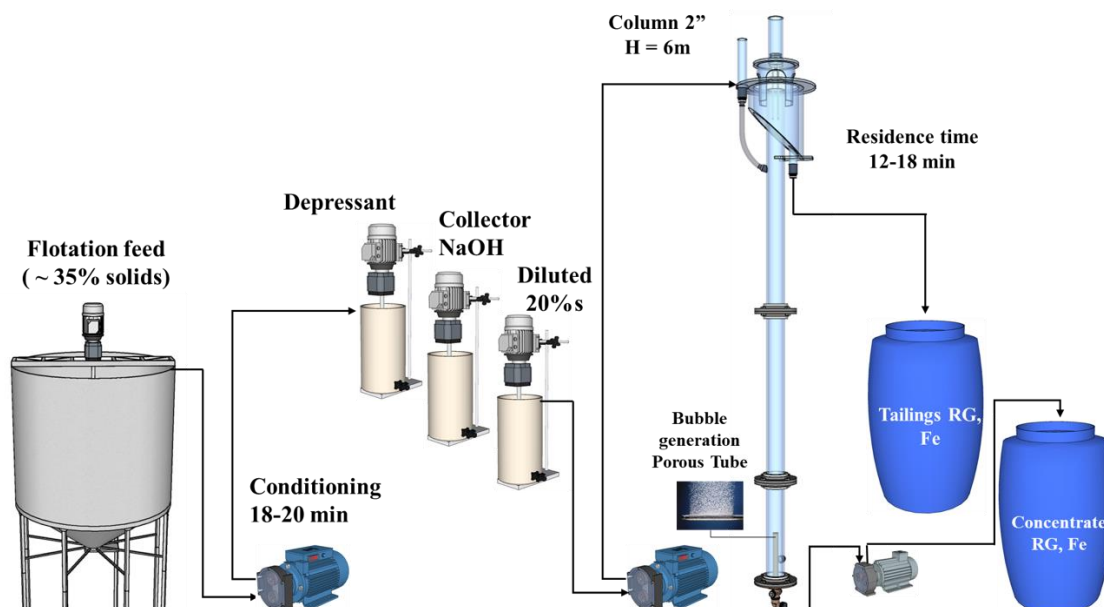


Figure 2. Schematic flowsheet for the iron concentration from Slime 1 in the 2'' column

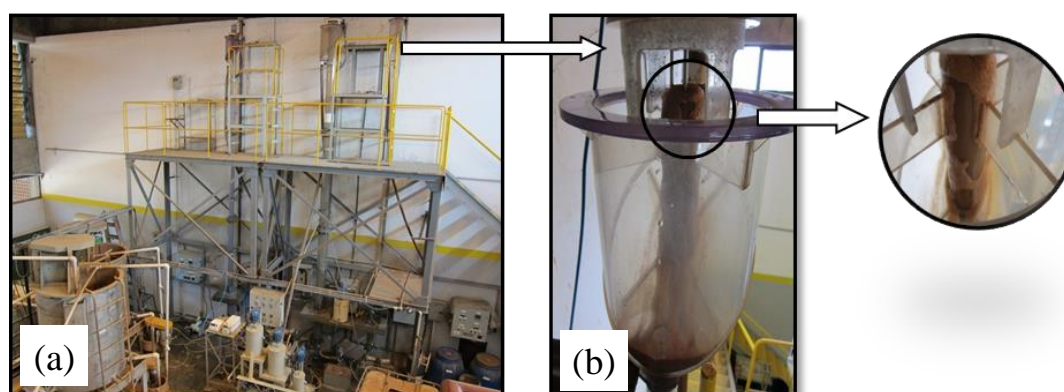


Figure 3. General view of the columns at CETEM's pilot plant (a) Column flotation 2'' (b)

Sample 1 - Column flotation 6''

Fig. 4 shows the schematic flowsheet considering the flotation stages for iron concentration from slime Sample 1. The column flotation studies developed in the column with an internal diameter of 6'' generally followed the same procedures as those in the 2'' column flotation studies. The pulp with 34–36% solid grade by weight fed the flotation circuit. The rougher flotation trials were performed using the column with an internal diameter of 6 in. and a height of 6.0 m. The effective volume of the column was 100 L. The solid feed rate in the circuit was 75 kg/h dry basis. From the storage tank, the pulp was pumped into a cylindrical tank where it was conditioned with the gelatinized corn starch depressant (when it was applied) with dosages ranging from 900 up to 1400 g/t. After conditioning with the depressant, the pulp was conditioned with the collector (Flotinator 5530) in a cylindrical tank and the pH was adjusted (between 8.5, 9.5 and 10.5) with NaOH. Flotinator 5530 ranged from 50 up to 200 g/t. The mean

residence time for conditioning was 10 min for the depressant and around 20 min for the collector. After conditioning, the pulp was diluted to 20% solids by weight and fed in the rougher column. The froth obtained in the rougher was discharged as final tailings (float stream), and the sink stream from the rougher was a final iron concentrate. The bubble generation of the 6" column flotation was through the recirculation of a portion of the pulp through a cavitation tube. The operational pressure in the cavitation was around 3.5 kgf/cm^2 .

The pulp/froth interface was controlled by a level sensor that was connected to the tailings pump and the wash water and air flow rate were controlled by a flow meter. The residence time was 15–23 min and the height of the foam layer in all tests ranged from 40 to 50 cm, and it was controlled by varying the tailings discharge flowrate. The superficial velocity of the air was set at 0.49 cm/s and the wash water ranged from 0.1 to 0.2 cm/s. After reaching the stationary stage (60–90 min), samples of the rougher tailings and rougher concentrate were collected simultaneously for 1–3 min for mass and metallurgical balances. The samples were flocculated and dried in an oven for 24 h at 80 °C and then weighed, disaggregated, and separated in aliquots for chemical analysis by X-ray fluorescence spectroscopy to determine the metallurgical balance.

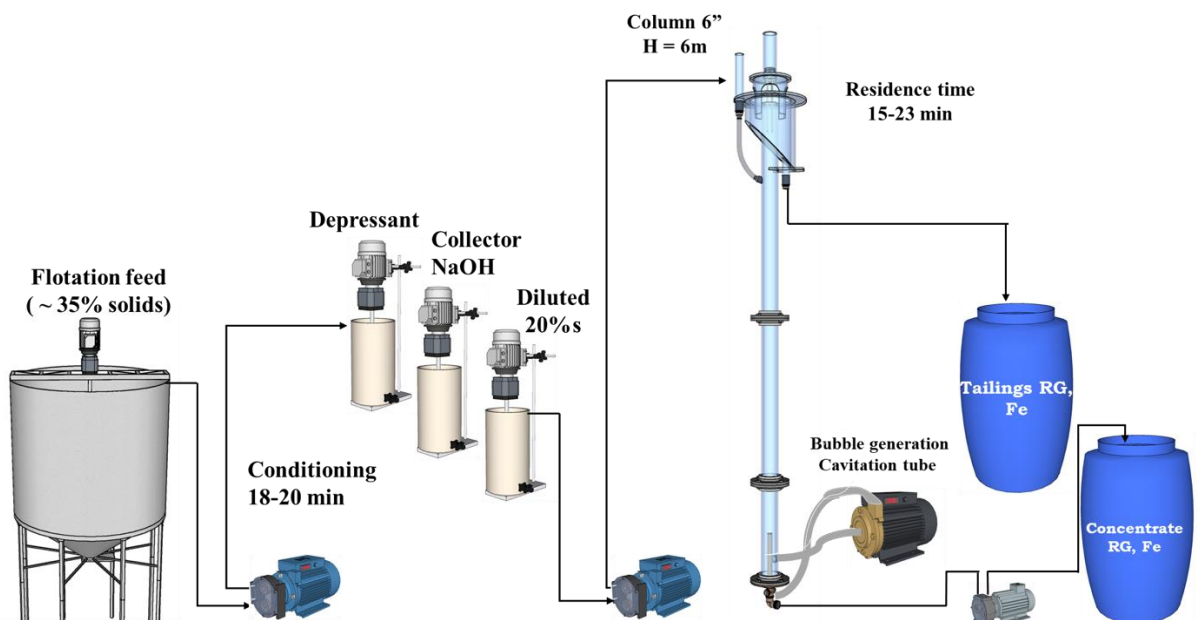


Figure 4. Schematic flowsheet for the iron concentration from Slime 1 in the 6" column

Sample 2 - Column flotation 3"

Fig. 5 shows the column flotation 3" applied to the rougher flotation studies from slime Sample 2. The rougher apatite flotation tests were carried out in a laboratory column with an internal diameter of 3 in., a height of 2.0 m, and an effective volume of 6.8 L, consisting of

three adjustable modules. The pulp with 35% solids by weight was conditioned in four flotation cells at the Mini Pilot Plant (MPP -Supplied by Eriez), being two for the depressant (Corn starch) and the other two for Flotinator 5530 and EDA-C as the collector. The average residence time in conditioning was around 9 min for both the collector and the depressant. The pH was adjusted using NaOH at 8.5, 9.5 and 10.5. After conditioning, the pulp was diluted to 20% solids by weight and it was fed straight into the column. The residence time was 12–20 min and the height of the foam layer in all tests ranged from 20 to 30 cm, and it was controlled by varying the tailings discharge flowrate.

The superficial velocity of the air ranged from 0.50 to 0.61 cm/s and the wash water was set at 0.13 cm/s. After flotation runs of around 60–90 min, the sample from the concentrate (sink stream) and the tailings (float stream) was collected for 5 min. The samples were flocculated and dried in an oven for 24 h at 80 °C and then weighed, disaggregated, and separated in aliquots for chemical analysis by X-ray fluorescence spectroscopy to determine the metallurgical balance.

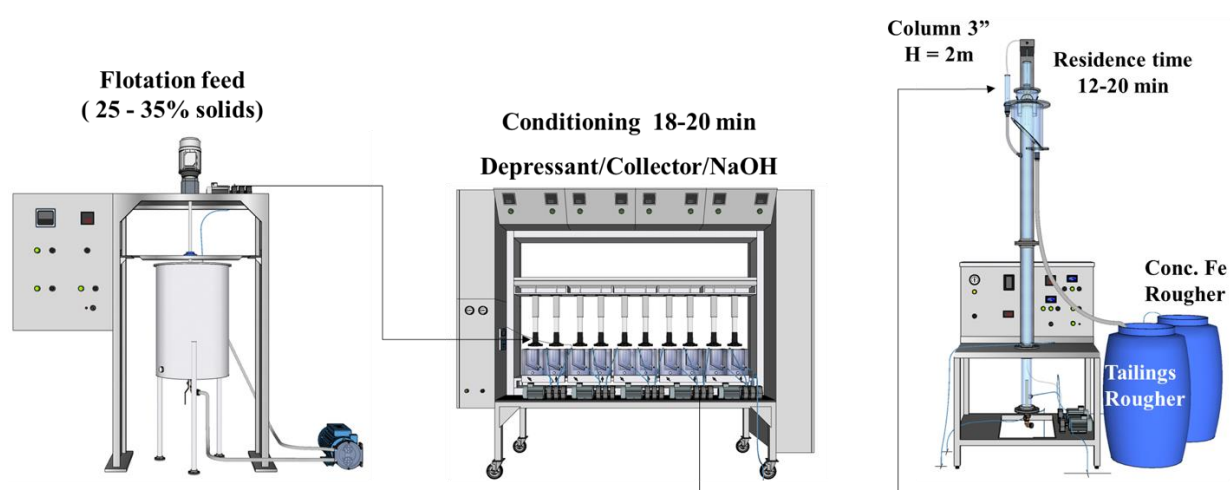


Figure 5. Schematic flowsheet for the iron concentration from Slime 2 in the 3'' column

Sample 2 - Column flotations 6'' and 4''

Fig. 6 shows the schematic flowsheet for the rougher/cleaner flotation studies from slime Sample 2. The rougher/cleaner flotation trials were performed using a column with an internal diameter of 6 in., a height of 6.0 m, and an effective volume of approximately 100 L, composed of acrylic modules joined by flanges for the rougher stage. The sink fraction obtained in the rougher fed the cleaner stage which was carried out in a column flotation with 4 in. in diameter and 6.0 m high (46 L volume).

The rougher and cleaner tailings streams (the froth) were discharged as final tailings. The pulp was conditioned with gelatinized corn starch and the pH was adjusted (10.5) with

NaOH and subsequently conditioned with Flotinor 5530 as a collector, in two cylindrical tanks. After conditioning, the pulp was diluted to 25–30% of solids by weight and fed at 1.26 m from the top of the rougher column. The sink fraction obtained in the rougher fed the cleaner, and both tailings were discharged as final tailings. Bubbles were generated with controlled pressure and flow via a forced air passage in a porous pipe at the base of the column. The pulp/froth interface was controlled by a level sensor that was attached to the tailings pump. The residence time was 15–23 min and the height of the foam layer in all tests ranged from 20 to 30 cm, and it was controlled by varying the tailings discharge flowrate. The superficial velocity of the air was set at 0.30 cm/s and the wash water was set at 0.20 cm/s. After flotation runs of around 60–90 min, product samples from the concentrate and tailings were collected for 5 min. The samples were flocculated and dried in an oven for 24 h at 80 °C and then weighed, disaggregated, and separated in aliquots for chemical analysis by X-ray fluorescence to determine the metallurgical balance.

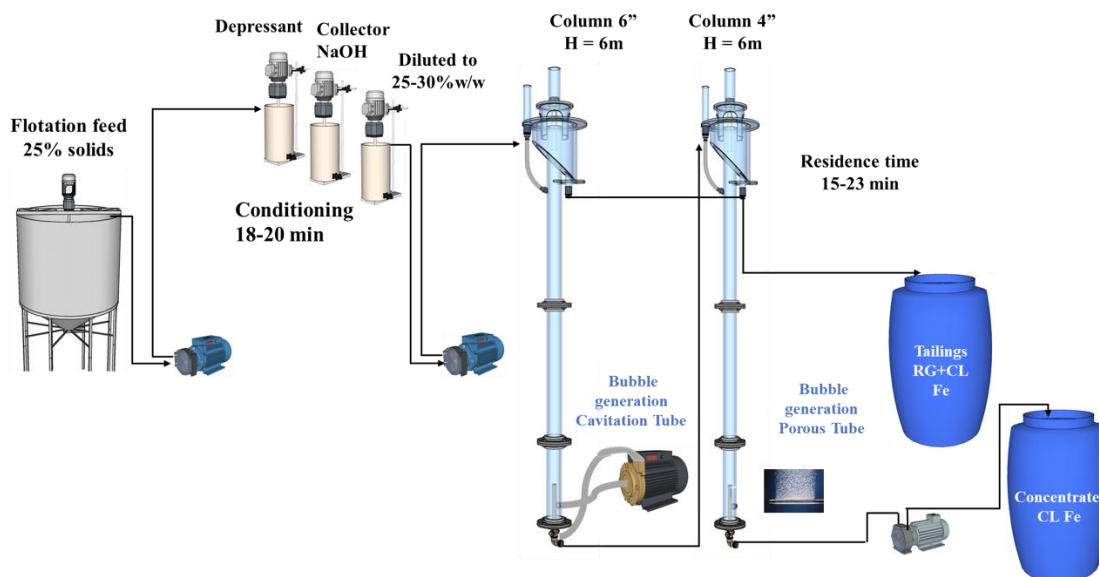


Figure 6. Schematic flowsheet for the iron concentration from Slime 2 in the 6" and 4" columns.

3. Results and Discussion

3.1. Flotation Studies – Sample 1

This topic presents the results and discussion on the iron flotation studies considering rougher flotation in the 6" and 2" diameter columns for Sample 1 where the influence of the collector dosage, the collector type, the depressant dosage and the pH were evaluated. Table 5 shows the results achieved from iron rougher flotation at a 2" diameter column flotation, the mass and metallurgical balance for Fe, SiO₂ and Al₂O₃, the impact of the collectors (EDA- C and Flotinor 5530) and the depressant (gelatinized corn starch) as well as the effect of the pH

(8.5, 9.5 and 10.5). Both collectors were evaluated in the presence and absence of the depressant. EDA-C dosages around 100 g/t were used in the absence of starch at pH values of 8.5, 9.5 and 10.5 and in the two tests the depressant dosage was tested around 500 g/t at pH values of 9.5 and 10.5. The best result (test 1) was in the absence of starch at pH 8.5, which produced a concentrate (sink stream) with an Fe grade of about 58% and mass and metallurgical recoveries of Fe of 68% and 88%, respectively. The SiO₂ and Al₂O₃ impurities grades were 10% and 3.5%. The increased of pH flotation from 8.5 to 9.5, with 100 g/t of EDA-C dosage in the absence of gelatinized corn starch, led to an increase of the Fe grade in the concentrate, despite the high mass and metallurgical Fe losses.

The tests performed in the presence of starch (\approx 500 g/t) for both pH values showed an inferior flotation performance, with a decrease in the Fe grade of the concentrate and in the mass and metallurgical Fe recoveries. Flotisor 5530 dosages of 100 and 230 g/t were tested in the presence of gelatinized corn starch (1100 g/t average) at pH values of 8.5, 9.5 and 10.5. The increased pH flotation to 10.5, in the presence or absence of gelatinized corn starch, led to an increase of the metallurgical recovery (from 94 to 96%). The test with a lower Flotisor 5530 dosage (152 g/t) and without the depressant (test 8), achieved 62.8% of Fe grade and a mass and metallurgical recovery of Fe of 68% and 94%, respectively. The SiO₂ and Al₂O₃ impurities grades were 3.2% and 2.5%. The tests performed in the presence of starch (\approx 1100 g/t) at pH 10.5 achieved 62.5% of Fe grade and a mass and metallurgical recovery of Fe of 67% and 92%, respectively. The SiO₂ and Al₂O₃ impurities grades were 4.7% and 2.4%.

Fig. 7 shows the comparative results for the Fe grade/recovery curve considering the rougher flotation in the 2" and 6" columns using Flotisor 5530 as a collector. The results for the circuit applied in the 2" column in the sink stream (concentrate) ranged from 52 to 64% of Fe grade, with an Fe recovery from 62% to almost 97%. Fe losses (froth phase) ranged from 3% to approximately 38%. Considering the average of the 29 tests in the concentrate, the Fe recovery was 85%, with an average of Fe grade of 59.8%. The results obtained for the 6" column rougher flotation studies in the sink concentrate indicated that the Fe grade ranged from approximately 48% to 63%, with an Fe recovery from 70% to almost 98%. Considering the average of the 18 tests in the concentrate, the Fe recovery was 91%, with an average of the Fe grade of 58.4%. Fig. 8 shows the correlation between the Fe grade and the main impurities grade (SiO₂ and Al₂O₃) in the final flotation concentrates considering the rougher flotation in the 2" and 6" columns using Flotisor 5530 as a collector. Analyzing the SiO₂ curve, the increase of Fe grade is mainly due to the reduction of the SiO₂ grade in the sink stream (concentrate). Regarding the SiO₂ grade ranged from maximum values of 25% to values below 3%. The

average SiO₂ grade, considering all tests, was around 8% whereas, the SiO₂ recovery in the concentrate ranged from 50% to 90%, with an average of 76%. Regarding the Al₂O₃ grade, the second most abundant impurity in the sample, there was little variation in the concentrate, ranging from 2.2% to values up to 4% (average of 3%). It was observed that SiO₂ showed a higher recovery in comparison to the alumina containing minerals.

Besides the low kaolinite recovery by the air bubbles, another explanation for the lower Al₂O₃ recovery in the froth phase can be the finely intergrown with martitic hematite of SiO₂, Al₂O₃ and P as reported/described by Lima and Abreu (2019) that reports to the sink fraction. In general terms, the flotation performance (grade and recovery) in the rougher circuit with the 2" column showed no significant differences compared to the rougher circuit with the 6" column. The difference in the feed rate between the two scales tested was in the order of ten times. However, the trend of results obtained could be considered the same. It is noteworthy, though, that adjustments in the levels of process variables may be necessary depending on the scale tested (Table 6). Table 7 shows the average results of the mineralogical characterization by XDR (Rietveld method) of ten concentrates (sink stream) and tailings (float stream), obtained in the flotation rougher circuits in the 2" and 6" columns.

Table 7 presents the mineralogical characterization of the concentrate and tailings referring to the flotation tests of Sample 1. The products chosen were the concentrates with a grade ranging from 58% to 62% Fe. For Fe-bearing minerals, the expected average mineralogical composition for the concentrates was around 73% hematite, 19% goethite and around 1% magnetite. As for contaminating minerals, the most abundant impurity was kaolinite with a grade of 3.5%, followed by quartz with 2.8%, 0.5% gibbsite and a 0.8% illite grade (Others). The tailings had an average mineralogical composition of around 71% quartz, 18% hematite, 5% kaolinite, 3% goethite, 0.2% magnetite and around 2% illite. The results obtained in the study with Sample 1 indicate a potential process route for the concentration of iron-bearing minerals from the slimes generated at this particular industrial plant. As determined at the pilot scale, the conceptual project considered cationic flotation (reverse configuration) with amidoamine as a collector (with or without corn starch as a depressant) and flotation column in a single rougher stage. For the purposes of scale up and industrial scale implementation, it was taken into account the physical–chemical aspects of the process - which involve the use of a different type of collector to the one massively employed in the iron ore industry - and the aspects related to the application of the column flotation technology for the concentration of ultrafine particles. The influence of performance variation at a different scale; the bubble generation system applied and the carrying capacity are discussed with the objective to define

the best process parameters for future industrial application. The application of amidoamine (Flotisor 5530) as a collector showed a very distinct trend in comparison with the classical cationic reverse flotation of iron ores using amines as a collector and starch as a depressant. In this work, it was possible to reach SiO_2 recoveries of up to 85% and Fe recoveries of up to 80%.

There are no cases reported in the literature indicating a satisfactory separation between silicates and iron-bearing minerals without the use of a depressant reagent, at least, with an Fe grade in the concentrate higher than 58%. In Brazil, for instance, corn starch has been extensively applied as an iron-bearing minerals depressant since 1978 and all industrial operations use this kind of reagent (Araujo et al., 2005). Regarding the aspects related to the application of column flotation, variations of flotation performance between different scales are always a concern related to scale-up considerations. The flotation results variations are related to aspects such as bubble generation system; mixing characteristics; H/D relation and carrying capacity (Yianatos, 1989). Bubble generation is recognized as a key aspect of the flotation column design (Harbort and Clarke, 2017). The flotation results achieved considering flotation in different size columns (2" and 6") indicate that the performance with the 2" column is slightly higher than that obtained in the 6" column. In this pilot-scale study, the bubble generation system (porous tube or cavitation tube) does not appear to be a determining factor in the metallurgical result. Since the growing popularization and application of flotation columns at industrial circuits in the 80s, the application of the bubble generation system at industrial scale has not been common sense.

Several studies have been carried out focusing on the evaluation of flotation performance as a function of the bubble generator at pilot scale (Mackay et al., 1988; Huls et al., 1991; Tortorelli et al., 1997; Peng and Yu, 2015; Matiolo et al., 2019). Mackay et al. (1988) reported research that led to the development of a simple method for externally generating bubbles for a flotation column or other application. This method for generating bubbles is strongly affected by pressure, frother concentration (solution surface tension), injection tip hole size, and tip velocity, but weakly affected by contact media size. This system, which permits extensive bubble size control at enhanced column air holdups compared with conventional porous spargers, has been successfully scaled up for use in commercial flotation columns and is currently being operated in a number of mineral processing plants and mineral beneficiation research laboratories.

Moreover, it is simple to construct, easy to operate, and it allows onstream maintenance. Huls et al. (1991) evaluated two sparging systems in a 0.9 m diameter pilot flotation: a cloth sparger and the external contacting system. By comparing copper recovery and nickel recovery,

it was seen that separation efficiency was virtually identical for both kinds of bubble generator. On the other hand, Matiolo et al. (2019) showed that with the same columns used in this study for the flotation of apatite ultrafine, the column equipped with a cavitation tube showed an apatite recovery around 5–8% greater than the column equipped with the porous tube. In the middle of the 90's, Finch (1995) in part IV of his review on the application of flotation column at industrial scale indicated that appropriate designs may be able to exploit dissolved air, and cavitation/nucleation to selectively “activate” particles by frosting them with fine bubbles and that future developments may be to combine bubble generation with particle collection in what might better be defined as a “reactor” rather than a sparger. The bubble generation for flotation columns at industrial scale includes jetting, static mixers and cavitation tube whereas at laboratory and pilot scale the most common device is porous tube (Bergh et al., 2018).

According to Harbort and Clarke (2017), at industrial scale, around 41% of the total installed capacity uses air/water mixture and cavitation tube less than 15% of the installed capacity. Bergh et al. (2018) reported that in Chile, for instance, the most common bubble generator applied is jetting sparger. In general, bubble size control and generation are best performed at pilot rather than at industrial scale. Not only is the bubble size obtained lower at pilot scale but also the size distribution does not change due to the sparger degradation, which is common at industrial plants (Bergh et al., 2018) and increases the bubble size. Kinetics decreases inversely to the bubble diameter leading to a lower recovery at the collection zone. Bergh et al. (2018) describes a methodology to estimate the economic impacts related to spargers degradation in flotation columns at industrial scale. The authors consider the use of jetting sparger since this is the bubble generator most columns have installed in Chile. The authors also reported that the water addition with air to avoid plugging is not a common practice due to the quality of the process water available. Thus, based on the conclusions from the present work, the authors would like to point out that the costs of implementing the procedure developed to quantify the magnitude of economic losses on an industrial scale due to the wear of the spargers are covered by the gains obtained with the adoption of a periodic maintenance program of the bubble generator device (jetting). Column flotation is by large the dominant technology in the phosphate and iron ore industry in Brazil (Harbort and Clarke, 2017).

The first industrial application of flotation columns in this country was silica flotation to concentrate iron ore at Samarco Mineração in the early 90's and soon a great expansion of the application of this technology was observed in the iron ore flotation circuits (Flint et al., 1992; Araujo and Peres, 1995). It is estimated that 67% of the installed iron ore column flotation capacity is in Brazil (Harbort and Clarke, 2017). The application of flotation column to the

concentration of phosphate ores represents 4% of the total installed column flotation capacity (Harbort and Clarke, 2017). In Brazil, the second application of flotation columns was in the beneficiation of phosphate ore. The first six columns started operating in 1993 in Araxá (Minas Gerais State) for barite, coarse apatite, and fine and ultrafine apatite flotation (Guimarães and Peres, 2003; Takata, 2009). Both in iron ore and phosphate application, the bubble generator applied was the CESL sparger that is an air/water mixture device. Over the twenty years of the application of this type of bubble generator, cloggings and wear of holes were observed at industrial plants, leading to recovery losses at the collection zone, not to mention an increase in maintenance costs. In mid-2000s, in the Araxá phosphate beneficiation plant, pilot trials were carried out using a column with 20" in diameter and 10 m tall (2 t/h solid feed) with the objective to evaluate, in a comparative way, the cavitation tube and the sparger with air/water.

With the results obtained in that study, starting in 2008, all spargers with air/water mixture were replaced by cavitation tubes at the industrial plant. Increases in recovery between 10 and 15% were observed especially for the fines circuit. In just a few years, all air/water mixture bubblers were replaced by cavitation tubes in all phosphate plants in Brazil. In iron mining, the same trend was observed and, finally, the world's largest pyrochlore concentration plant (located in Araxá) also reported the application of column flotation using cavitation tubes to generate bubbles. In fact, all the new column flotation projects developed in Brazil led, almost entirely, to the use of cavitation tubes in the generation of bubbles. Based on industrial practices as well as on this work, it is believed that the results obtained in this study were achieved at industrial scale, considering the adoption of hydrodynamic cavitation for bubble generation. In Brazil, the massive application of cavitation tubes for bubble generation of flotation columns at industrial scale seems to be a different trend to what is observed in other regions. Historically, the most popular form of bubble generation devices has been the fluid (plunging) jet and different varieties of air/water orifice types, with each having approximately 30% of the total installed column flotation capacity (Harbort and Clarke, 2017). Some of the advantages reported regarding hydrodynamic cavitation to bubble generation in mineral flotation include: enhanced particle aggregation by tiny bubbles bridging, giving rise to increase collision probability of the enlarged particle aggregates with large bubbles; accelerated particle-bubble attachment through coalescence of tiny bubbles frosted on particle surfaces with larger bubbles instead of the direct particle/bubble contact; and increasing in bubble/particle collision probability (Zhou et al., 1997, 2009; Tao et al., 2006; Li et al., 2015).

However, its application at industrial scale is still limited. The Brazilian experience in the use of this type of device to bubble generation in column flotation seems to be an important

trend to be followed. It is expected that significant benefits can be achieved in the concentration of different ores around the world. Another aspect to be taken into account for scale up purposes is the carrying capacity, which is the limitation that froth imposes to the maximum removal rate of floated solids (Finch and Dobby, 1991). Maximum loading of the bubbles is a possible limitation in flotation columns, especially in systems operating with fine particles ($< 20 \mu\text{m}$) requiring a high solids recovery into the froth phase (Yianatos, 1989). Both parameters are critical in the concentration of iron ore slimes since the expected d_{80} at the froth phase is below $30 \mu\text{m}$ and mass recovery is up to 30–40% and must be considered regarding scale up to industrial scale. The maximum carrying capacity, required for mineral transport on the bubble surface, determines the minimum bubble surface area flux for each operation. Thus, there is a close compromise between the mean bubble size and the superficial gas rate in order to generate the bubble surface area flux to accomplish the mass transport requirement across the interface (Yianatos and Henríquez, 2007). The carrying capacity for a given product can be increased by increasing the superficial bubble surface area rate, which in turn can be increased by increasing the aeration rate or by reducing the bubble size (Sastri, 1996).

Espinosa Gomez et al. (1988) proposed a model to the column carrying capacity as a function of particle size and particle density. Sastri (1996) revised the model proposed by Espinosa-Gomez et al. (1988) for the carrying capacities in flotation columns and was found to be satisfactory not only for predicting the maximum carrying capacity but also for the operating capacities of these columns. However, the constant proposed was found to yield too high values for the maximum carrying capacities. The results indicated by Patwardhan and Honaker (2000), which was consistent with previous findings, observed that the influence of the superficial gas velocity on the carrying capacity diminished above a value of 1.8 cm/s. At values lower than 1.8 cm/s, the impact of the superficial gas velocity was more significant for the flotation of relatively coarse material. Wang et al. (2019) evaluated the use of a fast-switching solenoid valve added to the air intake line of a 5cm diameter flotation column equipped with a sparger to change the flow pattern of air supply from steady to rapidly oscillatory. It was found that the use of oscillatory air supply to replace the steady air supply could significantly improve the throughput without sacrificing product yield and increase the carrying capacity of the column, which was consistent with the enhanced bubble surface area flux in the column.

Despite the high mass recovery to the froth zone ($> 30\%$) in the flotation of this sample in both columns, the J_g applied was very distinct, being 0.49 cm/s in the cavitation tube of the 6" diameter column and 1.15 cm/s in the 2" diameter porous sparger. In general, the bubbles generated by hydrodynamic cavitation were smaller when compared with the bubbles generated

by the other bubble generation devices which means higher S_b values. From experience, it is known that gas holdup increases with an increase in gas rate and decrease in bubble size (Gorain et al., 1999; Finch et al., 2000). For industrial purposes, a minimum 0.5 cm/s must be considered since the cavitation tube is applied as a bubble generator. Considering other devices, it is suggested higher J_g values (up to 1.0 cm/s) as minimum to guarantee the adequate S_b value, since the increment of J_g also results in higher S_b . Despite the fact that, in this study at pilot scale, the bubble generator device is not appointed as a key factor to the best metallurgical performance, it is strongly suggested the application of hydrodynamic cavitation as a bubble generator at industrial scale instead of fluid (plunging) jet or different varieties of air/water orifice types. The benefits include the possibility of application of lower J_g , a better control of bubble size and distribution as well as lower maintenance costs as it has already been observed at the phosphate and iron ore flotation columns in operation in Brazil.

Table 5. Effect of EDA-C, Flotisor 5530, Corn starch dosages and pH values on the flotation performance for experiments at the 2nd column flotation. Rougher flotation. $J_g = 1.15$ cm/s; $J_w = 0.49$ cm/s. Flotation studies with Sample 1

Test	Dosage (g/t)			pH	Recovery (%)		Grade (%)		
	EDA-C	Flotisor 5530	Corn Starch		Mass	Fe	Fe	SiO ₂	Al ₂ O ₃
1	105	0	0	8.5	67.8	88.3	57.7	10.7	3.4
2	113	0	0	9.5	47.1	67.1	64.0	3.7	2.2
3	115	0	0	10.5	28.3	34.8	55.6	6.4	5.2
4	100	0	493	10.5	30.7	37.5	54.9	7.3	5.2
5	101	0	497	9.5	55.1	71.5	59.2	5.8	3.8
6	0	152	0	8.5	63.5	87.0	61.9	4.1	3.1
7	0	149	0	9.5	57.6	79.0	62.0	3.6	2.9
8	0	152	0	10.5	67.7	94.1	62.8	3.2	2.5
9	0	200	0	10.5	67.6	93.2	62.3	3.3	2.6
10	0	109	1088	8.5	69.8	94.1	60.9	5.1	3.1
11	0	111	1113	9.5	66.9	92.4	62.4	4.3	3.0
13	0	230	1152	10.5	69.5	96.1	62.5	4.7	2.4

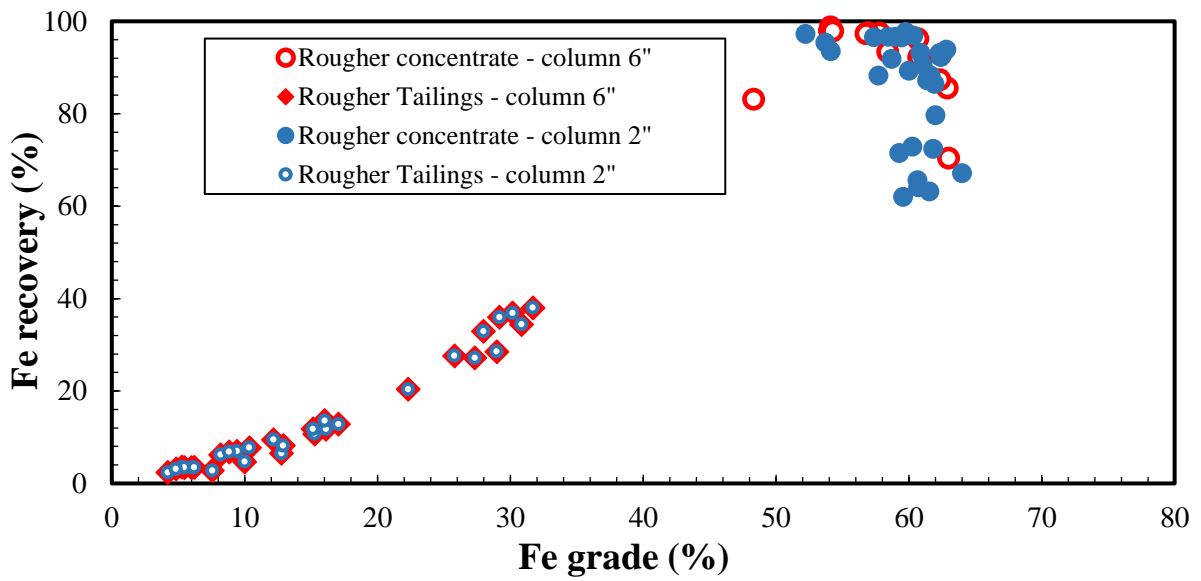


Figure 7. Fe grade/recovery curves for rougher flotation. Comparative results of the circuit with 6" and 2" column flotation.

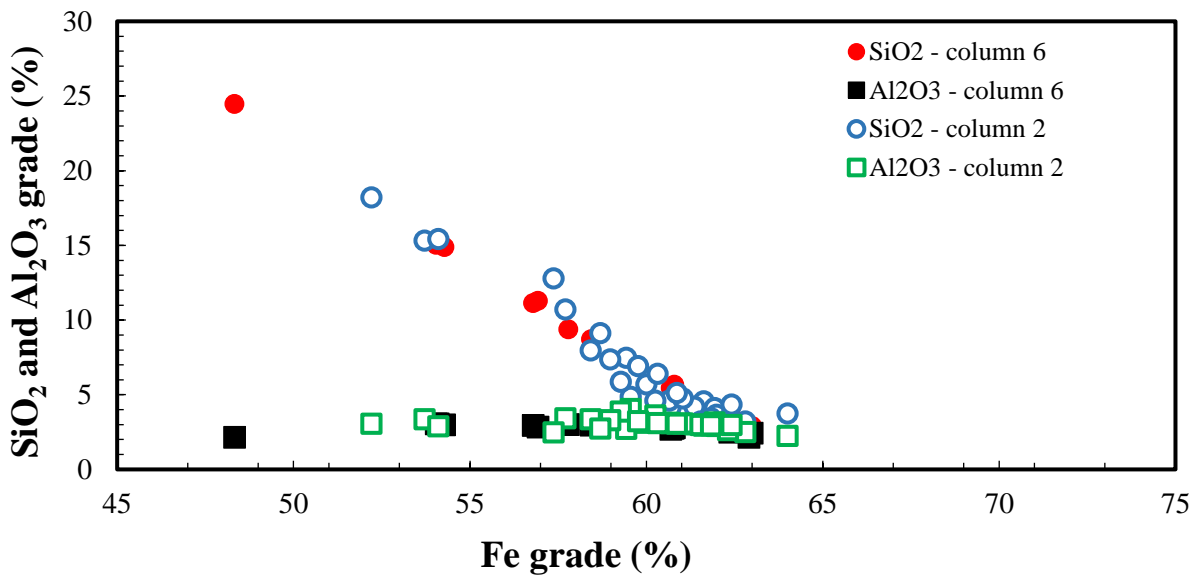


Figure 8. Fe grade vs SiO₂ and Al₂O₃ grade. Flotation studies in 2" and 6" diameter column flotation.

Table 6. Effect of Flotinator 5530 and corn starch dosages and pH values on the flotation performance for experiments in 2" and 6" columns flotation. Rougher flotation. Flotation studies with sample 1

Column	Reagents (g/t)		pH	Recovery (%)		Grade (%)		
	Flotinator 5530	Corn starch		Mass	Fe	Fe	SiO ₂	Al ₂ O ₃
6"	78	0	8.5	66.1	87.1	60.5	5.6	2.9
2"	101	0	8.5	65.7	90.5	61.0	4.7	3.1
6"	124	0	8.5	58.5	78.6	61.2	4.9	2.8
2"	152	0	8.5	62.3	86.4	61.9	4.1	3.1
6"	129	0	10.5	57.7	80.4	62.6	2.9	2.6
2"	152	0	10.5	66.5	93.8	62.8	3.2	2.5
6"	60	1200	8.5	77.8	96.4	55.8	12.2	3.0
2"	53	1062	8.5	74.7	97.7	59.8	6.9	3.2
6"	64	1273	9.5	70.1	93.3	58.4	8.7	3.0
2"	56	1116	9.5	71.5	96.9	60.3	6.4	3.1

Table 7. Mineralogical characterization of concentrate and tailings. Flotation of Sample 1

Product	Hematite	Goethite	Quartz	Kaolinite	Others
Concentrate	72.7	18.9	2.8	3.5	2.1
Tailings	18.5	3.0	71.4	4.9	2.2

3.2. Flotation Studies – Sample 2

This topic presents the results and discussion of the reverse iron flotation studies considering rougher flotation in the 3" diameter column and rougher/cleaner flotation in the 6" and 4" diameter columns for Sample 2. The influence of the collector dosage, the collector type, the depressant dosage and the pH were evaluated. Table 8 shows the results achieved in iron rougher flotation in the 3" diameter column flotation, the mass and metallurgical balance for Fe, SiO₂ and Al₂O₃, the impact of the collectors (EDA-C and Flotinator 5530) and the depressant (gelatinized corn starch), as well as the effect of the pH (9.5 and 10.5). EDA-C was evaluated in the presence and absence of a depressant. EDA-C dosages around 290 g/t were used in the absence of corn starch at pH value 10.5 and EDA-C dosages around 100 to 480 g/t were used in the presence of gelatinized corn starch with dosages of 500 to 1200 g/t, at pH values 9.5 and 10.5.

The best result (test 3) at 287 g/t of EDA-C was in the absence of starch at pH 10.5, which produced a concentrate (sink stream) with an Fe grade of about 52% and a mass and metallurgical recovery of Fe of 44% and 55%, respectively. The SiO₂ and Al₂O₃ impurities grades were 16% and 3.5%. The tests performed in the presence of corn starch (from 500 to

1200 g/t), around 105 to 480 g/t of EDA-C dosage and at pH values of 9.5 and 10.5 showed an inferior flotation performance, with a decrease in the concentrate of Fe grade (42% to 48%) and an increase in the mass (88%) and metallurgical Fe recoveries (95%). The Fe grade in the concentrate was extremely low in the presence of corn starch, below the values considered suitable for application of the concentrate as a pellet feed (in the order of 60%).

The results obtained with the application of EDA-C as a collector in association with gelatinized corn starch depressant indicated that this alternative should not be viable for the hematite concentration for Sample 2. As studied in Sample 1, Flotisor 5530 also was applied as a collector. It was evaluated the effect of a collector dosage in the absence and presence of gelatinized corn starch and the effect of pH values of 8.5; 9.5 and 10.5. Fig. 9 shows the curve of Fe grade versus recovery considering reverse iron flotation in the 3" diameter flotation column. The points presented at the graphic covered all tests, regardless of the process conditions applied, such as the corn starch dosage and pH values. As observed, the Fe grade ranged from 7.3% to 28% in the tailings. In the concentrate, the Fe grade ranged from 41% to 54%. Considering the average of the 33 tests in the concentrate, the Fe recovery was 86%, with an average of Fe grade of 47%. Unlike the results observed in Sample 1 when Flotisor 5530 was applied as a collector, the Fe grades were not reached in the concentrates with values close to 58–60%, a technical goal for pellet feed application from the concentrate.

An important point to highlight in the studies with Sample 2, even for collector dosages above 700 g/t, it was not possible to obtain concentrates with high Fe grades (above 58%). Fig. 10 shows the correlation between the Fe grade and the SiO₂ and Al₂O₃ impurity grades in the concentrates in the 3" diameter column flotation, rougher flotation, with the use of Flotisor 5530 reagent as a collector. As shown in Fig. 10, the Fe grade ranged from 41% to a maximum of 54%. As observed in Sample 1, the increase of the Fe grade in the concentrate was mainly due to the reduction of the SiO₂ grade. The SiO₂ grade in the concentrate ranged from maximum values of 30% to values below 14%. The SiO₂ recovery in the tailings (floated stream) ranged from 15% to a maximum of 78%, which was below the values observed in Sample 1 which reached values of up to 90%. Regarding the impurities of the Al₂O₃ grade, the second most abundant impurity in the sample, the values were below those observed in Sample 1, ranging from 3.2% to values up to 5%. Considering that the flotation circuit tested was the reverse configuration, the metallurgical recovery of Al₂O₃ impurities in the tailings (float) fraction was considered low, ranging from 27% to up to 65%. Table 9 shows the results achieved in iron rougher/cleaner flotation in the 6" and 4" diameter column flotation, the mass and metallurgical balance for Fe, SiO₂ and Al₂O₃, the impact of the collector (Flotisor 5530), dosages from 100

g/t to values above 600 g/t, in the absence of the depressant (gelatinized corn starch) at pH 10.5. The global mass recovery of the circuit ranged from 30% to values close to 80% and the Fe recovery ranged from 50% to 98%. The Fe grade in the final concentrates ranged from 44% to a maximum value of 55%-57%. The SiO₂ and Al₂O₃ impurities were around 12% and 3.5% for best results.

The best result achieved (test 1) was by using 678 g/t of Flotisor 5530, which produced a concentrate (sink stream) with an Fe grade of about 55% and a mass and Fe recovery of 58% and 83%, respectively. The SiO₂ and Al₂O₃ impurities grades were 13% and 4%. The flotation results obtained applying similar process conditions are very distinct between the two samples evaluated despite the similarity in terms of physical and mineralogical. Despite the very good results obtained with the sample 1 using the amidoamine collector, even when a more complex flotation circuit including a cleaner stage for treatment the sample 2, it was not possible to produce concentrates with iron grade higher than 55–57%, values that are considered too low for a commercial concentrate. This indicates that there is not a single solution for the recovery of the iron ore bearing minerals from slimes and it will be necessary continuous efforts to better understand the mechanisms involved in the hydrophobization of silicates minerals by amidoamine collectors. In case a suitable reagent system is identified (type of collector and depressant), the use of column flotation technology with the use of hydrodynamic cavitation for the bubble generation, must guarantee similar metallurgical performance obtained on a pilot scale.

Table 8. Effect of EDA-C, Corn starch dosages and pH values on the flotation performance for experiments at 3". Rougher flotation. Jg = 0.50 cm/s; Jw = 0.13 cm/s. Flotation studies with sample 2

Test	Dosage (g/t)		pH	Recovery (%)		Grade (%)		
	EDA-C	Corn		Mass	Fe	Fe	SiO ₂	Al ₂ O ₃
1	113	561	10.5	83.3	95.5	44.1	26.3	4.8
2	105	524	9.5	88.0	95.1	42.1	29.9	4.8
3	287	0	10.5	43.7	55.3	52.3	16.4	3.5
4	246	510	10.5	59.3	71.2	48.4	20.2	4.4
5	295	988	10.5	51.5	63.1	47.4	21.3	5.1
6	480	1199	10.5	31.8	41.3	48.5	19.2	5.0

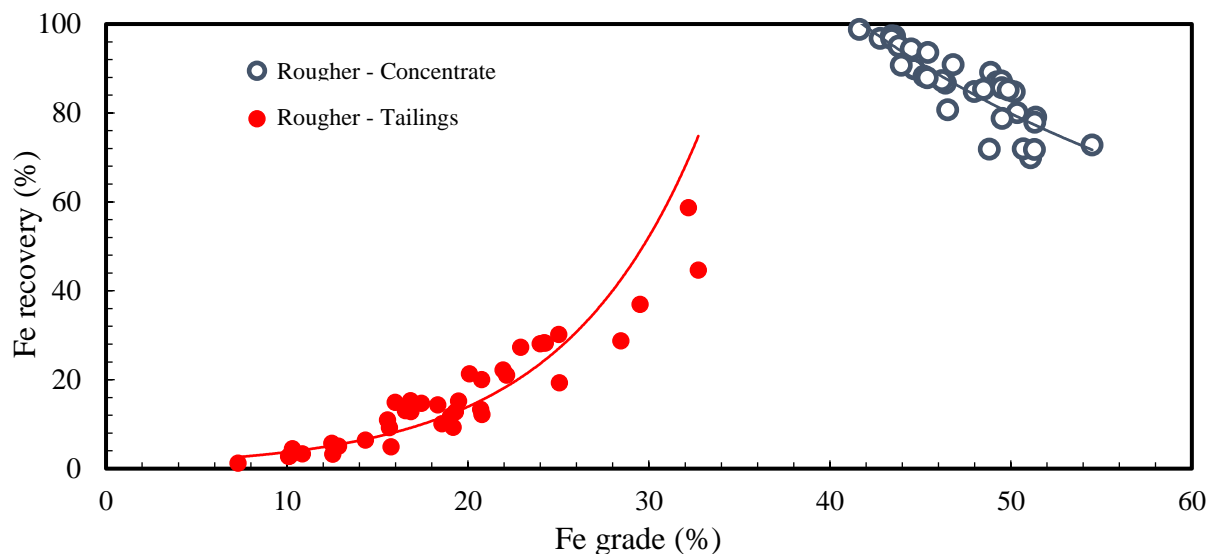


Figure 9. Grade vs recovery curve. Rougher flotation studies. Column 3” diameter. Sample 2

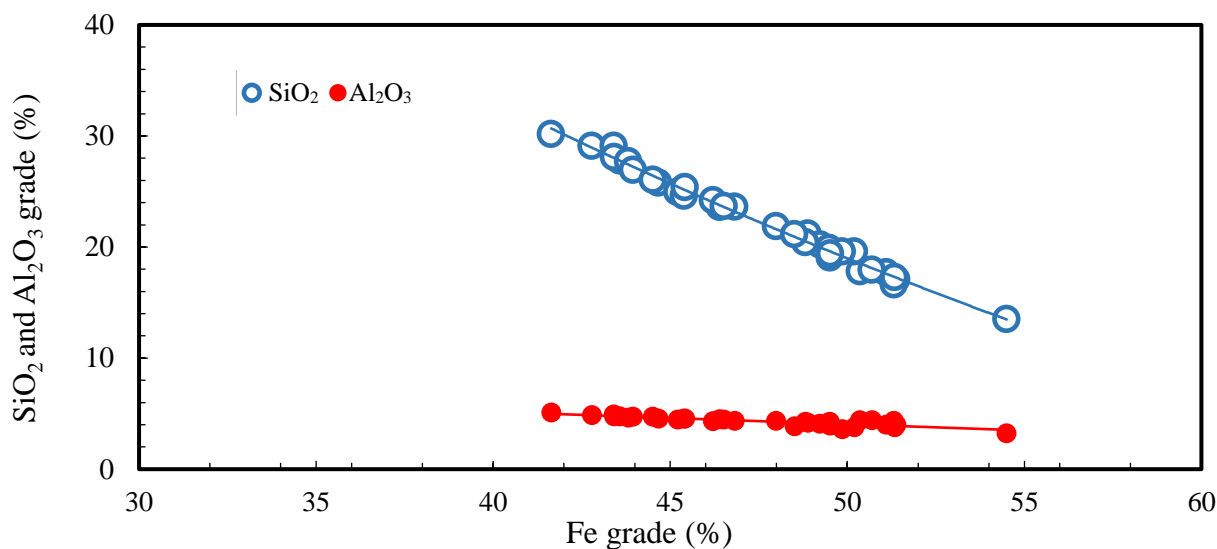


Figure 10. Correlation between Fe grade and SiO₂ and Al₂O₃ impurities grades in the final sink stream (concentrates). Column flotation of 3” diameter. Sample 2.

Table 9. Effect of Flotiner 5530 dosage on the flotation performance for experiments in the 6” and 4” column flotation. Rougher/cleaner flotation. (Rougher: Jg=0.30cm/s; Jw = 0.20 cm/s – Cleaner: Jg = 0.51 cm/s; Jw = 0.21 cm/s) pH = 10.5. Flotation studies with sample 2

Test	Dosage (g/t)	Mass Recovery (%)			Fe Recovery (%)			Grade (%)					
		RG	CL	Global	RG	CL	Global	Fe		SiO ₂		Al ₂ O ₃	
	Flotiner 5530	RG	CL	Global	RG	CL	Global	RG	CL	RG	CL	RG	CL
1	678	69.6	83.	58.0	89.9	92.2	82.9	49.9	55.2	20.5	12.8	4.1	4.1
2	411	34.7	88.	30.6	50.4	97.0	48.9	52.0	57.0	18.5	11.5	3.3	3.0
3	213	68.0	98.	67.0	84.7	99.8	84.5	46.3	46.9	26.5	25.7	3.5	3.5
4	106	88.4	89.	79.3	98.9	98.9	97.8	40.5	44.6	34.7	28.7	3.6	3.4
5	342	69.4	74.	51.4	81.9	96.1	78.7	40.0	52.0	35.3	18.0	3.6	3.2

4. Conclusions

The concentration of iron-bearing minerals from two slimes samples from two different industrial plants at Vale (Quadrilátero Ferrífero – MG) was evaluated at pilot scale considering the application of column flotation (reverse configuration), starch as a depressant and two kinds of silicates collector without previous desliming. It was possible to produce iron concentrates with grades higher than 60%, SiO₂ below 5% and Al₂O₃ 3% from only one of the two samples studied. The collector type had a great impact in the flotation results. The best results with Sample 1 were achieved with the collector type amidoamine (Flotisor 5530) instead of the classical amine collector extensively applied in the iron ore plants in Brazil. The results obtained with Sample 1 indicated that the results of the 2" column show consistently a higher recovery for similar grades than the 6" column. Despite the use of hydrodynamic cavitation for bubble generation at the 6" diameter column, which usually leads to better recovery, especially for ultrafine particles, the better results obtained with the column of 2" with porous tube as bubble generator can be attributed to better mixing characteristics of the smaller column. However, for industrial application, the use of cavitation tube is strongly recommended based on the successfully use of this kind of bubble generator at the iron industry in Brazil. For Sample 2, it was not possible to produce concentrates with iron grade higher than 55%, independent of the collector type and dosage and also flotation circuit. The results obtained in this study and from literature review indicate the non-existence of a standard solution for an efficient slimes processing in the iron ore industry. Therefore, continuous scientific and technological efforts must be made in order to reduce the iron losses at slimes at industrial iron ore concentration plants.

Acknowledgments

The authors are grateful to all the institutions supporting research in Brazil, namely CNPq for the scholarship to Amanda de Freitas and CETEM/MCTIC for the infrastructure. A special thanks to the industrial partner Vale for the financial support and permission to publish this work. A special thanks to Fabio Novaes for his support during the experimental work.

References

- Araujo, A., Peres, A.E.C. 1995. Froth Flotation. Relevant facts and the Brazilian case. Série Tecnologia Mineral. CETEM. 43 p.
- Araujo, A.C., Viana, P.R.M., Peres, A.E.C., 2005. Reagents in iron ores flotation. Minerals Engineering, 18. 219–224. <https://doi.org/10.1016/j.mineng.2004.08.023>.

Agência Nacional de Mineração (ANM). 2018. Anuário Mineral Brasileiro. Principais substâncias metálicas. http://www.anm.gov.br/dnpm/publicacoes/serie-estatisticas-e-economia-mineral/anuario-mineral/anuario-mineral-brasileiro/amb_2018.pdf. (accessed 24 April 2020) (In Portuguese).

Bergh, L., Yianatos, J., Acuña, C., Cantellano, C. 2018. Economic impact of spargers degradation in flotation columns. IFAC PapersOnLine. 51-21. 329-335. <https://doi.org/10.1016/j.ifacol.2018.09.441>

Castro, E., Peres, A.E.C. 2013. Production of pellet feed from slimes. Rem Rev. Esc. Minas 66. 391–395. <http://dx.doi.org/10.1590/S0370-44672013000300018>.

Clemmer, J.B. 1947. Flotation of Iron Ore. Duluth, Minnesota, USA, 8th Annual Mining Symposium.

Dey, S., Pani, S., Singh, R., Paul, G.M. 2015. Response of process parameters for processing of iron ore slime using column flotation. International Journal of Mineral Processing, 140. 58–65. <https://doi.org/10.1016/j.minpro.2015.04.013>.

Espinosa-Gomez, R., Finch, J.A., Yianatos, J.B., Dobby, G.S. 1988. Flotation column carrying capacity: particle size and density effects. Minerals Engineering, Vol. 1, N° 1. 77-79. [https://doi.org/10.1016/0892-6875\(88\)90068-4](https://doi.org/10.1016/0892-6875(88)90068-4)

Filippov, L.O., Filippova, I.V., Severov, V.V. 2010. The use of collectors mixture in the reverse cationic flotation of magnetite ore: The role of Fe-bearing silicates. Minerals Engineering, 23. 91–98. <https://doi.org/10.1016/j.mineng.2009.10.007>

Filippov, L.O., Severov, V. V., Filippova, I. V. 2014. An overview of the beneficiation of iron ores via reverse cationic flotation. International Journal of Mineral Processing, 127. 62–69. <https://doi.org/10.1016/j.minpro.2014.01.002>

Finch, J.A., Dobby, G.S. 1991. Column flotation: A selected review. Part I. International Journal of Mineral Processing, 33. 343-354. [https://doi.org/10.1016/0301-7516\(91\)90062-N](https://doi.org/10.1016/0301-7516(91)90062-N)

Finch, J.A. 1995. Column flotation: A selected review - Part IV: Novel flotation device. Minerals Engineering, Vol 8, N°6. 587-602. [https://doi.org/10.1016/0892-6875\(95\)00023-J](https://doi.org/10.1016/0892-6875(95)00023-J)

Finch, J.A., Xiao, J., Hardie, C., Gomez, C.O. 2000. Gas dispersion proprieties: bubble surface area flux and gas holdup. Minerals Engineering, Vol. 13, N°4. 365-372. [https://doi.org/10.1016/S0892-6875\(00\)00019-4](https://doi.org/10.1016/S0892-6875(00)00019-4).

Flint, I.M., Wyslouzil, H.E., Lima Andrade, V.L., Murdock, D.L. 1992. Column flotation of iron ore. Minerals Engineering, Vol. 5, N° 10-12. 1185-1194. [https://doi.org/10.1016/0892-6875\(92\)90158-6](https://doi.org/10.1016/0892-6875(92)90158-6)

Gorain, B.K., Franzidis, J.P., Manlapig, E.V. 1999. The empirical prediction of bubble surface area flux in mechanical flotation cells. *Minerals Engineering*, Vol 12, N° 3. 309-322. [https://doi.org/10.1016/S0892-6875\(99\)00008-4](https://doi.org/10.1016/S0892-6875(99)00008-4).

Guimarães, R.C., Peres, A.E.C. 2003. Production of phosphate concentrates from slimes: Brazilian experience. In: *Proceedings XXII International Mineral Processing Congress*, Cape-Town, South Africa, 606-612.

Harbort, G., Clarke, D. 2017. Fluctuations in the popularity and usage of flotation columns - An Overview. *Minerals Engineering*. 100. 17-30. <https://doi.org/10.1016/j.mineng.2016.09.025>

Houot. R.. 1983. Beneficiation of iron ore by flotation - Review of industrial and potential applications. *Int. J. Miner. Process.* 10. 183–204. [https://doi.org/10.1016/0301-7516\(83\)90010-8](https://doi.org/10.1016/0301-7516(83)90010-8).

Huls, B.J., Lachance, C.D., Dobby, G.S. 1991. Bubble generation assesement system for and industrial flotation columns. *Minerals Engineering*, Vol 4, N° 1. 37-42. [https://doi.org/10.1016/0892-6875\(91\)90116-D](https://doi.org/10.1016/0892-6875(91)90116-D)

Jena, S.K., Sahoo, H., Rath, S.S., Rao, D.S., Das, S.K., Das, B. 2015. Characterization and processing of iron ore slimes for recovery of iron values. *Mineral Processing and Extractive Metallurgy Review*, 36. 174–182. <https://doi.org/10.1080/08827508.2014.898300>

Knorr, K., Neumann, R., 2012. Advances in Quantitative X-Ray Mineralogy: Mixed Crystals in Bauxite. In: Broekmans, M.A.T.M. (Ed.), *Proceedings of the 10th International Congress for Applied Mineralogy (ICAM)*. Springer, Berlin Heidelberg. 377–384.

Kumar, R., Mandre, N.R. 2016. Characterization and Beneficiation of Iron Ore Tailings by Selective Flocculation. *Transactions of the Indian Institute of Metals*, 69. 1459–1466. <https://doi.org/https://doi.org/10.1007/s12666-015-0667-9>

Kumar, R., Mandre, N.R. 2017. Recovery of iron from iron ore slimes by selective flocculation. *Journal of the Southern African Institute of Mining and Metallurgy*, 117. 397–400. <https://doi.org/10.17159/2411-9717/2017/v117n4a12>.

Li, H., Afacan, A., Liu, Q., Xu, Z. 2015. Study interaction between fine particles and micro size bubbles generated by hydrodynamic cavitation. *Minerals Engineering*, 84. 106-115. <https://doi.org/10.1016/j.mineng.2015.09.023>.

Lima, R.M.F., Brandão, P.R.G., Peres, A.E.C. 2005. The infrared spectra of amine collectors used in the flotatation of iron ores. *Minerals Engineering*, 18. 267–273. <https://doi.org/10.1016/j.mineng.2004.10.016>

Lima, N.P., de Souza Pinto, T.C., Tavares, A.C., Sweet, J. 2016. The entrainment effect on the performance of iron ore reverse flotation. *Minerals Engineering*, 96–97. 53–58. <https://doi.org/10.1016/j.mineng.2016.05.018>

Lima, R.M.F., Abreu, F.P.V.F. 2019. Characterization and concentration by selective flocculation/magnetic separation of iron ore slimes from a dam of Quadrilátero Ferrífero - Brazil. *Journal of Materials Research and Technology*. Volume 9, Issue 2, March–April 2020. 2021-2027. <https://doi.org/10.1016/j.jmrt.2019.12.034>.

Ma. X., Bruckard, W.J., Holmes, R. 2009. Effect of collector, pH and ionic strength on the cationic flotation of kaolinite. *International Journal of Mineral Processing*, 93. 54-58. <https://doi.org/10.1016/j.minpro.2009.05.007>

Ma. X., Marques, M., Gontijo, C. 2011. Comparative studies of reverse cationic/anionic flotation of Vale iron ore. *International Journal of Mineral Processing*, 100. 179–183. <https://doi.org/10.1016/j.minpro.2011.07.001>

Ma. M. 2012. Froth flotation of iron ores. *International Journal of Mining Engineering and Mineral Processing* 2012. 1(2): 56-61. doi: 10.5923/j.mining.20120102.06.

Mackay, J.D., Foot, D.G., Shirts, M.B. 1988. Column flotation and bubble generation studies at the Bureau of Mines. In *Column Flotation '88. Proceedings of an International Symposium of Column Flotation*, Phoenix, AZ, January 25-28, Littleton, CO: SME. 173-176.

Matiolo, E., Couto, H., Teixeira, M.F.L., Almeida, R.N., Freitas, A.S. 2019. A comparative study of different column sizes for ultrafine apatite flotation. *Minerals*, 9(7), 391. <https://doi.org/10.3390/min9070391>.

Panda, L., Biswal, S.K., Venugopal, R., Mandre, N.R. 2018. Recovery of Ultra-Fine Iron Ore from Iron Ore Tailings. *Transactions of the Indian Institute of Metals*, 71. 463–468. <https://doi.org/10.1007/s12666-017-1177-8>

Patwardhan, A., Honaker, R.Q. 2000. Development of a carrying-capacity model for column froth flotation. *International Journal of Mineral Processing*, 59. 275-293. [https://doi.org/10.1016/S0301-7516\(99\)00081-2](https://doi.org/10.1016/S0301-7516(99)00081-2).

Peng, F., Yu, X. 2015. Pico–nano bubble column flotation using static mixer-venturi tube for Pittsburgh No. 8 coal seam. *International Journal of Mining Science and Technology*, 25. 347-354. <https://doi.org/10.1016/j.ijmst.2015.03.004>

Praes, P.E., de Albuquerque, R.O., Luz, A.F.O. 2013. Recovery of Iron Ore Tailings by Column Flotation. *Journal of Minerals and Materials Characterization and Engineering*, 01. 212–216. <https://doi.org/10.4236/jmmce.2013.15033>

Rocha, L., Canado, R.Z.L., Peres, A.E.C. 2010. Iron ore slimes flotation. *Minerals Engineering*, 23. 842–845. <https://doi.org/10.1016/j.mineng.2010.03.009>

Rao, D.S., VijayaKumar, T.V., Rao, S.S., Prabhakar, S., Raju, G.B. 2011. Effectiveness of sodium silicate as gangue depressants in iron ore slimes flotation. *International Journal of Minerals, Metallurgy, and Materials*, 18. 515–522. <https://doi.org/10.1007/s12613-011-0471-4>.

Rao, G.V., Markandeya, R., Sharma, S.K. 2016. Recovery of Iron Values from Iron Ore Slimes of Donimalai Tailing Dam. *Transactions of the Indian Institute of Metals*, 69. 143–150. <https://doi.org/https://doi.org/10.1007/s12666-015-0809-0>.

Sales, C.G. De. 2012. Rotas de beneficiamento para recuperação de minerais portadores de ferro do underflow do espessador de lamas da usina de Brucutu. Universidade Federal de Minas Gerais. (In Portuguese).

Sastri, S.R.S. 1996. Carrying capacity in flotation columns. *Minerals Engineering*, Vol 9, Nº 4. 465-468. [https://doi.org/10.1016/0892-6875\(96\)00031-3](https://doi.org/10.1016/0892-6875(96)00031-3).

Schulze. D.G. 1984. The influence of aluminum on iron oxides. VIII. Unit-cell dimensions of Al-substituted goethites and estimation of Al from them. *Clays and Clay Minerals*. 32 (1). 36-44. <https://doi.org/10.1346/CCMN.1984.0320105>

Singh, S., Sahoo, H., Rath, S.S., Sahu, A.K., Das, B. 2014. Recovery of iron minerals from Indian iron ore slimes using colloidal magnetic coating. *Powder Technology*, 269. 38–45. <https://doi.org/10.1016/j.powtec.2014.08.065>.

Sivamohan, R. 1990. The problem of recovering very fine particles in mineral processing - A review. *International Journal of Mineral Processing*, 28. 247-288. [https://doi.org/10.1016/0301-7516\(90\)90046-2](https://doi.org/10.1016/0301-7516(90)90046-2)

Souza, H.S., Testa, F.G., Braga, A.S., Kwitko-Ribeiro, R., Oliveira, A.H., Leal Filho, L.S. 2015. Desenvolvimento de uma rota de flotação com alternativa para concentração de minérios de manganês de baixo teor. XXVI Encontro Nacional de Tratamento de Minérios e Metalurgia Extrativa Poços de Caldas-MG, 18 a 22 de Outubro 2015 (In Portuguese).

Souza, H.S., Braga, A.S., Oliveira, A.H., Filho, L.S.L. 2016. Concentration of manganese tailings via reverse flotation in an acid medium. *Rem: Revista da Escola de Minas*, 69, Nº.1, Ouro Preto Jan./Mar. 2016. <https://doi.org/10.1590/0370-44672015690069>.

Takata, L.A. 2009. Flotação em coluna. Capítulo 3. Teoria e Prática do Tratamento de Minérios. A flotação no Brasil. Vol 4. Ed. Arthur Pinto Chaves. Sigmus Editora. 484 p. (In Portuguese).

Tammishetti, V., Kumar, D., Rai, B., Shukla, V., Patra, A.S., Chakraborty, D. P., Kumar, A. 2017. Selective Flocculation of Iron Ore Slimes_ Results of Successful Pilot Plant Trials at Tata Steel. Noamundi. *Trans. Indian Inst. Met.* 70. 411–419. <https://doi.org/https://doi.org/10.1007/s12666-016-1002-9>.

Tao, Y., Liu, J., Yu, S., Tao, D. 2006. Picobubble enhanced fine coal flotation. *Separation Science and Technology*, 41. 3597-3607. <https://doi.org/10.1080/01496390600957249>

Thella. J. S.. Mukherjee. A. K.. & Rajshekar. Y.. 2010. Recovering Iron Values From Iron Ore Slimes Using Cationic and Anionic Collectors. in: *Proceedings of the XI International Seminar on Mineral Processing Technology (MPT-2010)*. pp. 247–254.

Thella, J.S., Mukherjee, A.K., Srikakulapu, N.G. 2012. Processing of high alumina iron ore slimes using classification and flotation. *Powder Technology*, 217. 418–426. <https://doi.org/10.1016/j.powtec.2011.10.058>.

Tortorelli, J.P., Craven, J.W., Togun, J.M., Dobby, G.S., Agar, G.E. 1997. The effect of external gas/slurry contact on the flotation of fine particles. *Minerals Engineering*, Vol. 10, N° 10. 1127-1138. [https://doi.org/10.1016/S0892-6875\(97\)00099-X](https://doi.org/10.1016/S0892-6875(97)00099-X).

Yianatos, J.B., 1989. Column Flotation Modelling and Technology. *International Colloquium: Developments in Froth Flotation, Volume 2*. Cape Town, South Africa, 3-4 August. <http://www.saimm.co.za/Conferences/FrothFlotation/001-Yianatos.pdf>.

Yianatos, J.B., Henríquez, F. 2007. Boundary conditions for gas rate and bubble size at the pulp-froth interface in flotation equipment. *Minerals Engineering*, 20. 625-628. <https://doi.org/10.1016/j.mineng.2006.12.006>.

Wang, J., Park, H., Ng, C.Y., Wang, L. 2019. Use of oscillatory air supply for improving the throughput and carrying capacity of column flotation. *Powder Technology*, 353. 41-47. <https://doi.org/10.1016/j.powtec.2019.05.006>.

Wittelsheim, R.B., Ensisheim, M.M., Zimmerman, C. 1967. Amine-Amide collectors for the treatment of potash ores. *Unite States Patent* 3,596, 763.

Wyslouzil, H.E. 2009. The Use of Column Flotation for the Recovery of Ultra-Fine Phosphates. <http://en-ca.eriez.com/Products/Markets/mineralflotation>.

Zhou, Z.A., Xu, Z., Finch, J.A., Rao, S.R. 1997. Role of hydrodynamic cavitation in fine particle flotation. *International Journal of Mineral Processing*, 51. 139-149. [https://doi.org/10.1016/S0301-7516\(97\)00026-4](https://doi.org/10.1016/S0301-7516(97)00026-4)

Zhou Z.A., Xu, Z., Finch, J.A., Masliyah, J.H., Chow, R.S. 2009. On the role of cavitation in particle collection in flotation – A critical review II. *Minerals Engineering*, 22. 419-433. <https://doi.org/10.1016/j.mineng.2008.12.010>

Chapter 6 - Iron ore slimes flotation tests using column and amidoamine collector without depressant

Lev O. Filippov ^{1,*}, Klaydison Silva ^{1,2}, Alexandre Piçarra ¹, Neymayer Lima ², Iranildes Santos ³, Leandro Bicalho ⁴, Inna V. Filippova ¹ Antonio Eduardo Clark Peres ⁵

¹ Université de Lorraine, CNRS, GeoRessources, F54000 Nancy, France ; klaydison.silva@vale.com (K.S.); alexandre.palma-picarra@univ-lorraine.fr (A.P.); inna.filippova@univ-lorraine.fr (I.V.F.)

² VALE S.A.—Mineral Processing Development Department, Nova Lima CEP 34.006-200, MG, Brazil; neymayer.lima@vale.com

³ Vale Institute of Technology, Avenida Juscelino Kubitschek, Bauxita Ouro Preto 31, MG, Brazil; iranildes.santos@itv.org

⁴ Clariant, Av. Portugal, MG, 31710-400, Brazil; leandro.bicalho@clariant.com

⁵ Universidade Federal de Minas Gerais, Escola de Engenharia, 31270-901 Belo Horizonte, MG, Brazil; aecperes@demet.ufmg.br

Minerals 2021, 11(7), 699; <https://doi.org/10.3390/min11070699>

Received: 8 May 2021; Accepted: 21 June 2021; Published: 29 June 2021.

Abstract: This work describes the concentration of iron ore slimes on a pilot scale by using a 500- mm diameter flotation column and a novel collector, which renders the use of a depressant unnecessary. The pilot column was operated in series with the industrial plant Vargem Grande 2 (Iron Quadrangle, Brazil) receiving, as feed, part of the underflow from the desliming thickener. These pilot tests represented only the rougher stage of a flotation circuit. The novel collector used was an amidoamine (average collector dosage of 160 g/t), and the tests were carried out in the absence of starch, at pH 10.5 and with bubbles/microbubbles generated by cavitation tube. It was possible to achieve a concentrate, by reverse flotation, with an average iron content of 53% and an average metallurgical recovery of 91.5% The recovery of the silica in the froth was 53.1% in average for one stage of flotation. The high variability of the slime characteristics rendered difficult the stabilization of the SiO₂ recovery; however, the applicability of the amidoamine collector was proven. In an industrial scale circuit, the use of online analyzers for Fe and SiO₂ content and the adoption of control logics based on the adjustment of parameters such as reagents dosage and washing water flow rate

adjustment should contribute to the optimization of the results obtained in the pilot scale tests. Further studies adding a cleaner concentration stage should be performed.

Keywords: iron ore; slimes; column flotation; amidoamine; pilot plant; Vargem Grande 2

1. Introduction

1.1. Iron ore ultrafine concentration

The harmful effect of slime on quartz reverse flotation has been known since the beginning of iron ore flotation operations. The removal of slimes using hydrocyclones was introduced by United States Bureau of Mines (USBM) [1]. The high consumption of reagents and the difficulty to remove ultrafine quartz and the high amount of deleterious minerals, such as kaolinite, are the main issues due to the presence of slimes in the flotation [2].

The high stability of the froth is also an important characteristic regarding slimes presence in flotation systems. Achaye [3] showed that froth stability decreases with increasing particle size and fine particles had the greatest influence on froth stability. Some authors [4,5] investigated the relationship between froth stability, size distribution, and air recovery, demonstrating there is an ideal air rate for each particle size distribution.

The traditional view states that ultrafine particles have a lesser flotation selectivity than coarse particles, nevertheless, some ores must be ground to ultrafine sizes to reach the required liberation degree [6]. According to Haselhuhn and Kawatra [7], the selective flocculation and dispersion desliming followed by reverse cationic flotation is the only proven method for the beneficiation of fine-grained (<25 μm) hematite ores. This process was developed by USBM as an alternative method to the desliming process by hydrocyclones, which generates a high loss of iron in the slime [8].

Weissenborn et al. [9] studied the selective flocculation process for a plant of BHP Iron Ore and concluded that careful control of the many process variables was required to achieve optimum recovery. The industrial selective flocculation process was introduced at Tilden Mine prior to the flotation circuit, where the passing size of 80% of the grinding product (p80) is approximately 25 μm [7].

The flotation of itabirite iron ore slimes, without prior classification, is not yet adopted in any industrial iron ore plant due to some problems related to the characteristics of the slimes and to equipment limitations. In recent years, research aimed at concentrating ultrafine particles by flotation has received greater importance. Improvements in equipment, such as the use of

microbubbles in column flotation and the studies of new, more selective reagents, aim to contribute to the development of processes for iron ore slimes concentration by flotation.

1.2. Equipment Improvements for Ultrafine Flotation — Microbubbles

Trahar [10] investigated the relationship between particle size and flotation efficiency. In summary, the author stated that the collision efficiency is a function of particle size, and the adhesion efficiency depends on the mineral hydrophobicity degree and particle size. The collision and the adhesion efficiency increase with the hydrophobicity degree and decreases with particle size. The flotation of ultrafine particles may be improved by increasing the collision rate; thus, the flotation rate may be increased by enhanced aggregation, using smaller bubbles, increased residence time in the machine and providing countercurrent flows of particles and bubbles [11]. Flotation of very fine and large particles is facilitated with small bubbles [12].

Farrokhpay et al. [13] studied how microbubbles interact with fine quartz particles and facilitate the flotation of these particles in a conventional flotation system and as stated by the authors, the higher quartz flotation rate obtained in the presence of microbubbles can be attributed to a higher attachment efficiency of conventional bubbles with particles coated with microbubbles.

In the studies carried out by Oliveira et al. [14], the cavitation tube produced bubbles in a bimodal distribution, with a wide size range at the nano and micro scales, providing air holdup values as high as 16%, a bubble surface area flux S_b of 85 s^{-1} and a very high concentration of nanobubbles (Sauter mean diameter = 230–280 nm) of $6.4 \times 10^8 \text{ NBS} \cdot \text{mL}^{-1}$. According to Fan et al. [15], the application of the cavitation tube system for upgrading of fine and ultrafine phosphate ore in Brazil proved successful and makes it possible to extend the size range of particles that could be treated by flotation to 5–10 μm (originally, cut-size of the desliming stage at this plant was 25–30 μm).

1.3. Developments of Collectors Regarding the Brazilian Iron Ores Slimes

Characteristics

Regarding Brazilian iron ore processing plants, the typical flotation feed consists of particles in the size range between 10 μm and 300 μm and the desliming process is carried out by hydrocyclones [16]; thus, the Fe content in the Brazilian slimes is high in comparison to the slimes produced by the selective flocculation process.

Slimes samples were collected at 21 points in the tailings dam of Fundão, at the Samarco Mining, in the Iron Quadrangle, Brazil by Lima and Abreu [17], and they found that the main minerals detected were goethite, hematite, quartz, and kaolinite. Pure kaolinite is constituted by 39.5% of Al_2O_3 and 46.55% of SiO_2 and the reverse cationic flotation route is less selective for the separation between alumina/hematite than for quartz/hematite [18]. The particles size distribution of clay minerals, such as kaolinite, is also another issue regarding the flotation process; fine particles typically show slow recovery rates, owing to decreased particle–bubble collisions, and are prone to entrainment [19].

According to Ma and Bruckard [20], starch–kaolinite interactions are critically important for the successful removal of kaolinite from iron ore in selective flocculation and froth flotation processes. Ma et al. reported that the selective depression of hematite against kaolinite largely depends on strict pH control in iron ore flotation circuits and the level of ionic strength in pulp [18,20].

Nykänen et al. [21] studied the loss of iron-bearing minerals to the froth in two industrial mechanical flotation circuits (Conceição Itabiritos II and Pico). There are two mechanisms for this iron mineral loss, especially in the finer fractions ($-44 \mu\text{m}$): hydrodynamic dragging and true flotation and, according to the authors, at Conceição Itabiritos II, concerning the particles size below $44 \mu\text{m}$, 65.4% of the iron in this fraction was carried to the froth due to due inefficiency in the depression process. Thus, the adoption of a selective collector, without the need for the use of a depressant reagent, will contribute to the improvement of the metallurgical recovery of ultrafine particle flotation.

According to the studies performed by Filippov et al., Fe-Mg-Al-bearing silicates may form strong chemical complexes with starch molecules used as iron oxide depressants due to the presence of metal ions on the mineral surface [22–25]. Thus, the use of starch as a depressant in the reverse flotation containing deleterious minerals, as in some iron ore slimes, can reduce the selectivity of the process.

Recently, differently structured amines (modified amines or polyamines, amidoamines alone or mixed with etheramines, alkyl phosphonium) has drawn great attention in the field of reverse iron ore flotation [26]. Concerning Brazilian iron ore, recent studies [27] demonstrated the possibility of adopting a specific amidoamine type collector as a new collector reagent for reverse iron ore slimes flotation. The main advantage of this reagent is its high selectivity, eliminating the use of starch or other types of depressants. The authors carried out slime flotation studies with single particular sample from the Iron Quadrangle region using the amidoamine Flotisor 5530 as a collector in the absence of a depressant. It was possible to

obtain, using one rougher flotation stage, a product with iron content above 60% and Fe recovery above 90% for one sample tested.

The main active molecule of the Flotisor 5530 collector is amidoamine N-[3-(Dimethylamino)propyl]dodecanamide. Silva et al. [28] performed fundamental study with this amidoamine molecule and demonstrated its high selectivity by contact angle measurements and bench scale flotation tests. The increased volume of the amidoamine polar head group compared to the conventional cationic collectors like etheramine makes this molecule more susceptible to steric hindrance effects and defines the selective adsorption on the silicate minerals confirmed by the Fourier-transform infrared spectroscopy (FTIR) [28]. This difference in adsorption behavior is responsible for the selective and total flotation of the quartz.

On the other hand, the flotation behavior of kaolinite is similar to that of hematite, while the FTIR analysis showed a spectral profile similar to the quartz spectrum. In this case, the high specific surface area of kaolinite, coupled to its double-sheet structure may be an explanation for this behavior [19,20]. According to Silva et al., the most adequate hypothesis for the mechanism responsible for this selective flotation is a hindrance effect due to intermolecular interactions, such as molecular arrangements or interactions promoted by hydrogen bonds and/or electrostatic forces [28].

The main difference between the studies carried out by Matiolo and this present work is that they used only one slimes sample to carry out a series of flotation tests on small diameter pilot columns (2 and 6 inches). Therefore, the effect of the variability of slime characteristics due to the industrial process was not considered.

1.4. Objectives of this Paper

This paper presents the results of the continuous pilot campaign of reverse cationic flotation of the iron ore slimes (rougher stage) combining column flotation and a new collector reagent avoiding the use of a depressant, showing the fluctuation of some slimes characteristics (such as iron content and percentage of solids) in an industrial plant and discussing the effect of some operational parameters on the iron ore slime flotation performances.

The operation parameters of the column (air rate, carrying capacity, wash water rate) and the reagent dosage were evaluated based on the collected data on the Fe, SiO₂, Al₂O₃ contents in the concentrate. The need to implement automatic control systems for parameters such as collector dosage, washing water and air flow is discussed regarding an eventual industrial application of column flotation as rougher stage in a slime concentration process.

2. Materials and Methods

2.1. Industrial Plant

The pilot tests were carried out at Vargem Grande 2 iron ore processing plant, located in the Iron Quadrangle (IQ) in Minas Gerais, Brazil. The plant was designed to concentrate 22.36 million tons per year of ROM (run of mine) with the objective of producing concentrates with silica content ranging from 1.5% to 2.5%.

The industrial process route (Figure 1) basically consists of four crushing stages to reduce the run of mine (ROM) until d_{95} at 16 mm; the crushed ore is sent to a homogenization pile, where is reclaimed to feed four ball mills (4000 kw per mill) working in a closed circuit with 26 inches hydrocyclones. The product of the grinding stage (d_{95} at 0.15 mm) feeds the desliming circuit that consists of two stages (20 inch and 10 inch hydrocyclones). The underflow of the desliming circuit feeds the conditioner, where the starch is dosed. After the conditioning stage, the pulp feeds the conventional tank cell flotation circuit, where the amine is dosed as collector at pH 9.8–10.2. The concentrate feeds a thickener (diameter of 40 m) and its underflow is filtered by disc filters. The froth containing the non-valuable minerals is disposed to the tailings dam.

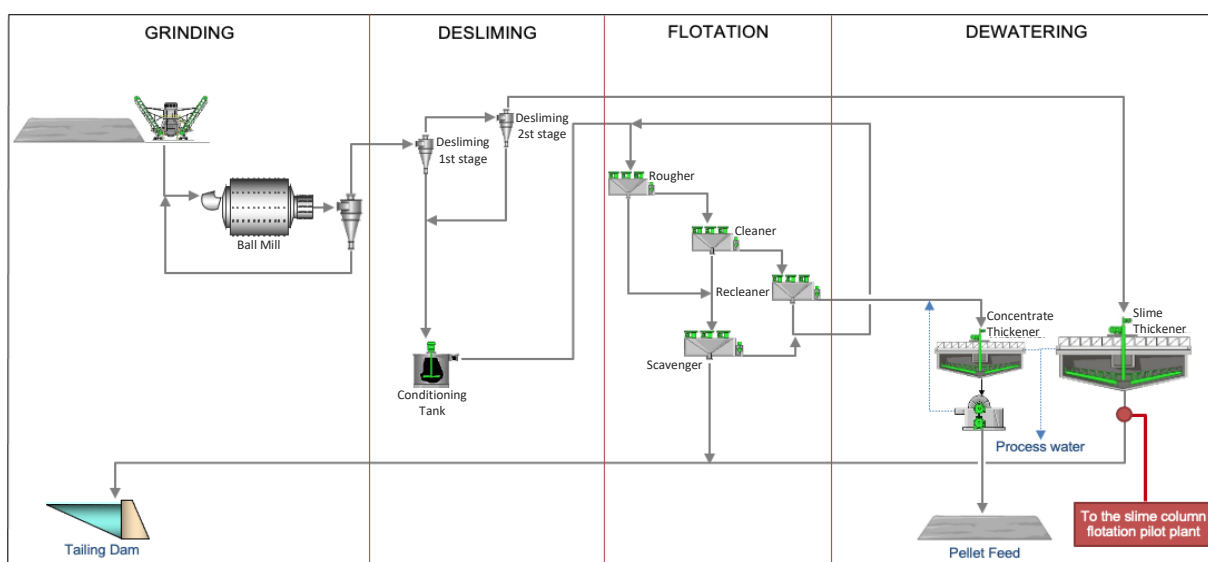


Figure 1. Simplified flowsheet of Vargem Grande 2 industrial plant.

The slime (overflow of second desliming stage—10inch hydrocyclones) feeds the slime thickener (diameter 100 m). The underflow of the slime thickener is sent to the tailings dam.

2.2. Pilot Plant

The pilot plant was constructed close to the slimes thickener and part of the stream from the thickener underflow was diverted towards this plant.

The tests were performed using a pilot flotation column of 500 mm diameter and 4000 mm height with a cavitation tube system for bubbles generation. The device consists of a centrifugal recycle pump with a sparger designed to induce cavitation and generate fine bubbles. A portion of the slurry underflow is drawn from the column and pumped to a cavitation tube sparger where the air is injected under pressure. The pilot plant flowsheet is shown in Figure 2.

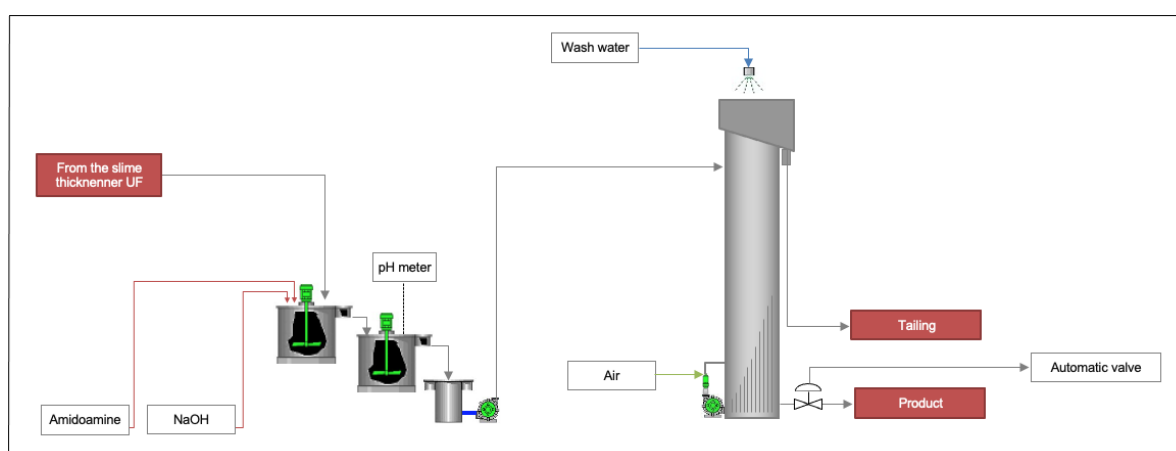


Figure 2. Pilot plant flowsheet.

2.3. Reagents

Information regarding the reagents is summarized in Table 1.

Table 1. Summary of all the reagents used in the experimental work.

Name	Type of Reagent/Role	Obs.:
Flotisor 5530	Collector	Amidoamine
Sodium hydroxide	pH Modifier	-

The amidoamine type collector Flotisor 5530 (Clariant, Belo Horizonte, Brazil), whose main active molecule is N-[3-(Dimethylamino)propyl]dodecanamide, was not adopted yet in the industrial iron ore flotation process and previous studies demonstrated that its application for the slimes flotation similar to the slimes from Vargem Grande 2 does not require a depressant [27].

2.4. Characterization

The chemical analyses were carried out by X-ray fluorescence at Vale's chemical analytical laboratories.

Wet sieving was used to minimize the loss of fine particles in dust form and to reduce minerals agglomeration in the slimes sample. A total of six size classes were chosen: >106, 106–80, 80–40, 20–10 and >10 μm .

The mineral phases were identified by X-ray diffraction using a Bruker AXS diffractometer.

2.5. Operational Parameters of Flotation Column

The superficial velocity (expressed in $\text{cm}\cdot\text{s}^{-1}$) is the ratio of the volumetric flow rate to the column cross-section.

Superficial feed velocity, for example, determines the column flotation results. It defines the value of the following parameters:

- Slurry residence time
- Liquid velocity
- Bubble rise velocity

In this paper, the superficial velocity of solids (J_S), water (J_L), slurry (J_{SL}) to the product, tailings and feed and the superficial velocity of washing water (J_W) was calculated. As the studies refer to the reverse flotation of iron ore, the tailing is the froth (floated) product.

Due to the countercurrent nature of the flows, air bubbles (or particle/bubble aggregates) should exceed a certain velocity to reach the froth otherwise they will report to tailings. This limits the utilization of fine bubbles.

The gas phase is also characterized by the superficial gas (air) velocity (J_g).

The effect of the air flow rate on flotation performance at a constant feed flow has a complex nature. Increased superficial air velocity causes a raise in the gas holdup and in the average bubble size due to the bubble coalescence. The bubble surface area defines bubble carrying capacity while increased bubble diameter reduces the collision probability.

An American Platinum Bubble Sizer (APBS) was adopted to measure the size of the bubbles (Sauter diameter— $d_{3,2}$) and the superficial gas velocity (J_g).

3. Results

3.1. Sample Characterization

Table 2 shows the chemical analysis of a typical slimes sample from the industrial plant.

Table 2. Chemical analysis of the slimes sample.

ID	Fe	SiO ₂	Al ₂ O ₃	P	LOI
Slimes Flotation Feed	44.31	31.09	2.85	0.079	2.15

The particles size analysis of this typical slime sample is presented in Figure 3. The results show that 83% of the total mass consists of particles below 20 μm , 3% above 106 μm , and 14% between 20 and 106 μm .

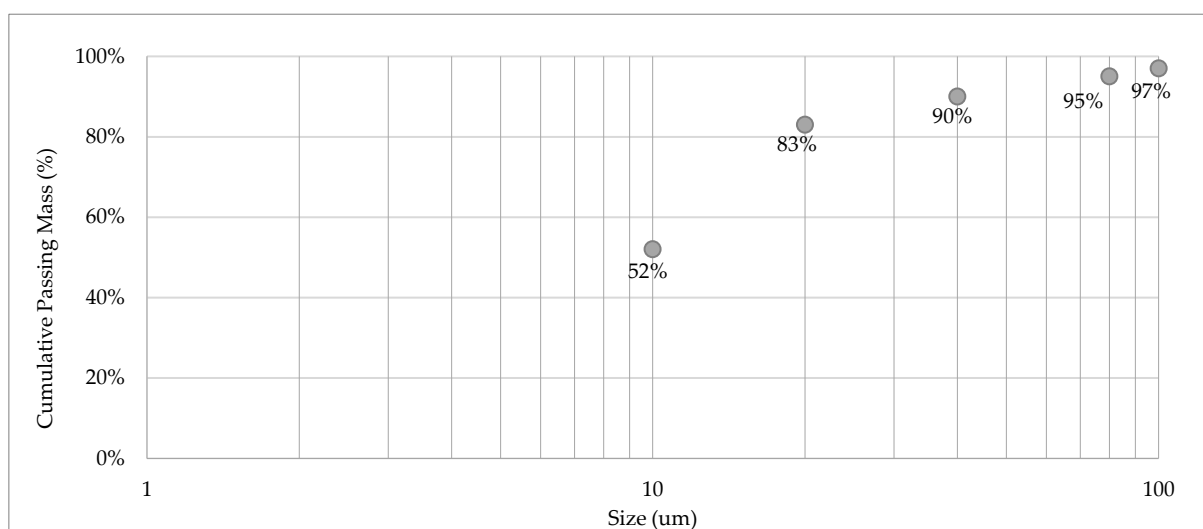


Figure 3. Particle size distribution of the slime sample.

Ma et al. [29] stated that the reverse cationic flotation tends to display unsatisfactory results for such fine-grain particles.

Figure 4 presents the element distribution by size fraction of this typical slimes sample. The majority of the iron (87%) is present in the fine particle size fractions (<20 μm). The presence of Fe in the fine fraction is problematic when aiming to achieve an efficient separation by reverse cationic flotation since fine hematite particles are susceptible to report to the froth product (tailings).

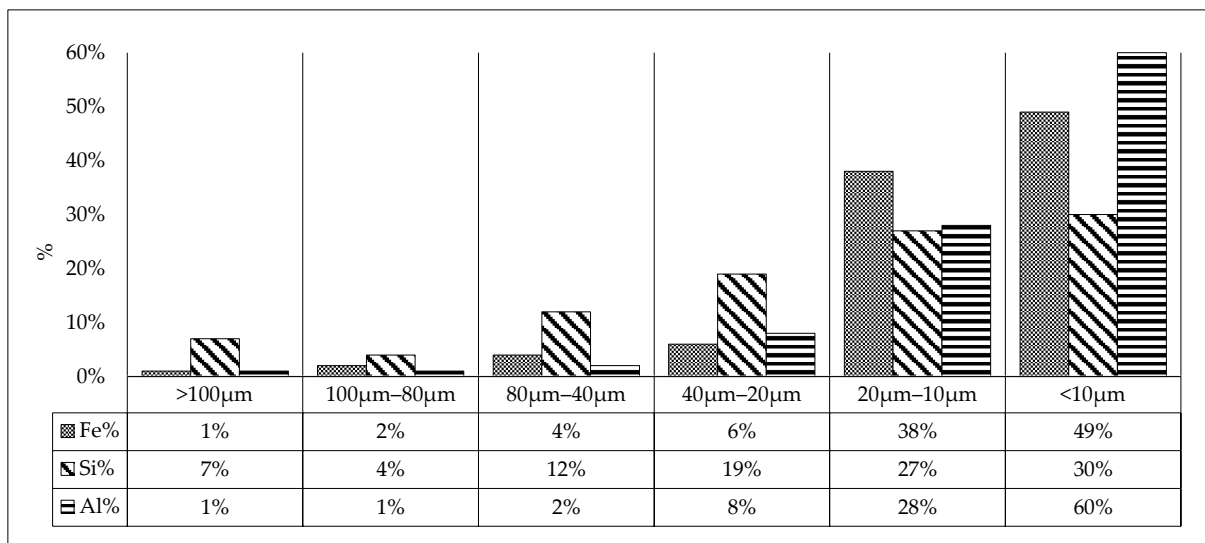


Figure 4. Fe, Si and Al in feed according to size fractions.

An important issue regarding this element distribution by size fraction is that in literature, it is often found that desliming is performed at 10 µm to obtain a good separation efficiency in the flotation process [30]. However, as previously stated, if the current sample is deslimed at 10 µm, approximately 49% of the total iron content will be lost.

XRD analysis was performed on the six size classes. A summary of the identified minerals and the corresponding size classes is displayed in Table 3.

Table 3. Summary of the identified minerals present in the slimes sample via XRD by different size classes

Size Class (µm)	Minerals Identified
>106	Hematite, Goethite, Quartz, Kaolinite, Muscovite
106-80	Hematite, Quartz, Kaolinite
80-40	Hematite, Goethite, Quartz, Kaolinite, Muscovite
40-20	Hematite, Goethite, Quartz, Kaolinite, Muscovite, Chlorite
10-20	Hematite, Goethite, Quartz, Kaolinite, Muscovite, Chlorite
10-0	Hematite, Goethite, Quartz, Kaolinite, Muscovite

Figure 5 shows the typical mineralogical composition of a slimes sample from the industrial plant.

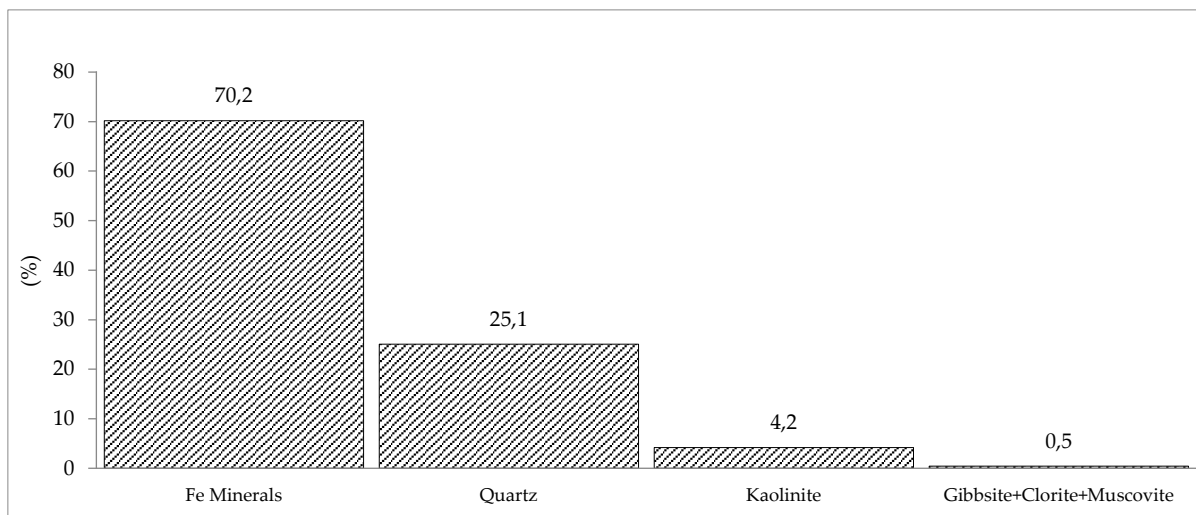


Figure 5. Typical mineralogical composition of a slimes sample from the industrial plant studied.

Both quartz (SiO_2) and kaolinite ($\text{Al}_4(\text{Si}_4\text{O}_{10})(\text{OH})_8$) are common gangue minerals associated with iron oxide slimes, while hematite and goethite are the main iron minerals. Depending on the goethite type, its presence could be problematic regarding the silica content in the concentrate. Goethite has three common forms, including brown, yellow ochreous and dark brown. The yellow ochreous is reported to contain considerable amounts of Al_2O_3 and SiO_2 (2–9%). It is still under debate if these impurities occur as inclusions in the goethite mineral or if it occurs by elemental substitution of Al in Si into the crystal lattice [31]. The presence of these impurities can cause selectivity problems in the reverse cationic flotation since the amines can adsorb onto the goethite. Moreover, the flotation does not provide successful removal of these impurities [32].

Figure 6 shows a selected SEM image for the slimes sample (Magnification: 500 \times) and the elemental mapping performed. Based on the EDS analysis, it is possible to state that in Figure 6a the white color particles represent hematite minerals, while the grey particles represent quartz. In the high-resolution elemental map (Figure 6b), Fe is represented by the red color, and Si is represented with the green color.

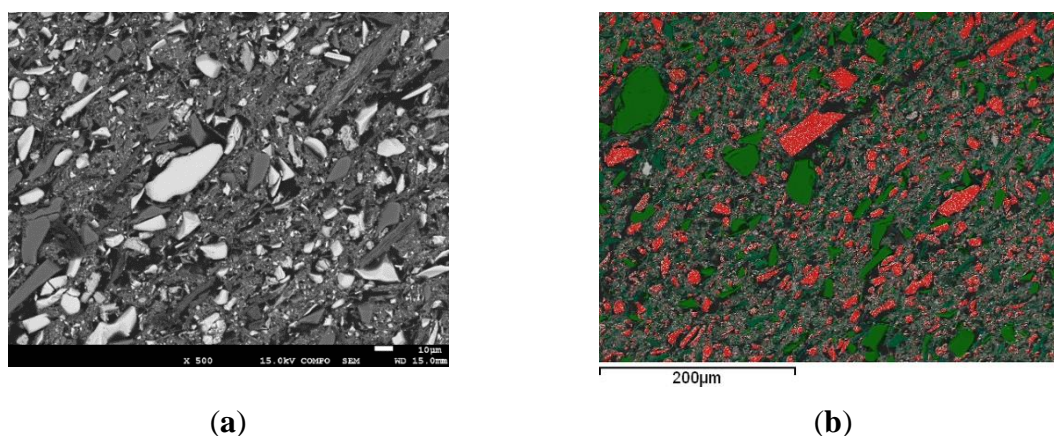


Figure 6. (a) Selected SEM image (500× magnification), (b) X ray elemental mapping image (500× magnification).

It is also notable the considerable presence of a very fine grain of hematite (iron oxides) in the smaller size fractions (<10 µm). This observation reinforces the statements made previously that desliming the sample at 10 µm would result in a significant loss of iron.

3.2. Pilot Flotation General Conditions

Amidoamine Flotisor 5530 was used as a collector at a dosage of 152–160 g/t in the absence of depressant. The flotation was performed in a 500-mm column at pH 10.5.

The flotation conditions in the pilot tests presented in this work were set to mimic the parameters (pH and collector dosage) reported by Matiolo [27], where the iron ore slimes flotation was performed in a 2” and 6” column. The measurements (Table 4) were performed to assess the hydrodynamic conditions of the flotation column during pilot tests at the Vargem Grande 2 site.

Table 4. Values obtained by the measurements carried out in the pilot column during the tests.

ID	Measured Value
Superficial gas velocity (J_g)	1.94 cm·s ⁻¹
Sauter diameter ($d_{3,2}$)	0.92m

3.3. Variability of the Slimes in the Industrial Plant

According to Trahar and Warren [33], the overall flotation performance deteriorates for the finer particles, but the precise effects of particle size on recovery, grade, and flotation rate are supposed to be more complex. Regarding the pilot tests in line with the industrial plant, several

factors can contribute to low SiO_2 recovery to the froth in some tests, such as collector dosage per SiO_2 content in the feed, washing water and industrial plant operation variations (i.e., grinding parameters, as p_{80}). Issues related to mineralogy and mineral particles liberation must also be considered.

Figures 7–10 show the variability of the % SiO_2 , %Fe, % Al_2O_3 and % solids in the flotation feed (underflow of the industrial thickener) during 67 pilot tests.

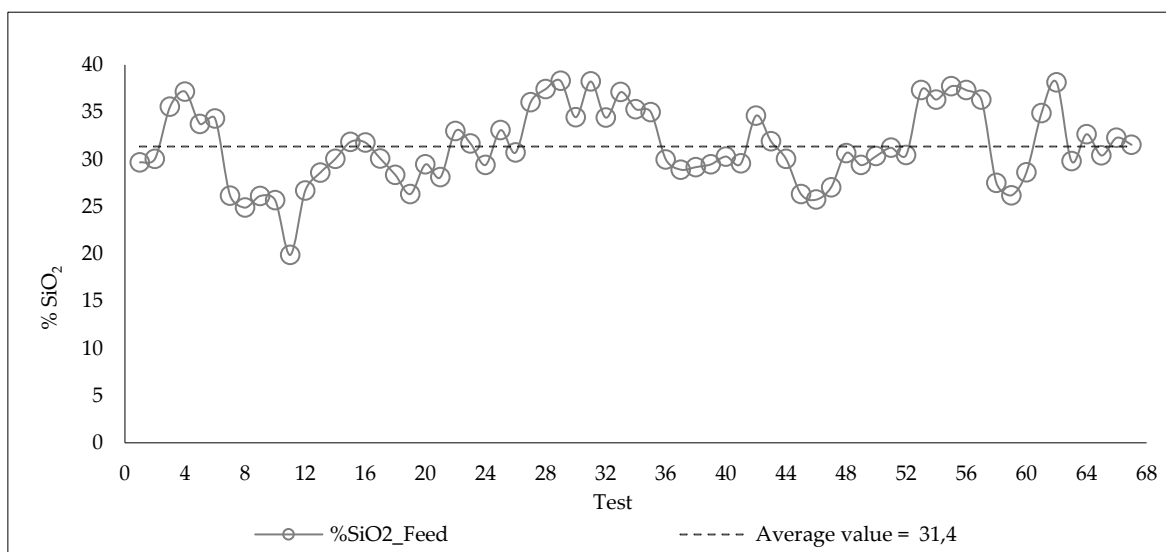


Figure 7. Variation of values concerning the SiO_2 content in the flotation feed during the pilot tests.

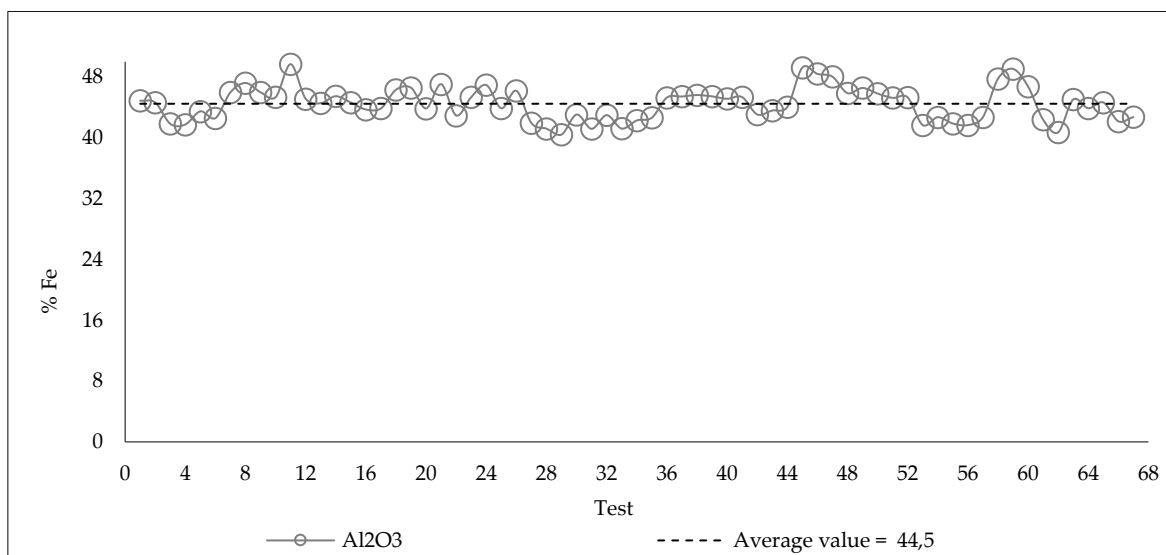


Figure 8. Variation of values concerning the Fe content in the flotation feed during the pilot tests.

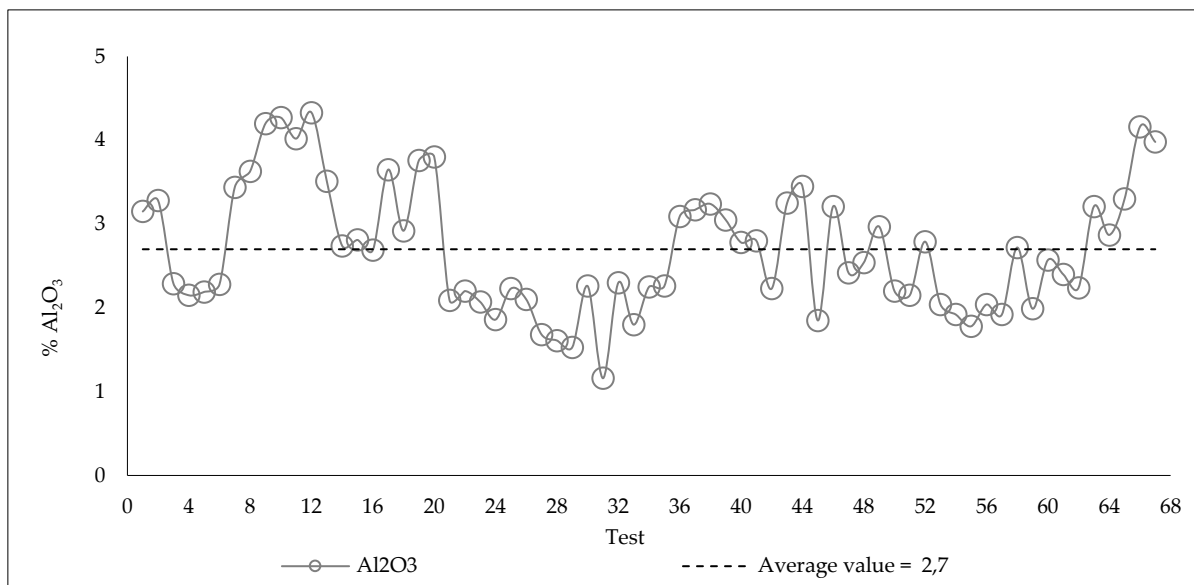


Figure 9. Variation of values concerning the Al₂O₃ content in the flotation feed during the pilot tests.

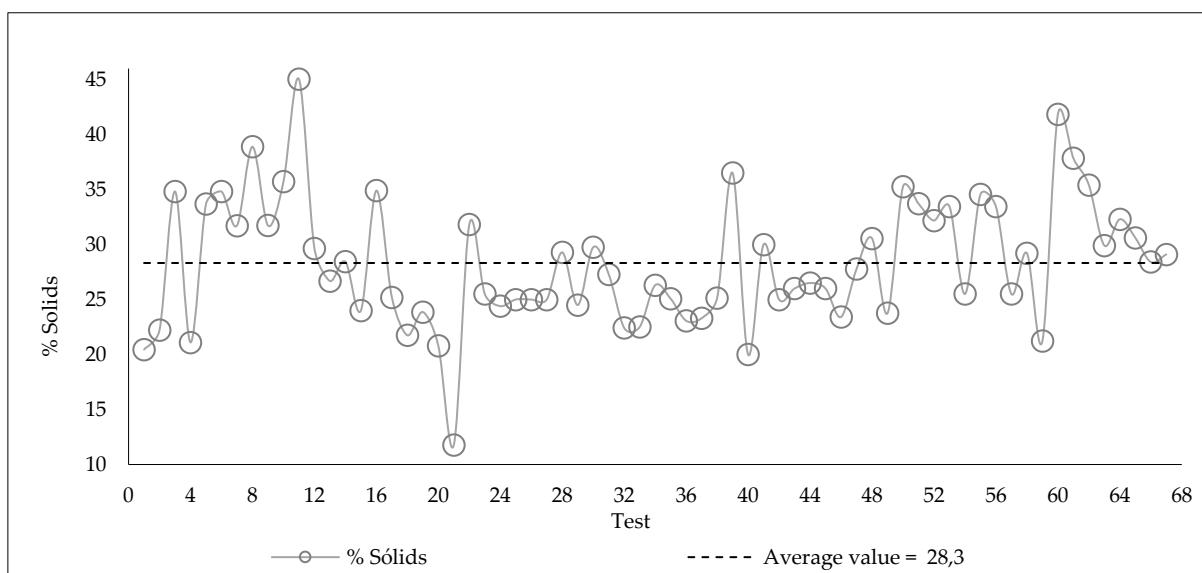


Figure 10. Variation of values concerning the percentage of solids in the flotation feed during the pilot tests.

The high variability in slimes characteristics can be explained by operational factors in the plant. The iron ore slimes are a reject fraction of the process, which is disposed of in the tailings dam. Therefore, regarding the slimes, the operational control of the plant aims to obtain the maximum percentage of solids in the slimes thickener underflow (provided that the quality of the overflow water is in accordance with the specifications of the industrial process water) and to reduce the amount of the slimes generated in the grinding and desliming process, since that the iron content in the final product and the metallurgical recovery of conventional flotation are maintained within acceptable values or even optimized.

Concerning the mining planning, in some cases, the mineralogical knowledge linked to the genesis of the ore may not be useful to predict the mineral processing responses in the industrial plant. For example, the mineralogy of the ore genesis identifies the presence of goethite, but it does not classify this mineral in terms of its chemical composition, such as aluminous goethite and siliceous goethite [34].

3.4. Initial Pilot Flotation Tests — Summary Results for a 6 Day Test Period

Considering the high variability of the slime characteristics, a six-day test period was selected in May 2018 to analyze the detailed results regarding the efficiency of the collector amidoamine in iron ore slimes flotation in the absence of a depressant. The objective of choosing a specific period was to reduce possible interferences in the pilot flotation results due to natural slime variations in the plant.

Results reported by Matiolo et al. [27] adopted a singular sample to carry out pilot slime flotation column tests using the amidoamine Flotisor 5530 as a collector without starch, where it was possible to achieve iron grades of approximately 62% in the concentrate and 8% in the tailings; however, there are no concentration plants by flotation for itabirite iron ore consisting of one single stage. As an example, Figure 1 shows that the industrial flowsheet for the flotation of the deslimed iron ore from the Vargem Grande 2 plant consists of four stages: rougher, cleaner, recleaner and scavenger.

Table 5. Results of the pilot tests from 9 to 16 May 2018.

Test ID	Mass (kg/h)	% Solids	Flowrate (l/h)	Water (l/h)	Grade (%)						
					Fe	SiO ₂	Al ₂ O ₃	P	Mn	LOI	
09/may	Feed	660	32.0	1582	1403	44.6	31.9	2.4	0.08	0.03	1.8
	Product	552	14.2	3490	3349	50.5	23.7	2.1	0.10	0.04	1.8
	Tailings	108	15.4	632	593	14.3	74.1	3.8	0.02	0.01	1.6
	Washing water (l/h)	2539		Recovery Fe Product		94.8	Recovery SiO ₂ Froth		37.9		
Test ID	Mass (kg/h)	% Solids	Flowrate (l/h)	Water (l/h)	Grade (%)						
					Fe	SiO ₂	Al ₂ O ₃	P	Mn	LOI	
10/may	Feed	640	31.2	1580	1412	47.5	28.9	1.7	0.06	0.01	1.4
	Product	467	13.3	3141	3034	58.5	12.6	1.8	0.08	0.02	1.7
	Tailings	174	26.8	535	475	17.7	72.4	1.5	0.01	0.01	0.7
	Washing water (l/h)	2097		Recovery Fe Product		89.9	Recovery SiO ₂ Froth		68.1		
Test ID	Mass (kg/h)	% Solids	Flowrate (l/h)	Water (l/h)	Grade (%)						
					Fe	SiO ₂	Al ₂ O ₃	P	Mn	LOI	
11/may	Feed	505	26.1	1565	1433	48.2	25.6	3.2	0.07	0.02	2.0
	Product	382	21.5	1485	1394	56.5	14.1	2.8	0.08	0.03	2.0
	Tailings	123	25.0	411	370	22.6	61.2	4.4	0.03	0.01	2.1
	Washing water (l/h)	331		Recovery Fe Product		88.6	Recovery SiO ₂ Froth		58.3		
Test ID	Mass (kg/h)	% Solids	Flowrate (l/h)	Water (l/h)	Grade (%)						
					Fe	SiO ₂	Al ₂ O ₃	P	Mn	LOI	
14/may	Feed	430	23.4	1519	1407	48.2	27.0	2.4	0.06	0.04	1.5
	Product	282	16.1	1528	1465	61.1	8.8	2.0	0.08	0.05	1.7
	Tailings	148	19.5	661	611	23.7	61.8	3.2	0.03	0.02	1.1
	Washing water (l/h)	669		Recovery Fe Product		83.1	Recovery SiO ₂ Froth		78.8		
Test ID	Mass (kg/h)	% Solids	Flowrate (l/h)	Water (l/h)	Grade (%)						
					Fe	SiO ₂	Al ₂ O ₃	P	Mn	LOI	
15/may	Feed	507	27.8	1449	1319	49.4	24.0	3.2	0.06	0.01	2.0
	Product	403	16.6	2125	2030	57.1	13.4	2.8	0.07	0.01	2.0
	Tailings	104	15.5	605	569	19.9	64.9	4.7	0.02	0.01	1.9
	Washing water (l/h)	1280		Recovery Fe Product		91.7	Recovery SiO ₂ Froth		55.5		
Test ID	Mass (kg/h)	% Solids	Flowrate (l/h)	Water (l/h)	Grade (%)						
					Fe	SiO ₂	Al ₂ O ₃	P	Mn	LOI	
16/may	Feed	600	30.6	1525	1364	45.6	30.5	2.5	0.05	0.01	1.6
	Product	384	14.1	2422	2336	61.0	8.1	2.5	0.07	0.01	1.9
	Tailings	216	23.8	766	691	18.2	70.2	2.6	0.01	0.01	1.1
	Washing water (l/h)	1663		Recovery Fe Product		85.7	Recovery SiO ₂ Froth		82.9		

Therefore, the results presented need to be evaluated at the first slime concentration stage where the product could feed a cleaner stage or even the conventional flotation circuit. Eventually, depending on the product obtained in the first stage, a cleaner stage can be bypassed, and the rougher product can be combined with the conventional pellet feed.

Table 5 shows the results concerning the period of 9–16 May 2018. The average parameters adopted during these tests were: collector dosage 160 g/ton, absence of starch, pH 10.5, froth height of 15 cm, and an average collector conditioning time of 10 min.

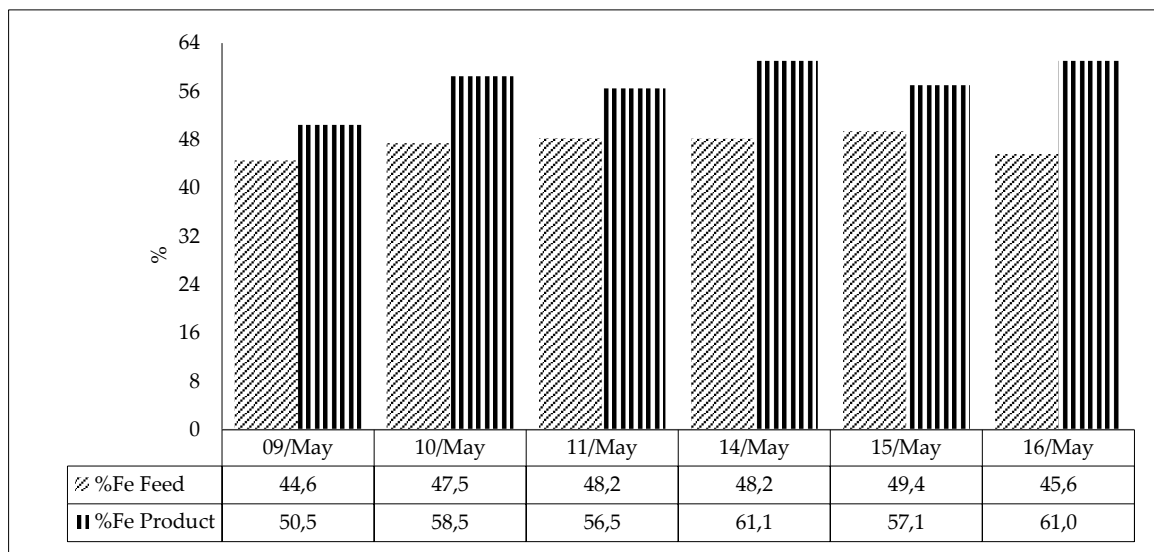


Figure 11. Fe content in feed and product.

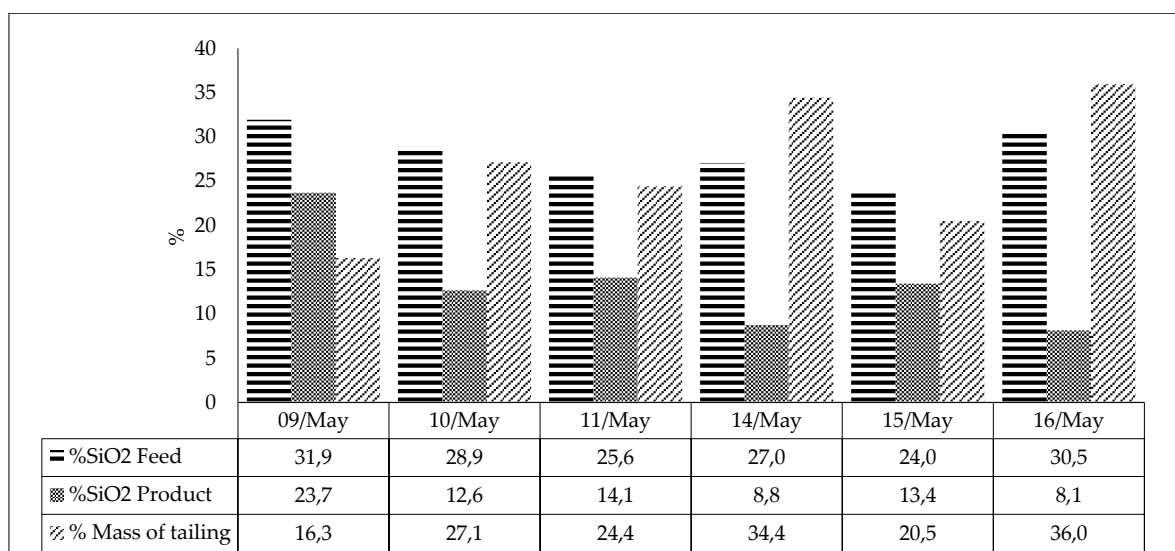


Figure 12. SiO₂ content in the flotation feed and product; percentage of mass in the tailings.

Figures 11 and 12 show that it was possible to recover in the froth percentages of mass varying from 16.3% to 36.0%, with an improvement in the iron content in the product varying from 5.9% (May 9) to 15.4% (May 16). The Figure 13 shows that, even the worst test result, carried out on May 9, recovered about 38% of all SiO₂ in the froth, losing only 5.2% of the iron. The recovery of SiO₂ reaches approximately 83%, with a loss of 14% of iron in the best of case (May 14). Therefore, considering the losses of iron in comparison with the floated SiO₂, the results show that this specific amidoamine collector could be adopted in slimes concentration since it provides a selective separation between ultrafine iron oxides and quartz (even in the absence of a depressant).

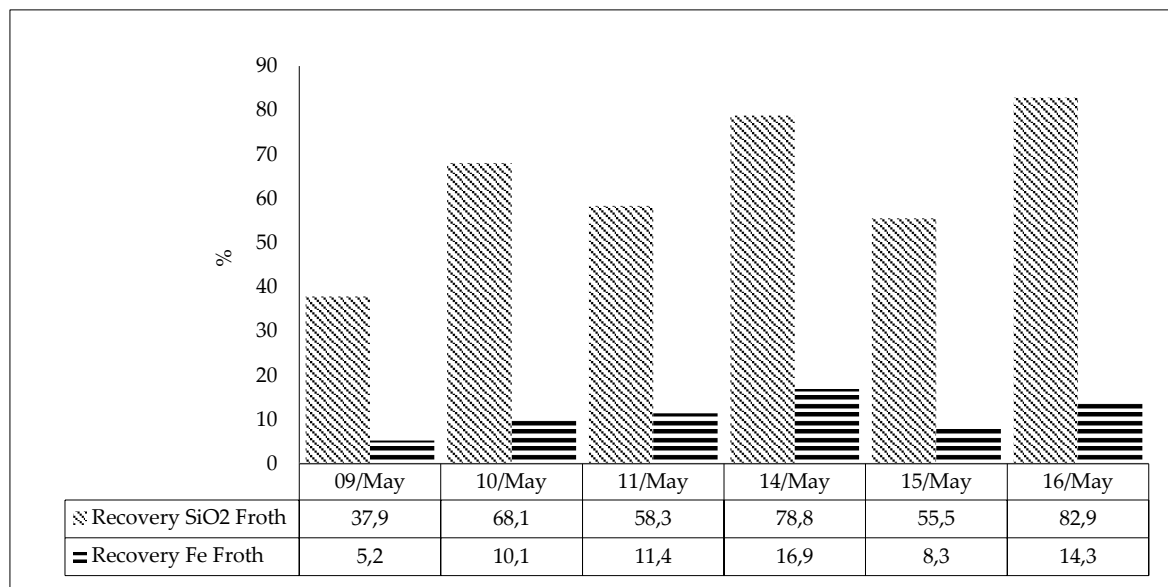


Figure 13. Recovery of SiO₂ and Fe to the tailings.

Some factors may have influenced the results regarding the variability of the SiO₂ recovery values to froth. Concerning quartz, a hypothesis for this recovery values range is that there may have been variations in its particle size at each test, influencing the specific surface areas of this mineral, requiring a higher specific dosage of the reagent for sufficient hydrophobization of its surface in some cases. The probability of a collision in the flotation process may be also impaired by particle size variation [35]. This probability captured the attention of several researchers, who showed that this parameter is directly related to physical variables, such as particle size and bubble diameter [30].

The minimum degree of hydrophobicity necessary for the flotation of a particle depends on its size [10]. The low recovery of fine particles is often attributed to their low mass and inertia, which leads to the low probability of particle colliding with bubbles, as demonstrated by some authors [36]. Another reason for the low floatability of fine particles is that they possess insufficient kinetic energy (due to low mass) to displace the thin water film between the colliding particle and bubble and form the three-phase line of contact [37]. Scheludko et al. [38] has proposed the existence of a critical contact angle necessary for the flotation of fine particles. According to Chipfunhu et al. [37], the poor floatability of fine particles is mainly because they have not reached their critical contact angle. Figure 5 demonstrated that the main alumina mineral in the slimes used in the pilot tests was kaolinite. The kaolinite structure has anisotropy, and this characteristic can explain its low recovery to froth in a flotation process. Souza et al. [39] showed that the application of amidoamine in kaolinite flotation in the beneficiation of manganese ore at acidic pH is feasible. However, according to Xu et al. [19],

in the cationic flotation, the pH dependence of kaolinite flotation is the opposite to that of oxides with a lower flotation recovery obtained at higher pH; therefore, the efficiency of kaolinite flotation using amidoamine is impaired at the pH adopted in the pilot tests (10.5). Kaolinite is a clay mineral; thus, the flotation of kaolinite is also impaired due to its small average size. Therefore, due to the issues regarding the kaolinite flotation, part of the SiO₂ content in the product of the pilot tests may be originated from the kaolinite. The kaolinite may also represent a higher consumption of collector due to its greater specific surface, decreasing the collector available to adsorb on the quartz surface.

3.5. Analysis of the Influence of Feed Variability and Operational Parameters on Flotation Results during the 67 Pilot Test Campaign

Results

Figure 14 shows the variability of the iron content values in the feed, product, and tailings during 67 pilot rougher flotation tests. The operational parameters adopted in these tests are, on average, the same adopted on the pilot tests shown in Table 5.

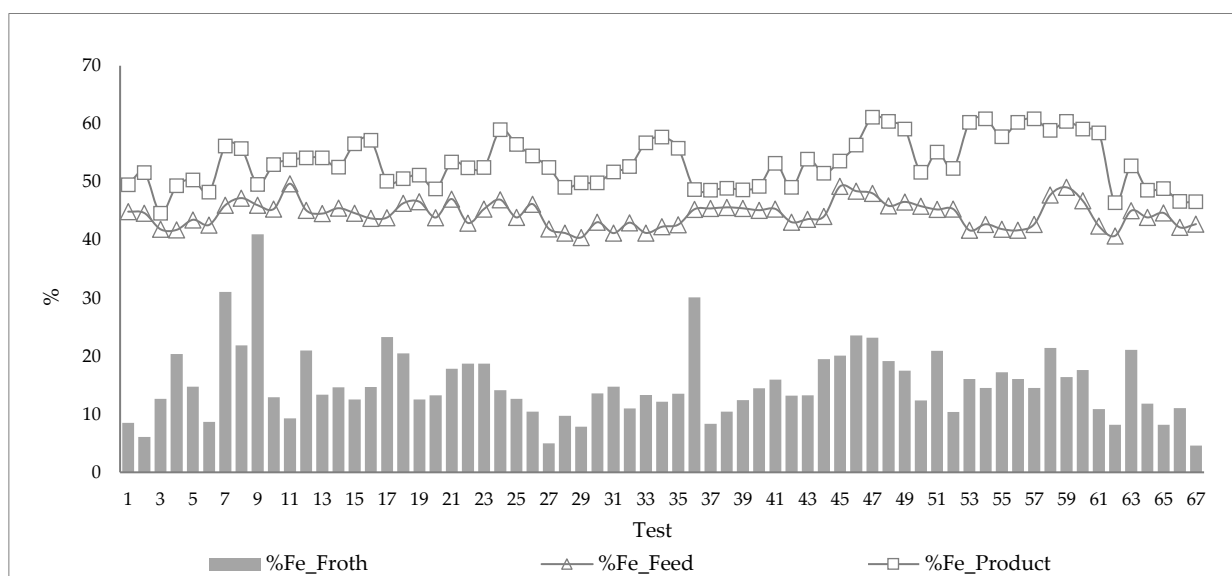


Figure 14. Results concerning the Fe content in the flotation feed, froth, and product during the pilot tests.

Figure 15 shows the results concerning the Fe and SiO₂ recoveries during the pilot tests.

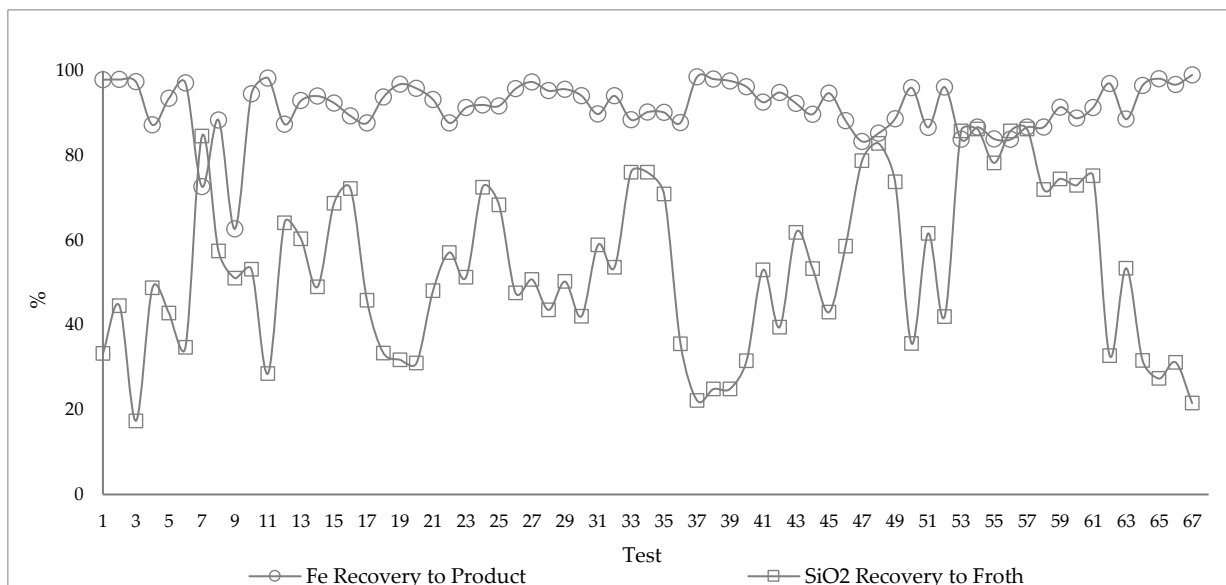


Figure 15. Results concerning the Fe and SiO₂ recoveries during the pilot tests.

The results presented in Table 6 shows that adopting only one slimes flotation stage (rougher), using the amidoamine Flotisor 5530 as a collector, in the absence of depressant, it was possible to float, on average, about 53.3% of SiO₂ present in the slimes, yielding Fe recovery above 86.1% in 90% of the tests carried out (10th percentile).

Table 6. Summary of results for 67 pilot tests.

ID	%Fe Feed	%Fe Product	%Fe Tailing	Mass Recovery	Fe Recovery Product	SiO ₂ Recovery Froth	
							Average Value
90th percentile	47.1	59.6	21.6	89.1	97.7	78.5	
Median	44.6	52.6	14.1	76.8	92.4	51.2	
10th percentile	41.7	48.6	8.4	62.8	86.1	30.0	
ID	J _L (cm·s ⁻¹)			J _{SL} (cm·s ⁻¹)			J _w (cm·s ⁻¹)
	Feed	Product	Tail	Feed	Product	Tail	
Average Value	0.18	0.25	0.07	0.20	0.26	0.08	0.14
90th percentile	0.20	0.29	0.13	0.22	0.31	0.14	0.19
Median	0.19	0.23	0.06	0.21	0.24	0.07	0.11
10th percentile	0.18	0.18	0.03	0.21	0.19	0.03	0.07

Due to the high variability of the slime characteristics during the pilot tests, the values obtained from these tests were grouped by ranges aiming at the analysis of trends related to parameters concerning the flotation tests (Table 7).

Table 7. Average values per range of variation of the collector, %Fe in the froth, J_L _product and carrying rate.

Range Collector (g/m ³ water_feed)/(%SiO ₂)	%SiO ₂ Product	%Water Froth	Range Fe Froth %	%Water Recovery_Froth	Jw/JSL Tail
from 0 to 0.75	0.6	25.1	75.7	12.4	2.6
from 0.75 to 1.85	1.5	19.2	77.8	18.3	2.4
from 1.85 to 2.95	2.2	19.0	81.7	25.0	1.7
from 2.95 to 4.05	3.3	14.0	82.6	28.8	1.4
from 4.05 to 5.15	4.2	14.1	87.5	34.9	1.2
from 5.15 to 6.25	5.7	11.2	87.0	66.3	0.9

Range Water Recovery_Product %	%Recovery Fe_Product	Range Carrying Rate (t/h·m ²)	%Fe Recovery Froth	%SiO ₂ Product
from 0 to 0,8	0,7	87,2	3,7	22,3
from 0,8 to 1,6	1,2	91,4	5,0	23,5
from 1,6 to 2,4	1,9	91,5	6,8	19,2
from 2,4 to 3,2	3,0	94,1	11,8	14,2
from 3,2 to 4	3,7	98,3	19,9	11,7
			13,7	11,2

Influence of Collector Dosage

The trend presented in Figure 16 shows that increasing the dosage of the collector results in a decrease in the silica content in the concentrate.

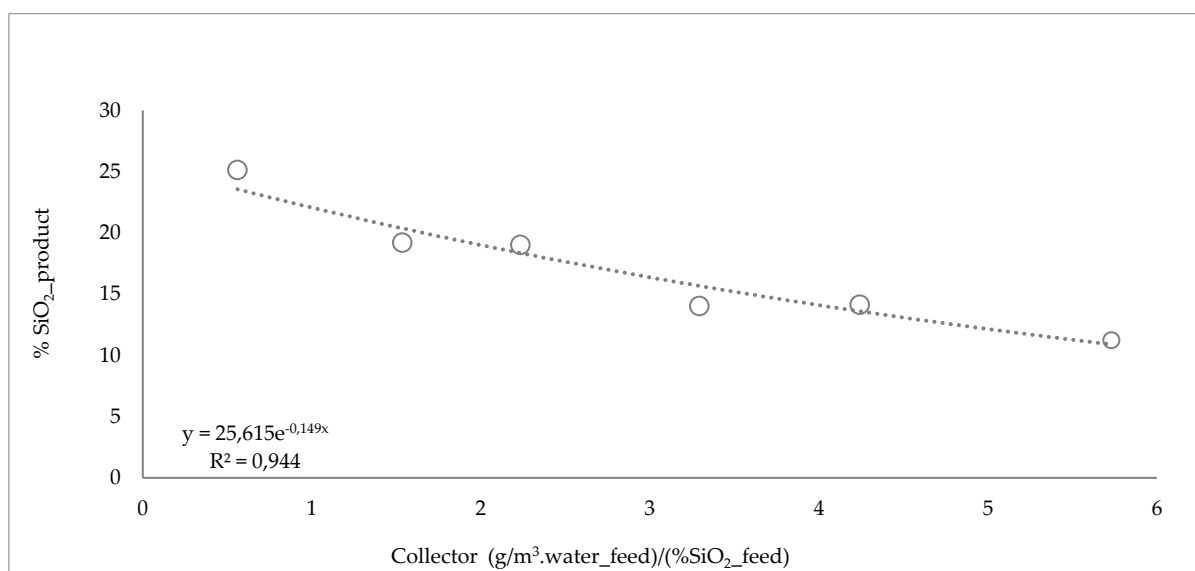


Figure 16. Trend between the amidoamine specific dosage and the SiO₂ content in the product concerning.

For a given gas holdup in the collection zone, different water-carrying capacities can be obtained by changing the frother type in the system [40]. The amidoamine is a surfactant, so this reagent performs two functions in the flotation process: collector and frother. Therefore,

by increasing the concentration of amidoamine, the bubbles will carry an increasing amount of water (Figure 17).

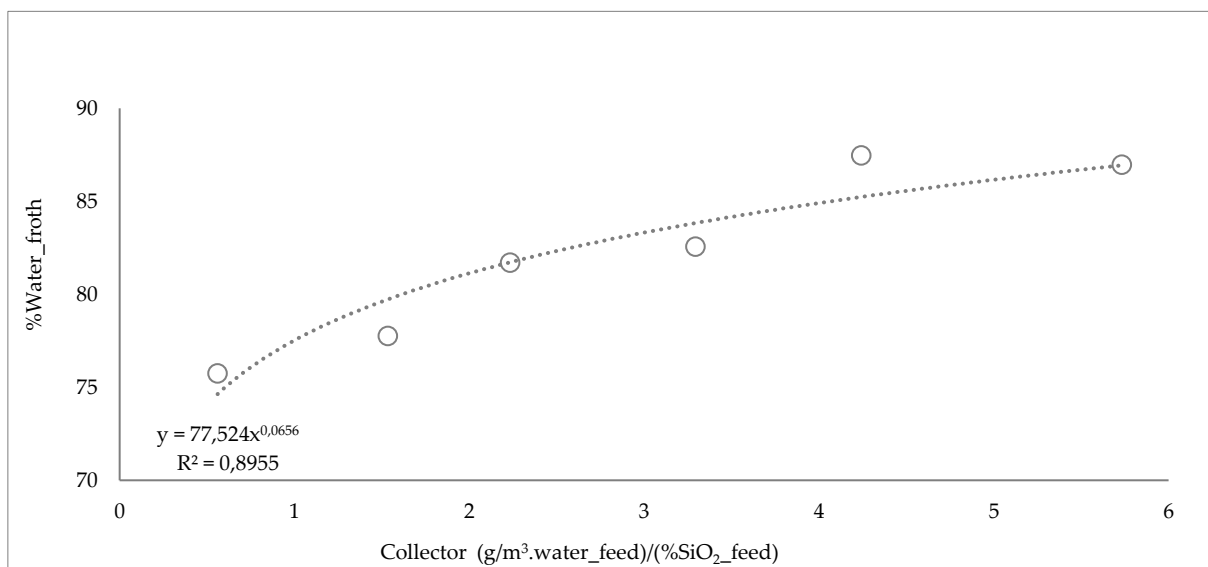


Figure 17. Trend between the amidoamine specific dosage and the %water in the froth content in the product.

The amount of water carried with bubbles affects many sub-processes taking place in the froth, which determine the froth product quality [41]. The recovery of fine hydrophilic particles in flotation is related to the recovery of water. Water may be carried by bubbles into the froth [42] and the water recovery is closely related to the nonselective transport of solid particles in the froth by entrainment [43].

Influence of Water Recovery

As the amidoamine Flotisor 5530 shows selective behavior for reverse flotation of quartz in iron ore without depressant, the loss of iron in the froth can be mainly attributed to entrainment. Figure 18 shows the trend of increasing the iron content in the froth due to the increased water recovery.

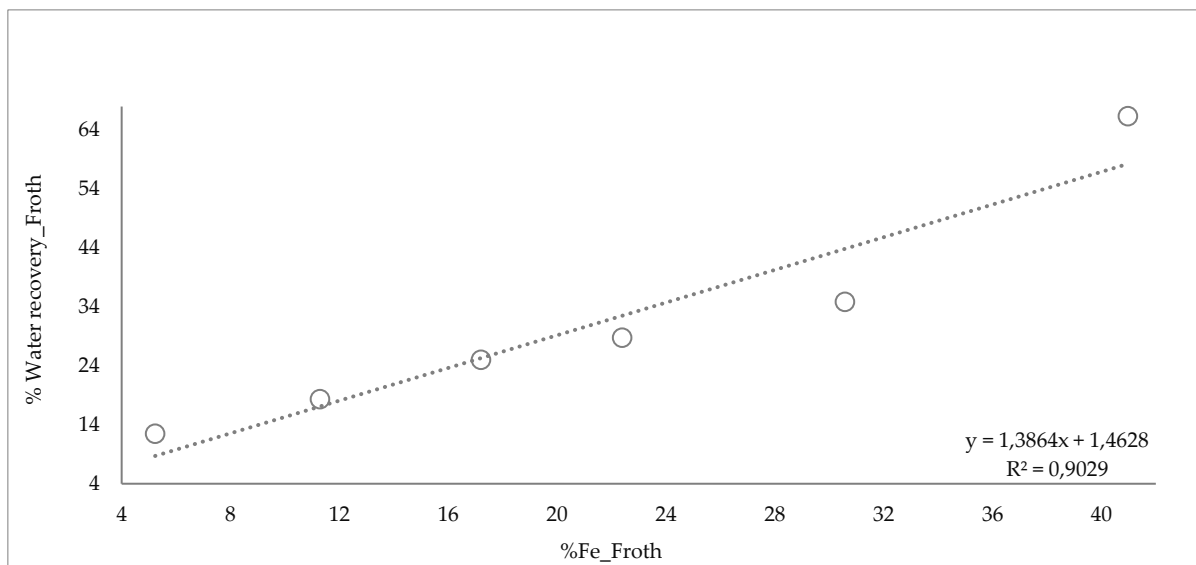


Figure 18. Trend between the Fe content in the froth and the water recovery in the froth.

Figure 19 shows that the improvement trend in iron recovery, due to the increase in water recovery, is observed for the non-floated product.

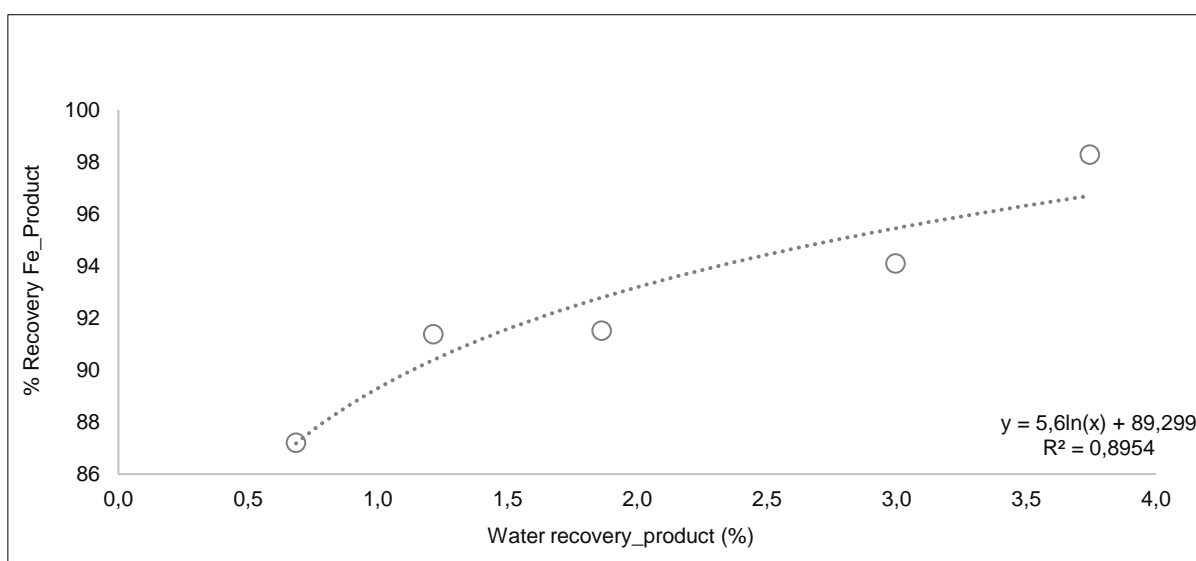


Figure 19. Trend between the water recovery to the product and the recovery of Fe to product.

Influence of Washing Water

According to Trahar [10], the entrainment effect can be reduced by decreasing the water flow to the froth, using a suitable choice of frothers and collectors or by reducing pulp densities. However, such methods rarely seem to provide an effective solution in industrial practices. Only column flotation combined with some form of refluxing and froth washing appears to reduce entrainment for the fine particle flotation [44].

Kursun [45] demonstrated that the effect of particle size on the entrainment factor is very significant. The washing water is used in flotation to increase the drainage rate of water within the froth phase, removing entrained (hydrophilic) particles [46]. According to Soto [47], washing water flow helps to stabilize the thick froth layer, reducing the entrainment of fine gangue particles (Figure 20). This makes column flotation a very selective process to separate finely ground minerals.

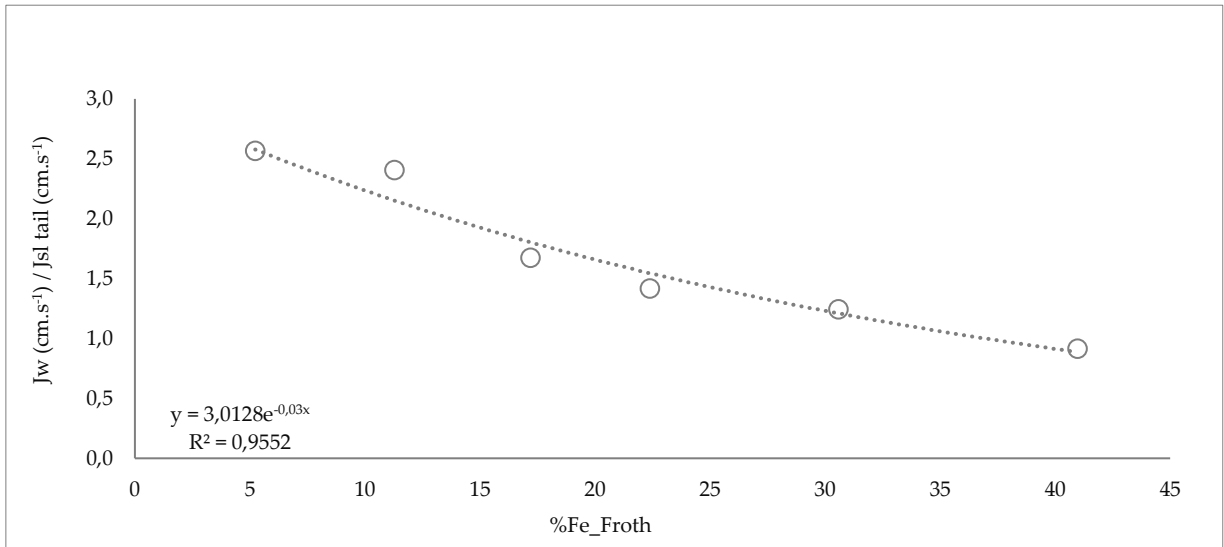


Figure 20. Trend between the Fe content and the J_w/J_{sl} tail.

Figure 21 shows the washing water system during the pilot tests.



Figure 21. Washing water system during the pilot tests.

Carrying Rates

To find the best column flotation circuit, the design objectives must be clear concerning the grades and recoveries and their allowed variance [48]. Maximum carrying capacity is a critical parameter in enrichment by column flotation [49]. According to Espinosa- Gomez et al. [50], the capacity of a flotation column can be limited by the rate of concentrate removal. Limiting carrying capacity was observed during pilot column flotation of very fine minerals at Mount Isa Mines (MIM), Australia [51].

Espinosa-Gomez et al. [50] showed that the maximum carrying capacity achieved from a flotation column is directly proportional to the product of the d_{80} particle size and the mean specific gravity of the concentrate. The carrying capacity parameter for iron ore slimes column flotation tends to be lower than the values for conventional iron ore flotation and may vary considerably due to operational adjustments and/or variations in ROM that will imply changes in the granulometry. The trends presented by the carrying capacity values and the SiO_2 content in the concentrate and the carrying capacity and recovery of iron in the froth are shown in Figures 22 and 23. These trends indicate that it is difficult to have a low loss of iron in the froth and obtain high iron content (low SiO_2) in the concentrate by adopting only one concentration stage.

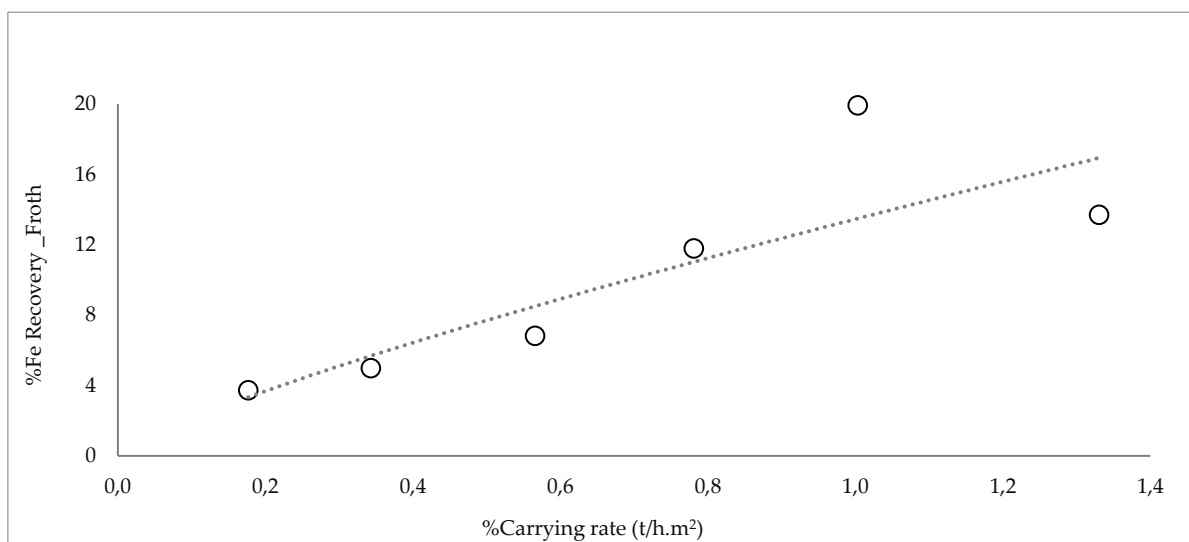


Figure 22. Trend between the carrying rate and Fe recovery to froth concerning the pilot tests results.

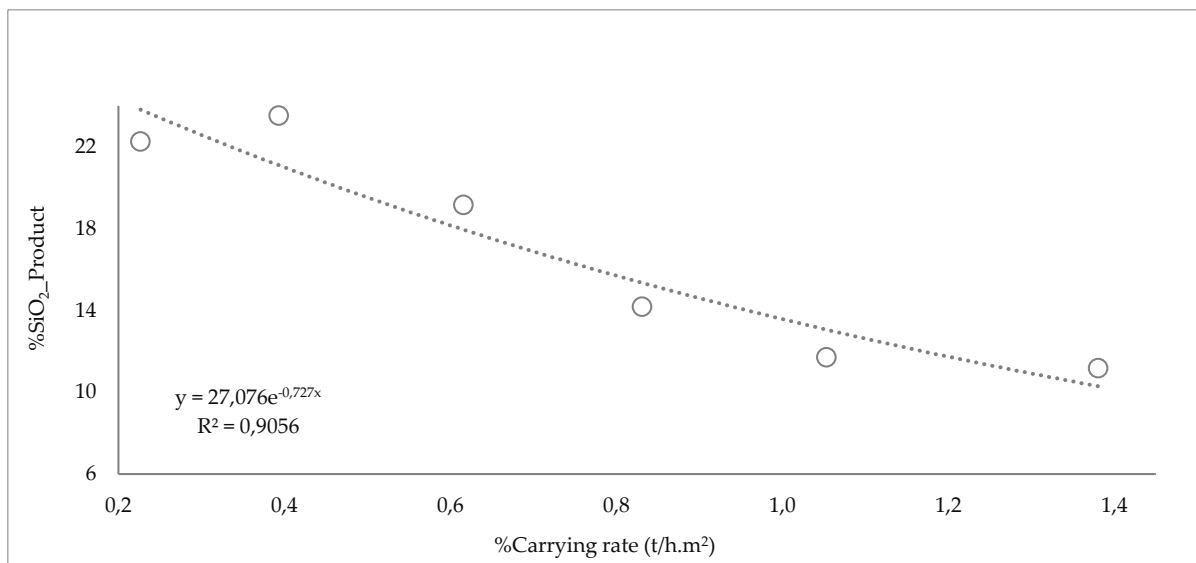


Figure 23. Trend between the carrying rate and SiO₂ content in the product concerning the pilot tests results.

3.6. General Discussions

Control System

According to Bergh and Yianatos [52], stable operation of flotation columns and consequent consistent metallurgical benefits can only be obtained if basic distributed control systems are implemented. Considering the high variation of the slime characteristics from the industrial plant (%Fe, %SiO₂, %Al₂O₃, %solids), the adoption of an industrial slimes flotation process as rougher stage needs to be supported by reagent dosing and wash water automatic control systems with online instrumentation to analyze the Fe and SiO₂ content.

The optimum superficial air velocity for each pilot test was not evaluated in this work. Mackay et al. [4] highlighted the importance of considering the connection between particle size, air rate and froth stability when determining flotation strategies. Thus, the implementation of automatic air flow control in the cavitation system can also contribute to improve the results obtained in a slime flotation industrial circuit since, in addition to the variability of the run of mine, some adjustments in the industrial plant may change the size distribution of the slimes flotation feed, requiring a new optimized air flow, since these changes in the particle size distribution require a change in the air rate to maximize mineral recovery [5].

Product Quality and the Challenge of Slimes Concentration in Brazil

Several factors may have influenced the results of the flotation process, such as mineralogical characteristics that may be related to gangue minerals or even to iron oxides. Figure 24 shows the tendency to reduce the iron content in the flotation product due to the increase in LOI (loss of ignition) in this same product.

The presence of goethite, gibbsite, and kaolinite leads to high LOI (loss on ignition) and high Blaine number (a technical parameter which quantifies the proportion of the clayey minerals, i.e., kaolinite) in the iron ore concentrate after beneficiation [53]. The iron oxides in the itabirite slimes of the Iron Quadrangle consist mainly of hematite and goethite. The more goethite is present in the slimes, in addition to the reduction of the Fe content due to the chemical composition of the goethite, the LOI associated with this iron oxide decreases the maximum possible iron content to be obtained in the concentrate. Considering the same mineralogical constitution, the higher the Blaine, the larger amount of reagent is needed to obtain the concentrates due to the increase in the mineral surfaces to absorb the collector. In relation to the flotation process, the increase in the dosage of the collector, in addition to the presence of more ultrafine particles and its mineralogical constitution, render it difficult to obtain products of high chemical quality without considerable reduction in mass recovery.

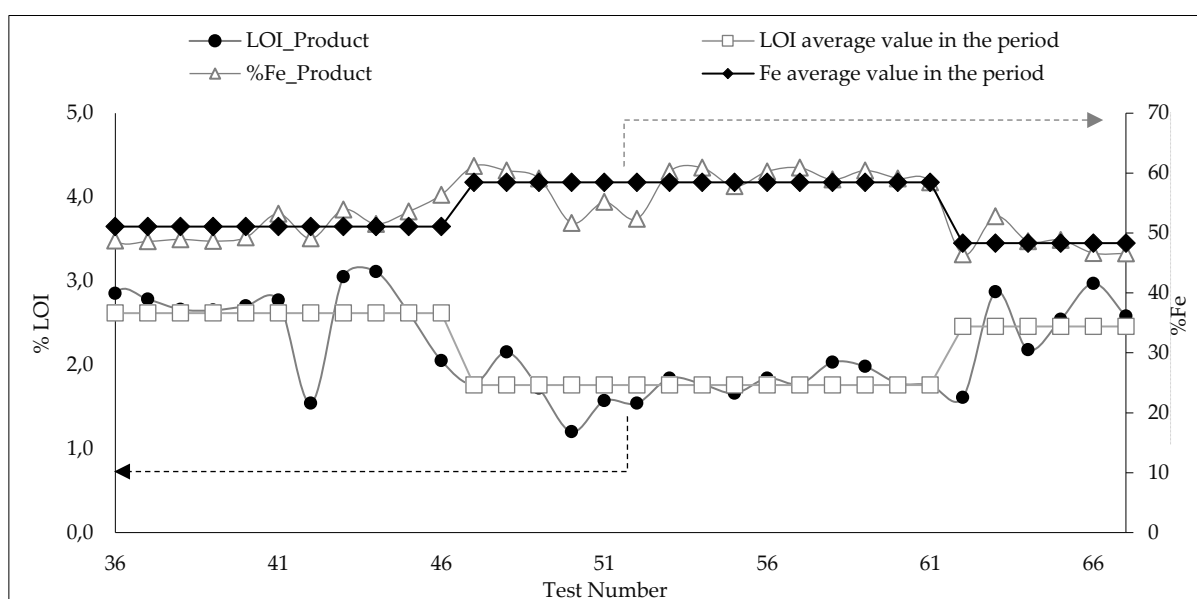


Figure 24. Trend regarding the reduction of the iron content in the product with the increase in the value of LOI for this concentrate.

Regarding another processes, such as the magnetic concentration, the relative importance of the particle size is a critical point in the process of magnetic concentration because, while the hydrodynamic drag force is proportional to the particle diameter, the magnetic and gravitational forces are proportional to the particle volume [54]. Thus, for ultrafine particle size, the magnetic concentration tends to generate high levels of iron in the tailings due to the increase in the hydrodynamic drag of these particles.

Studies have been carried out on the concentration and reuse of iron slimes in Brazil, considering not only unique processes, but also the combination of processes such as magnetic

concentration and flotation. The main objective of the Brazilian iron ore mining companies is to reduce the amount of slimes generated at their plants. The definition of the ore is based on economic criteria, therefore, the feasibility of a slime concentration process must be analyzed not only by the quality of the product generated, but, above all, by the avoided costs. Even generating lower quality products, the concentration of the slime decreases the volume of material sent to tailings dams, reducing environmental and safety risks.

4. Conclusion

The Flotiner 5530 amidoamine showed selective behavior as collector in reverse column flotation of quartz with no depressant from Vargem Grande 2 iron ore slimes. A concentrate with iron grade of up to 61% Fe and metallurgical recovery of 85.7% were achieved in one rougher stage only from the slimes containing 46.5% Fe. The fluctuation of the flotation performance of the continuous column flotation were related to the variability of the slimes characteristics in the industrial plant.

The loss of iron in the tailings was correlated with entrainment effect, thus the adjustment of the specific collector dosage and the relationship between the washing water and the froth volume are important factors to control the flotation performance. The implementation of automatic control systems regarding these parameters will improve the performance of an eventual slimes flotation industrial application.

The increased values of the carrying rate decreases the SiO₂ content in the iron concentrate to the detriment of the increased losses of iron in the froth product (tailings). Thus, there is no guarantee to reach high iron metallurgical recovery and low SiO₂ content in the concentrate, adopting only one column flotation stage during an industrial operation.

The iron content in the product varies according to the mineralogical characteristics of the slimes and, for high LOI values in the concentrate, there is a tendency to obtain low iron content in the nonfloated product.

Further studies regarding the adoption of a cleaner stage by flotation or magnetic concentration will contribute to the feasibility of implementing an iron ore slimes concentration circuit in the Vargem Grande 2 plant concentrator.

Acknowledgements

This paper was supported by VALE S.A in the context of developing beneficiation routes for iron ore slimes. The support of Clariant, Brazil is deeply appreciated. The support of Vale Institute of Technology is also acknowledged. L.F. and I.F. acknowledge the support provided by H2020 Fine Future project under grant agreement No. 821265.

References

1. Clemmer, J.B. Flotation of iron ore. In Proceedings of the 8th Annual Mining Symposium, 15 January 1947. The University of Minnesota: Duluth, MN, USA, 1947.
2. Filippov, L.; Severov, V.; Filippova, I. An overview of the beneficiation of iron ores via reverse cationic flotation. *Int. Natl. J. Miner. Process.* 2014, 127, 62–69.
3. Achaye, I. Effect of Mineral Particle Size on Froth Stability. Ph.D. Thesis, University of Cape Town, Cape Town, South Africa, March, 2017.
4. Mackay, I.; Videla, A.R.; Brito-Parada, P.R. The link between particle size and froth stability - Implications for reprocessing of flotation tailings. *J. Clean. Prod.* 2020, 242, 118436.
5. Norori-McCormac, A.; Brito-Parada, P.R.; Hadler, K.; Cole, K.; Cilliers, J.J. The effect of particle size distribution on froth stability in flotation. *Sep. Purif. Technol.* 2017, doi:10.1016/j.seppur.2017.04.022.
6. Rocha, L.; Cançado, R.Z.L.; Peres, A.E.C. Iron ore slimes flotation. *Miner. Eng.* 2010, 23, 842–845.
7. Haselhuhn, H.J.; Kawatra, K. Effects of Water Chemistry on Hematite Selective Flocculation and Dispersion. *Miner. Process. Extr. Metall. Rev.* 2015, 36, 305–309.
8. Houot, R. Beneficiation of iron ore by flotation—Review of industrial and potential applications. *Int. J. Miner. Process.* 1983, 10, 183–204.
9. Weissenborn, P.K.; Warren, L.J.; Dunn, J.G. Optimisation of selective flocculation of ultrafine iron ore. *Int. J. Miner. Process.* 1994, 42, 191–213.
10. Trahar, W.J. A rational interpretation of the role of particle size in flotation. *Int. J. Miner. Process.* 1981, 8, 289–327.
11. Sivamohan, R. The Problem of Recovering Very Fine Particles in Mineral Processing—A Review. *Int. J. Miner. Process.* 1990, 28, 247–288.
12. Gontijo, C.F.; Fornasiero, D.; Ralston, J. The Limits of Fine and Coarse Particle Flotation. *Can. J. Chem. Eng.* 2007, 85, 562–785.
13. Farrokhpay, S.; Filippova, I.; Filippov, L.; Picarra, A.; Rulyov, N. Flotation of fine particles in the presence of combined microbubbles and conventional bubbles. *Miner. Eng.* 2020, 155, doi:10.1016/j.mineng.2020.106439.
14. Oliveira, H.; Azevedo, A.; Rubio, J. Nanobubbles generation in a high-rate hydrodynamic cavitation tube. *Miner. Eng.* 2017, doi:10.1016/j.mineng.2017.10.020.

15. Fan, M.; Zhao, Y.; Tao, D. Fundamental studies of nanobubble generation and applications in flotation. In *Separation Technologies for Minerals Coal and Earth Resources*; SME: Littleton, CO, USA, 2012; pp. 457–469.
16. Lima, N.P.; Pinto, T.C.S.; Tavares, A.C.; Sweet, J. The entrainment effect on the performance of iron ore reverse flotation. *Miner. Eng.* 2016, doi:10.1016/j.mineng.2016.05.018.
17. Lima, R.M.F.; Abreu, F.P.V.F. Characterization and concentration by selective flocculation/magnetic separation of iron ore slimes from a dam of Quadrilátero Ferrífero—Brazil. *J. Mater. Res. Technol.* 2020, 9, 2021–2027.
18. Ma, X.; Bruckard, W.J.; Holmes, R. Effect of collector, pH and ionic strength on the cationic flotation of kaolinite. *Int. J. Miner. Process.* 2009, 93, 54–58.
19. Xu, L.; Hu, Y.; Faqin, D.; Hao, J.; Wu, H.; Zhen, W.; Ruohua, L. Effects of particle size and chain length on flotation of quaternary ammonium salts onto kaolinite. *Min. Pet.* 2014, doi:10.1007/s00710-014-0332-8.
20. Ma, X.; Bruckard, W.J. The effect of pH and ionic strength on starch–kaolinite interactions. *Int. J. Miner. Process.* 2010, 94, 111–114.
21. Nykänen, V.P.S.; Braga, A.S.; Pinto, T.C.S.; Matai, P.H.L.S.; Lima, N.P.; Filho, L.S.L.; Monte, M.B.M. True flotation versus entrainment in reverse cationic flotation for the concentration of iron ore at industrial scale. *Miner. Process. Extr. Metall. Rev.* 2018, 41, doi:10.1080/08827508.2018.1514298.
22. Filippov, L.; Filippova, I.; Severov, V. The use of collectors mixture of various molecular structure in the reverse cationic flotation of magnetite ore. *Miner. Eng.* 2020, 23, 91–98.
23. Filippov, L.; Severov, V.; Filippova, I. Mechanism of starch adsorption on Fe-Mg-Al-bearing amphiboles. *Int. J. Miner. Process.* 2013, 123, 120–128.
24. Severov, V.; Filippova, I.; Filippov, L. Floatability of Fe-bearing silicates in the presence of starch: Adsorption and spectroscopic studies. *J. Phys. Conf. Ser.* 2013, 416, 012017.
25. Veloso, C.H.; Filippov, L.O.; Filippova, I.; Ouvrard, S.; Araujo, A.C. Adsorption of polymers onto iron oxides: Equilibrium isotherms. *J. Mater. Res. Technol.* 2019, 9, 779–788.
26. Araujo, V.A.; Lima, N.P.; Azevedo, A.; Rubio, J. Column reverse rougher flotation of iron bearing fine tailings assisted by HIC and a new cationic collector. *Miner. Eng.* 2020, 156, doi:10.1016/j.mineng.2020.106531.
27. Matiolo, E.; Couto, H.J.B.; Lima, N.; Klaydison, S. Improving recovery of iron using column flotation of iron ore slimes. *Miner. Eng.* 2020, 158, doi:10.1016/j.mineng.2020.106608.

28. Klaydison, S.; Filippov, L.; Piçarra, A.; Filippova, I.; Lima, N.; Skliar, A.; Filho, L. New perspectives in iron ore flotation: Use of collector reagents without depressants in reverse cationic flotation of quartz. *Miner. Eng.* 2021, 170, doi:10.1016/j.mineng.2021.107004.
29. Ma, X.; Marques, M.; Gontijo, C. Comparative studies of reverse cationic/anionic flotation of Vale iron ore. *Int. J. Miner. Process.* 2011, 100, 179–183, doi:10.1016/j.minpro.2011.07.001.
30. Fornasiero, D.; Filippov, L. Innovations in the flotation of fine and coarse particles. *J. Phys. Conf. Ser.* 2017, 879, doi:10.1088/1742-6596/879/1/012002.
31. Clout, J.M.F.; Manuel, J.R. Minealógica, chemical and physical characteristics of iron ore. In *Iron Ore Mineralogy, Processing and Environmental Sustainability*; Elsevier: Amsterdam, The Netherlands, 2015.
32. Bruckard, W.J.; Smith, L.K.; Heyes, G.W. Developments in the physiochemical separation of iron ore. In *Iron Ore*; Woodhead Publishing: Sawston, UK, 2015; pp. 339–356, doi:10.1016/b978-1-78242-156-6.00011-3.
33. Trahar, W.J.; Warren, L.J. The flotability of very fine particles—A review. *Int. J. Miner. Process.* 1976, 3, 103–131.
34. Araujo, A.C.; Amarante, S.C.; Souza, C.C.; Silva, R.R.R. Ore mineralogy and its relevance for selection of concentration methods in processing of Brazilian iron ores. *Miner. Process. Extr. Metall.* 2003, 112, 54–64, doi:10.1179/037195503225011439.
35. Lima, N.P.; Valadão, G.E.S.; Peres, A.E.C. Effect of particles size range on iron ore flotation. *Rem: Rev. Esc. De Minas* 2013, 66, doi:10.1590/S0370-44672013000200018.
36. Schulze, H.J.; Radoev, B.; Geidel Th Stechemesser, H.; Topfer, E. Investigations of the Collision Process between Particles and Gas Bubbles in Flotation—A Theoretical Analysis. *Int. J. Miner. Process.* 1989, 27, 263–278.
37. Chipfunhu, D.; Zanin, M.; Grano, S. Flotation behaviour of fine particles with respect to contact angle. *Chem. Eng. Res. Des.* 2012, 90, 26–32.
38. Scheludko, A.; Toshev, B.V.; Bojadjiev, D.T. Attachment of Particles to a Liquid Surface (Capillary Theory of Flotation). *J. Chem. Soc. Faraday Trans. 1: Phys. Chem. Condens. Phases* 1976, 72, doi:10.1039/f19767202815.
39. Souza, H.S.; Braga, A.S.; Oliveira, A.H.; Filho, L.S.L. Concentration of manganese tailings via reverse flotation in an acid médium. *Rem: Rev. Esc. De Minas* 2016, 69, 85–90, doi:10.1590/0370-44672015690069.
40. Kracht, W.; Orozco, Y.; Acuña, C. Effect of surfactant type on the entrainment factor and selectivity of flotation at laboratory scale. *Miner. Eng.* 2016, 92, 216–220.

41. Melo, F.; Laskowski, J.S. Effect of frothers and solid particles on the rate of water transfer to froth. *Int. J. Miner. Process.* 2007, 84, 33–40, doi:10.1016/j.minpro.2007.04.003.
42. Moyo, P.; Gomes, C.O.; Finch, J.A. Characterizing frothers using water carrying rate. *Can. Metall. Q.* 2007, 46, 215–220.
43. Matos, V.E.; Nogueira, S.C.S.; Silva, G.; Kowalczyk, P.B. Differences in Etheramines Froth Properties and the Effects on Iron Ore Flotation. Part II: Three-Phase Systems. *Miner. Process. Extr. Metall. Rev.* 2021, doi:10.1080/08827508.2021.1888725.
44. Somasundaran, P. Fine particles treatment. In *Workshop on Research Needs in Mineral Processing*; Columbia University: New York, NY, USA, 1976.
45. Kursun, H. Effect of Fine Particles' Entrainment on Conventional and Column Flotation. Part. *Sci. Technol.* 2014, 32, 251–256, doi:10.1080/02726351.2013.855684.
46. Tan, J.; Wang, J.; Nguyen, A.V.; Xie, G. Regimes of drainage instability caused by wash water. *Miner. Eng.* 2020, 148, 160202, doi:10.1016/j.mineng.2020.106202.
47. Soto, H.S. Column flotation with negative bias. In *Proceedings of the International Symposium on Processing of Complex Ores*, Halifax, UK, 20–24 August 1989; pp. 379–385.
48. Flint, I.M.; Wyslouzil, H.E.; Andrade, V.L.L.; Murdock, D.J. Column flotation of iron ore. *Miner. Eng.* 1992, 10–12, 1185–1194.
49. Kursun, H. Determination of Carrying Capacity Using Talc in Column Flotation. *Arab. J. Sci. Eng.* 2011, 36, 703.
50. Espinosa-Gomez, R.; Finch, J.A.; Yianatos, J.B.; Dobby, G.S. Technical Note: Flotation Column Carrying Capacity: Particle SIZE and Density Effects. *Miner. Eng.* 1988, 1 N1, 77–79.
51. Yianatos, J.B.; Contreras, F.A. On the Carrying Capacity Limitation in Large Flotation Cells. *Can. Metall. Q.* 2010, 49, 345–352.
52. Bergh, L.G.; Yianatos, J.B. Flotation column automation: state of the art. *Control Eng. Pract.* 2003, 11, 67–72.
53. Beuria, P.C.; Biswal, S.K.; Mishra, B.K.; Roy, G.G. Study on kinetics of thermal decomposition of low LOI goethetic hematite iron ore. *Int. J. Min. Sci. Technol.* 2017, doi:10.1016/j.ijmst.2017.06.018.
54. Svoboda, J.; Fujita, T. Recent developments in magnetic methods of material separation. *Miner. Eng.* 2003, 16, 785–792.

Chapter 7 - Why flotation for iron ore slimes?

This thesis aims to study issues related to amidoamine (N-[3-(dimethylamino)propyl] dodecanamide) as a collector in iron ore slime flotation; however, it is important to provide a small explanation of the question. The desliming is adopted, in the concentration of iron ore, precisely to improve the results in the reverse cationic flotation of quartz, so: *Why study flotation in iron ore slimes concentration? Is there a different process more suitable for this purpose?*

Magnetic separation is also a process that can be applied, on an industrial scale, also to concentrate iron ore slimes. The efficiency of this process depends on some characteristics, such as granulometric distribution and mineralogy. For example, the presence of goethite can hamper the process due to its lower magnetic susceptibility when compared to hematite. Considering that iron ore slimes are composed of ultrafine particles (almost 50% below 10 microns), significant loss of iron to tailings can occur due to the “competition” between magnetic force and hydraulic drag in the process, especially when iron oxide predominant is goethite. Therefore, flotation can be an alternative to concentrate some iron ore slimes.

Skosana (2008) investigated the iron ore slime beneficiation process in order to concentrate the Sishen Mine slime. The most promising results were obtained by two stages of VPHGMS magnetic separators (rougher and cleaner), which presented a final concentrate with 66.5%Fe and a yield of 40%. The average iron content in this slime was 54% and, in relation to the granulometric distribution, despite the d50 being close 7 μm , the d90 was close 100 μm .

Some iron ore slimes from the Iron Quadrangle region (Brazil) presents, in average, close 44%Fe, that means 10% lower than the slimes from Sishen mine. Concerning the granulometric distribution, the d90 is, generally finer than that from Sishen mine, because the ore with particles distribution between 150 μm and 10 μm is concentrated by conventional flotation

Studies adopting magnetic concentration for the iron ore slime from Vargem Grande 2 plant were carried out by Pinto (2020). The best results obtained by the author showed values above 3.4% of SiO_2 in the concentrate and iron content in the tailings above 30% when adopting the WHIMS (high intensity wet magnetic separator). Concerning the VPHGMS (vertically pulsating high gradient magnetic separator), the results showed values higher than 4.8% SiO_2 in the concentrate and higher than 21%Fe in the tailings. The iron content in the feed of the slimes magnetic concentration was close to 44% (Table 1 - 2).

Table 1. Vargem Grande 2 iron ore slimes magnetic concentration pilot tests results adopting WHIMS. Copied from (Pinto, 2020)

ID	Matrix	% Solids	Medium Wash Water (kgf/cm ²)	Speed of ring (r/min)	Volumetric Flowrate (l/h)	Magnetic Field Intensity (T)	Stream	Yield		%	
								% Total Mass	Fe	Fe	SiO ₂
1	conventional 0.5 mm	30	1.0	4	Nominal (manufacturer's default)	1.8	Feed	100.0	51.1	44.06	30.15
							Product	36.1		62.43	7.35
							Tailing	63.9		33.69	43.33
2	conventional 1.1 mm	30	1.0	4	Nominal (manufacturer's default) Nominal (manufacturer's default)	1.8	Feed	100.0	48.5	43.95	30.53
							Product	33.2		64.32	5.01
							Tailing	66.8		33.83	43.29
3	conventional 1.5 mm	30	1.0	4	Nominal (manufacturer's default)	1.8	Feed	100.0	40.2	43.87	30.48
							Product	27.4		64.36	4.81
							Tailing	72.6		36.15	40.26
4	Big flux 0.5 mm	30	1.0	4	Nominal (manufacturer's default)	1.8	Feed	100.0	54.9	43.99	30.41
							Product	38.9		62.17	7.19
							Tailing	61.1		32.43	45.28
5	Big flux 1.1 mm	30	1.0	4	Nominal (manufacturer's default)	1.8	Feed	100.0	36.4	43.76	30.69
							Product	25.5		62.42	6.99
							Tailing	74.5		37.35	38.82
6	Big flux 1.5 mm	30	1.0	4	Nominal (manufacturer's default)	1.8	Feed	100.0	25.5	43.89	30.49
							Product	18.1		61.85	7.69
							Tailing	81.9		39.92	35.53
7	Wave 1.5 mm	30	1.0	4	Nominal (manufacturer's default)	1.8	Feed	100.0	40.8	43.34	32.08
							Product	29.2		60.63	20.00
							Tailing	70.8		36.21	39.77
8	conventional 1.1 mm	30	0.0	4	Nominal (manufacturer's default)	1.8	Feed	100.0	47.2	43.92	30.56
							Product	33.3		62.26	7.52
							Tailing	66.7		34.77	42.21
9	conventional 1.1 mm	30	2.0	4	Nominal (manufacturer's default)	1.8	Feed	100.0	41.0	44.06	30.64
							Product	27.7		65.27	4.16
							Tailing	72.3		35.95	40.78
10	conventional 1.1 mm	30	3.0	4	Nominal (manufacturer's default)	1.8	Feed	100.0	39.3	44.30	30.22
							Product	26.4		65.89	3.44
							Tailing	73.6		36.54	39.84
11	conventional 1.1 mm	30	1.0	3	Nominal (manufacturer's default)	1.8	Feed	100.0	38.2	43.77	31.05
							Product	25.4		65.95	3.40
							Tailing	74.6		36.23	40.45
12	conventional 1.1 mm	30	1.0	7	Nominal (manufacturer's default)	1.8	Feed	100.0	47.5	43.91	30.83
							Product	34.1		61.12	9.17
							Tailing	65.9		34.99	42.05
13	conventional 1.1 mm	30	1.0	4	-60%	1.8	Feed	100.0	64.1	44.34	30.23
							Product	45.3		62.68	6.49
							Tailing	54.7		29.14	49.72
14	conventional 1.1 mm	30	1.0	4	-40%	1.8	Feed	100.0	54.7	44.37	30.08
							Product	37.6		64.56	4.70
							Tailing	62.4		32.20	45.38
15	conventional 1.1 mm	30	1.0	4	-20%	1.8	Feed	100.0	51.4	44.19	30.17
							Product	35.3		64.36	4.98
							Tailing	64.7		33.20	43.91
16	conventional 1.1 mm	30	1.0	4	20%	1.8	Feed	100.0	42.5	44.36	29.95
							Product	29.1		64.71	4.77
							Tailing	70.9		36.00	40.29
17	conventional 1.1 mm	30	1.0	4	40%	1.8	Feed	100.0	42.0	44.17	30.22
							Product	28.9		64.24	5.34
							Tailing	71.1		36.02	40.33
18	conventional 1.1 mm	30	1.0	4	Nominal (manufacturer's default)	1.9	Feed	100.0	48.1	43.81	30.05
							Product	32.6		64.67	5.08
							Tailing	67.4		33.72	42.22
19	conventional 1.1 mm	30	1.0	4	Nominal (manufacturer's default)	1.6	Feed	100.0	44.6	44.09	30.30
							Product	30.6		64.26	5.21
							Tailing	69.4		35.20	41.15
20	conventional 1.1 mm	30	1.0	4	Nominal (manufacturer's default)	1.5	Feed	100.0	41.0	44.11	30.29
							Product	28.0		64.60	4.96
							Tailing	72.0		36.16	40.22
21	conventional 1.1 mm	22	1.0	4	Nominal (manufacturer's default)	1.8	Feed	100.0	59.5	44.95	29.28
							Product	41.5		64.43	4.71
							Tailing	58.5		31.11	46.72

Table 2. Vargem Grande 2 iron ore slimes magnetic concentration pilot tests results adopting VPHGMS. Copied from (Pinto, 2020)

ID	Speed of ring (r/min)	Pulsating speed (per/min)	Magnetic Field (T)	% Solids	Volumetric Flowrate (l/h)	Stream	Yield		%	
							% Total Mass	Fe	Fe	SiO ₂
1	0.5	300	1.4	23	200	Feed	100.0	70.9	42.40	34.08
						Product	47.0		63.96	5.61
						Tailing	53.0		23.30	59.30
2	1.0	300	1.4	23	200	Feed	100.0	75.7	41.66	35.07
						Product	50.0		63.00	6.87
						Tailing	50.0		20.30	63.30
3	2.0	300	1.4	23	200	Feed	100.0	78.8	42.40	34.07
						Product	53.1		63.01	6.75
						Tailing	46.9		19.11	64.95
4	3.0	300	1.4	23	200	Feed	100.0	83.1	42.43	34.04
						Product	57.1		61.81	8.29
						Tailing	42.9		16.67	68.27
5	1.0	100	1.4	23	200	Feed	100.0	70.5	41.90	34.48
						Product	59.1		49.99	23.26
						Tailing	40.9		30.24	50.65
6	1.0	200	1.4	23	200	Feed	100.0	77.6	42.00	34.35
						Product	54.7		59.61	10.59
						Tailing	45.3		20.75	63.05
7	1.0	300	0.8	23	200	Feed	100.0	73.2	41.93	34.47
						Product	48.1		63.80	5.85
						Tailing	51.9		21.67	61.00
8	1.0	300	1.0	23	200	Feed	100.0	78.3	42.12	34.16
						Product	51.6		63.92	5.47
						Tailing	48.4		18.87	64.74
9	1.0	300	1.2	23	200	Feed	100.0	79.8	42.09	34.18
						Product	52.8		63.56	5.84
						Tailing	47.2		18.06	65.90
10	1.0	300	1.4	32	200	Feed	100.0	61.5	42.71	32.79
						Product	41.0		64.03	5.07
						Tailing	59.0		27.86	52.09
11	1.0	300	1.4	23	200	Feed	100.0	65.0	42.90	32.29
						Product	43.7		63.80	5.29
						Tailing	56.3		26.69	53.25
12	1.0	300	1.4	13	200	Feed	100.0	61.5	43.09	31.97
						Product	41.3		64.13	4.84
						Tailing	58.7		28.26	51.09
13	1.0	300	1.4	6	200	Feed	100.0	75.5	43.51	31.16
						Product	51.4		63.93	4.98
						Tailing	48.6		21.95	58.82
14	1.0	300	1.4	23	100	Feed	100.0	61.9	40.73	33.32
						Product	40.1		62.84	5.64
						Tailing	59.9		25.93	51.85
15	1.0	300	1.4	23	300	Feed	100.0	56.6	40.43	33.88
						Product	36.1		63.42	5.29
						Tailing	63.9		27.44	50.04
16	1.0	300	1.4	23	400	Feed	100.0	52.9	40.91	34.00
						Product	34.0		63.61	5.37
						Tailing	66.0		29.21	48.76
17	1.0	300	1.4	23	500	Feed	100.0	49.0	40.91	33.78
						Product	31.5		63.54	5.41
						Tailing	68.5		30.49	46.84

To answer the question presented in this chapter, some exploratory pilot tests, adopting the magnetic concentration, were performed with Vargem Grande 2 plant slimes to compare the

results between magnetic concentration and flotation with amidoamine (N-[3-(dimethylamino)propyl]dodecanamide). As for the magnetic concentration, the results agree with those presented by Pinto (2020), and it is not possible to obtain values with a silica content in the concentrate lower than 3.4%.

The equipment adopted in these magnetic concentration exploratory tests was the VPHGMS (Figure 1). According to Altin et al (2016), the VPHGMS allows the processing of fine and weakly magnetic particles through the combined magnetic force field, pulsation in the separation zone, gravity, and vertical rotating ring.

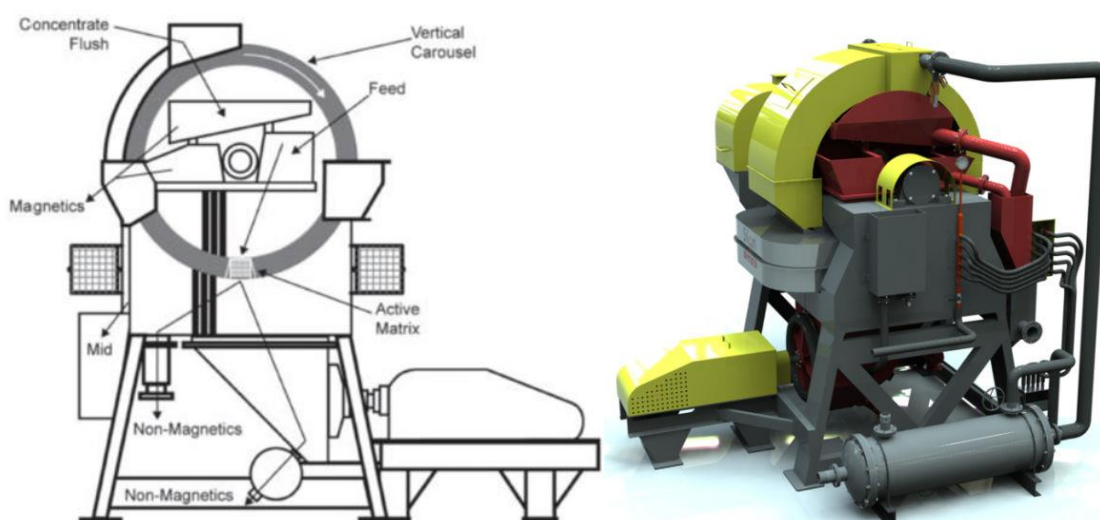


Figure 1. VPHGMS Copied from (Altin et al., 2016; www.slonmagnetics2020.en.made-in-china.com)

Flotation column pilot tests were also performed, and three different circuit configurations were evaluated. The mass balance was calculated with the average value obtained from the optimized tests. Regarding the VPHGMS, the best operating parameters were flowrate: 300 l/h, ring speed: 3 revolutions per minute, magnetic field: 13 T. The VPHGMS adopted in the pilot tests was the Longi LGS-EX, with a ring diameter of 500 mm (Figure 5). Flotation tests parameters were presented in chapter 6. This thesis does not aim to detail studies related to the magnetic concentration in iron ore slimes, therefore, only the final results for each evaluated route are presented in figures 2 to 4.

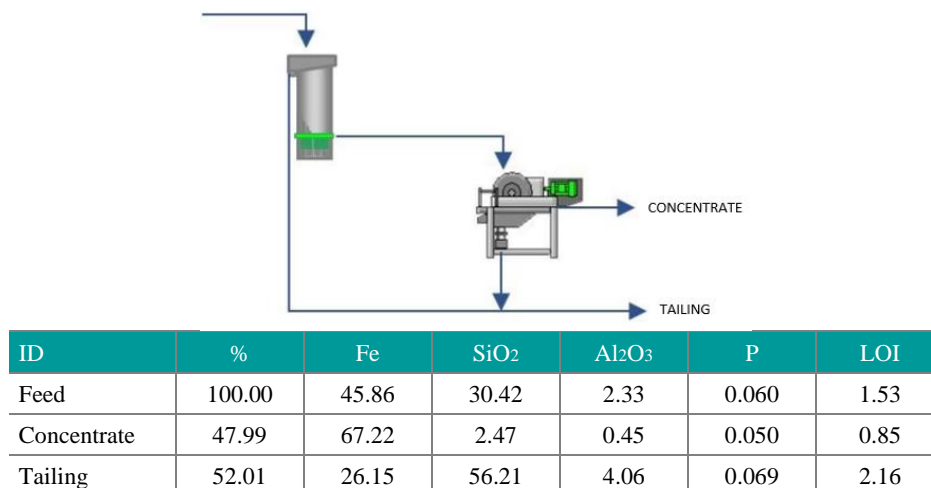


Figure 2. Flotation + VPHGMS simplified flowsheet and mass balance

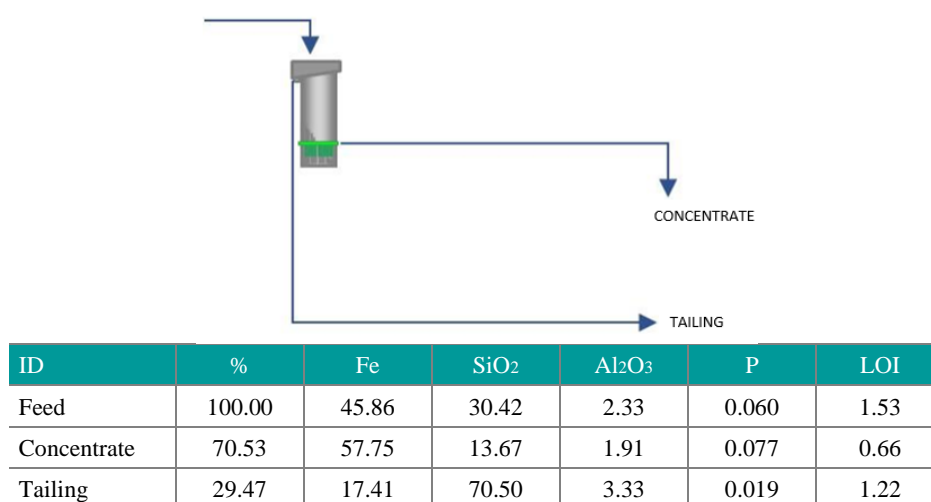


Figure 3. Flotation simplified flowsheet and mass balance

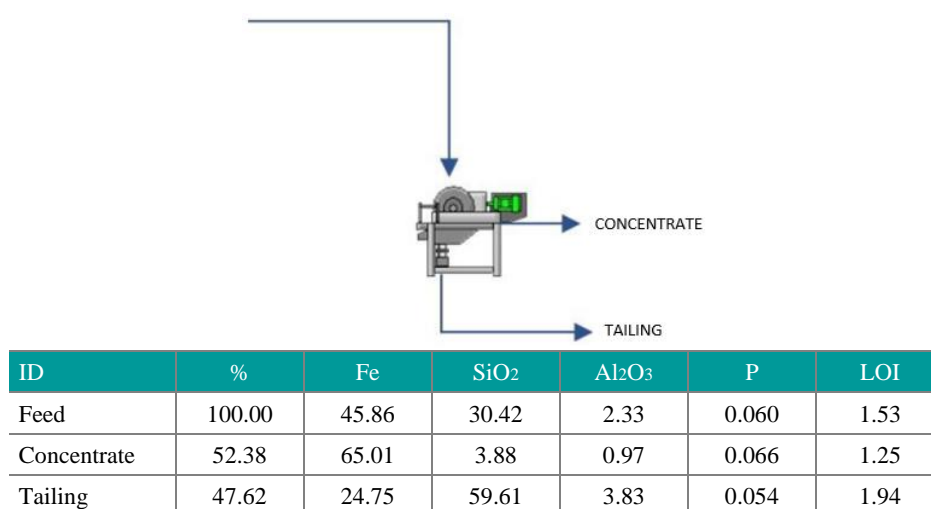


Figure 4. VPHGMS simplified flowsheet and mass balance



Figure 5. VPHGMS LGS-EX adopted in the exploratory pilot tests to evaluate the magnetic concentration of iron ore slimes from the Vargem Grande 2 plant.

As demonstrated by the pilot test results in Chapter 6, concerning the flotation, to improve the iron content in the concentrate, a cleaner stage is needed. The exploratory studies of magnetic concentration and flotation showed that the synergy between these two distinct processes can be, in some cases, an adequate option to guarantee less iron loss in the tailings and higher iron content in the concentrate. Therefore, a suitable process route for the concentration of iron ore slime from the Vargem Grande 2 plant could be the rougher phase by column flotation with amidoamine (N-[3-(dimethylamino)propyl]dodecanamide) and the cleaner by adopting magnetic concentration with VPGHMS. Table 3 presents the results of the pilot tests adopting the VPGHMS to concentrate the column flotation product referring to the pilot tests shown in Table 5 of chapter 6 while Table 4 presents some results obtained in the exploratory pilot tests adopting only a rougher stage by the VPHGMS.

Table 3. Pilot tests results considering 2 concentration stages (flotation as rougher and VPHGMS as cleaner)

Data	Flotation (%Fe)			VPHGMS (%Fe)			Global Results				
	Feed	Product	Tailing	Feed	Product	Tailing	Final Tailings		Final Product		Yield (%)
							Fe	SiO ₂	Fe	SiO ₂	
09 may	44.6	50.5	14.3	50.5	66.4	32.7	27.4	54.7	66.4	2.9	44.0
10 may	47.5	58.5	17.7	58.5	67.6	41.1	29.0	53.5	67.6	2.0	47.8
11 may	48.2	56.5	22.6	56.5	67.4	36.6	29.9	48.4	67.4	1.7	48.9
14 may	48.2	61.1	23.7	61.1	67.1	39.7	28.4	53.3	67.1	1.9	51.1
15 may	49.4	57.1	19.9	57.1	67.4	33.7	27.4	51.2	67.4	1.8	55.0
16 may	45.6	61.0	18.2	61.0	67.6	36.3	23.1	60.3	67.6	1.4	50.7
Average Value	47.2	57.4	19.4	57.4	67.3	36.7	27.5	53.6	67.3	2.0	49.6

Table 4. Pilot tests results adopting 1 concentration stage by VPHGMS

ID	Feed		Product		Tailing	
	Fe	SiO ₂	Fe	SiO ₂	Fe	SiO ₂
1	48.9	24.0	62.3	7.4	19.4	64.7
2	48.9	24.0	62.3	7.4	19.4	64.7
3	44.8	29.8	63.6	5.7	19.9	66.3
4	47.8	27.2	65.6	3.0	27.4	53.4
5	48.6	25.6	64.9	3.9	26.9	51.8
6	46.6	25.4	65.9	2.4	24.5	52.9
7	45.4	27.1	66.0	2.4	26.8	49.9
8	47.3	26.5	64.9	3.4	28.5	51.3
Average Value	47.3	26.2	64.4	4.4	24.1	56.9

Comparing Tables 3 and 4, it is possible to observe that better results for the final product were obtained by adopting the route with flotation and VPGHMS. Regarding the iron ore slimes from the Vargem Grande 2 plant, feeding the magnetic concentrator with high quartz content results in a higher silica content in the concentrate due to the trapping of non-magnetic particles in the equipment matrix. In this case, a cleaner stage also performed with magnetic concentration tends to generate greater iron loss in the final tailings when compared to flotation performed as a rougher stage.

In this work, a different flotation from conventional flotation was developed, because, due to the specificities of the collector, it does not require the use of starch. Due to the selectivity of this reagent in the specific case of Vargem Grande 2, the loss of iron in the tailings is lower when flotation is compared to the magnetic concentration process, but the magnetic concentration generates products with lower SiO₂ content and with less variation in chemical quality of the concentrate when compared to flotation. Thus, the combination of the two processes (flotation and magnetic concentration) tends to generate a route with lower iron losses in the tailings (compared to the route with only magnetic concentration) and better chemical quality of the final product (when compared to a route where there is only flotation).

Therefore, depending on the desired iron content in the final concentrate and the characteristics of the slimes, this new flotation process (without depressant), may be a suitable process as a rougher stage to reduce iron loss to the final tailings when compared to the two-step VPHGMS route.

In an industrial project, it is possible, for example, to design a flexible circuit to operate according to slime characteristics and specific objectives (improve mass recovery or improve concentrate quality, for example) by adopting the configuration shown in Figure 2 and options for bypass of the column or magnetic concentration.

Thus, answering the question posed at the beginning of this chapter, the best iron ore slime concentration process depends on the characteristics of these slimes, therefore magnetic concentration, selective flocculation, flotation, or other processes must be developed and evaluated. The best processing route for a given iron ore slime can be achieved through just one process or through synergy between different processes.

References

Skosana, D.J.; 2008, Process Alternatives to Recover High-Grade Iron Ore Concentrate from the Thickener Underflow Slimes of Sishen Beneficiation Plant, MetPlan (Metallurgical Plant Design and Operating Strategies), 18 – 19 august, Perth, WA

Pinto, Pedro Henrique Ferreira, 2020. Aproveitamento de lamas de minério de ferro do Quadrilátero Ferrífero por concentração magnética de alta intensidade de campo magnético. Tese (doutorado) – Escola Politécnica da Universidade de São Paulo. Departamento de Engenharia de Minas e Petróleo. <https://www.teses.usp.br/teses/disponiveis/3/3134/tde-24082020134547/publico/PedroHenriqueFerreiraPintoCorr20.pdf>

Altin, G.; Inal, S.; ALP, I.; Lekili, M.E.; 2016; Recovery of chromite from processing plant tailing by vertical ring and pulsating high-gradient magnetic separation, International Black Sea Mining & Tunnelling Symposium, 2-4 November, Trabzon-Turkey

Chapter 8 - Final comments

In this chapter, it will be discussed, in a simplified way, a relationship between the topics presenting the main conclusions obtained from this thesis. This topic also aims, somehow, to emphasize the importance of developing new reagents for iron ore flotation to, perhaps, instigate new lines of research on the subject.

As shown in Chapter 1, the iron ore mining industry in the Iron Quadrangle, Brazil, is currently at the stage called by some authors The Third Wave, that means, due to the iron ore characteristics, the most suitable concentration process is the reverse cationic flotation. The third wave of the iron ore mining industry generates some undesirable consequences, such as increased environmental impacts related to tailings dams. Therefore, the study of the concentration process contributing to the reduction of the amount of tailings is very important for the progress of the mining industry in that region.

Issues related to the use of starch in some specific conditions that can hinder the flotation process were discussed. Some authors have shown that starch can be adsorbed on silicate surfaces containing Fe-Mg-Al, impairing flotation. At high dosages of amine and/or starch in flotation, it is possible that interactions between these reagents occur, reducing the efficiency of the process. On the other hand, some works aimed at the development of new, more selective flotation collectors, which eliminate the need for depressants, have shown that some reagents, with bulky polar head group, can present a selective behavior in the flotation of some minerals, due to the phenomenon steric hindrance.

Thus, it was proposed in this thesis to develop studies on the scientific hypothesis that some collectors, with molecular structure containing a bulky polar head group, which do not require depressants, can improve the flotation efficiency of some complex iron ore minerals. Considering the iron content of the slimes in the Iron Quadrangle region, its mineral composition (containing other minerals in addition to hematite and quartz, with a significant presence of kaolinite) and particle size distribution (generating a high specific surface, increasing the consumption of reagents and loss of iron in tailings by drag), we can consider these slimes as a “complex iron ore”. In order to test the scientific hypothesis, we adopted the amidoamine N-[3-(dimethylamino)propyl]dodecanamide to be studied as collector. The development of an iron ore slimes flotation process will reduce the amount of ultrafine tailings, also improving metallurgical recovery and contributing to the replacement of tailings dams by

piles, since some studies have shown that there is a maximum ratio between ultrafine tailings and flotation tailings, which makes filtering and stacking of the total tailings viable.

The Chapter 2 was dedicated to discussing the harmful effects of iron slimes on the reverse flotation of quartz (the main effects refer to the increase of reagents consumption, the lower selectivity and the froth stability). It was also discussed the anomalous flotation behavior of kaolinite, that can be explained based on crystal structure. Fine kaolinite particles have more edges to adsorb fewer cationic collectors than that of coarse kaolinite particles, which is responsible for its poorer floatability. Slimes have higher surface area, which increases the consumption of reagents and can result in high froth volumes.

It was analyzed a slime iron ore sample from the Iron Quadrangle, which almost 91% of the alumina (mainly kaolinite) were distributed in the size fraction below 20 μm . Flotation tests showed that the addition of corn starch during desliming feed sedimentation tests increased the kaolinite depression. Considering that kaolinite is the main alumina mineral in the iron ore slime from the Iron Quadrangle region, its presence can affect the quartz flotation due the kaolinite depression by the corn starch. The starch adsorption on kaolinite surface may impairs the starch adsorption on the hematite, increasing the iron content in the flotation tail. The kaolinite depression due the starch adsorption, also impairs the quality of the product due the increase of silica and alumina content in the concentrate of flotation. Thus, considering an iron ore with high kaolinite content, increasing the starch dosage to enhance the hematite depression may generate, as consequence, the decrease of the flotation process selectivity.

Another important issue presented in this chapter is related to the particle size distribution of minerals present in the iron ore slimes. It was possible to verify that the hematite present in the slime sample studied was much finer than the silicates (D50 of hematite was 9 μm , while d50 of the silicates is 20 μm). The high hematite specific surface in the slimes may requires higher starch dosages in the flotation process. As discussed, high starch dosages may generate, kaolinite depression and also the quartz depression due the co-adsorption of starch with amine on the quartz surface (high dosages of reagents may also impairs the flotation process due the clathrates formation).

Therefore, studies carried out on the Chapter 2 contributed to demonstrate that the scientific hypothesis presented in the Chapter 1 (the development of collector that dispense the need for a depressant reagent in iron ore cationic reverse flotation may contributes to obtain a more efficient iron ore slime flotation process) is a suitable hypothesis.

It is important, however, to emphasize that the magnetic concentration results presented in the Chapter 2 showed that, even after three cleaner stages, the tailings contained 17.06% Fe,

which may indicate some association between gangue minerals and Fe minerals. Therefore, the finer size distribution of the Fe minerals and their associations with the gangue minerals indicate challenges and difficulties to concentrate the iron ore slimes even with a collector reagent without need for depressant.

From the Chapter 3 to the Chapter 6, the studies were based on the analysis of the amidoamine N-[3-(diethylamino)propyl]dodecanamide as collector reagent, without depressant.

The Chapter 3 was focused on the classic fundamental studies related to the interaction between the hematite, quartz, and kaolinite minerals with the amidoamine, amine and starch. It was discussed the results of the zeta potential, contact angle measurements, pure and mixed minerals flotation tests and FTIR analysis. Although smaller than the contact angles for etheramine, the angles obtained with amidoamine at pH 8 and 10 showed that this collector could hydrophobicise the quartz surface to promote its flotation. The zeta potential increased significantly at pH 8 for amidoamine, whereas the zeta potential variation for etheramine was slightly pronounced at pH 10. Thus, the biggest difference in the adsorption behaviour between both collectors occurs at pH 8 and 10 (this difference can be explained due to the pka of each reagent, while the etheramine pka value is close to 10, the amidoamine pka value is close to 8).

The flotation tests showed that is possible to obtain selective flotation of quartz from hematite in the reverse approach, without a depressant. But, to reach the same recovery level as that achieved using the amine collector, it is necessary to adopt a higher amidoamine dosage than etheramine.

The infrared spectroscopy results showed that an increase in amidoamine concentration did not result in a significant variation in peak intensity (stretching bands of CH₃ and CH₂) for hematite spectrum, while the peaks intensity on the quartz and kaolinite were increased significantly, therefore since for this amidoamine collector the structure of the adsorption layer is controlled by the collector concentration, occurs hindrance effect for hematite. Thus, the amidoamine N-[3-(dimethylamino)propyl]dodecanamide is able to promote the selective flotation of quartz from hematite without a depressant agent, such as starch. Despite the flotation behavior of kaolinite, adopting the amidoamine, was similar to those of hematite, the FTIR spectrum analysis was similar to the of quartz. The high specific surface area coupled with double sheet structure may be an explanation for this behavior. Therefore, this reagent can be an advantageous alternative to conventional amines in the reverse cationic flotation of iron ores slimes, depending on the amount of kaolinite present, since high kaolinite content may also impair the selectivity of flotation even adopting the amidoamine as collector.

The deep understanding of the adsorption mechanism related this specific amidoamine may contribute to the development of a new class of reagents, more effective for the reverse iron ore flotation, reducing or eliminating the need for the depressant reagent, also contributing to a decrease of iron loss to tailings. Therefore, in the Chapter 4, studies concerning the molecular modeling, comparing the adsorption of the etheramine and amidoamine on the hematite in on quartz surface were carried out to explain the hindrance mechanism presented by the FTIR analysis in the Chapter 3.

The molecular modeling studies demonstrated that, concerning the surface D2 of the hematite, the selectivity behavior for the quartz-hematite system flotation with amidoamine can be explained by the combination of the “shield” formed by the coordinating water molecules on this surface with the large amidoamine head group molecular volume, due the methyl bonded to nitrogen in the tertiary amine, generating steric hindrance and impairing the adsorption on its surface, even considering the protonated amidoamine (pH 8,5). In relation to etheramine, the neutral collector adsorption is impaired by the coordinating water on the hematite-(D2) surface, but the protonated molecule (etherammonium) can penetrate and bind on this surface due the electrostatic driving force. Thus, the analysis presented in the Chapter 4, contributed to explain the occurrence of steric hindrance on the hematite surface and the absence of this behavior on the quartz surface. Others hematite surfaces did not be studied, so depending on of the iron ore characteristics, the selectivity behavior of this amidoamine may be different.

In order to evaluate the amidoamine industrial application on the iron ore slimes flotation, the Chapter 5 was dedicated to study two different slimes samples in a column flotation pilot plant. The slime sample containing higher amount of kaolinite presented worst flotation performance. These results are according to the analysis related to the fundamental studies carried out in this thesis. The amidoamine showed potential to be adopted, without depressant, in a slimes flotation process for the sample with the lowest percentage of kaolinite.

The several tests presented in Chapter 4 were performed in a controlled plant, thus they did not consider process variations due to plant operation or even slimes characteristics variability that occurs in an industrial plant. Therefore, to conclude about the industrial application of the amidoamine in the iron ore slimes flotation, without depressant, it was necessary to evaluate its performance considering the issues related to the continuous operation.

Thus, studies presented in the Chapter 6 demonstrated that, regarding an industrial application of the iron ore slimes flotation with the amidoamine N-[3-(dimethylamino)propyl]dodecanamide, without depressant, the variability of the flotation feed significantly impairs the results. It was analyzed the influence of the mains operational

parameters and it was possible to conclude that, different of the results obtained in the controlled environment presented in the Chapter 5, it was not possible to maintain a suitable flotation efficiency during the continuous operation adopting only one concentration. The importance of implementing automated silica and iron analyzers was also demonstrated, as well as automatic parameter controls, such as washing water and reagent dosage, in an eventual industrial application.

Chapter 7 suggests that a suitable process to use as a cleaner step in the concentration of slimes from the Vargem Grande 2 plant, after flotation with the amidoamine N-[3-(dimethylamino)propyl]dodecanamide, could be the concentration magnetic. This chapter presents exploratory studies, which are outside the scope of this thesis and should be further explored.

This thesis was focused on the selectivity behavior related to the amidoamine N-[3-(dimethylamino)propyl]dodecanamide in the flotation of iron ore slimes composed basically by hematite and quartz and represents a small contribution to the development of new iron ore flotation collectors.

With the advancement of technology, the use of computational tools has an increasingly important role in the most varied areas of knowledge, as demonstrated using molecular modeling in this thesis, for example.

The scientific development of a given subject is done by several hands. It is a construction in which each researcher places a brick to build new and more solid knowledge. Thus, there are still several issues related to the research presented in this thesis that can be further developed, such as: the adsorption behavior in relation to different sizes of mineral particles, the influence of the percentage of solids and froth characteristics on the hydrodynamics and efficiency of the process. Furthermore, the study of reagent optimization through changes in its structure or mixture with other reagents is an important line of research to be evaluated.